



Founded 1905

**ADAPTIVE NEURAL CONTROL OF NONLINEAR
SYSTEMS WITH HYSTERESIS**

BEIBEI REN
(B.Eng. & M.Eng.)

**A THESIS SUBMITTED
FOR THE DEGREE OF DOCTOR OF PHILOSOPHY
DEPARTMENT OF ELECTRICAL & COMPUTER ENGINEERING
NATIONAL UNIVERSITY OF SINGAPORE
2009**

Acknowledgements

First of all, I would like to express my heartfelt gratitude to my PhD supervisor, Professor Shuzhi Sam Ge, for his time, thoughtful guidance, and selfless sharing of experiences in all things research and more, that are so conducive to the work that I have undertaken. His broad knowledge, deep insights, outstanding leadership, and great personality impressed me, inspired me, and changed me. The experience of working with him is a lifelong treasure to me, which is challenging, enjoyable and rewarding.

Thanks also go to Professor Tong Heng Lee, my PhD co-supervisor, for his enthusiastic encouragements, suggestions and help on all matters concerning my research despite his busy schedule during the course of my PhD study. I also would like to thank Professor Chun-Yi Su, from Concordia University, and his research group for their excellent research works, and helpful advice and guidance on my research.

I am also grateful to all other staffs, fellow colleagues and friends in the Mechatronics and Automation Lab, and the Social Robotics Laboratory for their kind companionship, generous help, friendship, collaborations and brainstorming, that are always filled with creativity, inspiration and crazy ideas. Thanks to them for bringing me so many enjoyable memories.

Acknowledgement is extended to National University of Singapore for awarding me the research scholarship, providing me the research facilities and challenging environment, and the highly efficient administration of my candidature matters throughout my PhD course.

In addition, my great appreciation goes to the distinguished examiners for their time and effort in examining my work.

Last, but certainly not the least, I am deeply indebted to my family for always being there with their constant love, trust, support and encouragement, without which, I would never be where I am today.

Contents

| | |
|--|------------|
| Acknowledgements | ii |
| Contents | iii |
| Summary | vii |
| List of Figures | ix |
| Notation | xii |
| 1 Introduction | 1 |
| 1.1 Background and Motivation | 1 |
| 1.1.1 Hysteresis and Systems Control | 1 |
| 1.1.2 Neural Networks | 4 |
| 1.1.3 Adaptive Neural Control of Nonlinear Systems | 6 |
| 1.2 Objectives and Structure of the Thesis | 9 |
| 2 Mathematical Preliminaries | 12 |
| 2.1 Introduction | 12 |

| | | |
|----------|---|-----------|
| 2.2 | Hysteresis Models and Properties | 12 |
| 2.2.1 | Backlash-Like Hysteresis Model | 13 |
| 2.2.2 | Classic Prandtl-Ishlinskii Hysteresis Model | 14 |
| 2.2.3 | Generalized Prandtl-Ishlinskii Hysteresis Model | 18 |
| 2.3 | Function Approximation | 19 |
| 2.3.1 | NN Approximation | 20 |
| 2.3.2 | MNNs | 21 |
| 2.3.3 | RBFNNs | 22 |
| 2.4 | Useful Definitions, Theorems and Lemmas | 25 |
| 3 | Systems with Backlash-Like Hysteresis | 29 |
| 3.1 | Strict-Feedback Systems | 29 |
| 3.1.1 | Introduction | 29 |
| 3.1.2 | Problem Formulation and Preliminaries | 31 |
| 3.1.3 | Adaptive Dynamic Surface Control Design | 33 |
| 3.1.4 | Simulation Results | 42 |
| 3.2 | Output Feedback Systems | 43 |
| 3.2.1 | Introduction | 43 |
| 3.2.2 | Problem Formulation and Preliminaries | 46 |
| 3.2.3 | State Estimation Filter and Observer Design | 48 |
| 3.2.4 | Adaptive Observer Backstepping Design | 51 |
| 3.2.5 | Simulation Results | 60 |
| 3.3 | Conclusion | 62 |

| | | |
|----------|--|------------|
| 4 | Systems with Classic Prandtl-Ishlinskii Hysteresis | 68 |
| 4.1 | Introduction | 68 |
| 4.2 | Problem Formulation and Preliminaries | 70 |
| 4.3 | Control Design and Stability Analysis | 73 |
| 4.3.1 | Adaptive Variable Structure Neural Control for SISO Case ($m = 1$) | 74 |
| 4.3.2 | Adaptive Variable Structure Neural Control for MIMO Case ($m \geq 2$) | 85 |
| 4.4 | Simulation Results | 92 |
| 4.4.1 | SISO Case | 92 |
| 4.4.2 | MIMO Case | 95 |
| 4.5 | Conclusion | 96 |
| 5 | Systems with Generalized Prandtl-Ishlinskii Hysteresis | 106 |
| 5.1 | Introduction | 106 |
| 5.2 | Problem Formulation and Preliminaries | 108 |
| 5.3 | Control Design and Stability Analysis | 112 |
| 5.4 | Simulation Results | 125 |
| 5.5 | Conclusion | 127 |
| 6 | Conclusions and Further Research | 131 |
| 6.1 | Conclusions | 131 |
| 6.2 | Recommendations for Further Research | 133 |
| | Bibliography | 135 |

Contents

| | |
|-----------------------|-----|
| Author's Publications | 152 |
|-----------------------|-----|

Summary

Control of nonlinear systems preceded by unknown hysteresis nonlinearities is a challenging task and has received increasing attention in recent years with growing industrial demands involving varied applications. The most common approach is to construct an inverse operator, which, however, has its limits due to the complexity of the hysteresis characteristics. Therefore, there is a need to develop a general control framework to achieve the stable output tracking performance for the concerned systems and mitigation of the effects of hysteresis without constructing the hysteresis inverse, especially in the presence of unmodelled dynamics and uncertain hysteresis models.

The main purpose of the research in this thesis is to develop adaptive neural control strategies for uncertain nonlinear systems preceded by several different hysteresis models, including the backlash-like hysteresis, the classic Prandtl-Ishlinskii (PI) hysteresis, and the generalized PI hysteresis. By investigating the characteristics of these hysteresis models, neural network (NN) based control approaches fused with these hysteresis models are presented for four classes of uncertain nonlinear systems.

For the control of a class of strict-feedback nonlinear systems preceded by unknown backlash-like hysteresis, adaptive dynamic surface control (DSC) is developed without constructing a hysteresis inverse by exploring the characteristics of backlash-like hysteresis, which can be described by two parallel lines connected via horizontal line segments. Through transforming the backlash-like hysteresis model into a linear-in-control term plus a bounded “disturbance-like” term, standard robust adaptive control used for dealing with bounded disturbances is applied.

Furthermore, the control of a class of output feedback nonlinear systems subject to function uncertainties and backlash-like hysteresis is studied. Adaptive observer backstepping using NN is adopted for state estimation and function on-line approximation using only output measurements. In particular, a Barrier Lyapunov Function (BLF) is introduced to address two open and challenging problems in the neuro-control area: (i) for any initial compact set, how to determine *a priori* the compact superset, on which NN approximation is valid; and (ii) how to ensure that the arguments of the unknown functions remain within the specified compact superset. By ensuring boundedness of the BLF, we actively constrain the argument of the unknown functions to remain within a compact superset such that the NN approximation conditions hold.

Thirdly, adaptive variable structure neural control is proposed for a class of uncertain multi-input multi-output (MIMO) nonlinear systems under the effects of classic PI hysteresis and time-varying state delays. Although there are some works that deal with hysteresis, or time delay, individually, the combined problem, despite its practical relevance, is largely open in the literature to the best of the author's knowledge. The unknown time-varying delay uncertainties are compensated for using appropriate Lyapunov-Krasovskii functionals in the design. Unlike backlash-like hysteresis, standard robust adaptive control used for dealing with bounded disturbances cannot be applied here, since no assumptions can be made on the boundedness of the hysteresis term of the classic PI model. In this thesis, new solution is provided to mitigate the effect of the uncertain PI classic hysteresis.

Finally, a class of unknown nonlinear systems in pure-feedback form with the generalized PI hysteresis input is considered. Compared with the backlash-like hysteresis model and the classic PI hysteresis model, the generalized PI hysteresis model can capture the hysteresis phenomenon more accurately and accommodate more general classes of hysteresis shapes by adjusting not only the density function but also the input function. The difficulty of the control of such class of systems lies in the nonaffine problem in both system unknown nonlinear functions and unknown input function in the generalized PI hysteresis model. To overcome this difficulty, in this thesis, the Mean Value Theorem is applied successively, first to the functions in the pure-feedback plant, and then to the hysteresis input function.

List of Figures

| | | |
|-----|---|----|
| 2.1 | Backlash-like hysteresis curves | 15 |
| 2.2 | Classic Prandtl-Ishlinskii hysteresis curves | 17 |
| 2.3 | Generalized Prandtl-Ishlinskii hysteresis curves | 19 |
| 2.4 | Schematic illustration of (a) symmetric and (b) asymmetric barrier functions | 27 |
| 3.1 | Compact sets for NN approximation | 45 |
| 3.2 | Tracking performance for the strict-feedback system with backlash-like hysteresis | 63 |
| 3.3 | Control inputs for the strict-feedback system with backlash-like hysteresis | 63 |
| 3.4 | Neural weights for the strict-feedback system with backlash-like hysteresis | 64 |
| 3.5 | Estimate of disturbance bound for the strict-feedback system with backlash-like hysteresis | 64 |
| 3.6 | Tracking performance for the output feedback system with backlash-like hysteresis | 65 |
| 3.7 | Tracking error z_1 (top) and control input w (bottom) for the output feedback system with backlash-like hysteresis | 65 |
| 3.8 | Function approximation results: $f_1(y)$ (top) and $f_2(y)$ (bottom) for the output feedback system with backlash-like hysteresis | 66 |

| | | |
|------|---|-----|
| 3.9 | Parameter adaptation results for the output feedback system with backlash-like hysteresis: norm of neural weights $\ \hat{\theta}_1\ $ (top); norm of neural weights $\ \hat{\theta}_2\ $ (middle) and bounding parameter $\hat{\psi}$ (bottom) | 66 |
| 3.10 | Output trajectories for the output feedback system with backlash-like hysteresis with different initial conditions | 67 |
| 4.1 | Compact sets | 84 |
| 4.2 | Output tracking performance of SISO plant S_1 with classic PI hysteresis | 97 |
| 4.3 | Control signals of SISO plant S_1 with classic PI hysteresis | 97 |
| 4.4 | Tracking error comparison result of SISO plant S_1 with classic PI hysteresis and w/o v_h | 98 |
| 4.5 | Learning behavior of neural networks of SISO plant S_1 with classic PI hysteresis | 98 |
| 4.6 | Norm of NN weights of SISO plant S_1 with classic PI hysteresis | 99 |
| 4.7 | The behavior of the estimate values of the density function, $\hat{p}(t, r)$ | 99 |
| 4.8 | Tracking error comparison result of SISO plant S_1 with classic PI hysteresis for different k_1 | 100 |
| 4.9 | Tracking error comparison result of SISO plant S_1 with classic PI hysteresis for different η | 100 |
| 4.10 | Tracking error comparison result of SISO plant S_1 with classic PI hysteresis for different ϵ | 101 |
| 4.11 | Tracking error comparison result of SISO plant S_1 with classic PI hysteresis for different delay Δt as pointed in Remark 4.8 (the sampling time $T = 0.005$) | 101 |
| 4.12 | Output tracking performance of MIMO plant S_2 with classic PI hysteresis | 102 |
| 4.13 | Control signals of MIMO plant S_2 with classic PI hysteresis | 102 |

List of Figures

| | | |
|------|--|-----|
| 4.14 | Norm of NN weights of MIMO plant S_2 with classic PI hysteresis . . . | 103 |
| 4.15 | Other states of MIMO plant S_2 with classic PI hysteresis | 103 |
| 4.16 | Learning behavior of neural networks of MIMO plant S_2 with classic PI hysteresis | 104 |
| 4.17 | Tracking error comparison result of MIMO plant S_2 with classic PI hysteresis for different k_{11} and k_{21} | 104 |
| 4.18 | Tracking error comparison result of MIMO plant S_2 with classic PI hysteresis for different η_1 and η_2 | 105 |
| 4.19 | Tracking error comparison result of MIMO plant S_2 with classic PI hysteresis for different ϵ | 105 |
| 5.1 | Tracking performance for the pure-feedback system with generalized PI hysteresis | 128 |
| 5.2 | State x_2 for the pure-feedback system with generalized PI hysteresis . | 128 |
| 5.3 | Control signals for the pure-feedback system with generalized PI hys- teresis | 129 |
| 5.4 | Norm of NN weights for the pure-feedback system with generalized PI hysteresis | 129 |
| 5.5 | Nussbaum function signals for the pure-feedback system with general- ized PI hysteresis | 130 |
| 5.6 | Estimation of disturbance bound, \hat{d} , for the pure-feedback system with generalized PI hysteresis | 130 |

Notation

| | |
|---------------------------|--|
| \mathbb{R} | Field of real numbers |
| \mathbb{R}^n | Linear space of n-dimensional vectors with elements in \mathbb{R} |
| $\mathbb{R}^{n \times m}$ | Set of $n \times m$ -dimensional matrices with elements in \mathbb{R} |
| $\ x\ $ | Euclidean vector norm of a vector x |
| $\hat{(\cdot)}$ | Estimate of (\cdot) |
| $\tilde{(\cdot)}$ | $\hat{(\cdot)} - (\cdot)$ |
| $\lambda_{\min}(A)$ | Minimum eigenvalue of the matrix A where all eigenvalues are real |
| $\lambda_{\max}(A)$ | Maximum eigenvalue of the matrix A where all eigenvalues are real |
| \bar{x}_i | $[x_1, \dots, x_i]^T$ |
| \bar{z}_i | $[z_1, z_2, \dots, z_i]^T$ |
| $\bar{\lambda}_i$ | $[\lambda_1, \lambda_2, \dots, \lambda_i]^T$ |
| $\bar{y}_r^{(i)}$ | $[y_r, y_r^{(1)}, \dots, y_r^{(i)}]^T$ |
| $q(x c)$ | $\begin{cases} 1 & \text{if } x \geq c \\ 0 & \text{if } x < c \end{cases}, \forall x \in \mathbb{R}, \text{ with any given positive constant } c > 0$ |
| $A \subset B$ | Set A is contained in Set B |
| $f : A \rightarrow B$ | f maps the domain A into the codomain B |

Chapter 1

Introduction

1.1 Background and Motivation

1.1.1 Hysteresis and Systems Control

In recent decades, dealing with hysteresis in control design has become an important research topic, driven by practical needs and theoretical challenges. Hysteresis nonlinearities exist in many industrial processes, especially in position control of smart material-based actuators, including piezoceramics and shape memory alloys [1]. The principal characteristic of hysteresis is that the output of the system depends not only on the instantaneous input, but also on the history of its operation. When a nonlinear plant is preceded by the hysteresis nonlinearity, the system usually exhibits undesirable inaccuracies or oscillations and even instability [2, 3] due to the nondifferentiable and nonmemoryless character of the hysteresis. Interest in control of dynamic systems with hysteresis is also motivated by the fact that they are nonlinear systems with nonsmooth nonlinearities for which traditional control methods are insufficient and thus requiring development of alternate effective approaches [4]. Development of a general frame for control of a system in the presence of unknown hysteresis nonlinearities is a quite challenging task.

To address such a challenge, the thorough characterization of these nonlinearities forms the foremost task. Appropriate hysteresis models may then be applied to

1.1 Background and Motivation

describe the nonsmooth nonlinearities for their potential usage in formulating the control algorithms. Hysteresis models can be roughly classified into physics based models and purely phenomenological models. Physics-based models are built on first principles of physics. Phenomenological models, on the other hand, are used to produce behaviors similar to those of the physical systems without necessarily providing physical insight into the problems [5]. The basic idea consists of the modeling of the real complex hysteresis nonlinearities by the weighted aggregate effect of all possible so-called elementary hysteresis operators. Elementary hysteresis operators are non-complex hysteretic nonlinearities with a simple mathematical structure. The reader may refer to [6] for a review of the hysteresis models.

With the developments in various hysteresis models, it is by nature to seek means to fuse these hysteresis models with the available control techniques to mitigate the effects of hysteresis, especially when the hysteresis is unknown, which is a typical case in many practical applications. However, the discussions on the fusion of the available hysteresis models with the available control techniques is sparse in the literature [7].

In the literature, the most common approach to mitigate the effects of hysteresis is to construct an inverse operator, which was pioneered by Tao and Kokotovic [3]. For hysteresis with major and minor loops, they used a simplified linear parameterized model to develop an adaptive hysteresis inverse model with parameters updated on line by adaptive laws. Model based compensation of hysteresis has been addressed in many research papers. The main issue is how to find the inverse of the hysteresis [8].

Compensation of hysteresis effects in smart material actuation systems using Preisach model based control architectures has been studied by many researchers [8]. Ge and Jouaneh [9] proposed a static approach to reduce the hysteresis effects in tracking control of a piezoceramic actuator for desired sinusoidal trajectory. The relationship between input and output of the actuator was first initialized by a linear approximation model of a specific hysteresis. The Preisach model of the hysteresis was then used to redefine the corresponding input signals for the desired output of the actuator displacements. Proportional-integral-derivative (PID) feedback controller was used to adjust the tracking errors. The developed methods worked for both specific trajectories and required resetting for different inputs. Galinaitis [10] analytically

1.1 Background and Motivation

investigated the inverse properties of the Preisach model and proved that a Preisach operator can only be locally invertible. He presented a closed form inverse formula when the weight function of the Preisach model was taking a specific form. Mittal and Meng [11] developed a method of hysteresis compensation in electromagnetic actuator through inversion of numerically expressed Preisach model in terms of first-order reversal curves and the input history. Croft, Shed and Devasia [12] used a different approach. Instead of modelling the forward hysteresis in piezoceramic actuators and then finding the inverse, they directly formulated the inverse hysteresis effect using Preisach model. Also in [13], an inverse Preisach model was proposed with magnetic flux density and its rate as inputs, and the magnetic fields as the output.

Methods based on the inverse of Krasnosel'skii-Pokrovskii (KP) model can be found in [10, 14]. Galinaitis mathematically investigated the properties and the discrete approximation method of the KP operators [10]. Webb defined a parameterized discrete inverse KP model, combined with adaptive laws to adjust the parameters on line to compensate hysteresis effects [14]. Recently, a feed-forward control design based on the inverse of Prandtl-Ishlinskii (PI) model was also applied to reduce hysteresis effects in piezoelectric actuators [15].

Essentially, the inversion problem depends on the phenomenological modelling methods and strongly influences practical applications of controller design. Due to the complexity of the hysteresis characteristics, especially the multi-value and nonsmoothness features, it is quite a challenge to find the inverse hysteresis models. Thus, those inverse based methods are sometimes complicated, computationally costly and highly sensitive to the model parameters with unknown measurement errors. These issues are directly linked to the difficulty of stability analysis of the systems except for certain special cases [3]. Therefore, other advanced control techniques to mitigate the effects of hysteresis have been called upon and have been studied for decades.

In [16], robust adaptive control was investigated for a class of nonlinear systems with unknown backlash-like hysteresis, for which, adaptive backstepping control was designed in [17]. In [18] and [19], adaptive variable structure control and adaptive backstepping methods were proposed, respectively, for a class of continuous-time

1.1 Background and Motivation

nonlinear dynamic systems preceded by hysteresis nonlinearity with the Prandtl-Ishlinskii (PI) hysteresis model representation.

However, in most of the above works, the dynamics of systems were expressed in the linear-in-parameters form, for which the regressor is exactly known and the uncertainty is parametric and time-invariant. It is therefore of interest to develop methods to deal with the case with functional uncertainties, so as to enlarge the class of applicable systems. With the celebrated success and rapid development of approximation based control in solving functional uncertainties, there is a need to carry out investigations within this framework and develop new tools to deal with uncertain nonlinear systems preceded by hysteresis, without the need of constructing an inverse operator for the hysteresis.

1.1.2 Neural Networks

Artificial neural networks (ANNs) are inspired by biological neural networks, which usually consist of a number of simple processing elements, call neurons, that are interconnected to each other. In most cases, one or more layers of neurons are connected to each other in a feedback or recurrent way. Since McCulloch and Pitts [20] introduced the idea of studying the computational abilities of networks composed of simple models of neurons in the 1940s, neural network techniques have undergone great development and have been successfully applied in many fields such as learning, pattern recognition, signal processing, modelling and system control. The approximation abilities of neural networks have been proven in many research works [21, 22, 23, 24, 25, 26, 27, 28]. The major advantages of highly parallel structure, learning ability, nonlinear function approximation, fault tolerance and efficient analog VLSI implementation for real-time applications, greatly motivate the usage of neural networks in nonlinear system control and identification.

The early works of neural network applications for controller design were reported in [29, 30]. The popularization of backpropagation (BP) algorithm [31] in the late 1980s greatly boosted the development of neural control and many neural control approaches have been developed [32, 33, 34, 35, 36]. Most early works on neural control

1.1 Background and Motivation

described creative ideas and demonstrated neural controllers through simulation or by particular experimental examples, but were short of analytical analysis on stability, robustness and convergence of the closed-loop neural control systems. The theoretical difficulty arose mainly from the nonlinearly parametrized networks used in the approximation. The analytical results obtained in [37, 38] showed that using multi-layer neural networks as function approximators guaranteed the stability and convergence results of the systems when the initial network weights chosen were sufficiently close to the ideal weights. This implies that for achieving a stable neural control system using the gradient learning algorithms such as BP, sufficient off-line training must be performed before neural network controllers are put into the systems.

Due to their universal approximation abilities, parallel distributed processing abilities, learning, adaptation abilities, natural fault tolerance and feasibility for hardware implementation, neural networks are made one of the effective tools in approximation based control problems. Recently neural networks (NNs) have been made particularly attractive and promising for applications to modelling and control of nonlinear systems. For NN controller design of general nonlinear systems, several researchers have suggested to use neural networks as emulators of inverse systems. The main idea is that for a system with finite relative degree, the mapping between system input and system output is one-to-one, thus allowing the construction of a “left-inverse” of the nonlinear system using NN. Using the implicit function theory, the NN control methods proposed in [38, 39] have been used to emulate the “inverse controller” to achieve the desired control objectives. Based on this idea, an adaptive controller has been developed using high order neural networks with stable internal dynamics in [40] and applied in [41]. As an alternative, neural networks have been used to approximate the implicit desired feedback controller (IDFC) in [42]. A multi-layer neural network control method for single-input single-output (SISO) non-affine systems without zero dynamics was also proposed in that paper. In this thesis, we mainly investigate the implementation of neural networks as function approximators for the desired feedback control, which can realize exact tracking.

Except that neural networks can be used as function approximators to emulate the “inverse” control in nonlinear system research, there are many other areas, in which neural networks play an important role. For example, neural networks combined

1.1 Background and Motivation

backstepping design are reported in [43], using neural networks to construct observers can be found in [44, 45], neural network control in robot manipulators are reported in [46, 47, 48, 49], neural identification of chemical processes by using dynamics neural networks can be found in [50, 51], neural control for distillation column are reported in [52, 53], etc. It should be noted, similar to neural networks, fuzzy system is another kind of system, which has “intelligence” and has attracted many research interests. It can also be used as function approximators. Research works in fuzzy system can be found in [54, 55, 56].

1.1.3 Adaptive Neural Control of Nonlinear Systems

Research in adaptive control for nonlinear systems have a long history of intense activities that involve rigorous problems for formulation, stability proof, robustness design, performance analysis and applications. The advances in stability theory and the progress of control theory in the 1960s improved the understanding of adaptive control and contributed to a strong interest in this field. By the early 1980’s, several adaptive approaches have been proven to provide stable operation and asymptotic tracking. The adaptive control problem since then, was rigorously formulated and several leading researchers have laid the theoretical foundations for many basic adaptive schemes. In the mid 1980s, research of adaptive control mainly focused on the robustness problem in the presence of unmodeled dynamics and/or bounded disturbances. A number of redesigns and modifications were proposed and analyzed to improve the robustness of the adaptive controllers, e.g., by applying normalization techniques in controller design and modification of adaptation laws using projection method [57], dead zone modifications [58, 59], ϵ -modification [60] and σ -modification [61].

In last decades, in continuous-time domain, feedback linearization technique [62, 63, 64], backstepping design [65], neural network control and identification [46, 66] and tuning function design have attracted much attention. Many remarkable results in this area have been obtained [55, 67, 68, 69, 70, 71, 72, 73, 74, 75, 76].

1.1 Background and Motivation

For SISO continuous-time nonlinear systems, the feasibility of applying neural networks for modelling unknown functions in dynamic systems has been demonstrated in several studies. It was shown that for stable and efficient on-line control using the BP learning algorithm, the identification of systems must be sufficiently accurate before control action is initiated [32, 50, 38]. Recently, several good NN control approaches have been proposed based on Lyapunov's stability theory [66, 77, 78, 79, 80]. One main advantage of these schemes is that the adaptive laws are derived based on the Lyapunov synthesis method and therefore guaranteed the stability of continuous-time systems without the requirement of off-line training. For strict-feedback nonlinear SISO system, adaptive control scheme is still an active topic in nonlinear system control area. Using the backstepping design procedures, a systematic approach of adaptive controller design was presented for a class of nonlinear systems transformable to a parametric strict-feedback canonical form, which guarantees the global and asymptotic stability of the closed-loop system [65, 66, 81]. Using the implicit function theory, the NN control methods proposed in [38, 39] have been used to emulate the "inverse controller" to achieve the desired control objectives. Based on this idea, an adaptive controller has been developed using high order neural networks with stable internal dynamics in [40] and applied in [41]. As an alternative, neural networks have been used to approximate the implicit desired feedback controller in [42]. Multi-layer neural network control method was also proposed for SISO non-affine systems without zero dynamics in that paper. Furthermore, previous works on nonlinear non-affine systems controller design [82] proposed a new control law for non-affine nonlinear system for a class of deterministic time-invariant discrete system which is free of the usual restrictions, such as minimum phase, known plant states etc. A general form of control structure of adaptive feedback linearization is $u = \hat{N}(x)/\hat{D}(x)$, where $\hat{D}(x)$ must be bounded away from zero to avoid the possible controller singularity problem [79]. The approach is only applicable to the class of systems whose dynamics are linear-in-the-parameters and satisfy the so-called matching conditions. The matching condition was relaxed to the extended matching condition in [83] and [84], and the extended matching barrier was broken in [81] by using adaptive backstepping design [65, 66, 85]. For single input multi outputs systems, some results can be found in [86, 87].

1.1 Background and Motivation

For multi-input multi-output (MIMO) continuous-time nonlinear systems, there are few results available, due primarily to the difficulty in handling the coupling matrix between different inputs. In [88], a stable neural network adaptive controller was developed for a class of nonlinear multi-variable systems, the control inputs are in triangular form and integral Lyapunov function was used to analyze the stability. In [89], a numerically robust approximate algorithms was given for input-output decoupling nonlinear MIMO systems. Several algorithms have been proposed in the literature for solving the problem of exact decoupling for nonlinear MIMO systems, see for examples [90, 91, 92, 93]. All these algorithms need the determination of the inverse, the so-called decoupling matrix. In [94], the problem of semi-global robust stabilization was investigated for a class of MIMO uncertain nonlinear system, which cannot be transformed into lower dimensional zero dynamics representation, via change of coordinates or state feedback. Both the partial state and dynamic output controllers were explicitly constructed via the design tools such as semi-global backstepping and high-gain observer. In [95], an adaptive fuzzy systems approach to state feedback input-output linearizing controller was outlined. The analysis was based on a general nonlinear MIMO system, with minimum phase zero dynamics and uncertainties satisfying the matching condition.

Adaptive neural network control of nonlinear strict-feedback systems is well documented in the literature. However, results for general nonlinear pure-feedback systems are relatively fewer than those for strict-feedback systems. In addition, the systems considered are often in special forms [42, 96, 97, 98, 99]. The pure-feedback system represents a more general class of nonlinear systems than its strict-feedback counterpart, with the important feature being that the virtual or practical controls are non-affine. In practice, many physical systems such as chemical reactions, pH neutralization and distillation columns are inherently non-affine and nonlinear. In recent years, control of non-affine nonlinear systems have captured the attention of researchers and poses a challenge to control theorists. The main impediment in solving this control problem directly is that even if the inverse is known to exist, it may be impossible to construct it analytically. Consequently, no control system design is possible along the lines of classic model based control. Fundamental research is called upon for this class of nonlinear systems because of the relatively fewer tools available

1.2 Objectives and Structure of the Thesis

in comparison with that for affine nonlinear system. In [96], inverse dynamic control was applied to deal with the non-affine problem under contraction mapping condition. For the same class of systems, a different approach using the Implicit Function Theorem and the Mean Value Theorem, was employed in [42], and then extended to the case with zero dynamics in [99]. In [97], a special class of pure-feedback systems was considered, wherein the n order system is assumed to be affine in the control and in the x_n state variable for the \dot{x}_{n-1} equation to avoid a circular argument in the control design and stability analysis. In [98], the system considered has the first $n - 1$ equations non-affine, and the main result heavily relied on the assumption that $1 - \frac{\partial \alpha_{n-1}}{\partial x_n} \neq 0$, which is only effective when the input gain functions are known.

For the control of completely non-affine pure-feedback systems, however, few results are available in the literature. In [100], small gain theorem was combined with input-to-state stability analysis for control design. In [101], Nussbaum-Gain function was utilized along with Mean Value Theorem to develop an adaptive NN control for non-affine pure-feedback systems. For such systems, the main difficulty is in dealing with non-affine functions, particularly in the final step of backstepping, where circular argument of control may appear.

In spite of the development of neural network control techniques and their successful applications, there still remain several fundamental problems yet to be further investigated. For example, it is well known that NN approximation-based control relies on universal approximation property in a compact set in order to approximate unknown nonlinearities in the plant dynamics. However, as pointed out in [102], how to determine *a priori* the compact set and how to ensure the arguments of the unknown functions remain within the compact set, are still two open and challenging problems in the neuro-control area.

1.2 Objectives and Structure of the Thesis

In general, the objective of this thesis is to develop constructive and systematic adaptive neural control methods for uncertain nonlinear systems preceded by hysteresis.

1.2 Objectives and Structure of the Thesis

By investigating different characteristics of several different hysteresis models, neural network (NN) based control approaches fused with these hysteresis models are proposed to achieve the stable output tracking performance for the concerned systems and mitigate the effects of hysteresis without constructing the inverse hysteresis nonlinearity.

The remainder of the thesis is organized as follows. In Chapter 2, we provide some mathematical preliminaries, which will be used throughout this thesis. Three types of hysteresis models and their properties are introduced, including backlash-like hysteresis model, classic Prandtl-Ishlinskii (PI) hysteresis model as well as generalized PI hysteresis model. Then, a brief introduction for function approximation using neural networks (NNs) is given, followed by some useful definitions, theorems, and technical lemmas for completeness.

Chapter 3 considers the control of two classes of nonlinear systems with unknown backlash-like hysteresis. Firstly, for a class of strict-feedback nonlinear systems preceded by unknown backlash-like hysteresis, adaptive dynamic surface control (DSC) is developed without constructing a hysteresis inverse by exploring the characteristics of backlash-like hysteresis, which can be described by two parallel lines connected via horizontal line segments. Through transforming the backlash-like hysteresis model into a linear-in-control term plus a bounded “disturbance-like” term, standard robust adaptive control used for dealing with bounded disturbances is applied. The explosion of complexity in traditional backstepping design is avoided by utilizing DSC. Function uncertainties are compensated for using neural networks due to their universal approximation capabilities. The bounds of the “disturbance-like” terms and neural network approximation errors, are handled on-line by an adaptive bounding design.

Furthermore, the control of a class of output feedback nonlinear systems subject to function uncertainties and backlash-like hysteresis is studied. Adaptive observer backstepping using NN is adopted for state estimation and function on-line approximation using only output measurements. In particular, a Barrier Lyapunov Function (BLF) is introduced to address two open and challenging problems in the neuro-control area: (i) for any initial compact set, how to determine *a priori* the compact superset, on which NN approximation is valid; and (ii) how to ensure that the arguments of the

unknown functions remain within the specified compact superset. By ensuring boundedness of the BLF, we actively constrain the argument of the unknown functions to remain within a compact superset such that the NN approximation conditions hold. The stable output tracking with guaranteed performance bounds can be achieved in the semi-global sense.

In Chapter 4, adaptive variable structure neural control is proposed for a class of uncertain multi-input multi-output (MIMO) nonlinear systems under the effects of classic PI hysteresis and time-varying state delays. Although there are some works that deal with hysteresis, or time delay, individually, the combined problem, despite its practical relevance, is largely open in the literature to the best of the author's knowledge. The unknown time-varying delay uncertainties are compensated for using appropriate Lyapunov-Krasovskii functionals in the design. Unlike backlash-like hysteresis, standard robust adaptive control used for dealing with bounded disturbances cannot be applied here, since no assumptions can be made on the boundedness of the hysteresis term of the classic PI model. In this thesis, new solution is provided to mitigate the effect of the uncertain PI classic hysteresis.

In Chapter 5, a class of unknown nonlinear systems in pure-feedback form with the generalized PI hysteresis input is considered. Compared with the backlash-like hysteresis model and the classic PI hysteresis model, the generalized PI hysteresis model can capture the hysteresis phenomenon more accurately and accommodate more general classes of hysteresis shapes by adjusting not only the density function but also the input function. The difficulty of the control of such class of systems lies in the nonaffine problem in both system unknown nonlinear functions and unknown input function in the generalized PI hysteresis model. To overcome this difficulty, in this thesis, the mean-value theorem is applied successively, first to the functions in the pure-feedback plant, and then to the hysteresis input function.

Finally, Chapter 6 concludes the contributions of the thesis and makes recommendation on future research works.

Chapter 2

Mathematical Preliminaries

2.1 Introduction

In this chapter, we provide some mathematical preliminaries, which will be used throughout this thesis. The chapter is organized as follows. Firstly, three types of hysteresis models considered in this thesis, namely backlash-like hysteresis model, classic Prandtl-Ishlinskii (PI) hysteresis model, generalized PI hysteresis model, as well as their properties are introduced in Section 2.2. Then, a brief introduction for function approximation using neural networks (NNs) is given in Section 2.3, followed by Section 2.4 about some useful definitions, theorems, and technical lemmas for completeness.

2.2 Hysteresis Models and Properties

Generally, modeling hysteresis nonlinearities is still a research topic, since hysteresis is a very complex phenomenon. The readers may refer to [6] for a review. Hysteresis models can be roughly classified into physics based models and purely phenomenological models. Physics-based models are built on first principles of physics. Phenomenological models, on the other hand, are used to produce behaviors similar to those of the physical systems without necessarily providing physical insight into the problems

2.2 Hysteresis Models and Properties

[5]. The basic idea consists of the modeling of the real complex hysteresis nonlinearities by the weighted aggregate effect of all possible so-called elementary hysteresis operators. Elementary hysteresis operators are noncomplex hysteretic nonlinearities with a simple mathematical structure. A hysteresis nonlinearity can be denoted as an operator

$$w(t) = H(v(t)) \quad (2.1)$$

with $v(t)$ as input, $w(t)$ as output and $H(\cdot)$ as operator. For different kinds of hysteresis models, different operators should be adopted, as will be discussed in detail in the forthcoming subsections.

2.2.1 Backlash-Like Hysteresis Model

Traditionally, a backlash hysteresis nonlinearity can be described by

$$\begin{aligned} w(t) &= BH(v(t)) \\ &= \begin{cases} c(v(t) - B), & \text{if } \dot{v}(t) > 0 \text{ and } w(t) = c(v(t) - B) \\ c(v(t) + B), & \text{if } \dot{v}(t) < 0 \text{ and } w(t) = c(v(t) + B) \\ w(t_-), & \text{otherwise} \end{cases} \end{aligned} \quad (2.2)$$

where $c > 0$ is the slope of the lines and $B > 0$ is the backlash distance. This model is itself discontinuous and may not be amenable to controller design for the nonlinear systems.

Instead of using the above model, we define a continuous-time dynamic model to describe a class of backlash-like hysteresis, as given by [16]:

$$\frac{dw}{dt} = \alpha \left| \frac{dv}{dt} \right| (cv - w) + B_1 \frac{dv}{dt} \quad (2.3)$$

where α , c , and B_1 are constants, $c > 0$ is the slope of lines satisfying $c > B_1$.

Equation (2.3) can be solved explicitly for v piecewise monotone

$$w(t) = cv(t) + d(v) \quad (2.4)$$

with

$$d(v) = [w_0 - cv_0]e^{-\alpha(v-v_0)\text{sgn}(\dot{v})} + e^{-\alpha v \text{sgn}(\dot{v})} \int_{v_0}^v [B_1 - c]e^{\alpha \zeta \text{sgn}(\dot{v})} d\zeta \quad (2.5)$$

2.2 Hysteresis Models and Properties

for \dot{v} constant and $w(v_0) = w_0$. Analyzing (2.4), we see that it is composed of a line with the slope c , together with a term $d(v)$. For $d(v)$, it can be easily shown that if $w(v; v_0; w_0)$ is the solution of (2.4) with initial values $(v_0; w_0)$, then, if $\dot{v} > 0$ ($\dot{v} < 0$) and $v \rightarrow +\infty$ ($-\infty$), one has

$$\lim_{v \rightarrow +\infty} d(v) = \lim_{v \rightarrow +\infty} [w(v; v_0; w_0) - cv] = -\frac{c - B_1}{\alpha} \quad (2.6)$$

$$\lim_{v \rightarrow -\infty} d(v) = \lim_{v \rightarrow -\infty} [w(v; v_0; w_0) - cv] = \frac{c - B_1}{\alpha} \quad (2.7)$$

It should be noted that the above convergence is exponential at the rate of α . Solution (2.4) and properties (2.6) and (2.7) show that $w(t)$ eventually satisfies the first and second conditions of (2.2). Furthermore, setting $\dot{v} = 0$ results in $\dot{w} = 0$ which satisfies the last condition of (2.2). This implies that the dynamic equation (2.3) can be used to model a class of backlash-like hysteresis and is an approximation of backlash hysteresis (2.2). In particular, $w(t)$ switches exponentially from the line $cv(t) - ((c - B_1)/\alpha)$ to $cv(t) + ((c - B_1)/\alpha)$ to generate backlash-like hysteresis curves. Figure 2.1 shows that the model (2.3) indeed generates a class of backlash-like hysteresis curve, where $\alpha = 1.0$, $c = 3.1635$, $B_1 = 0.345$ and the input signal $v = 6.5 \sin(2.3t)$.

It is important to note that (2.6) and (2.7) imply that

Property 2.1 *There exists a uniform bound η such that*

$$|d(v)| \leq \eta \quad (2.8)$$

If the values of backlash slope c and distance bound η are not known implicitly, then adaptation will be used to estimate them. This will be clarified in Chapter 3 about control design of systems with backlash-like hysteresis.

2.2.2 Classic Prandtl-Ishlinskii Hysteresis Model

The classic Prandtl-Ishlinskii (PI) hysteresis model involves some basic well-known hysteresis operators. A detailed discussion on this subject can be found in the monographs [103, 104, 105].

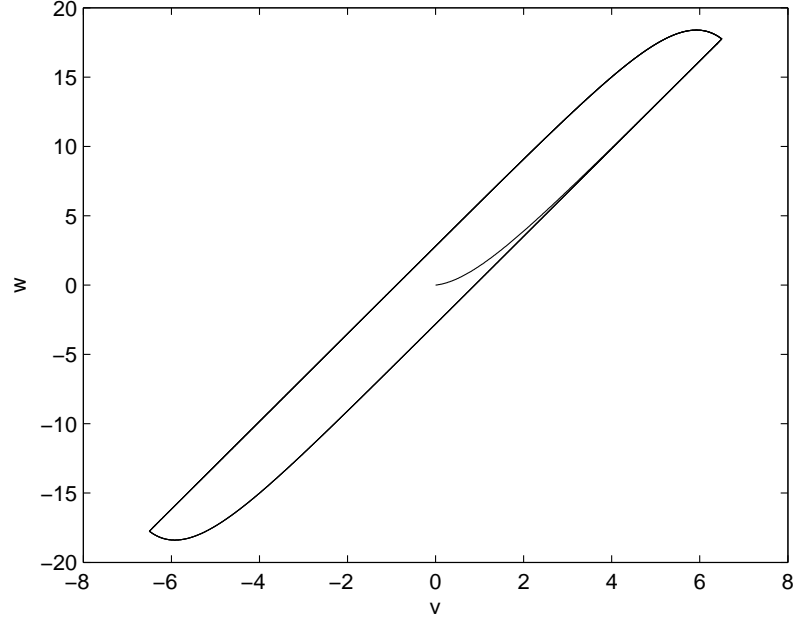


Figure 2.1: Backlash-like hysteresis curves

Stop and Play Operators

One of the basic elements of the theory of hysteresis operators is borrowed from continuum mechanics for elastic-perfectly plastic constitutive laws. As long as the stress w is smaller than the yield stress r , the strain v is related to w through the linear Hooke's law. This input-output relation can be expressed by an elastic-plastic, or stop, operator, $w(t) = E_r[v](t)$ with threshold r . Analytically, suppose $C_m[0, t_E]$ is the space of piecewise monotone continuous functions, for any input $v(t) \in C_m[0, t_E]$, the stop operator E_r , for any $r \geq 0$, can be defined by the inductive definition:

$$\begin{aligned} E_r[v](0) &= e_r(v(0)) \\ E_r[v](t) &= e_r(v(t) - v(t_i) + E_r[v](t_i)) \\ &\quad \text{for } t_i < t \leq t_{i+1} \text{ and } 0 \leq i \leq N-1 \end{aligned} \tag{2.9}$$

with $e_r(v) = \min(r, \max(-r, v))$, where $0 = t_0 < t_1 < \dots < t_N = t_E$ is a partition of $[0, t_E]$ such that the function v is monotone on each of the subintervals $(t_i, t_{i+1}]$. The argument of the operator is written in square brackets to indicate the functional

2.2 Hysteresis Models and Properties

dependence, since it maps a function to a function. The stop operator, however, is mainly characterized by its threshold parameter r which determines the height of the hysteresis region in the (v, w) plane.

Another basic hysteresis operator is the play operator $F_r[v](t)$ with threshold r . For a given input $v(t) \in C_m[0, t_E]$, the play operator F_r with threshold r is then inductively defined by

$$\begin{aligned} F_r[v](0) &= f_r(v(0), 0) \\ F_r[v](t) &= f_r(v(t), F_r[v](t_i)) \\ &\text{for } t_i < t \leq t_{i+1} \text{ and } 0 \leq i \leq N-1 \end{aligned} \quad (2.10)$$

with $f_r(v, w) = \max(v - r, \min(v + r, w))$, where $0 = t_0 < t_1 < \dots < t_N = t_E$ is the same kind of partition as given previously. From definitions (2.9) and (2.10), it can be proved [104] that for any $v(t) \in C_m[0, t_E]$, F_r is the complement of E_r , i.e., they are closely related through the equation

$$E_r[v](t) + F_r[v](t) = v(t) \quad \forall r \geq 0 \quad (2.11)$$

Due to the nature of play and stop operators, the above discussions are based on $v \in C_m[0, t_E]$ of continuous and piecewise monotone functions; however, they can be extended to the space $C[0, t_E]$ of continuous functions.

Classic PI hysteresis model

The classic PI hysteresis model was introduced to formulate the elastic-plastic behavior through a weighted superposition of basic elastic-plastic elements $E_r[v]$, or stop as follows:

$$w(t) = \int_0^R p(r) E_r[v](t) dr \quad (2.12)$$

where $p(r)$ is a given density function, satisfying $p(r) \geq 0$ with $\int_0^\infty rp(r)dr < \infty$, and is expected to be identified from experimental data. With the defined density function, this operator maps $C[t_0, \infty)$ into $C[t_0, \infty)$, i.e., Lipschitz continuous inputs will yield Lipschitz continuous outputs [103]. Since the density function $p(r)$ vanishes

2.2 Hysteresis Models and Properties

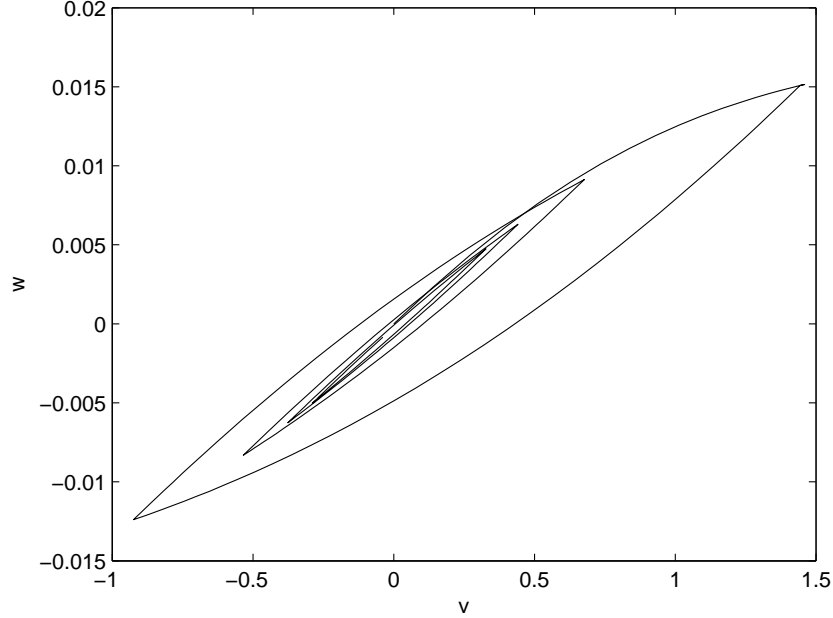


Figure 2.2: Classic Prandtl-Ishlinskii hysteresis curves

for large values of r , the choice of $R = \infty$ as the upper limit of integration in the literature is just a matter of convenience [104].

It can be seen that the stop operator E_r serves as the building element in the classic PI hysteresis model (2.12). We should mention that the stop and the play are rate-independent thus the classic PI hysteresis model is rate-independent. As an illustration, Figure 2.2 shows $w(t)$ generated by (2.12), with $p(r) = 0.01e^{-0.505(r-0.5)^2}$, $r \in [0, 100]$, and the input $v(t) = 2\sin(4t)/(1+t)$, $t \in [0, 2\pi]$. This numerical result shows the classic PI hysteresis model (2.12) indeed generates hysteresis curves and is well-suited to model the rate-independent hysteresis behavior.

Since F_r is the complement of E_r , the classic PI hysteresis model can also be represented through the play operator. Using (2.11) and substituting E_r in (2.12) by F_r , the classic PI hysteresis model defined by the play operator is

$$w(t) = p_0 v(t) - \int_0^R p(r) F_r[v](t) dr \quad (2.13)$$

where $p_0 = \int_0^R p(r) dr$ is constant and depends on the density function. It should be noted that (2.13) decomposes the hysteresis behavior into two terms. The first

2.2 Hysteresis Models and Properties

term is a linear reversible component and the second is a nonlinear hysteretic component. This decomposition is crucial since it facilitates the utilization of the currently available robust adaptive control techniques for the controller design.

2.2.3 Generalized Prandtl-Ishlinskii Hysteresis Model

Based on the definition of the play operator in (2.10), the generalized Prandtl-Ishlinskii (PI) model can be expressed as [106]:

$$w(t) = h(v)(t) - \int_0^D p(r) F_r[v](t) dr \quad (2.14)$$

where $p(r)$ is a given density function, satisfying $p(r) \geq 0$ with $\int_0^\infty rp(r)dr < \infty$ and is expected to be identified from experimental data; D is a constant so that density function $p(r)$ vanishes for large values of D ; $F_r[v](t)$ is the play operator defined in (2.10); and $h(v)$ is the hysteresis input function that satisfies the following assumptions [106]:

Assumption 2.1 *The function $h : \mathbb{R} \rightarrow \mathbb{R}$ is odd, non-decreasing, locally Lipschitz continuous, and satisfies $\lim_{v \rightarrow \infty} h(v) \rightarrow \infty$ and $\frac{dh(v)}{dv} > 0$ for almost every $v \in \mathbb{R}$.*

Assumption 2.2 *The growth of the hysteresis function $h(v)$ is smooth, and there exist positive constants h_0 and h_1 such that $0 < h_0 \leq \frac{dh(v)}{dv} \leq h_1$.*

Remark 2.1 *It should be noted that the classic PI hysteresis model in (2.13) is only a special case of the generalized PI hysteresis model described in (2.14). If we select the input function $h(v)(t) = p_0 v$ with $p_0 = \int_0^D p(r)dr$ in (2.14), then the generalized PI hysteresis model becomes a classic PI hysteresis model. For the classic PI hysteresis model, the different hysteresis shapes are formulated by adjusting the density function only. However, for the generalized PI hysteresis model, both the density function and the input function can be adjusted to describe a more general class of hysteresis characteristics.*

As an illustration, using the same density function and input with the hysteresis curves of the classic PI model in Figure 2.2, the hysteresis curves of the generalized

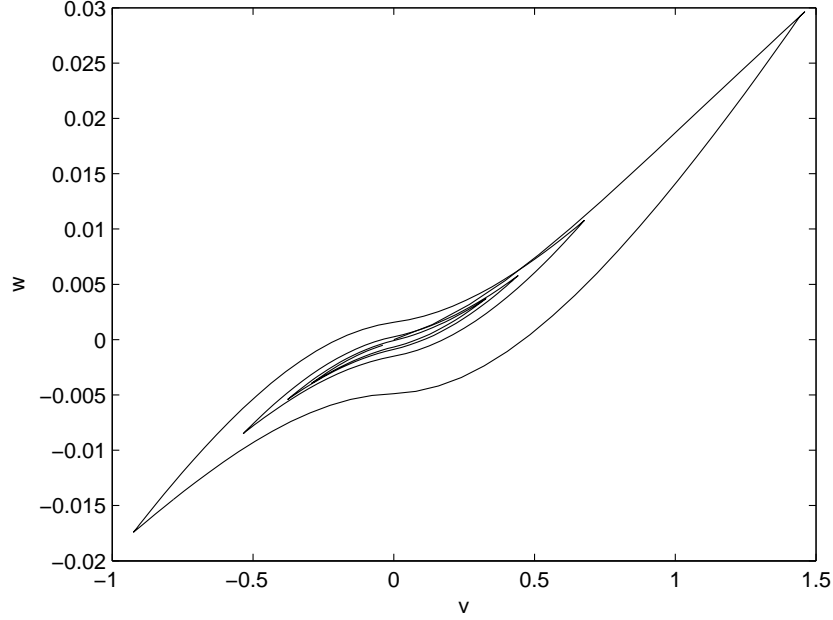


Figure 2.3: Generalized Prandtl-Ishlinskii hysteresis curves

PI model described by $w(t) = h(v)(t) - \int_0^D p(r)F_r[v](t)dr$ is shown in Figure 2.3 with $h(v)(t) = 0.02(|u| \arctan(u) + 0.4u)$. It can be observed that, the generalized PI model can describe more general hysteresis shapes.

2.3 Function Approximation

In adaptive neural control design, neural networks (NNs) are mostly used as function approximators. The unknown nonlinearities in the systems or in the controllers are approximated by linearly or nonlinearly parameterized neural networks, such as radial basis function neural networks (RBF NNs) and multilayer neural networks (MNNs). The purpose of this section is to give a brief introduction to NN approximation. The reasons for choosing RBF NNs in the thesis are also explained.

2.3.1 NN Approximation

The development of mathematical analysis during the past two hundred years has lead to the discovery and study of important classes of approximating functions, such as polynomials, trigonometric series, orthogonal functions, splines, etc. Since McCulloch and Pitts [20] introduced the idea of studying the computational abilities of networks composed of simple models of neurons in the 1940s, neural network techniques have undergone great developments and have been successfully applied in many fields such as learning, pattern recognition, signal processing, modeling and system control. From 1980s, neural networks were constructed and empirically demonstrated (using simulation studies) to approximate quite well nearly all functions encountered in practical applications. The elegant results by Funahashi [23], Cybenko [21] and Hornik *et. al.* [24] proved that neural networks are capable of universal approximation in a very precise and satisfactory sense. These results lead the study of neural networks from its empirical origins to a mathematical discipline.

The NN approximation problem can be stated following the definition of function approximation:

Definition 2.1 (Function Approximation) *If $f(x) : \mathbb{R}^n \rightarrow \mathbb{R}$ is a continuous function defined on a compact set Ω , and $f_{nn}(W, x) : \mathbb{R}^s \times \mathbb{R}^n \rightarrow \mathbb{R}$ is an approximating function that depends continuously on W and x , then, the approximation problem is to determine the optimal parameters W^* , for some metric (or distance function) d , such that*

$$d(f_{nn}(W^*, x), f(x)) \leq \epsilon \quad (2.15)$$

for an acceptable small ϵ [107].

To approximate the unknown function $f(x)$ by using neural networks, the approximating function $f_{nn}(W, x)$ is firstly chosen. The neural network weights W are then adjusted by a training set. Thus, there are two distinct problems in NN approximation, namely, the representation problem which deals with the selection of the approximating function $f_{nn}(W, x)$, and the learning problem which is to find the

2.3 Function Approximation

training method to ensure that the optimal neural network weights W^* are obtained. In the literature of NN approximation, two types of NNs are usually employed, i.e., linearly parameterized approximators (e.g, RBF NNs), and nonlinearly parameterized approximators (e.g., MNNs).

2.3.2 MNNs

MNN is one of the most widely used neural networks in system modeling and control. It is a static feedforward network that consists of a number of layers, and each layer consists of a number of McCulloch-Pitts neurons [20]. Once these have been selected, only the adjustable weights have to be determined to specify the networks completely. Since each node of any layer is connected to all the nodes of the following layer, it follows that a change in a single parameter at any one layer will generally affect all the outputs in the following layers. The structure of MNNs can be expressed in the following form

$$f_{nn}(Z) = \sum_{j=1}^l \left[w_j s \left(\sum_{k=1}^n v_{jk} z_k + \theta_{vj} \right) \right] + \theta_w \quad (2.16)$$

where $Z = [z_1, z_2, \dots, z_n]^T$ is the input vector, v_{jk} are the first-to-second layer interconnection weights, w_j are the second-to-third layer interconnection weights, θ_w and θ_{vj} are the threshold offsets. The activation function $s(\cdot)$ can be chosen as the continuous and differentiable nonlinear sigmoidal

$$s(z) = \frac{1}{1 + e^{-\gamma z}}, \quad \forall z \in \mathbb{R} \quad (2.17)$$

with $\gamma > 0$ being a constant, or a hyperbolic tangent function

$$s(z) = \frac{e^z - e^{-z}}{e^z + e^{-z}} \quad (2.18)$$

MNN with one or more hidden layers can approximate any continuous nonlinear function arbitrarily well over a compact set, provided sufficient hidden neurons are available [21, 23, 24]. MNN has many good properties for function approximation, e.g., global approximator due to the nature of the global active neuron functions within the networks, the ability of reducing the effect of the “curse of dimensionality”

2.3 Function Approximation

problem [108]. However, MNN is often referred to as a nonlinearly parameterized network, which means that the network output is related to the neural weights in a nonlinear fashion. This property often makes the analysis of systems containing MNN difficult and the results obtained conservative. Further, the adjustment of a single weight of the networks affects the output globally. All the weights have to be adjusted simultaneously for each training data set. Thus, slow convergence rate were obtained in the phase of MNN learning, which is inappropriate for online adaptation of neural networks in closed-loop control systems [47]. On the other hand, RBF NN, with its properties of linear parameterization and localization, renders it feasible to be applied to uncertain nonlinear system modeling and control. Since the network output of RBF NN is related to the adjustable weights in a linear manner, on-line adaptation laws for neural weights and the convergence results can be derived using the available adaptive control techniques [61].

2.3.3 RBFNNs

The RBF NNs can be considered as a two-layer network in which the hidden layer performs a fixed nonlinear transformation with no adjustable parameters, i.e., the input space is mapped into a new space. The output layer then combines the outputs in the latter space linearly. Therefore, they belong to a class of linearly parameterized networks. For a continuous function $f(Z) : \mathbb{R}^q \rightarrow \mathbb{R}$, it has been shown (see, e.g., [109]) that an RBF NNs, $W^T S(Z)$, can be used to approximate $f(Z)$ over a compact set $\Omega_Z \subset \mathbb{R}^q$ with arbitrary accuracy, i.e.,

$$f(Z) = W^{*T} S(Z) + \epsilon, \quad \forall Z \in \Omega_Z \quad (2.19)$$

where the input vector $Z \in \Omega_Z \subset \mathbb{R}^q$, the weight vector $W = [w_1, w_2, \dots, w_l]^T \in \mathbb{R}^l$, W^* represents the ideal constant weights, and ϵ is the approximation error that can be arbitrarily small, $S(Z) = [s_1(Z), \dots, s_l(Z)]^T \in \mathbb{R}^l$. The ideal weight vector W^* is an “artificial” quantity required for analysis. W^* is defined as the value of W that minimizes $|\epsilon|$ for all $Z \in \Omega_Z \subset \mathbb{R}^q$, i.e.,

$$W^* \triangleq \arg \min_{W \in \mathbb{R}^l} \left\{ \sup_{Z \in \Omega_Z} |f(Z) - W^T S(Z)| \right\} \quad (2.20)$$

2.3 Function Approximation

It has been justified in [110] that for a continuous positive function $s(\cdot)$ on $[0, \infty)$, if its first derivative is completely monotonic, then this function can be used as a radial basis function. Commonly used RBFs are the Gaussian functions, which have the form

$$s_i(Z) = \exp \left[\frac{-(Z - \mu_i)^T (Z - \mu_i)}{\eta_i^2} \right], \quad i = 1, 2, \dots, l \quad (2.21)$$

where $\mu_i = [\mu_{i1}, \mu_{i2}, \dots, \mu_{iq}]^T$ is the center of the receptive field and η_i is the width of the Gaussian function. The radial basis functions can also be chosen as Hardy's multiquadric form [110]

$$s_i(Z) = \sqrt{\sigma_i^2 + (Z - \mu_i)^T (Z - \mu_i)} \quad (2.22)$$

or Inverse Hardy's multiquadric form [110]

$$s_i(Z) = \frac{1}{\sqrt{\sigma_i^2 + (Z - \mu_i)^T (Z - \mu_i)}} \quad (2.23)$$

Universal approximation results in [111] indicate that, for any continuous function $f(Z) : \mathbb{R}^n \rightarrow \mathbb{R}^l$, if l is sufficiently large, then there exists an ideal constant weight vector W^* such that

$$\max_{Z \in \Omega_Z} |f(Z) - W^{*T} S(Z)| < \epsilon, \quad \forall Z \in \Omega_Z \quad (2.24)$$

with an arbitrary constant $\epsilon > 0$.

Throughout this thesis, RBF NNs will be used as function approximators in adaptive NN control design. The useful properties of RBF NNs, such as linear parametrization and localization, will be exploited to simplify the design and analysis. The problems with using RBF NNs, such as the curse of dimensionality and the requirement of prior knowledge for the studied systems will be overcome or minimized.

- RBF NN belongs to a class of linearly parametrized networks where the network output is related to the adjustable weights in a linear manner, assuming the basis function centers and variances are fixed a priori. Thus, on-line learning rules can be used to update the weights and the convergence results can be derived using the available linear adaptive techniques.

2.3 Function Approximation

- The activation functions of RBF networks are localized, thus these networks store information locally in a transparent fashion. The adaptation in part of the input spaces does not affect knowledge stored in a different area, i.e., they have spatially localized learning capability. Therefore, if the basis functions are correctly chosen, the learning speed of RBF NNs is in generally better than that of MNNs.
- One of the problems of RBF NNs is that the number of basis functions for RBF networks tends to increase exponentially with the dimension of the input space. The approximation will become practically infeasible when the dimensionality of the input space is very high, which is often referred to as “the curse of dimensionality” [109]. To overcome this problem, in this thesis, the number of inputs to RBF NN is made minimal by defining intermediate variables, which are available through the computation of all the variables of the unknown functions. Thus, the introductions of intermediate variables help to avoid the curse of dimensionality, and make the proposed neural control scheme computationally implementable.
- Another problem of using RBF NNs is that the network structure, the number of basis functions, their location and shape, must be chosen a priori by considering the working space. According to [111], Gaussian RBF NNs arranged on a regular lattice can uniformly approximate sufficiently smooth functions on closed, bounded subsets. Moreover, given only crude estimates of the smoothness of the function being approximated, it is feasible to select the centers and variances of a finite number of Gaussian nodes, so that the resulting NNs are capable of uniformly approximating the required function to a chosen tolerance everywhere on a pre-specified subset. In practical applications, some rough knowledge of the system states, including those of the plant and the reference model, is usually assumed to be known. Thus, the centers and widths of RBFs can be selected on a regular lattice in the respective compact sets.

Thus, by exploiting the useful properties and minimizing the disadvantages, RBF NNs will be used to approximate the unknown nonlinearities in adaptive NN control design

2.4 Useful Definitions, Theorems and Lemmas

throughout this thesis. Simulation studies will be conducted to show the effectiveness of RBF NNs.

Remark 2.2 *Although RBFNN is employed in our control design, it can be replaced by other linearly parameterized function approximators such as high-order neural networks, fuzzy systems, polynomials, splines and wavelet networks without difficulty. For a unified framework of different approximation structures in adaptive approximation based control, interested readers can refer to [112].*

2.4 Useful Definitions, Theorems and Lemmas

Definition 2.2 (SGUUB) [66] *The solution $X(t)$ of a system is semi-globally uniformly ultimately bounded (SGUUB) if, for any compact set Ω_0 and all $X(t_0) \in \Omega_0$, there exists an $\mu > 0$ and $T(\mu, X(t_0))$ such that $\|X(t)\| \leq \mu$ for all $t \geq t_0 + T$.*

Lemma 2.1 (Implicit Function Theorem) [97] *For a continuously differentiable function $f(x, u) : \mathbb{R}^n \times \mathbb{R} \rightarrow \mathbb{R}$, if there exists a positive constant δ such that $|\partial f(x, u)/\partial u| > \delta > 0$, $\forall (x, u) \in \mathbb{R}^n \times \mathbb{R}$. Then there exists a continuous (smooth) function $u^* = u(x)$ such that $f(x, u^*) = 0$.*

Lemma 2.2 (Mean Value Theorem) [113] *Assume that $f(x, y) : \mathbb{R}^n \times \mathbb{R} \rightarrow \mathbb{R}$ has a derivative (finite or infinite) at each point of an open set $\mathbb{R}^n \times (a, b)$, and assume also that it is continuous at both endpoints $y = a$ and $y = b$. Then there is a point $\xi \in (a, b)$ such that $f(x, b) - f(x, a) = f'(x, \xi)(b - a)$.*

Lemma 2.3 (First Mean Value Theorem for Integration) *If $G : [a, b] \rightarrow \mathbb{R}$ is a continuous function and $\phi : [a, b] \rightarrow [0, \infty)$ is an integrable function, then there exists a number x in $[a, b]$ such that*

$$\int_a^b G(t)\phi(t)dt = G(x) \int_a^b \phi(t)dt$$

In particular, if $\phi(t) = 1$ for all t in $[a, b]$, then there exists x in $[a, b]$ such that

$$\int_a^b G(t)dt = G(x)(b - a).$$

2.4 Useful Definitions, Theorems and Lemmas

Definition 2.3 (Nussbaum-type Function) *A function $N(\zeta)$ is called a Nussbaum-type function if it has the following properties:*

$$\begin{aligned} \text{(i)} \quad & \lim_{s \rightarrow +\infty} \sup \frac{1}{s} \int_0^s N(\zeta) d\zeta = +\infty \\ \text{(ii)} \quad & \lim_{s \rightarrow +\infty} \inf \frac{1}{s} \int_0^s N(\zeta) d\zeta = -\infty \end{aligned}$$

For clarity, the even Nussbaum function, $N(\zeta) = \exp(\zeta^2) \cos((\pi/2)\zeta)$ is used in this thesis.

Lemma 2.4 [114] *Let $V(\cdot)$, $\zeta(\cdot)$ be smooth functions defined on $[0, t_f)$ with $V(t) \geq 0$, $\forall t \in [0, t_f)$, and $N(\cdot)$ be an even smooth Nussbaum-type function. If the following inequality holds:*

$$V(t) \leq c_0 + e^{-c_1 t} \int_0^t [g(\cdot)N(\zeta) + 1] \dot{\zeta} e^{c_1 \tau} d\tau, \quad \forall t \in [0, t_f)$$

where c_0 represents some suitable constant, c_1 is a positive constant, and $g(\cdot)$ is a time-varying parameter which takes values in the unknown closed intervals $I = [l^-, l^+]$, with $0 \notin I$, then $V(t)$, $\zeta(t)$, $\int_0^t g(\cdot)N(\zeta)\dot{\zeta}d\tau$ must be bounded on $[0, t_f)$.

Lemma 2.5 [115] *For any continuous function $h(\xi_1, \dots, \xi_n) : \mathbb{R}^{m_1} \times \dots \times \mathbb{R}^{m_n} \rightarrow \mathbb{R}$ satisfying $h(0, \dots, 0) = 0$, where $\xi_j \in \mathbb{R}^{m_j} (j = 1, 2, \dots, n, m_j > 0)$, there exist positive smooth functions $\varrho_j(\xi_j) : \mathbb{R}^{m_j} \rightarrow \mathbb{R} (j = 1, 2, \dots, n)$ satisfying $\varrho_j(0) = 0$ such that*

$$h(\xi_1, \dots, \xi_n) \leq \sum_{j=1}^n \varrho_j(\xi_j) \tag{2.25}$$

Definition 2.4 (Barrier Lyapunov Function) [116] *A Barrier Lyapunov Function (BLF) is a scalar function $V(x)$, defined with respect to the system $\dot{x} = f(x)$ on an open region \mathcal{D} containing the origin, that is continuous, positive definite, has continuous first-order partial derivatives at every point of \mathcal{D} , has the property $V(x) \rightarrow \infty$ as x approaches the boundary of \mathcal{D} , and satisfies $V(x(t)) \leq b \forall t \geq 0$ along the solution of $\dot{x} = f(x)$ for $x(0) \in \mathcal{D}$ and some positive constant b .*

2.4 Useful Definitions, Theorems and Lemmas

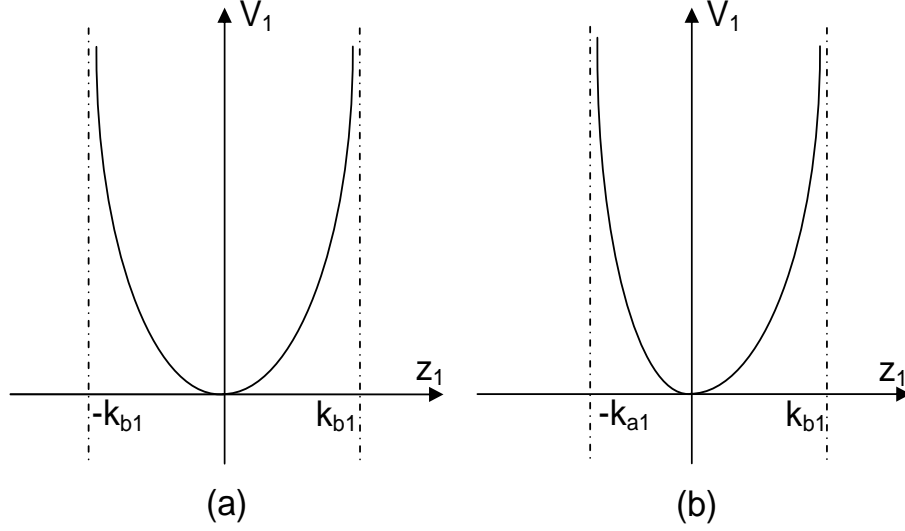


Figure 2.4: Schematic illustration of (a) symmetric and (b) asymmetric barrier functions

As discussed in [116], there are many functions $V_1(z_1)$ satisfying Definition 2.4, which may be symmetric ($\mathcal{D} = (-k_{b_1}, k_{b_1})$) or asymmetric ($\mathcal{D} = (-k_{a_1}, k_{b_1})$) as illustrated in Figure 2.4 with some positive constants k_{a_1} and k_{b_1} . Asymmetric barrier functions are more general than their symmetric counterparts, and thus can offer more flexibility for control design to obtain better performance. However, they are considerably more difficult to construct analytically, and to employ for control design. For clarity, the following symmetric BLF candidate considered in [116, 117] is used in this thesis:

$$V_1 = \frac{1}{2} \log \frac{k_{b_1}^2}{k_{b_1}^2 - z_1^2} \quad (2.26)$$

where $\log(\cdot)$ denotes the natural logarithm of \cdot , and k_{b_1} the constraint on z_1 , i.e., $|z_1| < k_{b_1}$. As seen from the schematic illustration of $V_1(z_1)$ in Figure 2.4 (a), the BLF escapes to infinity at $|z_1| = k_{b_1}$. It can be shown that V_1 is positive definite and C^1 continuous in the set $|z_1| < k_{b_1}$, and thus a valid Lyapunov function candidate in the set $|z_1| < k_{b_1}$. The control design and results can be extended to the asymmetric BLF case. Interested readers can refer to [116].

Lemma 2.6 [118] *For any positive constant k_{b_1} , let $\mathcal{Z}_1 := \{z_1 \in \mathbb{R} : |z_1| < k_{b_1}\} \subset \mathbb{R}$ and $\mathcal{N} := \mathbb{R}^l \times \mathcal{Z}_1 \subset \mathbb{R}^{l+1}$ be open sets. Consider the system*

$$\dot{\eta} = h(t, \eta) \quad (2.27)$$

2.4 Useful Definitions, Theorems and Lemmas

where $\eta := [w, z_1]^T \in \mathcal{N}$ is the state, and the function $h : \mathbb{R}_+ \times \mathcal{N} \rightarrow \mathbb{R}^{l+1}$ satisfies conditions of the existence and uniqueness of solution ([119], p.476, Theorem 54). Suppose that there exist continuously differentiable and positive definite functions $U : \mathbb{R}^l \rightarrow \mathbb{R}_+$ and $V_1 : \mathcal{Z}_1 \rightarrow \mathcal{R}_+$, $i = 1, \dots, n$, such that

$$V_1(z_1) \rightarrow \infty \quad \text{as} \quad |z_1| \rightarrow k_{b_1} \quad (2.28)$$

$$\gamma_1(\|w\|) \leq U(w) \leq \gamma_2(\|w\|) \quad (2.29)$$

with γ_1 and γ_2 as class K_∞ functions. Let $V(\eta) := V_1(z_1) + U(w)$, and $z_1(0) \in \mathcal{Z}_1$. If the inequality holds:

$$\dot{V} = \frac{\partial V}{\partial \eta} h \leq -\mu V + \lambda \quad (2.30)$$

in the set $z_1 \in \mathcal{Z}_1$, and μ and λ are positive constants, then $z_1(t) \in \mathcal{Z}_1$, $\forall t \in [0, \infty)$.

Remark 2.3 In Lemma 2.6, we split the state variable into z_1 and w , where z_1 is the state to be constrained, and w are the free states, along with the adaptive parameters if adaptive control is involved. The constrained state z_1 requires the use of a barrier function V_1 to prevent it from reaching the limits $-k_{b_1}$ and k_{b_1} . The free states require the use of Lyapunov function candidates in the usual sense, i.e., defined over the entire state space, a common choice being quadratic functions.

Lemma 2.7 [118] For any positive constant k_{b_1} , the following inequality holds for all z_1 in the interval $|z_1| < k_{b_1}$:

$$\log \frac{k_{b_1}^2}{k_{b_1}^2 - z_1^2} < \frac{z_1^2}{k_{b_1}^2 - z_1^2} \quad (2.31)$$

Chapter 3

Systems with Backlash-Like Hysteresis

In this chapter, adaptive NN control schemes are investigated for nonlinear systems with backlash-like hysteresis. The chapter is organized as follows. Firstly, for a class of strict-feedback nonlinear systems preceded by unknown backlash-like hysteresis, adaptive dynamic surface control (DSC) is developed without constructing a hysteresis inverse in Section 3.1. Then, for a class of output feedback nonlinear systems in the presence of unknown functions and bounded time-varying disturbances, an output feedback control scheme is proposed in Section 3.2. Conclusions are made in Section 3.3.

3.1 Strict-Feedback Systems

3.1.1 Introduction

Hysteresis nonlinearities are common in many industrial processes, especially in position control of smart material-based actuators, including piezoceramics and shape memory alloys. The existence of hysteresis nonlinearities severely limit system performance such as giving rise to undesirable inaccuracy or oscillations and even may lead to instability [3]. Since hysteresis is a very complex phenomenon, modeling a

3.1 Strict-Feedback Systems

general type of hysteresis is still an active research topic and there exist many hysteresis models in the literature, such as the Preisach model, the Ishlinskii hysteresis operator, the Prandtl-Ishlinskii hysteresis model, the Duhem hysteresis operator, the Bouc Wen model, and so on. Interested readers can refer to [6] for a review of the hysteresis models. Among of them, the backlash hysteresis model is the most familiar and simple model, which can be described by two parallel lines connected via horizontal line segments and will be considered in this chapter.

Due to the nonsmooth characteristics of hysteresis nonlinearities, traditional control methods are inadequate in dealing with the effects of unknown hysteresis. Therefore, advanced control techniques to mitigate the effects of hysteresis have been called upon and have been studied for decades. One of the most common approaches is to construct an inverse operator to cancel the effects of the hysteresis as in [3] and [120]. However, it is a challenging task to construct the inverse operator for the hysteresis, due to its complexity and uncertainty. To circumvent these difficulties, alternative control approaches that do not need an inverse model have also been developed. In [16] and [17], robust adaptive control and adaptive backstepping control were, respectively, investigated for a class of nonlinear systems in a Brunovsky form with unknown backlash-like hysteresis and system parameters.

Motivated by the above works [16] and [17], in this section, we extend the system to a class of nonlinear systems in strict-feedback form with unknown functions and disturbances. The function uncertainties are compensated for by neural networks due to their universal approximation capabilities [46, 66, 112]. For the control of strict-feedback nonlinear systems, though backstepping is one of the popular design methods, an obvious drawback in the traditional backstepping design is the problem of “explosion of complexity”, which is caused by the repeated differentiations of certain nonlinear functions such as virtual controls. To overcome the “explosion of complexity”, dynamic surface control (DSC) was proposed for a class of strict-feedback nonlinear systems with known $f_i(x_1, \dots, x_i)$ and $g_i = 1$ by introducing first-order filtering of the synthetic virtual control input at each step of traditional backstepping approach [121]. The result was extended to a class of strict-feedback nonlinear systems with unknown functions f_i and virtual coefficients $g_i = 1$ by combining DSC control and neural networks [122]. In this section, the virtual coefficients g_i of the

3.1 Strict-Feedback Systems

strict-feedback nonlinear systems are considered as unknown constants further. The bounds of the “disturbance-like” terms, including disturbances and neural network approximation errors, are estimated by adaptive control.

The organization of this section is as follows. The problem formulation and preliminaries are given in Section 3.1.2. In Section 3.1.3, adaptive dynamic surface control is developed for a class of unknown nonlinear systems in strict-feedback form with the unknown backlash-like hysteresis. The closed-loop system stability is analyzed as well. Results of extensive simulation studies are shown to demonstrate the effectiveness of the approach in Section 3.1.4.

3.1.2 Problem Formulation and Preliminaries

Consider a class of nonlinear systems in strict-feedback form described as follows:

$$\begin{aligned}
 \dot{x}_1 &= f_1(x_1) + g_1 x_2 + d_1(t) \\
 &\vdots \\
 \dot{x}_i &= f_i(\bar{x}_i) + g_i x_{i+1} + d_i(t), \quad i = 2, \dots, n-1 \\
 &\vdots \\
 \dot{x}_n &= f_n(\bar{x}_n) + g_n u(v) + d_n(t) \\
 y &= x_1
 \end{aligned} \tag{3.1}$$

where $\bar{x}_i = [x_1, \dots, x_i]^T \in \mathbb{R}^i$, $i = 1, \dots, n$ are the states, y is the system output, g_i are the unknown constant virtual coefficients, $f_i(\cdot)$ are the unknown smooth functions, $d_i(\cdot)$ are the unknown bounded time varying disturbances, and $u \in \mathbb{R}$ is the system input and the output of the backlash-like hysteresis, which is described as follows:

$$\frac{du}{dt} = \alpha \left| \frac{dv}{dt} \right| (cv - u) + B_1 \frac{dv}{dt} \tag{3.2}$$

where α , c , and B_1 are constants, $c > 0$ is the slope of lines satisfying $c > B_1$.

Based on the analysis in Section 2.2.1 of Chapter 2, (3.2) can be solved explicitly as follows:

$$u(t) = cv(t) + h(v) \tag{3.3}$$

3.1 Strict-Feedback Systems

where

$$h(v) = [u_0 - cv_0]e^{-\alpha(v-v_0)\text{sgn}\dot{v}} + e^{-\alpha v\text{sgn}\dot{v}} \int_{v_0}^v [B_1 - c]e^{\alpha\zeta(\text{sgn}\dot{v})} d\zeta \quad (3.4)$$

Substituting (3.3) into (3.1), we have:

$$\begin{aligned} \dot{x}_1 &= f_1(x_1) + g_1x_2 + d_1(t) \\ &\vdots \\ \dot{x}_i &= f_i(\bar{x}_i) + g_ix_{i+1} + d_i(t), \quad i = 2, \dots, n-1 \\ &\vdots \\ \dot{x}_n &= f_n(\bar{x}_n) + g_ncv(t) + g_nh(v) + d_n(t) \\ y &= x_1 \end{aligned} \quad (3.5)$$

The control objective is to design adaptive control law $v(t)$ for system (3.5) such that the output y follows the specified desired trajectory y_d .

To facilitate the control design later in Section 3.1.3, the following assumptions are needed.

Assumption 3.1 *The signs of g_i are known, and there exist constants $g_{i\max} \geq g_{i\min} > 0$ such that $g_{i\min} \leq |g_i| \leq g_{i\max}$.*

Assumption 3.2 *The desired trajectory vectors are continuous and available, and $[y_d, \dot{y}_d, \ddot{y}_d]^T \in \Omega_d$ with known compact set $\Omega_d = \{[y_d, \dot{y}_d, \ddot{y}_d]^T : y_d^2 + \dot{y}_d^2 + \ddot{y}_d^2 \leq B_0\} \subset \mathbb{R}^3$, whose size B_0 is a known positive constant.*

Assumption 3.3 *There exist constants c_{\min} and c_{\max} such that the slope c in (3.2) satisfies $c \in [c_{\min}, c_{\max}]$.*

Assumption 3.4 *There exist a constant h_{\max} such that $h(v) \leq h_{\max}$.*

Assumption 3.5 *There exist constants $d_{i\max}$ such that $d_i(t) \leq d_{i\max}$.*

3.1 Strict-Feedback Systems

Remark 3.1 *Assumption 3.1 implies that unknown constants g_i are strictly either positive or negative. Without losing generality, we will only consider the case when $g_i > 0$. Assumptions 3.3 and 3.4 assume the slop range of a backlash hysteresis and the upper bound of the hysteresis loop, which are reasonable according to the analysis in Section 2.2.1 of Chapter 2. In Assumption 3.5, the disturbances are also required to be bounded, which is practical in reality. It should be noted that all these bounds g_{\max} , g_{\min} , c_{\min} , c_{\max} , h_{\max} and $d_{i\max}$ are not required in implementation proposed control design. They are used only for analytical purposes.*

3.1.3 Adaptive Dynamic Surface Control Design

In this section, we will combine the dynamic surface control with backstepping and adaptive control for the n th-order system described by (3.5). Similar to traditional backstepping, the design of adaptive dynamic surface control is based on the following change of coordinates: $z_1 = x_1 - y_d$, $z_i = x_i - \omega_i$, $i = 2, \dots, n$, where ω_i is the output of a first order filter with α_{i-1} as the input, and α_{i-1} is an intermediate control which shall be developed for the corresponding $(i - 1)$ th subsystem. Finally, an overall control law v is constructed at step n . The major difference of dynamic surface control with traditional backstepping is to replace, at each step of recursion, the quantity $\dot{\alpha}_{i-1}$ by $\dot{\omega}_i$ in determining the virtual control α_i . As a result, the operation of differentiation can be replaced by simpler algebraic operation. Before proceeding with the adaptive control, some notations are presented below: $\bar{z}_i = [z_1, \dots, z_i]^T$, $\bar{y}_j = [y_2, \dots, y_j]^T$, $\bar{W}_i = [\hat{W}_1^T, \dots, \hat{W}_i^T]^T$, where $i = 1, \dots, n$, $y_j = \omega_j - \alpha_{j-1}$, $j = 2, \dots, n$.

Step 1: Since $z_1 = x_1 - y_d$, and its derivative is

$$\dot{z}_1 = \dot{x}_1 - \dot{y}_d = f_1(x_1) + g_1 x_2 + d_1(t) - \dot{y}_d \quad (3.6)$$

Consider the following Lyapunov function candidate:

$$V_{z_1} = \frac{1}{2g_1} z_1^2 \quad (3.7)$$

Its derivative along (3.6) is

$$\dot{V}_{z_1} = \frac{1}{g_1} z_1 \dot{z}_1 = z_1 [Q_1(Z_1) + x_2 + \frac{1}{g_1} d_1(t)] \quad (3.8)$$

3.1 Strict-Feedback Systems

where $Q_1(Z_1) = g_1^{-1}f_1(x_1) - g_1^{-1}\dot{y}_d$ with $Z_1 = [x_1, \dot{y}_d] \in \Omega_{Z_1} \subset \mathbb{R}^2$.

To compensate for the unknown function $Q_1(Z_1)$, we can use the radial basis function neural networks (RBFNNs) in Section 2.3.3, $\hat{W}_1^T S(Z_1)$, with $\hat{W}_1 \in \mathbb{R}^{l \times 1}$, $S(Z_1) \in \mathbb{R}^{l \times 1}$, and the NN node number $l > 1$, to approximate the function $Q_1(Z_1)$ on the compact set Ω_{Z_1} as follows

$$Q_1(Z_1) = \hat{W}_1^T S(Z_1) - \tilde{W}_1^T S(Z_1) + \varepsilon_1(Z_1) \quad (3.9)$$

where the approximation error $\varepsilon_1(Z_1)$ satisfies $|\varepsilon_1(Z_1)| \leq \varepsilon_1^*$ with a positive constant ε_1^* .

Substituting (3.9) into (3.8) and according to Assumptions 3.1 and 3.5, we obtain

$$\dot{V}_{z_1} \leq z_1[\hat{W}_1^T S(Z_1) - \tilde{W}_1^T S(Z_1) + x_2] + |z_1|D_1 \quad (3.10)$$

where $D_1 = \frac{d_{1max}}{g_{1min}} + \varepsilon_1^*$.

Since $x_2 = z_2 + y_2 + \alpha_1$, (3.10) becomes

$$\dot{V}_{z_1} \leq z_1[\hat{W}_1^T S(Z_1) - \tilde{W}_1^T S(Z_1) + z_2 + y_2 + \alpha_1] + |z_1|D_1 \quad (3.11)$$

Choose the following virtual control law and adaptation laws:

$$\alpha_1 = -k_1 z_1 - \hat{W}_1^T S(Z_1) - \tanh\left(\frac{z_1}{\epsilon}\right)\hat{D}_1 \quad (3.12)$$

$$\dot{\hat{W}}_1 = \Gamma_1[z_1 S(Z_1) - \sigma_1 \hat{W}_1] \quad (3.13)$$

$$\dot{\hat{D}}_1 = \gamma_{d_1}[z_1 \tanh\left(\frac{z_1}{\epsilon}\right) - \sigma_{d_1} \hat{D}_1] \quad (3.14)$$

where $k_1 > 0$, $\epsilon > 0$, \hat{D}_1 is the estimate of D_1 , $\Gamma_1 = \Gamma_1^T \in \mathbb{R}^{l \times l} > 0$, $\sigma_1 > 0$, $\gamma_{d_1} > 0$ and $\sigma_{d_1} > 0$.

Substituting (3.12) into (3.11), and using the following property of the hyperbolic tangent function $\tanh(\cdot)$:

$$0 \leq |z_1| - z_1 \tanh\left(\frac{z_1}{\epsilon}\right) \leq 0.2785\epsilon \quad (3.15)$$

we obtain that

$$\dot{V}_{z_1} \leq -k_1 z_1^2 + z_1 z_2 + z_1 y_2 - z_1 \tilde{W}_1^T S(Z_1) - z_1 \tanh\left(\frac{z_1}{\epsilon}\right)\tilde{D}_1 + |z_1|D_1$$

3.1 Strict-Feedback Systems

$$\begin{aligned}
& -z_1 \tanh\left(\frac{z_1}{\epsilon}\right) D_1 \\
\leq & -k_1 z_1^2 + z_1 z_2 + z_1 y_2 - z_1 \tilde{W}_1^T S(Z_1) - z_1 \tanh\left(\frac{z_1}{\epsilon}\right) \tilde{D}_1 \\
& + 0.2785\epsilon D_1
\end{aligned} \tag{3.16}$$

where $\tilde{D} = \hat{D} - D$.

Using the Young's inequality, the following inequalities hold:

$$z_1 z_2 \leq z_1^2 + \frac{1}{4} z_2^2 \tag{3.17}$$

$$z_1 y_2 \leq z_1^2 + \frac{1}{4} y_2^2 \tag{3.18}$$

Substituting (3.17) and (3.18) into (3.16) leads to

$$\begin{aligned}
\dot{V}_{z_1} \leq & -(k_1 - 2)z_1^2 + \frac{1}{4}z_2^2 + \frac{1}{4}y_2^2 - z_1 \tilde{W}_1^T S(Z_1) - z_1 \tanh\left(\frac{z_1}{\epsilon}\right) \tilde{D}_1 \\
& + 0.2785\epsilon D_1
\end{aligned} \tag{3.19}$$

Define the filtered virtual control ω_2 in the following manner:

$$\tau_2 \dot{\omega}_2 + \omega_2 = \alpha_1, \quad \omega_2(0) = \alpha_1(0), \tag{3.20}$$

where τ_2 is a design constant that we will choose later.

Due to $y_2 = \omega_2 - \alpha_1$, from (3.20), we have

$$\dot{\omega}_2 = -\frac{y_2}{\tau_2} \tag{3.21}$$

Therefore, we have

$$\begin{aligned}
\dot{y}_2 &= \dot{\omega}_2 - \dot{\alpha}_1 \\
&= -\frac{y_2}{\tau_2} + [k_1 \dot{z}_1 + \dot{W}_1^T S(Z_1) + \hat{W}_1^T \dot{S}(Z_1) + \tanh\left(\frac{z_1}{\epsilon}\right) \dot{\hat{D}}_1 \\
&\quad + (1 - \tanh^2\left(\frac{z_1}{\epsilon}\right)) \dot{z}_1 \hat{D}_1]
\end{aligned} \tag{3.22}$$

As such,

$$\left| \dot{y}_2 + \frac{y_2}{\tau_2} \right| \leq \zeta_2(\bar{z}_2, y_2, \hat{W}_1, \hat{D}_1, y_d, \dot{y}_d, \ddot{y}_d) \tag{3.23}$$

where $\zeta_2(\bar{z}_2, y_2, \hat{W}_1, \hat{D}_1, y_d, \dot{y}_d, \ddot{y}_d)$ is a continuous function.

3.1 Strict-Feedback Systems

From (3.22) and (3.23), using the Young's inequality, we obtain that

$$\begin{aligned} y_2 \dot{y}_2 &\leq -\frac{y_2^2}{\tau_2} + |y_2| \zeta_2 \\ &\leq -\frac{y_2^2}{\tau_2} + y_2^2 + \frac{1}{4} \zeta_2^2 \end{aligned} \quad (3.24)$$

Consider the following Lyapunov function candidate:

$$V_1 = V_{z_1} + \frac{1}{2} \tilde{W}_1^T \Gamma_1^{-1} \tilde{W}_1 + \frac{1}{2\gamma_{d_1}} \tilde{D}_1^2 + \frac{1}{2} y_2^2 \quad (3.25)$$

Its time derivative along (3.19) and (3.24) is

$$\begin{aligned} \dot{V}_1 &= \dot{V}_{z_1} + \tilde{W}_1^T \Gamma_1^{-1} \dot{\tilde{W}}_1 + \frac{1}{\gamma_{d_1}} \tilde{D}_1 \dot{\tilde{D}} + y_2 \dot{y}_2 \\ &\leq -(k_1 - 2) z_1^2 + \frac{1}{4} z_2^2 - z_1 \tilde{W}_1^T S(Z_1) - z_1 \tanh\left(\frac{z_1}{\epsilon}\right) \tilde{D}_1 + 0.2785\epsilon D_1 \\ &\quad + \tilde{W}_1^T \Gamma_1^{-1} \dot{\tilde{W}}_1 + \frac{1}{\gamma_{d_1}} \tilde{D}_1 \dot{\tilde{D}} - \frac{y_2^2}{\tau_2} + \frac{1}{4} y_2^2 + \frac{1}{4} \zeta_2^2 \end{aligned} \quad (3.26)$$

Substituting (3.13) and (3.14) into (3.26) results in

$$\begin{aligned} \dot{V}_1 &\leq -(k_1 - 2) z_1^2 + \frac{1}{4} z_2^2 - \sigma_1 \tilde{W}_1^T \hat{W}_1 - \sigma_{d_1} \tilde{D}_1 \hat{D}_1 - \frac{y_2^2}{\tau_2} + \frac{1}{4} y_2^2 + \frac{1}{4} \zeta_2^2 \\ &\quad + 0.2785\epsilon D_1 \end{aligned} \quad (3.27)$$

Step i ($2 \leq i < n$): The time derivative of z_i is

$$\dot{z}_i = f_i(\bar{x}_i) + g_i x_{i+1} + d_i(t) - \dot{\omega}_i \quad (3.28)$$

Consider the following Lyapunov function candidate:

$$V_{z_i} = \frac{1}{2g_i} z_i^2 \quad (3.29)$$

Its derivative along (3.28) is

$$\dot{V}_{z_i} = \frac{1}{g_i} z_i \dot{z}_i = z_i [Q_i(Z_i) + x_{i+1} + \frac{1}{g_i} d_i(t)] \quad (3.30)$$

where $Q_i(Z_i) = g_i^{-1} f_i(\bar{x}_i) - g_i^{-1} \dot{\omega}_i$ with $Z_i = [\bar{x}_i, \dot{\omega}_i] \in \Omega_{Z_i} \subset \mathbb{R}^{i+1}$.

To compensate for the unknown function $Q_i(Z_i)$, we can use the RBFNNs, $\hat{W}_i^T S(Z_i)$, with $\hat{W}_i \in \mathbb{R}^{l \times 1}$, $S(Z_i) \in \mathbb{R}^{l \times 1}$, and the NN node number $l > 1$, to approximate the function $Q_i(Z_i)$ on the compact set Ω_{Z_i} as follows

$$Q_i(Z_i) = \hat{W}_i^T S(Z_i) - \tilde{W}_i^T S(Z_i) + \varepsilon_i(Z_i) \quad (3.31)$$

3.1 Strict-Feedback Systems

where the approximation error $\varepsilon_i(Z_i)$ satisfies $|\varepsilon_i(Z_i)| \leq \varepsilon_i^*$ with a positive constant ε_i^* .

Substituting (3.31) into (3.30), we obtain

$$\dot{V}_{z_i} \leq z_i[\hat{W}_i^T S(Z_i) - \tilde{W}_i^T S(Z_i) + x_{i+1}] + |z_i|D_i \quad (3.32)$$

where $D_i = \frac{d_{1\max}}{g_{1\min}} + \varepsilon_i^*$.

Since $x_{i+1} = z_{i+1} + y_{i+1} + \alpha_i$, (3.32) becomes

$$\dot{V}_{z_i} \leq z_i[\hat{W}_i^T S(Z_i) - \tilde{W}_i^T S(Z_i) + z_{i+1} + y_{i+1} + \alpha_i] + |z_i|D_i \quad (3.33)$$

Choose the following virtual control law and adaptation laws:

$$\alpha_i = -k_i z_i - \hat{W}_i^T S(Z_i) - \tanh\left(\frac{z_i}{\epsilon}\right)\hat{D}_i \quad (3.34)$$

$$\dot{\hat{W}}_i = \Gamma_i[z_i S(Z_i) - \sigma_i \hat{W}_i] \quad (3.35)$$

$$\dot{\hat{D}}_i = \gamma_{d_i}[z_i \tanh\left(\frac{z_i}{\epsilon}\right) - \sigma_{d_i} \hat{D}_i] \quad (3.36)$$

where $k_i > 0$, $\epsilon > 0$, \hat{D}_i is the estimate of D_i , $\Gamma_i = \Gamma_i^T \in \mathbb{R}^{l \times l} > 0$, $\sigma_i > 0$, $\gamma_{d_i} > 0$ and $\sigma_{d_i} > 0$.

Substituting (3.34) into (3.33) and using the property of the hyperbolic tangent function as (3.15), we obtain

$$\begin{aligned} \dot{V}_{z_i} \leq & -k_i z_i^2 + z_i z_{i+1} + z_i y_{i+1} - z_i \tilde{W}_i^T S(Z_i) - z_i \tanh\left(\frac{z_i}{\epsilon}\right)\tilde{D}_i \\ & + 0.2785\epsilon D_i \end{aligned} \quad (3.37)$$

Using the Young's inequality, the following inequalities hold:

$$z_i z_{i+1} \leq z_i^2 + \frac{1}{4} z_{i+1}^2 \quad (3.38)$$

$$z_i y_{i+1} \leq z_i^2 + \frac{1}{4} y_{i+1}^2 \quad (3.39)$$

Substituting (3.38) and (3.39) into (3.37) leads to

$$\begin{aligned} \dot{V}_{z_i} \leq & -(k_i - 2)z_i^2 + \frac{1}{4}z_{i+1}^2 + \frac{1}{4}y_{i+1}^2 - z_i \tilde{W}_i^T S(Z_i) - z_i \tanh\left(\frac{z_i}{\epsilon}\right)\tilde{D}_i \\ & + 0.2785\epsilon D_i \end{aligned} \quad (3.40)$$

3.1 Strict-Feedback Systems

Define the filtered virtual control ω_{i+1} in the following manner:

$$\tau_{i+1}\dot{\omega}_{i+1} + \omega_{i+1} = \alpha_i, \quad \omega_{i+1}(0) = \alpha_i(0), \quad (3.41)$$

where τ_{i+1} is a design constant that we will choose later.

Due to $y_{i+1} = \omega_{i+1} - \alpha_i$, from (3.41), we have

$$\dot{\omega}_{i+1} = -\frac{y_{i+1}}{\tau_{i+1}} \quad (3.42)$$

Therefore, we have

$$\begin{aligned} \dot{y}_{i+1} &= \dot{\omega}_{i+1} - \dot{\alpha}_i \\ &= -\frac{y_{i+1}}{\tau_{i+1}} + [k_i \dot{z}_i + \dot{W}_i^T S(Z_i) + \hat{W}_i^T \dot{S}(Z_i) + \tanh(\frac{z_i}{\epsilon}) \dot{D}_i \\ &\quad + (1 - \tanh^2(\frac{z_i}{\epsilon})) \dot{z}_i \hat{D}_i] \end{aligned} \quad (3.43)$$

As such,

$$\left| \dot{y}_{i+1} + \frac{y_{i+1}}{\tau_{i+1}} \right| \leq \zeta_{i+1}(\bar{z}_{i+1}, \bar{y}_{i+1}, \bar{W}_i, \bar{D}_i, y_d, \dot{y}_d, \ddot{y}_d) \quad (3.44)$$

where $\zeta_{i+1}(\bar{z}_{i+1}, \bar{y}_{i+1}, \bar{W}_i, \bar{D}_i, y_d, \dot{y}_d, \ddot{y}_d)$ is a continuous function.

From (3.43) and (3.44), using the Young's inequality, we obtain that

$$\begin{aligned} y_{i+1}\dot{y}_{i+1} &\leq -\frac{y_{i+1}^2}{\tau_{i+1}} + |y_{i+1}|\zeta_{i+1} \\ &\leq -\frac{y_{i+1}^2}{\tau_{i+1}} + y_{i+1}^2 + \frac{1}{4}\zeta_{i+1}^2 \end{aligned} \quad (3.45)$$

Consider the following Lyapunov function candidate:

$$V_i = V_{z_i} + \frac{1}{2}\tilde{W}_i^T \Gamma_i^{-1} \tilde{W}_i + \frac{1}{2\gamma_{d_i}} \tilde{D}_i^2 + \frac{1}{2}y_{i+1}^2 \quad (3.46)$$

Its time derivative along (3.40) and (3.45) is

$$\begin{aligned} \dot{V}_i &= \dot{V}_{z_i} + \tilde{W}_i^T \Gamma_i^{-1} \dot{\tilde{W}}_i + \frac{1}{\gamma_{d_i}} \tilde{D}_i \dot{\tilde{D}}_i + y_{i+1} \dot{y}_{i+1} \\ &\leq -(k_i - 2)z_i^2 + \frac{1}{4}z_{i+1}^2 - z_i \tilde{W}_i^T S(Z_i) + \tilde{W}_i^T \Gamma_i^{-1} \dot{\tilde{W}}_i + \frac{1}{\gamma_{d_i}} \tilde{D}_i \dot{\tilde{D}}_i \\ &\quad - \frac{y_{i+1}^2}{\tau_{i+1}} + \frac{1}{4}y_{i+1}^2 + \frac{1}{4}\zeta_{i+1}^2 \end{aligned} \quad (3.47)$$

3.1 Strict-Feedback Systems

Substituting (3.35) and (3.36) into (3.47) results in

$$\begin{aligned}\dot{V}_i \leq & -(k_i - 2)z_i^2 + \frac{1}{4}z_{i+1}^2 - \sigma_i \tilde{W}_i^T \hat{W}_i - \sigma_{d_i} \tilde{D}_i \hat{D}_i - \frac{y_{i+1}^2}{\tau_{i+1}} + 1 \frac{1}{4}y_{i+1}^2 \\ & + \frac{1}{4}\zeta_{i+1}^2 + 0.2785\epsilon D_i\end{aligned}\quad (3.48)$$

Step n: In this final step, we will design the control input $v(t)$. Since $z_n = x_n - \omega_n$, the time derivative of z_n is

$$\dot{z}_n = f_n(\bar{x}_n) + g_n c v(t) + g_n h(v) + d_n(t) - \dot{\omega}_n \quad (3.49)$$

Consider the following Lyapunov function candidate:

$$V_{z_n} = \frac{1}{2g_n c} z_n^2 \quad (3.50)$$

Its derivative along (3.49) is

$$\dot{V}_{z_n} = \frac{1}{g_n c} z_n \dot{z}_n = z_n [Q_n(Z_n) + v(t) + \frac{h(v)}{c} + \frac{1}{g_n c} d_n(t)] \quad (3.51)$$

where $Q_n(Z_n) = (g_n c)^{-1} f_n(\bar{x}_n) - (g_n c)^{-1} \dot{\omega}_n$ with $Z_n = [\bar{x}_n, \dot{\omega}_n] \in \Omega_{Z_n} \subset \mathbb{R}^{n+1}$.

To compensate for the unknown function $Q_n(Z_n)$, we can use the RBFNNs, $\hat{W}_n^T S(Z_n)$, with $\hat{W}_n \in \mathbb{R}^{l \times 1}$, $S(Z_n) \in \mathbb{R}^{l \times 1}$, and the NN node number $l > 1$, to approximate the function $Q_n(Z_n)$ on the compact set Ω_{Z_n} as follows

$$Q_n(Z_n) = \hat{W}_n^T S(Z_n) - \tilde{W}_n^T S(Z_n) + \varepsilon_n(Z_n) \quad (3.52)$$

where the approximation error $\varepsilon_n(Z_n)$ satisfies $|\varepsilon_n(Z_n)| \leq \varepsilon_n^*$ with a positive constant ε_n^* .

Substituting (3.52) into (3.55) and according to Assumptions 3.1, 3.3-3.5, we obtain that

$$\dot{V}_{z_n} \leq z_n [\hat{W}_n^T S(Z_n) - \tilde{W}_n^T S(Z_n) + v(t)] + |z_n| D_n \quad (3.53)$$

where $D_n = \frac{h_{\max}}{c_{\min}} + \frac{d_n \max}{g_n \min c_{\min}} + \varepsilon_n^*$.

Choose the following control law:

$$v(t) = -k_n z_n - \hat{W}_n^T S(Z_n) - \tanh\left(\frac{z_n}{\epsilon}\right) \hat{D}_n \quad (3.54)$$

3.1 Strict-Feedback Systems

where $k_n > 0$, $\epsilon > 0$, \hat{D}_n is the estimate of D_n .

Substituting (3.54) into (3.53), and using the property of the hyperbolic tangent function as (3.15), we obtain that

$$\begin{aligned}\dot{V}_{z_n} &\leq -k_n z_n^2 - z_n \tilde{W}_n^T S(Z_n) + z_n \varepsilon_n(Z_n) - z_n \tanh\left(\frac{z_n}{\epsilon}\right) \hat{D} + |z_n| D \\ &\leq -k_n z_n^2 - z_n \tilde{W}_n^T S(Z_n) + z_n \varepsilon_n(Z_n) - z_n \tanh\left(\frac{z_n}{\epsilon}\right) \tilde{D} + |z_n| D - z_n \tanh\left(\frac{z_n}{\epsilon}\right) D \\ &\leq -k_n z_n^2 - z_n \tilde{W}_n^T S(Z_n) - z_n \tanh\left(\frac{z_n}{\epsilon}\right) \tilde{D}_n + 0.2785\epsilon D_n\end{aligned}\quad (3.55)$$

where $\tilde{D}_n = \hat{D}_n - D_n$.

Consider the following Lyapunov function candidate:

$$V_n = V_{z_n} + \frac{1}{2} \tilde{W}_n^T \Gamma_n^{-1} \tilde{W}_n + \frac{1}{2\gamma_{d_n}} \tilde{D}_n^2 \quad (3.56)$$

where $\Gamma_n = \Gamma_n^T \in \mathbb{R}^{l \times l} > 0$, $\gamma_{d_n} > 0$.

Its time derivative along (3.55) is

$$\begin{aligned}\dot{V}_n &= \dot{V}_{z_n} + \tilde{W}_n^T \Gamma_n^{-1} \dot{\tilde{W}}_n + \frac{1}{\gamma_{d_n}} \tilde{D}_n \dot{\tilde{D}}_n \\ &\leq -k_n z_n^2 - z_n \tilde{W}_n^T S(Z_n) - z_n \tanh\left(\frac{z_n}{\epsilon}\right) \tilde{D}_n + 0.2785\epsilon D_n \\ &\quad + \tilde{W}_n^T \Gamma_n^{-1} \dot{\tilde{W}}_n + \frac{1}{\gamma_{d_n}} \tilde{D}_n \dot{\tilde{D}}_n\end{aligned}\quad (3.57)$$

Choose the following adaptation laws:

$$\dot{\tilde{W}}_n = \Gamma_n [z_n S(Z_n) - \sigma_n \tilde{W}_n] \quad (3.58)$$

$$\dot{\tilde{D}}_n = \gamma_{d_n} [z_n \tanh\left(\frac{z_n}{\epsilon}\right) - \sigma_{d_n} \tilde{D}_n] \quad (3.59)$$

where $\sigma_n > 0$ and $\sigma_{d_n} > 0$.

Substituting (3.58) and (3.59) into (3.57) results in

$$\dot{V}_n \leq -k_n z_n^2 - \sigma_n \tilde{W}_n^T \tilde{W}_n - \sigma_{d_n} \tilde{D}_n \hat{D}_n + 0.2785\epsilon D_n \quad (3.60)$$

The following theorem shows the stability and control performance of the closed-loop adaptive system.

3.1 Strict-Feedback Systems

Theorem 3.1 *Consider the closed-loop system consisting of the plant (3.5) under Assumptions 3.1-3.5, the controller (3.54), and adaption laws (3.35)(3.36). For bounded initial conditions, there exist constants $p > 0$, $k_i > 0$, $\tau_i > 0$, $\lambda_{\max}(\Gamma_i^{-1})$, $\sigma_i > 0$, γ_{d_i} and $\sigma_{d_i} > 0$, satisfying $V = \sum_{i=1}^n V_i \leq p$, such that the overall closed-loop control system is semi-globally stable in the sense that all of the signals in the closed-loop system are bounded, and the tracking error is smaller than a prescribed error bound.*

Proof: Consider the Lyapunov function candidate

$$V = \sum_{i=1}^n V_i$$

The derivative of V with respect to time is:

$$\dot{V} = \sum_{i=1}^n \dot{V}_i \quad (3.61)$$

Substitute (3.27), (3.48) and (3.60) into (3.61), it follows that

$$\begin{aligned} \dot{V} \leq & -(k_1 - 2)z_1^2 - \sum_{i=2}^{n-1} (k_i - 2\frac{1}{4})z_i^2 - (k_n - \frac{1}{4})z_n^2 - \sum_{i=1}^n \sigma_i \tilde{W}_i^T \hat{W}_i - \sum_{i=1}^n \sigma_{d_i} \tilde{D}_i \hat{D}_i \\ & + \sum_{i=1}^{n-1} \left[-\frac{y_{i+1}^2}{\tau_{i+1}} + 1\frac{1}{4}y_{i+1}^2 + \frac{1}{4}\zeta_{i+1}^2 \right] + \sum_{i=1}^n 0.2785\epsilon D_i \end{aligned} \quad (3.62)$$

Since for any $B_0 > 0$ and $p > 0$, the sets $\Omega_d = \{(y_d, \dot{y}_d, \ddot{y}_d) : y_d^2 + \dot{y}_d^2 + \ddot{y}_d^2 \leq B_0\}$ and $\Omega_i = \{[\bar{z}_i^T, \bar{y}_i^T, \bar{\tilde{W}}_i^T]^T : \sum_{j=1}^i V_j \leq p\}$, $i = 1, \dots, n$ are compact in \mathbb{R}^3 and $\mathbb{R}^{2i-1+\sum_{j=1}^i l_j}$, respectively. Therefore, ζ_{i+1} has a maximum M_{i+1} on $\Omega_d \times \Omega_i$.

By completion of squares, the following inequalities hold:

$$-\sigma_i \tilde{W}_i^T \hat{W}_i \leq -\frac{\sigma_i \|\tilde{W}_i\|^2}{2} + \frac{\sigma_i \|W_i^*\|^2}{2} \quad (3.63)$$

$$-\sigma_{d_i} \tilde{D}_i \hat{D}_i \leq -\frac{\sigma_{d_i} \tilde{D}_i^2}{2} + \frac{\sigma_{d_i} D_i^2}{2} \quad (3.64)$$

Substituting (3.63) and (3.64) into (3.62) leads to

$$\begin{aligned} \dot{V} \leq & -(k_1 - 2)z_1^2 - \sum_{i=2}^{n-1} (k_i - 2\frac{1}{4})z_i^2 - (k_n - \frac{1}{4})z_n^2 - \sum_{i=1}^n \frac{\sigma_i \|\tilde{W}_i\|^2}{2} \\ & - \sum_{i=1}^n \frac{\sigma_{d_i} \tilde{D}_i^2}{2} + \sum_{i=1}^{n-1} \left[-\frac{y_{i+1}^2}{\tau_{i+1}} + 1\frac{1}{4}y_{i+1}^2 \right] + \mu \end{aligned} \quad (3.65)$$

3.1 Strict-Feedback Systems

where

$$\mu = \sum_{i=1}^n \frac{\sigma_i \|W_i^*\|^2}{2} + \sum_{i=1}^n \frac{\sigma_{d_i} D_i^2}{2} + \frac{1}{4} \sum_{i=1}^{n-1} M_{i+1}^2 + \sum_{i=1}^n 0.2785 \epsilon D_i \quad (3.66)$$

Choosing

$$\begin{aligned} \alpha_0 &\leq \min\{\sigma_{d_i} \gamma_{d_i}, \frac{\sigma_i}{\lambda_{\max}(\Gamma_i^{-1})}\}, \quad i = 1, \dots, n \\ k_1 &\geq 2 + \frac{\alpha_0}{2g_{1\min}} \\ k_i &\geq 2\frac{1}{4} + \frac{\alpha_0}{2g_{i\min}}, \quad i = 2, \dots, n-1 \\ k_n &\geq \frac{1}{4} + \frac{\alpha_0}{2g_{n\min}c_{\min}} \\ \frac{1}{\tau_i} &\geq 1\frac{1}{4} + \frac{\alpha_0}{2}, \quad i = 2, \dots, n \end{aligned} \quad (3.67)$$

and substituting them into (3.62), we obtain that

$$\dot{V} \leq -\alpha_0 V + \mu \quad (3.68)$$

If $V = p$ and $\alpha_0 > \frac{\mu}{p}$, then $\dot{V} \leq 0$. It implies that $V(t) \leq p, \forall t \geq 0$ for $V(0) \leq p$. Multiplying (3.68) by $e^{\alpha_0 t}$ and integrating over $[0, t]$ yields

$$0 \leq V(t) \leq \frac{\mu}{\alpha_0} + \left[V(0) - \frac{\mu}{\alpha_0}\right] e^{-\alpha_0 t} \quad (3.69)$$

Therefore, all signals of the closed-loop system, i.e., z_i, y_i and \hat{W}_i are uniformly ultimately bounded. Furthermore, x_i, α_i and Ω_i are also uniformly ultimately bounded. From (3.66) and (3.67), we know that for any given constants B_0, p, σ_{d_i} and σ_i , we can decrease $\lambda_{\max}(\Gamma_i^{-1})$ to make $\frac{\mu}{\alpha_0}$ arbitrarily small. Thus, the tracking error z_1 becomes arbitrarily small. This completes the proof. ■

3.1.4 Simulation Results

To demonstrate the effectiveness of the proposed approach, we consider the plant used in [16, 17]:

$$\begin{aligned} \dot{x} &= a \frac{1 - e^{-x(t)}}{1 + e^{-x(t)}} + bu(v) \\ y &= x \end{aligned} \quad (3.70)$$

3.2 Output Feedback Systems

where $a = 1$, $b = 1$, and $u(v)$ represents an output of the following backlash-like hysteresis:

$$\frac{du}{dt} = \alpha \left| \frac{dv}{dt} \right| (cv - u) + B_1 \frac{dv}{dt} \quad (3.71)$$

with $\alpha = 1$, $c = 3.1635$, and $B_1 = 0.345$. As discussed in [16], without control, i.e., $u(v) = 0$, (3.70) is unstable, since $\dot{x} = a \frac{1-e^{-x(t)}}{1+e^{-x(t)}} > 0$ for $x > 0$, and $\dot{x} = a \frac{1-e^{-x(t)}}{1+e^{-x(t)}} < 0$ for $x < 0$. The objective is to control the system output y to follow a desired trajectory $y_d = 12.5 \sin(2.3t)$.

We adopt the control law and adaption laws in (3.54) (3.58) (3.59). The following initial conditions and control design parameters are chosen as: $x(0) = u(0) = v(0) = 0.0$, $\hat{W}(0) = \hat{D}(0) = 0.0$, $k_1 = 0.3$, $\Gamma = 0.1I_{25}$, $\sigma = 0.1$, $\gamma_d = 0.1$, $\sigma_d = 0.1$, $\epsilon = 0.05$.

The simulation results are shown in Figures 3.2- 3.5. From Figure 3.2, we observe that good tracking performance is achieved and the tracking error converges to a small neighborhood of zero. At the same time, the control signal v and hysteresis output u are kept bounded, as seen in Figure 3.3. It is noted that there is a large difference between the signals v and u in Figure 3.3, which indicates the significant hysteresis effect. From Figures 3.4- 3.5, we can see that the boundedness of neural weights $\|\hat{W}\|$ and estimate of disturbance bound \hat{D} as well.

3.2 Output Feedback Systems

3.2.1 Introduction

Since the seminal work [32], great progress has been witnessed in neural networks (NNs) control of nonlinear systems, which has evolved to become a well-established technique of advanced adaptive control systems. In the earlier NN control schemes, optimization techniques were mainly used to derive parameter adaptation laws, and the feasibility of such neural control schemes were demonstrated via numerous empirical studies in off-line environments with little formal mathematical stability proofs, and firm performance guarantees. Thereafter, considerable research efforts have been

3.2 Output Feedback Systems

centered on developing on-line neural control structures and algorithms based on rigorous mathematical analysis. Several elegant adaptive NN control approaches based on Lyapunov's stability theory have been proposed for nonlinear systems with certain types of matching conditions [37, 77, 111, 123], as well as nonlinear triangular systems without the requirement of matching conditions [78, 124]. The advantage of these schemes is that the parameter adaptation laws are derived based on Lyapunov synthesis and therefore stability of the closed-loop system is guaranteed. The performance and robustness properties are readily determined. In the above works, the states of the system are required to be directly measured. However, in practice, the states might not be directly measured. Therefore, neural network output feedback control schemes have been investigated in [102, 125, 126, 127, 128]. The main trend in recent neural control research is to integrate NN, including multi-layer networks[77], radial basis function networks[111] and recurrent ones [28], with main nonlinear control design methodologies. Such integration significantly enhances the capability of control methods in handling many practical systems that are characterized by nonlinearity, uncertainty, and complexity [46, 47, 66, 112].

It is well known that NN approximation-based control relies on universal approximation property in a compact set in order to approximate unknown nonlinearities in the plant dynamics. For any initial compact set Ω^0 , as long as the arguments of the unknown function start from Ω^0 and remain within a compact superset Ω , as shown in Figure 3.1, NN approximation is valid.

Therefore, how to determine *a priori* the compact superset Ω and how to ensure the arguments of the unknown function remain within the compact superset Ω , are two open and challenging problems in the neuro-control area in [102]. One method of ensuring that the NN approximation condition holds is by careful selection of the control parameters, via rigorous transient performance analysis, so that the system states do not transgress the compact superset of approximation Ω [66, 129, 130], but the compact superset Ω is only given qualitatively, not quantitatively. Another method is to rely on sliding mode control operating in parallel to the approximation-based control, such that the compact superset Ω is rendered positively invariant [112, 131]. The compact superset Ω can be specified *a priori*, but there exist some implementation issues, such as the fixed-point problem in the input signal.

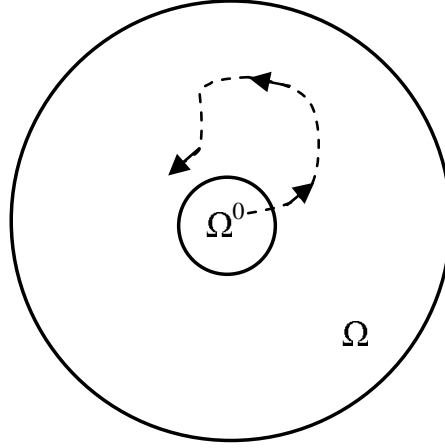


Figure 3.1: Compact sets for NN approximation

Recently, the design of barrier functions in Lyapunov synthesis has been proposed for constraint handling in Brunovsky-type systems [117], nonlinear systems in strict feedback form [116], and electrostatic microactuators [132]. Unlike conventional Lyapunov functions, which are well-defined over the entire domain and radially unbounded for global stability, a Barrier Lyapunov Function (BLF) possesses the special property of approaching infinity whenever its arguments approach some limits. By ensuring boundedness of the BLF along the system trajectories, transgression of constraints is prevented. We note that the BLF based control design methodology appears very promising in providing yet another means of tackling the NN approximation-based control problems, by actively constraining the states of the system to remain within the compact set of approximation.

In this section, we present adaptive neural control for a class of output feedback nonlinear systems preceded by unknown backlash-like hysteresis, subject to function uncertainties and bounded time-varying disturbances. The unknown functions are compensated for via on-line NN function approximation using only output measurements. To address two important neural control concerns mentioned above, the BLF is incorporated into Lyapunov synthesis by following the constructive procedures of adaptive observer backstepping design in [65]. First, for any initial compact set Ω^0 where the the argument of the unknown function belongs to, we can always construct an *a priori* compact superset Ω . Second, by ensuring the boundedness of the BLF,

3.2 Output Feedback Systems

we guarantee that the argument of the unknown function remains within the compact superset Ω , on which the NN approximation is valid. Then, the stable output tracking with guaranteed performance bounds can be achieved in the semi-global sense. In addition, the uncertainties due to the NN reconstruction error and the time-varying disturbances are collectively bounded by an unknown constant, which is handled on-line by an adaptive bounding design.

The organization of this section is as follows. The problem formulation and preliminaries are given in Section 3.2.2. Section 3.2.3 presents the state estimation filter and observer design. In Section 3.2.4, the constructive procedures of adaptive observer backstepping design are provided and the closed-loop system stability is analyzed as well. Section 3.2.5 demonstrates the feasibility of the proposed approach using a numerical example.

3.2.2 Problem Formulation and Preliminaries

Consider a class of SISO output feedback nonlinear system described by:

$$\begin{aligned}
 \dot{x}_1 &= x_2 + f_1^0(y) + f_1(y) + d_1(t) \\
 &\vdots \\
 \dot{x}_{\rho-1} &= x_{\rho} + f_{\rho-1}^0(y) + f_{\rho-1}(y) + d_{\rho-1}(t) \\
 \dot{x}_{\rho} &= x_{\rho+1} + f_{\rho}^0(y) + f_{\rho}(y) + d_{\rho}(t) + \bar{b}_m u \\
 &\vdots \\
 \dot{x}_{n-1} &= x_n + f_{n-1}^0(y) + f_{n-1}(y) + d_{n-1}(t) + \bar{b}_1 u \\
 \dot{x}_n &= f_n^0(y) + f_n(y) + d_n(t) + \bar{b}_0 u \\
 y &= x_1
 \end{aligned} \tag{3.72}$$

where x_1, \dots, x_n are system states, y is the output; $f_i^0(y)$, $i = 1, \dots, n$ are known smooth functions, which represent nominal parts of the plant and may be available using some prior physical or expert information ($f_i^0(y) = 0$ if no prior knowledge of the nonlinearity); $f_i(y)$, $i = 1, \dots, n$ are unknown smooth functions, which represent model uncertainties due to modeling errors or unmodeled dynamics; $d_i(t)$ are bounded time-varying disturbances with unknown constant bounds; $\bar{b}_m, \dots, \bar{b}_0$ are uncertain

3.2 Output Feedback Systems

constant parameters; and $u \in \mathbb{R}$ is the system input and the output of the backlash-like hysteresis, which is described as follows:

$$\frac{du}{dt} = \alpha \left| \frac{dw}{dt} \right| (cw - u) + B_1 \frac{dw}{dt} \quad (3.73)$$

where α , c , and B_1 are constants, $c > 0$ is the slope of lines satisfying $c > B_1$.

Based on the analysis in Section 2.2.1 of Chapter 2, (3.73) can be solved explicitly as follows:

$$u(t) = cw(t) + h(w) \quad (3.74)$$

where

$$h(w) = [u_0 - cw_0]e^{-\alpha(w-w_0)\text{sgn}\dot{w}} + e^{-\alpha w \text{sgn}\dot{w}} \int_{w_0}^w [B_1 - c]e^{\alpha\zeta(\text{sgn}\dot{w})} d\zeta \quad (3.75)$$

Remark 3.2 When $f_i(y)$ in (3.72) satisfy the linear-in-the-parameters (LIP) condition, i.e., $f_i(y) = \phi_i^T(y)\theta$, with $\phi_i \in \mathbb{R}^r$ known nonlinear function vector and $\theta \in \mathbb{R}^r$ unknown constant vector, system (3.72) becomes the standard output feedback nonlinear system and has been intensively investigated in [65, 133, 134]. When $f_i(y)$ do not satisfy LIP condition and $\rho = n$, adaptive observer backstepping control using neural networks has been presented for system (3.72) in [102], but without addressing two open and challenging problems in the neuro-control area mentioned in Introduction. Motivated by [102], we will incorporate a Barrier Lyapunov Function (BLF) into Lyapunov synthesis to address these two problems in the neuro-control area in this section.

Assumption 3.6 The unknown disturbance $d_i(t)$ satisfies $|d_i(t)| \leq \bar{d}_i$, where \bar{d}_i is an unknown constant.

Assumption 3.7 The sign of the high frequency gain $b_m = \bar{b}_m c$ is known.

Assumption 3.8 The relative degree $\rho = n - m$ is known and the system is minimum phase, i.e., the polynomial $B(s) = \bar{b}_m s^m + \dots + \bar{b}_1 s + \bar{b}_0$ is Hurwitz.

3.2 Output Feedback Systems

Assumption 3.9 *There exist positive constants $\underline{Y}_0, \bar{Y}_0, A_0, Y_1, Y_2, \dots, Y_n$ satisfying $\max\{\underline{Y}_0, \bar{Y}_0\} \leq A_0$ such that the reference signal $y_r(t)$ and its p th order derivatives are piecewise continuous, known and bounded, which satisfy $-\underline{Y}_0 \leq y_r(t) \leq \bar{Y}_0$, $|\dot{y}_r(t)| < Y_1$, $|\ddot{y}_r(t)| < Y_2$, ..., $|y_r^{(n)}(t)| < Y_n$, $\forall t \geq 0$.*

Assumption 3.10 *There exist a constant h_{\max} such that $h(w) \leq h_{\max}$.*

Assuming that only the output signal y is measured, the control objective is to drive the output y to track the given reference signal $y_r(t)$ within a neighborhood of zero, while keeping that all of the signals in the closed-loop system bounded.

3.2.3 State Estimation Filter and Observer Design

Since only the output signal y is measured, some filters should be designed first which will provide “virtual estimates” of the unmeasured state variables x_2, \dots, x_n . The unknown function $f_i(y) : \mathbb{R} \rightarrow \mathbb{R}$ in the plant (3.72) is approximated by the radial basis function neural networks (RBFNNs) in Section 2.3.3:

$$f_i(y) = \phi_i^T(y)\theta_i^* + \varepsilon_i(y) \quad (3.76)$$

where the input $y \in \Omega_y \subset \mathbb{R}$; $\theta_i^* = [\theta_{i1}^*, \dots, \theta_{il_i}^*]^T$ are ideal constant weights; and $\varepsilon_i(y)$ is the approximation error satisfying $|\varepsilon_i(y)| \leq \varepsilon_i^*$ with constant $\varepsilon_i^* > 0$ for all $y \in \Omega_y$; the vector of smooth basis functions $\phi_i = [\phi_{i1}, \phi_{i2}, \dots, \phi_{il_i}]^T \in R^{l_i}$, $\phi_{ij}(y)$ being chosen as the commonly used Gaussian functions $\phi_{ij}(y) = \exp\left[\frac{-(y-\mu_{ij})^T(y-\mu_{ij})}{\eta_i^2}\right]$, $j = 1, 2, \dots, l_i$, where μ_{ij} is the center of the receptive field and η_i is the width of the Gaussian function.

Remark 3.3 *The stability results obtained in NN control literature are semiglobal in the sense that, as long as the input variable of the NNs remains within some specified compact set $\Omega_y \subset \mathbb{R}$, where Ω_y can be made as large as desired, there exists a controller with sufficiently large number of NN nodes such that all the signals in the closed-loop remain bounded. However, how to determine the compact set Ω_y and make the input variable of the NNs remain within the compact set are two open and challenging problems in the NN control field as suggested in [102]. One possible solution*

3.2 Output Feedback Systems

is by careful selection of the control parameters via rigorous transient performance analysis [66, 129, 130], but the compact set is only given qualitatively, not quantitatively. Another method is to rely on a sliding mode control mechanism to render the compact set positively invariant [112, 131]. The compact set can be specified a priori, but there exist some implementation issues, such as the fixed-point problem about the input signal. Therefore, new solutions are sought.

Remark 3.4 To address two open and challenging problems in the neuro-control area mentioned in Remark 3.3, the Barrier Lyapunov Function (BLF), $V_1 = \frac{1}{2} \log \frac{k_{b_1}^2}{k_{b_1}^2 - z_1^2}$, introduced in Section 2.4, will be adopted, which was proposed for handling constraints of states and output in [116, 117, 132]. We note that the BLF based control design methodology appears very promising in providing yet another means of tackling the NN approximation-based control problems, by actively constraining the states of the system to remain within the compact set of approximation.

Substituting (3.74) and (3.76) into (3.72) and after some manipulations, we obtain that

$$\dot{x} = Ax + F^0(y) + \Phi(y)\theta^* + \Delta(y, t) + \begin{bmatrix} 0 \\ b \end{bmatrix} w \quad (3.77)$$

where

$$\begin{aligned} A &= \begin{bmatrix} 0 & 1 & 0 & \cdots & 0 \\ 0 & 0 & 1 & \cdots & 0 \\ \vdots & \vdots & \vdots & \ddots & \vdots \\ 0 & 0 & 0 & \cdots & 1 \\ 0 & 0 & 0 & \cdots & 0 \end{bmatrix} \in \mathbb{R}^{n \times n}, \quad F^0(y) = \begin{bmatrix} f_1^0(y) \\ \vdots \\ f_n^0(y) \end{bmatrix} \in \mathbb{R}^{n \times 1}, \\ \Phi(y) &= \begin{bmatrix} \Phi_1^T(y) \\ \vdots \\ \Phi_n^T(y) \end{bmatrix} = \begin{bmatrix} \phi_1^T(y) & 0 & \cdots & 0 \\ 0 & \phi_2^T(y) & \cdots & 0 \\ \vdots & \vdots & \ddots & \vdots \\ 0 & 0 & \cdots & \phi_n^T(y) \end{bmatrix} \in \mathbb{R}^{n \times ln}, \\ \theta^* &= \begin{bmatrix} \theta_1^* \\ \vdots \\ \theta_n^* \end{bmatrix} \in \mathbb{R}^{ln \times 1}, \quad b = \begin{bmatrix} b_m \\ \vdots \\ b_0 \end{bmatrix} = \begin{bmatrix} \bar{b}_m c \\ \vdots \\ \bar{b}_0 c \end{bmatrix} \in \mathbb{R}^{(m+1) \times 1}, \end{aligned}$$

3.2 Output Feedback Systems

$$\Delta(y, t) = \begin{bmatrix} \Delta_1(y, t) \\ \vdots \\ \Delta_{\rho-1}(y, t) \\ \Delta_\rho(y, t) \\ \vdots \\ \Delta_n(y, t) \end{bmatrix} = \begin{bmatrix} \varepsilon_1(y) + d_1(t) \\ \vdots \\ \varepsilon_{\rho-1}(y) + d_{\rho-1}(t) \\ \varepsilon_\rho(y) + d_\rho(t) + \bar{b}_m h(w) \\ \vdots \\ \varepsilon_n(y) + d_n(t) + \bar{b}_0 h(w) \end{bmatrix} \in \mathbb{R}^{n \times 1} \quad (3.78)$$

From Assumptions 3.6 and 3.10, we know that there exists a bounding parameter ψ such that $|\Delta_i(y, t)| \leq \psi$, where ψ is unknown and will be estimated by $\hat{\psi}$.

Choose the K-filters [65] as follows:

$$\dot{\xi} = A_0 \xi + ky + F^0(y) \quad (3.79)$$

$$\dot{\Xi} = A_0 \Xi + \Phi(y) \quad (3.80)$$

$$\dot{\lambda} = A_0 \lambda + e_n w \quad (3.81)$$

$$v_i = A_0^i \lambda, \quad i = 0, 1, \dots, m \quad (3.82)$$

where $k = [k_1, \dots, k_n]^T$ such that $A_0 = A - ke_1^T$ is Hurwitz, and e_i is the i th coordinate vector in \mathbb{R}^n .

By constructing the state estimates as follows:

$$\hat{x}(t) = \xi + \Xi^T \theta^* + \sum_{i=0}^m b_i v_i \quad (3.83)$$

it is straightforward to verify that the dynamics of the observation error, $\tilde{x} = x - \hat{x}$, are given by

$$\dot{\tilde{x}} = A_0 \tilde{x} + \Delta(y, t) \quad (3.84)$$

Since A_0 is Hurwitz, it can be shown that the error system (3.84) with state \tilde{x} is input state stable (ISS) with respect to the term $\Delta(y, t)$. Furthermore, the dynamic equation of y can be expressed as

$$\begin{aligned} \dot{y} &= x_2 + f_1^0(y) + \Phi_1^T(y) \theta^* + \Delta_1(y, t) \\ &= b_m v_{m,2} + \xi_2 + f_1^0(y) + \bar{\Omega}^T \Theta + \Delta_1(y, t) + \tilde{x}_2 \end{aligned} \quad (3.85)$$

3.2 Output Feedback Systems

with

$$\begin{aligned}\Theta &= [b_m, \dots, b_0, \theta^{*T}]^T \\ \Omega &= [v_{m,2}, v_{m-1,2}, \dots, v_{0,2}, \Xi_2 + \Phi_1^T]^T \\ \bar{\Omega} &= [0, v_{m-1,2}, \dots, v_{0,2}, \Xi_2 + \Phi_1^T]^T\end{aligned}$$

where \tilde{x}_2 , $v_{i,2}$, ξ_2 and Ξ_2 denote the second entries of \tilde{x} , v_i , ξ and Ξ , respectively, and y , v_i , ξ and Ξ are all available signals.

Combining system (3.85) with the filters (3.79)-(3.82), system (3.72) is represented as

$$\dot{y} = b_m v_{m,2} + \xi_2 + f_1^0(y) + \bar{\Omega}^T \Theta + \Delta_1(y, t) + \tilde{x}_2 \quad (3.86)$$

$$\dot{v}_{m,i} = v_{m,i+1} - k_i v_{m,1}, \quad i = 2, 3, \dots, \rho - 1 \quad (3.87)$$

$$\dot{v}_{m,\rho} = v_{m,\rho+1} - k_\rho v_{m,1} + w \quad (3.88)$$

In the next section, adaptive observer backstepping design will be presented for the system (3.86)-(3.88) with constructive procedures, where states y , $v_{m,2}$, \dots , $v_{m,\rho}$ are available.

3.2.4 Adaptive Observer Backstepping Design

In this section, we present the adaptive control design using the backstepping technique with tuning functions in ρ steps.

Define the following error coordinates:

$$z_1 = y - y_r \quad (3.89)$$

$$z_i = v_{m,i} - \alpha_{i-1} - \hat{\varrho} y_r^{(i-1)}, \quad i = 2, 3, \dots, \rho \quad (3.90)$$

where $\hat{\varrho}$ is an estimate of $\varrho = \frac{1}{b_m}$ and α_{i-1} is the stabilizing functions at each step and will be defined later.

Step 1: From (3.86) and (3.89), the derivative of z_1 is given by

$$\dot{z}_1 = b_m v_{m,2} + \xi_2 + f_1^0(y) + \bar{\Omega}^T \Theta + \Delta_1(y, t) + \tilde{x}_2 - \dot{y}_r \quad (3.91)$$

3.2 Output Feedback Systems

By substituting (3.90) for $i = 2$ into (3.91) and using $\tilde{\varrho} = \varrho - \hat{\varrho}$, we have

$$\dot{z}_1 = b_m \alpha_1 + \xi_2 + f_1^0(y) + \bar{\Omega}^T \Theta + \Delta_1(y, t) + \tilde{x}_2 - b_m \tilde{\varrho} \dot{y}_r + b_m z_2 \quad (3.92)$$

For any initial compact set $\Omega_y^0 := \{y \in \mathbb{R} \mid |y| \leq k_0, k_0 > 0\} \subset \mathbb{R}$, which $y(0)$ belongs to, we can always specify another compact set $\Omega_y := \{y \in \mathbb{R} \mid |y| \leq k_{c1}, k_{c1} > k_0 + A_0 + |y_r(0)|\} \subset \mathbb{R}$, which is a superset of Ω_y^0 and can be made as large as desired. As long as the input variable of the NNs, y , remains within this prefixed compact Ω_y , the NN approximation is valid. Borrowing the idea of the BLF based control in [116, 132], to design a control that does not drive y out of the interval $|y| < k_{c1}$, we require that $|z_1| < k_{b1}$ with $k_{b1} = k_{c1} - A_0$ and choose the following Lyapunov function candidate, which incorporate the symmetric Barrier Lyapunov Function candidate introduced in Remark 3.4:

$$V_1 = \frac{1}{2} \log \frac{k_{b1}^2}{k_{b1}^2 - z_1^2} + \frac{1}{2} \tilde{\Theta}^T \Gamma^{-1} \tilde{\Theta} + \frac{|b_m|}{2\gamma_\varrho} \tilde{\varrho}^2 + \frac{1}{2\gamma_\psi} \tilde{\psi}^2 + \frac{1}{2\gamma_1} \tilde{x}^T P \tilde{x} \quad (3.93)$$

where $\tilde{\Theta} = \Theta - \hat{\Theta}$, $\hat{\Theta}$ is the estimate of Θ , $\tilde{\psi} = \psi - \hat{\psi}$, Γ is a positive definite design matrix, γ_ϱ , γ_ψ and γ_1 are positive design parameters, and P is a definite positive matrix such that

$$PA_0 + A_0^T P = -I$$

where $P = P^T > 0$.

The derivative of V_1 along (3.92) is given by

$$\begin{aligned} \dot{V}_1 &= \frac{z_1 \dot{z}_1}{k_{b1}^2 - z_1^2} - \tilde{\Theta}^T \Gamma^{-1} \dot{\tilde{\Theta}} - \frac{|b_m|}{\gamma_\varrho} \tilde{\varrho} \dot{\tilde{\varrho}} - \frac{1}{\gamma_\psi} \tilde{\psi} \dot{\tilde{\psi}} - \frac{1}{2\gamma_1} \tilde{x}^T \dot{\tilde{x}} \\ &= \frac{z_1}{k_{b1}^2 - z_1^2} [b_m \alpha_1 + \xi_2 + f_1^0(y) + \bar{\Omega}^T \Theta + \Delta_1(y, t) + \tilde{x}_2 - b_m \tilde{\varrho} \dot{y}_r + b_m z_2] \\ &\quad - \tilde{\Theta}^T \Gamma^{-1} \dot{\tilde{\Theta}} - \frac{|b_m|}{\gamma_\varrho} \tilde{\varrho} \dot{\tilde{\varrho}} - \frac{1}{\gamma_\psi} \tilde{\psi} \dot{\tilde{\psi}} - \frac{1}{2\gamma_1} \tilde{x}^T \dot{\tilde{x}} \end{aligned} \quad (3.94)$$

Design the following stabilizing functions:

$$\alpha_1 = \hat{\varrho} \bar{\alpha}_1 \quad (3.95)$$

$$\bar{\alpha}_1 = -c_1 z_1 - \xi_2 - f_1^0(y) - \bar{\Omega}^T \hat{\Theta} - \frac{\gamma_1 z_1}{k_{b1}^2 - z_1^2} - \hat{\psi} \tanh \left(\frac{\frac{z_1}{k_{b1}^2 - z_1^2}}{\delta_1} \right) \quad (3.96)$$

3.2 Output Feedback Systems

where c_1 and δ_1 are positive design parameters.

It is easy to know that

$$b_m \alpha_1 = b_m \hat{\varrho} \bar{\alpha}_1 = \bar{\alpha}_1 - b_m \tilde{\varrho} \bar{\alpha}_1 \quad (3.97)$$

Substituting (3.95)-(3.97) into (3.94) leads to

$$\begin{aligned} \dot{V}_1 \leq & -\frac{c_1 z_1^2}{k_{b_1}^2 - z_1^2} + \frac{z_1}{k_{b_1}^2 - z_1^2} (\bar{\Omega}^T \tilde{\Theta} + b_m z_2) - \frac{z_1}{k_{b_1}^2 - z_1^2} b_m \tilde{\varrho} (\dot{y}_r + \bar{\alpha}_1) + \frac{z_1 \tilde{x}_2}{k_{b_1}^2 - z_1^2} \\ & - \gamma_1 \left(\frac{z_1}{k_{b_1}^2 - z_1^2} \right)^2 + \psi \left| \frac{z_1}{k_{b_1}^2 - z_1^2} \right| - \hat{\psi} \frac{z_1}{k_{b_1}^2 - z_1^2} \tanh \left(\frac{\frac{z_1}{k_{b_1}^2 - z_1^2}}{\delta_1} \right) - \tilde{\Theta}^T \Gamma^{-1} \dot{\tilde{\Theta}} \\ & - \frac{|b_m|}{\gamma_{\varrho}} \tilde{\varrho} \dot{\varrho} - \frac{1}{\gamma_{\psi}} \tilde{\psi} \dot{\psi} - \frac{1}{2\gamma_1} \tilde{x}^T \tilde{x} \end{aligned} \quad (3.98)$$

For the second term in the right hand of (3.98), we can rewrite it as

$$\begin{aligned} \frac{z_1}{k_{b_1}^2 - z_1^2} (\bar{\Omega}^T \tilde{\Theta} + b_m z_2) &= \frac{z_1}{k_{b_1}^2 - z_1^2} [\bar{\Omega}^T \tilde{\Theta} + (v_{m,2} - \hat{\varrho} \dot{y}_r - \alpha_1) e_1^T \tilde{\Theta} + \hat{b}_m z_2] \\ &= \frac{z_1}{k_{b_1}^2 - z_1^2} \{ [\Omega - \hat{\varrho} (\dot{y}_r + \bar{\alpha}_1) e_1]^T \tilde{\Theta} + \hat{b}_m z_2 \} \end{aligned} \quad (3.99)$$

By using Young's inequality, the fourth term in the right hand of (3.98) becomes

$$\frac{z_1 \tilde{x}_2}{k_{b_1}^2 - z_1^2} \leq \gamma_1 \left(\frac{z_1}{k_{b_1}^2 - z_1^2} \right)^2 + \frac{\tilde{x}_2^2}{4\gamma_1} \leq \gamma_1 \left(\frac{z_1}{k_{b_1}^2 - z_1^2} \right)^2 + \frac{1}{4\gamma_1} \tilde{x}^T \tilde{x} \quad (3.100)$$

Due to $\tilde{\psi} = \psi - \hat{\psi}$ and the property of the hyperbolic tangent function

$$0 \leq |\eta| - \eta \tanh\left(\frac{\eta}{\delta}\right) \leq 0.2785\delta \quad (3.101)$$

the sixth and seventh terms in the right hand of (3.98) becomes

$$\begin{aligned} & \psi \left| \frac{z_1}{k_{b_1}^2 - z_1^2} \right| - \hat{\psi} \frac{z_1}{k_{b_1}^2 - z_1^2} \tanh \left(\frac{\frac{z_1}{k_{b_1}^2 - z_1^2}}{\delta_1} \right) \\ &= \psi \left\{ \left| \frac{z_1}{k_{b_1}^2 - z_1^2} \right| - \frac{z_1}{k_{b_1}^2 - z_1^2} \tanh \left(\frac{\frac{z_1}{k_{b_1}^2 - z_1^2}}{\delta_1} \right) \right\} + \tilde{\psi} \frac{z_1}{k_{b_1}^2 - z_1^2} \tanh \left(\frac{\frac{z_1}{k_{b_1}^2 - z_1^2}}{\delta_1} \right) \\ &\leq 0.2785\delta_1 \psi + \tilde{\psi} \frac{z_1}{k_{b_1}^2 - z_1^2} \tanh \left(\frac{\frac{z_1}{k_{b_1}^2 - z_1^2}}{\delta_1} \right) \end{aligned} \quad (3.102)$$

3.2 Output Feedback Systems

Substituting (3.99)-(3.102) into (3.98), we have

$$\begin{aligned} \dot{V}_1 \leq & -\frac{c_1 z_1^2}{k_{b_1}^2 - z_1^2} + \frac{\hat{b}_m z_1 z_2}{k_{b_1}^2 - z_1^2} + \tilde{\Theta}^T \left\{ \frac{z_1}{k_{b_1}^2 - z_1^2} [\Omega - \hat{\varrho}(\dot{y}_r + \bar{\alpha}_1)e_1] - \Gamma^{-1} \dot{\hat{\Theta}} \right\} \\ & - \frac{|b_m|}{\gamma_\varrho} \tilde{\varrho} \left[\gamma_\varrho \text{sign}(b_m)(\dot{y}_r + \bar{\alpha}_1) \frac{z_1}{k_{b_1}^2 - z_1^2} + \dot{\hat{\varrho}} \right] \\ & + \tilde{\psi} \left[\frac{z_1}{k_{b_1}^2 - z_1^2} \tanh \left(\frac{\frac{z_1}{k_{b_1}^2 - z_1^2}}{\delta_1} \right) - \frac{1}{\gamma_\psi} \dot{\hat{\psi}} \right] - \frac{1}{4\gamma_1} \tilde{x}^T \tilde{x} + 0.2785\delta_1\psi \end{aligned} \quad (3.103)$$

Choose the adaptation law $\dot{\hat{\varrho}}$ and the tuning functions $\tau_{1\theta}$ and $\tau_{1\psi}$ as follows:

$$\dot{\hat{\varrho}} = -\gamma_\varrho \left[\text{sign}(b_m)(\dot{y}_r + \bar{\alpha}_1) \frac{z_1}{k_{b_1}^2 - z_1^2} + \sigma_\varrho \hat{\varrho} \right] \quad (3.104)$$

$$\tau_{1\theta} = \frac{z_1}{k_{b_1}^2 - z_1^2} [\Omega - \hat{\varrho}(\dot{y}_r + \bar{\alpha}_1)e_1] - \sigma_\theta \hat{\Theta} \quad (3.105)$$

$$\tau_{1\psi} = \frac{z_1}{k_{b_1}^2 - z_1^2} \tanh \left(\frac{\frac{z_1}{k_{b_1}^2 - z_1^2}}{\delta_1} \right) - \sigma_\psi \hat{\psi} \quad (3.106)$$

Substituting (3.104) and (3.106) into (3.103) results in

$$\begin{aligned} \dot{V}_1 \leq & -\frac{c_1 z_1^2}{k_{b_1}^2 - z_1^2} + \frac{\hat{b}_m z_1 z_2}{k_{b_1}^2 - z_1^2} + \tilde{\Theta}^T (\tau_{1\theta} - \Gamma^{-1} \dot{\hat{\Theta}}) + \tilde{\psi} (\tau_{1\psi} - \frac{1}{\gamma_\psi} \dot{\hat{\psi}}) + \sigma_\theta \tilde{\Theta} \hat{\Theta} + \sigma_\psi \tilde{\psi} \hat{\psi} \\ & + \sigma_\varrho |b_m| \tilde{\varrho} \hat{\varrho} - \frac{1}{4\gamma_1} \tilde{x}^T \tilde{x} + 0.2785\delta_1\psi \end{aligned} \quad (3.107)$$

with the coupling term $\frac{\hat{b}_m z_1 z_2}{k_{b_1}^2 - z_1^2}$ to be canceled in the subsequent step.

Step 2: The derivative of z_2 can be obtained from (3.87) and (3.90) as follows

$$\begin{aligned} \dot{z}_2 &= \dot{v}_{m,2} - \dot{\alpha}_1 - \hat{\varrho} \dot{y}_r - \hat{\varrho} \ddot{y}_r \\ &= v_{m,3} - k_2 v_{m,1} - \dot{\alpha}_1 - \hat{\varrho} \dot{y}_r - \hat{\varrho} \ddot{y}_r \end{aligned} \quad (3.108)$$

From (3.95) and (3.96), we know that α_1 is a function of $y, \xi, \Xi, \hat{\Theta}, \hat{\varrho}, \hat{\psi}, y_r, \bar{\lambda}_{m+1}$, thus, its derivative $\dot{\alpha}_1$ can be expressed as

$$\begin{aligned} \dot{\alpha}_1 &= \frac{\partial \alpha_1}{\partial y} (b_m v_{m,2} + \xi_2 + f_1^0(y) + \bar{\Omega}^T \Theta + \Delta_1(y, t) + \tilde{x}_2) + \frac{\partial \alpha_1}{\partial y_r} \dot{y}_r \\ &+ \sum_{j=1}^{m+1} \frac{\partial \alpha_1}{\partial \lambda_j} (-k_j \lambda_1 + \lambda_{j+1}) + \frac{\partial \alpha_1}{\partial \xi} (A_0 \xi + ky + F^0(y)) \\ &+ \frac{\partial \alpha_1}{\partial \Xi} (A_0 \Xi^T + \Phi(y)) + \frac{\partial \alpha_1}{\partial \hat{\Theta}} \dot{\hat{\Theta}} + \frac{\partial \alpha_1}{\partial \hat{\varrho}} \dot{\hat{\varrho}} + \frac{\partial \alpha_1}{\partial \hat{\psi}} \dot{\hat{\psi}} \end{aligned} \quad (3.109)$$

3.2 Output Feedback Systems

Substituting (3.109) into (3.108), we have

$$\dot{z}_2 = v_{m,3} - \hat{\rho}\ddot{y}_r - \beta_2 - \frac{\partial\alpha_1}{\partial y}(\Omega^T\tilde{\Theta} + \Delta_1(y, t) + \tilde{x}_2) - \frac{\partial\alpha_1}{\partial\hat{\Theta}}\dot{\Theta} - \frac{\partial\alpha_1}{\partial\hat{\psi}}\dot{\psi} \quad (3.110)$$

where

$$\begin{aligned} \beta_2 = & \frac{\partial\alpha_1}{\partial y} \left(\xi_2 + f_1^0(y) + \Omega^T\hat{\Theta} \right) + k_2 v_{m,1} + \frac{\partial\alpha_1}{\partial y_r} \dot{y}_r + \left(\frac{\partial\alpha_1}{\partial\hat{\rho}} + \dot{y}_r \right) \hat{\rho} \\ & + \sum_{j=1}^{m+1} \frac{\partial\alpha_1}{\partial\lambda_j} (-k_j \lambda_1 + \lambda_{j+1}) + \frac{\partial\alpha_1}{\partial\xi} (A_0\xi + ky + F^0(y)) \\ & + \frac{\partial\alpha_1}{\partial\Xi} (A_0\Xi^T + \Phi(y)) \end{aligned} \quad (3.111)$$

Taking $v_{m,3}$ as a virtual control input and using $z_3 = v_{m,3} - \alpha_2 - \hat{\rho}\ddot{y}_r$, we have

$$\dot{z}_2 = z_3 + \alpha_2 - \beta_2 - \frac{\partial\alpha_1}{\partial y}(\Omega^T\tilde{\Theta} + \Delta_1(y, t) + \tilde{x}_2) - \frac{\partial\alpha_1}{\partial\hat{\Theta}}\dot{\Theta} - \frac{\partial\alpha_1}{\partial\hat{\psi}}\dot{\psi} \quad (3.112)$$

Since z_2 does not need to be constrained, we choose Lyapunov function candidate by augmenting V_1 with a quadratic function as follows

$$V_2 = V_1 + \frac{1}{2}z_2^2 + \frac{1}{2\gamma_2}\tilde{x}^T P \tilde{x} \quad (3.113)$$

where γ_2 is a positive design parameter.

The derivative of V_2 along (3.107) and (3.112) is given by

$$\begin{aligned} \dot{V}_2 \leq & -\frac{c_1 z_1^2}{k_{b_1}^2 - z_1^2} + \frac{\hat{b}_m z_1 z_2}{k_{b_1}^2 - z_1^2} + z_2 \left[z_3 + \alpha_2 - \beta_2 - \frac{\partial\alpha_1}{\partial y}(\Omega^T\tilde{\Theta} + \Delta_1(y, t) + \tilde{x}_2) \right. \\ & \left. - \frac{\partial\alpha_1}{\partial\hat{\Theta}}\dot{\Theta} - \frac{\partial\alpha_1}{\partial\hat{\psi}}\dot{\psi} \right] + \tilde{\Theta}^T(\tau_{1\theta} - \Gamma^{-1}\dot{\Theta}) + \tilde{\psi}(\tau_{1\psi} - \frac{1}{\gamma_\psi}\dot{\psi}) + \sigma_\theta\tilde{\Theta}\dot{\Theta} + \sigma_\psi\tilde{\psi}\dot{\psi} \\ & + \sigma_\rho|b_m|\tilde{\rho}\dot{\rho} - \frac{1}{4\gamma_1}\tilde{x}^T\tilde{x} + 0.2785\delta_1\psi - \frac{1}{2\gamma_2}\tilde{x}^T\tilde{x} \end{aligned} \quad (3.114)$$

Choose the second stabilizing function α_2 and tuning function τ_2 :

$$\begin{aligned} \alpha_2 = & -\frac{\hat{b}_m z_1}{k_{b_1}^2 - z_1^2} - c_2 z_2 + \beta_2 + \frac{\partial\alpha_1}{\partial\hat{\Theta}}\Gamma\tau_{2\theta} + \frac{\partial\alpha_1}{\partial\hat{\psi}}\gamma_\psi\tau_{2\psi} - \hat{\psi}\frac{\partial\alpha_1}{\partial y}\tanh\left(\frac{z_2\frac{\partial\alpha_1}{\partial y}}{\delta_2}\right) \\ & - \gamma_2\left(\frac{\partial\alpha_1}{\partial y}\right)^2 z_2 \end{aligned} \quad (3.115)$$

$$\tau_{2\theta} = \tau_{1\theta} - z_2\frac{\partial\alpha_1}{\partial y}\Omega \quad (3.116)$$

$$\tau_{2\psi} = \tau_{1\psi} + z_2\frac{\partial\alpha_1}{\partial y}\tanh\left(\frac{z_2\frac{\partial\alpha_1}{\partial y}}{\delta_2}\right) \quad (3.117)$$

3.2 Output Feedback Systems

where c_2 and δ_2 are positive design parameters.

Substituting (3.115) and (3.117) into (3.118), we have

$$\begin{aligned} \dot{V}_2 \leq & -\frac{c_1 z_1^2}{k_{b_1}^2 - z_1^2} - c_2 z_2^2 + z_2 z_3 + \tilde{\Theta}^T (\tau_{2\theta} - \Gamma^{-1} \dot{\hat{\Theta}}) + \tilde{\psi} (\tau_{2\psi} - \frac{1}{\gamma_\psi} \dot{\hat{\psi}}) \\ & + z_2 \frac{\partial \alpha_1}{\partial \hat{\Theta}} (\Gamma \tau_{2\theta} - \dot{\hat{\Theta}}) + z_2 \frac{\partial \alpha_1}{\partial \hat{\psi}} (\gamma_\psi \tau_{2\psi} - \dot{\hat{\psi}}) + \sigma_\theta \tilde{\Theta} \hat{\Theta} + \sigma_\psi \tilde{\psi} \hat{\psi} + \sigma_\rho |b_m| \tilde{\theta} \hat{\theta} \\ & - \sum_{i=1}^2 \frac{1}{4\gamma_i} \tilde{x}^T \tilde{x} + \sum_{i=1}^2 0.2785 \delta_i \psi \end{aligned} \quad (3.118)$$

Step $i = 3, \dots, \rho$. Similar to the procedures in Step 2, choose the following stabilizing functions α_i and tuning functions τ_i for $i = 3, \dots, \rho$:

$$\begin{aligned} \alpha_i = & -z_{i-1} - c_i z_i + \beta_i + \frac{\partial \alpha_{i-1}}{\partial \hat{\Theta}} \Gamma \tau_{i\theta} + \frac{\partial \alpha_{i-1}}{\partial \hat{\psi}} \gamma_\psi \tau_{i\psi} - \hat{\psi} \frac{\partial \alpha_{i-1}}{\partial y} \tanh \left(\frac{z_i \frac{\partial \alpha_{i-1}}{\partial y}}{\delta_i} \right) \\ & - \gamma_i \left(\frac{\partial \alpha_{i-1}}{\partial y} \right)^2 z_i - \left(\sum_{k=2}^{i-1} z_k \frac{\partial \alpha_{k-1}}{\partial \hat{\Theta}} \right) \Gamma \frac{\partial \alpha_{i-1}}{\partial y} \Omega \\ & - \left(\sum_{k=2}^{i-1} z_k \frac{\partial \alpha_{k-1}}{\partial \hat{\psi}} \right) \gamma_\psi \frac{\partial \alpha_{i-1}}{\partial y} \tanh \left(\frac{z_i \frac{\partial \alpha_{i-1}}{\partial y}}{\delta_i} \right) \end{aligned} \quad (3.119)$$

$$\tau_{i\theta} = \tau_{(i-1)\theta} - z_i \frac{\partial \alpha_{i-1}}{\partial y} \Omega \quad (3.120)$$

$$\tau_{i\psi} = \tau_{(i-1)\psi} + z_i \frac{\partial \alpha_{i-1}}{\partial y} \tanh \left(\frac{z_i \frac{\partial \alpha_{i-1}}{\partial y}}{\delta_i} \right) \quad (3.121)$$

where

$$\begin{aligned} \beta_i = & \frac{\partial \alpha_{i-1}}{\partial y} \left(\xi_2 + f_1^0(y) + \Omega^T \hat{\Theta} \right) + k_i v_{m,1} + \sum_{j=1}^{i-1} \frac{\partial \alpha_{i-1}}{\partial y_r^{(j-1)}} y_r^{(j)} + \left(\frac{\partial \alpha_{i-1}}{\partial \hat{\theta}} + y_r^{(i-1)} \right) \dot{\hat{\theta}} \\ & + \sum_{j=1}^{m+i-1} \frac{\partial \alpha_{i-1}}{\partial \lambda_j} (-k_j \lambda_1 + \lambda_{j+1}) + \frac{\partial \alpha_{i-1}}{\partial \xi} (A_0 \xi + ky + \Psi(y)) \\ & + \frac{\partial \alpha_{i-1}}{\partial \Xi} (A_0 \Xi^T + \Phi(y)) \end{aligned} \quad (3.122)$$

In the last step ρ , the actual control law w and the adaptation law $\dot{\hat{\Theta}}$ are given as follows:

$$w = \alpha_\rho - v_{m,\rho+1} + \hat{\psi} y_r^{(\rho)} \quad (3.123)$$

3.2 Output Feedback Systems

$$\dot{\hat{\Theta}} = \Gamma \tau_{\rho\theta} \quad (3.124)$$

$$\dot{\hat{\psi}} = \gamma_{\psi} \tau_{\rho\psi} \quad (3.125)$$

The final Lyapunov function V_{ρ} can be written as

$$V_{\rho} = \frac{1}{2} \log \frac{k_{b_1}^2}{k_{b_1}^2 - z_1^2} + \sum_{i=2}^{\rho} \frac{1}{2} z_i^2 + \frac{1}{2} \tilde{\Theta}^T \Gamma^{-1} \tilde{\Theta} + \frac{|b_m|}{2\gamma_{\varrho}} \tilde{\varrho}^2 + \frac{1}{2\gamma_{\psi}} \tilde{\psi}^2 + \sum_{i=1}^{\rho} \frac{1}{2\gamma_i} \tilde{x}^T P \tilde{x} \quad (3.126)$$

Substituting (3.118)-(3.125) into the derivative of V_{ρ} , we obtain

$$\begin{aligned} \dot{V}_{\rho} \leq & -\frac{c_1 z_1^2}{k_{b_1}^2 - z_1^2} - \sum_{i=2}^{\rho} c_i z_i^2 + \sigma_{\theta} \tilde{\Theta} \hat{\Theta} + \sigma_{\psi} \tilde{\psi} \hat{\psi} + \sigma_{\rho} |b_m| \tilde{\varrho} \hat{\varrho} - \sum_{i=1}^{\rho} \frac{1}{4\gamma_i} \tilde{x}^T \tilde{x} \\ & + \sum_{i=1}^{\rho} 0.2785 \delta_i \psi \end{aligned} \quad (3.127)$$

By completion of squares, (3.127) becomes

$$\begin{aligned} \dot{V}_{\rho} \leq & -\frac{c_1 z_1^2}{k_{b_1}^2 - z_1^2} - \sum_{i=2}^{\rho} c_i z_i^2 - \frac{\sigma_{\theta}}{2} \|\tilde{\Theta}\|^2 - \frac{\sigma_{\psi}}{2} \tilde{\psi}^2 - \frac{\sigma_{\varrho}}{2} |b_m| \tilde{\varrho}^2 - \sum_{i=1}^{\rho} \frac{1}{4\gamma_i} \tilde{x}^T \tilde{x} \\ & + \frac{\sigma_{\theta}}{2} \|\Theta\|^2 + \frac{\sigma_{\psi}}{2} \psi^2 + \frac{\sigma_{\varrho}}{2} |b_m| \varrho^2 + \sum_{i=1}^{\rho} 0.2785 \delta_i \psi \end{aligned} \quad (3.128)$$

Theorem 3.2 Consider the closed-loop system consisting of the plant (3.72), filters (3.79)-(3.82), stabilizing functions (3.95)(3.115)(3.119), control law (3.123) and adaptation laws (3.104)(3.124), under Assumptions 3.6-3.10. Then, for any initial compact set Ω_y^0 , which $y(0)$ belongs to,

- (i) there always exists a sufficiently large compact set Ω_y , such that $y(t) \in \Omega_y$, $\forall t > 0$;
- (ii) all closed loop signals are bounded; and
- (iii) the output tracking error converges to a neighborhood of zero, which can be made arbitrarily small by appropriate selection of design parameters.

Proof:

3.2 Output Feedback Systems

- (i) For any initial compact set $\Omega_y^0 := \{y \in \mathbb{R} \mid |y| \leq k_0, k_0 > 0\} \subset \mathbb{R}$, which $y(0)$ belongs to, we can always specify another compact set $\Omega_y := \{y \in \mathbb{R} \mid |y| \leq k_{c_1}, k_{c_1} > k_0 + A_0 + |y_r(0)|\} \subset \mathbb{R}$, which is a superset of Ω_y^0 and can be made as large as desired. Now, we prove that y , the input variable of the NNs, remains within this specified compact set for all time, which means that $y(t) \in \Omega_y$, $\forall t > 0$.

Borrowing the idea of the BLF based control in [116][132], to design a control that does not drive y out of the interval $|y| < k_{c_1}$, we require that $|z_1| < k_{b_1}$ with $k_{b_1} = k_{c_1} - A_0$. According to Lemma 2.7, $-\frac{k_{b_1}^2}{k_{b_1}^2 - z_1^2} < -\log \frac{k_{b_1}^2}{k_{b_1}^2 - z_1^2}$ in the set $|z_1| < k_{b_1}$. Therefore, (3.128) can be further represented as

$$\begin{aligned} \dot{V}_\rho &\leq -c_1 \log \frac{k_{b_1}^2}{k_{b_1}^2 - z_1^2} - \sum_{i=2}^{\rho} c_i z_i^2 - \frac{\sigma_\theta}{2} \|\tilde{\Theta}\|^2 - \frac{\sigma_\psi}{2} \tilde{\psi}^2 - \frac{\sigma_\varrho}{2} |b_m| \tilde{\varrho}^2 - \sum_{i=1}^{\rho} \frac{1}{4\gamma_i} \tilde{x}^T \tilde{x} \\ &\quad + \frac{\sigma_\theta}{2} \|\Theta\|^2 + \frac{\sigma_\psi}{2} \psi^2 + \frac{\sigma_\varrho}{2} |b_m| \varrho^2 + \sum_{i=1}^{\rho} 0.2785 \delta_i \psi \\ &\leq -\mu_1 V_\rho + \mu_2 \end{aligned} \quad (3.129)$$

in the set $|z_1| < k_{b_1}$, where

$$\mu_1 = \min \left\{ 2c_i, \frac{\sigma_\theta}{\lambda_{\max}(\Gamma^{-1})}, \sigma_\varrho \gamma_\varrho, \sigma_\psi \gamma_\psi, \frac{1}{2\lambda_{\max}(P)} \right\} \quad (3.130)$$

$$\mu_2 = \frac{\sigma_\theta}{2} \|\Theta\|^2 + \frac{\sigma_\psi}{2} \psi^2 + \frac{\sigma_\varrho}{2} |b_m| \varrho^2 + \sum_{i=1}^{\rho} 0.2785 \delta_i \psi \quad (3.131)$$

We can rewrite the closed loop system consisting of the plant (3.72), filters (3.79)-(3.82), stabilizing functions (3.95)(3.115)(3.119), control law (3.123) and adaptation laws (3.104)(3.124), as $\dot{\eta} = h(t, \eta)$, where $\eta = [\bar{z}_n^T, \tilde{\Theta}^T, \tilde{\varrho}, \tilde{\psi}]^T$. Then, it can be shown that $h(t, \eta)$ satisfies the conditions of the existence and uniqueness of solution ([119], p.476, Theorem 54) for $\eta \in \Omega = \left\{ \bar{z}_n \in \mathbb{R}^n, \tilde{\Theta} \in \mathbb{R}^{ln+m+1}, \tilde{\varrho} \in \mathbb{R}, \tilde{\psi} \in \mathbb{R} \mid |z_1| < k_{b_1} \right\}$. Since $z_1(0) = y(0) - y_r(0)$, $y(0) \leq k_0$ in the definition of Ω_y^0 and $k_{c_1} > k_0 + A_0 + |y_r(0)|$ in the definition of Ω_y , we obtain that $|z_1(0)| < k_{b_1}$. Therefore, we can conclude that the set Ω is an invariant set. Together with (3.129), we infer, from Lemma 2.6, that $|z_1(t)| < k_{b_1}$, $\forall t > 0$. Since $y(t) = z_1(t) + y_r(t)$ and $|y_r(t)| \leq A_0$ in Assumption 3.9, we obtain that

3.2 Output Feedback Systems

$|y(t)| \leq |z_1(t)| + |y_r(t)| < k_{b_1} + A_0 = k_{c_1}$, $\forall t > 0$. As such, we can conclude that for any initial compact set Ω_y^0 , which $y(0)$ belongs to, there always exists a sufficiently large compact set Ω_y , such that $y \in \Omega_y$, $\forall t > 0$.

(ii) Let $\mu_0 = \frac{\mu_2}{\mu_1}$, then (3.129) satisfies

$$0 \leq V_\rho(t) \leq \mu_0 + (V_\rho(0) - \mu_0)e^{-\mu_1 t} \leq \mu_0 + V_\rho(0) \quad (3.132)$$

Therefore, from (3.126), we infer that \bar{z}_n , $\hat{\Theta}$, $\hat{\rho}$, $\hat{\psi}$, \tilde{x} are bounded. Since z_1 and y_r are bounded, y is also bounded. Then, from (3.79) and (3.80), we conclude that ξ and Ξ are bounded as A_0 is Hurwitz. Assumption 3.8 and (3.81) imply that $\bar{\lambda}_{m+1}$ are bounded. From the coordinate change (3.90), it follows that

$$v_{m,i} = z_i + \hat{\rho} y_r^{(i-1)} + \alpha_{i-1}(y, \xi, \Xi, \hat{\Theta}, \hat{\rho}, \hat{\psi}, \bar{\lambda}_{m+i-1}, \bar{y}_r^{(i-2)}), \quad i = 2, 3, \dots, \rho \quad (3.133)$$

For $i = 2$, the boundedness of $\bar{\lambda}_{m+1}$, along with the boundedness of z_2 and $y, \xi, \Xi, \hat{\Theta}, \hat{\rho}, \hat{\psi}, y_r, \dot{y}_r$, proves that $v_{m,2}$ is bounded. From (3.82), it follows that λ_{m+2} is bounded. Following the same procedure recursively, the boundedness of λ is established. Finally, from (3.83) and the boundedness of $\xi, \Xi, \lambda, \tilde{x}$, we conclude that x is bounded. Furthermore, $w(t)$ is bounded. Hence, all closed loop signals are bounded.

(iii) From (3.126) and (3.132), we obtain that

$$\frac{1}{2} \log \frac{k_{b_1}^2}{k_{b_1}^2 - z_1^2} \leq \mu_0 + (V_\rho(0) - \mu_0)e^{-\mu_1 t} \quad (3.134)$$

Taking exponentials on both sides of (3.134) results in

$$\frac{k_{b_1}^2}{k_{b_1}^2 - z_1^2} \leq e^{2[\mu_0 + (V_\rho(0) - \mu_0)e^{-\mu_1 t}]} \quad (3.135)$$

Since $|z_1(t)| < k_{b_1}$ is obtained in (i), we have, that $k_{b_1}^2 - z_1^2 > 0$. Multiplying both sides by $(k_{b_1}^2 - z_1^2)$ and after some manipulations lead to

$$|z_1(t)| \leq k_{b_1} \sqrt{1 - e^{-2[\mu_0 + (V_\rho(0) - \mu_0)e^{-\mu_1 t}]}} \quad (3.136)$$

3.2 Output Feedback Systems

It follows that given any $\mu > k_{b_1}\sqrt{1 - e^{-2\mu_0}}$, there exists T such that for all $t > T$,

$$|z_1(t)| \leq \mu \quad (3.137)$$

As $t \rightarrow \infty$,

$$|z_1(t)| \leq k_{b_1}\sqrt{1 - e^{-2\mu_0}} \quad (3.138)$$

which implies that

$$|y - y_r| \leq k_{b_1}\sqrt{1 - e^{-2\mu_0}}, \text{ as } t \rightarrow \infty \quad (3.139)$$

Due to $\mu_0 = \frac{\mu_2}{\mu_1}$, and from the definitions of μ_1 (3.130) and μ_2 (3.131), we see that $y - y_r$ can be made arbitrarily small by appropriate selection of design parameters. ■

3.2.5 Simulation Results

In this section, the feasibility and effectiveness of the proposed approach are illustrated by an example. Consider a second-order output feedback system as follows

$$\begin{aligned} \dot{x}_1 &= x_2 + (y^3 - y)/(1 + y^4) + 0.1 \sin(0.1t) \\ \dot{x}_2 &= y^2 + \sin(y) + 0.1 \cos(0.1t) + u(w) \\ y &= x_1 \end{aligned} \quad (3.140)$$

where x_1, x_2 are system states, y is the output; $f_1(y) = (y^3 - y)/(1 + y^4)$ and $f_2(y) = y^2 + \sin(y)$ are unknown functions; the bounded time-varying disturbances $d_1(t) = 0.01 \sin(0.1t)$ and $d_2(t) = 0.01 \cos(0.1t)$ satisfy that $|d_1(t)| \leq 0.01$, $|d_2(t)| \leq 0.01$; and $u(w)$ represents an output of the following backlash-like hysteresis:

$$\frac{du}{dt} = \alpha \left| \frac{dw}{dt} \right| (cw - u) + B_1 \frac{dw}{dt} \quad (3.141)$$

with $\alpha = 1$, $c = 3.1635$, and $B_1 = 0.345$. The objective is for y to track the desired trajectory y_r , which is generated by a second-order filter

$$y_r = \frac{w_n^2}{s^2 + 2\zeta w_n s + w_n^2} y_{ref} \quad (3.142)$$

3.2 Output Feedback Systems

with $w_n = 1.5$, $\zeta = 0.8$, and for y_{ref} defined to be a square wave of amplitude $A_0 = 0.05$, period $T = 20$ s.

The initial conditions and the control design parameters used in the simulation are as follows: $x_1(0) = 0.0$, $x_2(0) = 0.0$, $\xi_i(0) = \Xi_i(0) = v_{0,i}(0) = 0.0$, $i = 1, 2$, $k_1 = k_2 = 5.0$, $c_1 = c_2 = 0.8$, $\delta_1 = \delta_2 = 7.0$, $\gamma_1 = \gamma_2 = 0.1$, $\Gamma_{\theta_1} = 0.2I$, $\Gamma_{\theta_2} = 0.1I$, $\gamma_\psi = 0.05$, $\sigma_{\theta_1} = 0.4$, $\sigma_{\theta_2} = 0.8$, $\sigma_\psi = 0.4$. For the unknown functions $f_1(y)$ and $f_2(y)$, we use the RBFNNs to approximate them on-line as $f_1(y) = \phi_1^T(y)\hat{\theta}_1$ and $f_2(y) = \phi_2^T(y)\hat{\theta}_2$ respectively, where the input of the neural networks is only the output signal y . If the initial compact set is chosen as $\Omega_y^0 := \{y \in \mathbb{R} \mid |y| \leq k_0\}$, where $k_0 = 0.5$, we can specify another compact set $\Omega_y := \{y \in \mathbb{R} \mid |y| \leq k_{c_1}\}$, where $k_{c_1} = 0.6 > k_0 + A_0 + |y_r(0)| = 0.55$. Thus, we have that $k_{b_1} = k_{c_1} - A_0 = 0.55$. Our proposed control can ensure that the input variable of the NNs, y , remains within this prefixed compact Ω_y all the time, and thus, the NN approximation is valid. For both function approximators, the numbers of nodes are chosen as $l_1 = l_2 = 5$; the centers of the receptive fields as $\mu_1 = \mu_2 = [-0.6, -0.3, 0.0, 0.3, 0.6]^T$, the widths of the Gaussian function as $\eta_1 = 0.2$ and $\eta_2 = 0.1$. The initial values for all weights $\hat{\theta}_1$ and $\hat{\theta}_2$ are set to zero (i.e., no initial knowledge).

The simulation results are shown in Figures 3.6-3.10. Figure 3.6 shows the output tracking performance. It can be seen that the output y remains within the compact set $\Omega_y := \{y \in \mathbb{R} \mid |y| \leq 0.6\}$ and tracks the desired trajectory y_r to a neighborhood of zero when the proposed BLF based control is used. The tracking error $z_1 = y - y_r$ and the control u are shown in Figure 3.7. It is noted that there are some spikes in the control signal $u(t)$ at $t = nT/2$ ($n = 1, 2, \dots$). This is caused by the nonlinear term $\frac{z_1}{k_{b_1}^2 - z_1^2}$ in (3.96) and (3.115). For the square wave reference signal defined in (3.142), there are some jumps at $t = nT/2$ ($n = 1, 2, \dots$), which result in jumps for the tracking error signal z_1 . Before $z_1(t)$ tends to approach the barriers at $z_1 = \pm 0.55$, the nonlinear term $\frac{z_1}{k_{b_1}^2 - z_1^2}$ grows rapidly and leads to a large control effort that prevents z_1 from the barriers. It can be seen that z_1 remains in the set $|z_1| < k_{b_1}$ in Figure 3.7, and thus, $|y| < k_{c_1}$, such that NN approximation is valid. From Figure 3.8, we can see that the approximations to the functions f_1 and f_2 are converging to a neighborhood of the actual functions. The boundedness of the norm of neural weights $\|\hat{\theta}_1\|$ and $\|\hat{\theta}_2\|$, and

the bounding parameter adaptation $\hat{\psi}$ are shown in Figure 3.9 as well. In addition, Figure 3.10 shows output trajectories for different initial conditions. It indicates that with the proposed BLF based control, the output y , starting from a initial compact set $\Omega_y^0 := \{y \in R \mid |y| \leq 0.5\}$, can always stay within the specified compact set $\Omega_y := \{y \in R \mid |y| \leq 0.6\}$ for all time, which ensures that NN approximation is valid.

3.3 Conclusion

In this chapter, firstly, adaptive dynamic surface control (DSC) using neural networks has been proposed for a class of nonlinear systems in strict-feedback form with back-lash hysteresis input, where the hysteresis is modeled as a differential equation. The developed adaptive control can guarantee that all signals involved are semi-globally uniformly ultimately bounded (SGUUB) without constructing a hysteresis inverse. Simulation results have been provided to show the effectiveness of the proposed approach. Secondly, adaptive observer backstepping using neural network (NN) has been adopted for state estimation and function on-line approximation using only output measurements to achieve the output tracking for a class of output feedback nonlinear systems with back-lash hysteresis input. The Barrier Lyapunov Function (BLF) has been incorporated into Lyapunov synthesis to address two open and challenging problems in the neuro-control area. By ensuring the boundedness of the BLF, we can actively (i) determine the compact set *a priori*, on which NN approximation is valid; and (ii) ensure the argument of the unknown function remain within the specified set. The semi-globally uniformly ultimately bounded (SGUUB) stability of the closed-loop system has been provided and the effectiveness of the proposed approach has been illustrated using a numerical example.

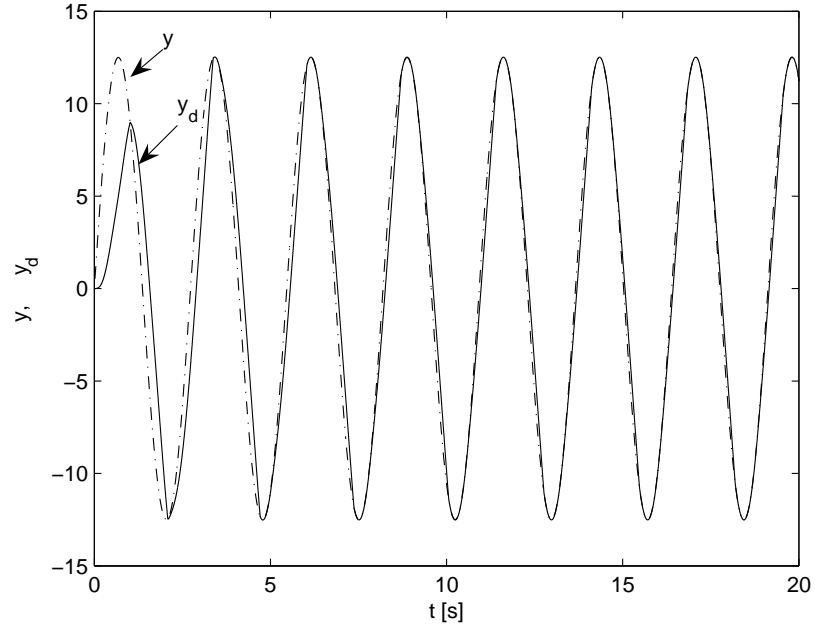


Figure 3.2: Tracking performance for the strict-feedback system with backlash-like hysteresis

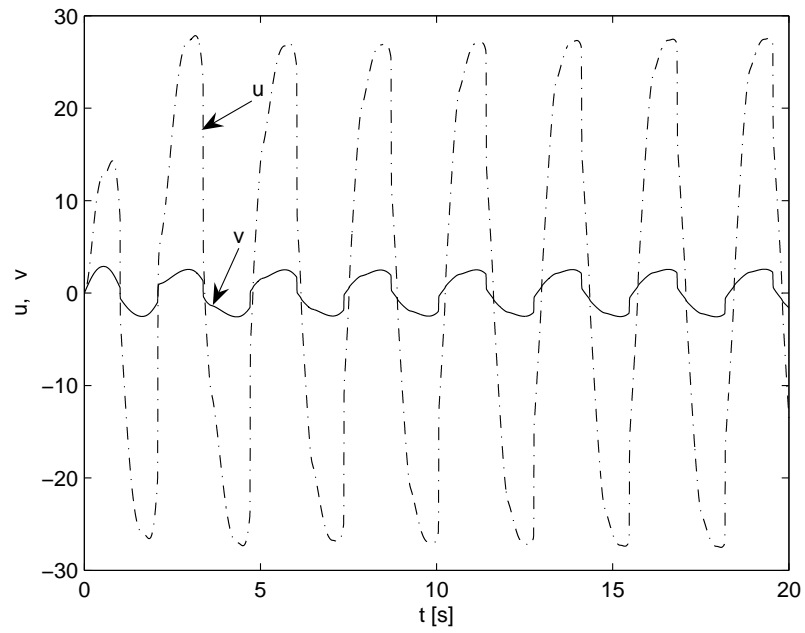


Figure 3.3: Control inputs for the strict-feedback system with backlash-like hysteresis

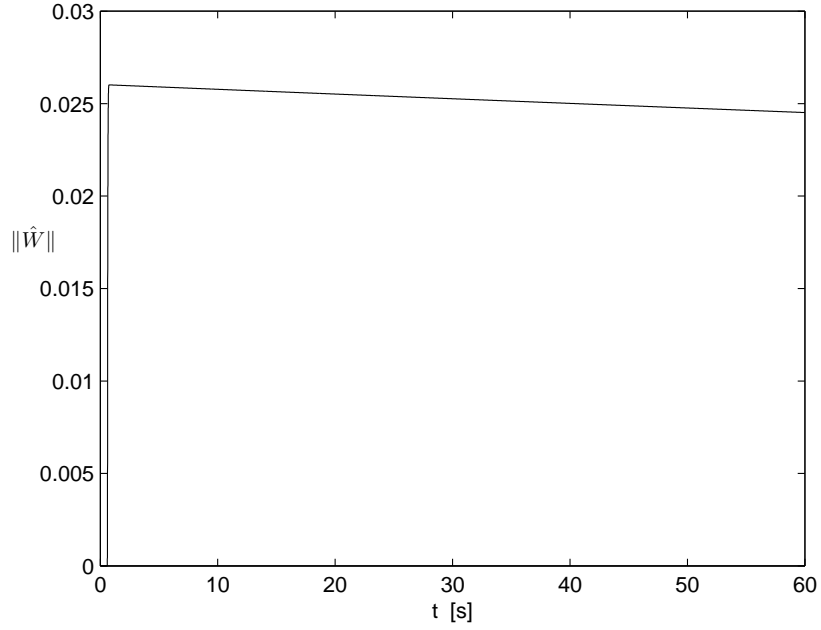


Figure 3.4: Neural weights for the strict-feedback system with backlash-like hysteresis

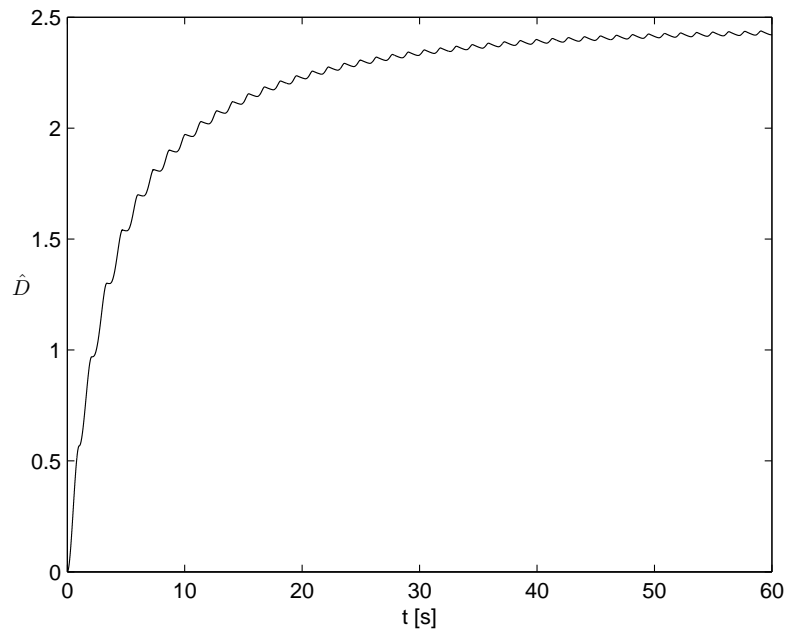


Figure 3.5: Estimate of disturbance bound for the strict-feedback system with backlash-like hysteresis

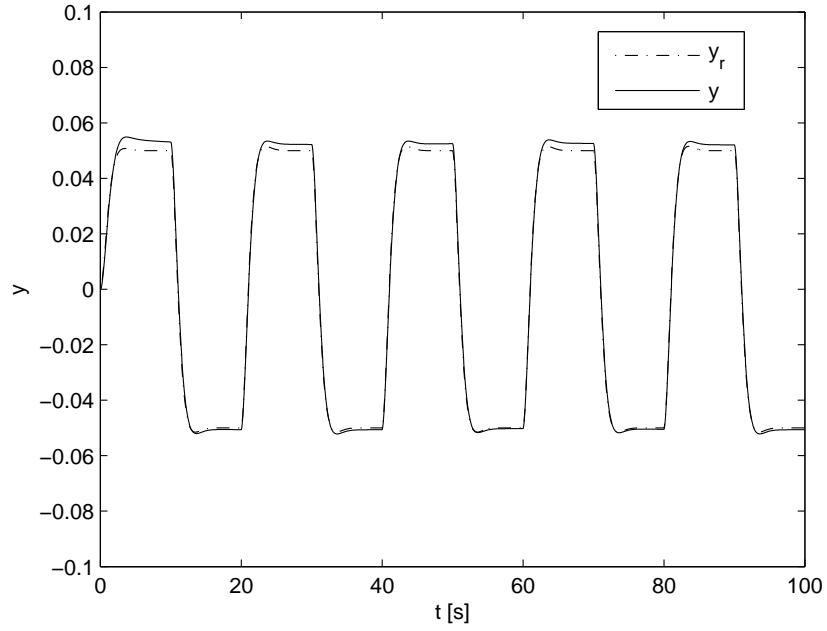


Figure 3.6: Tracking performance for the output feedback system with backlash-like hysteresis

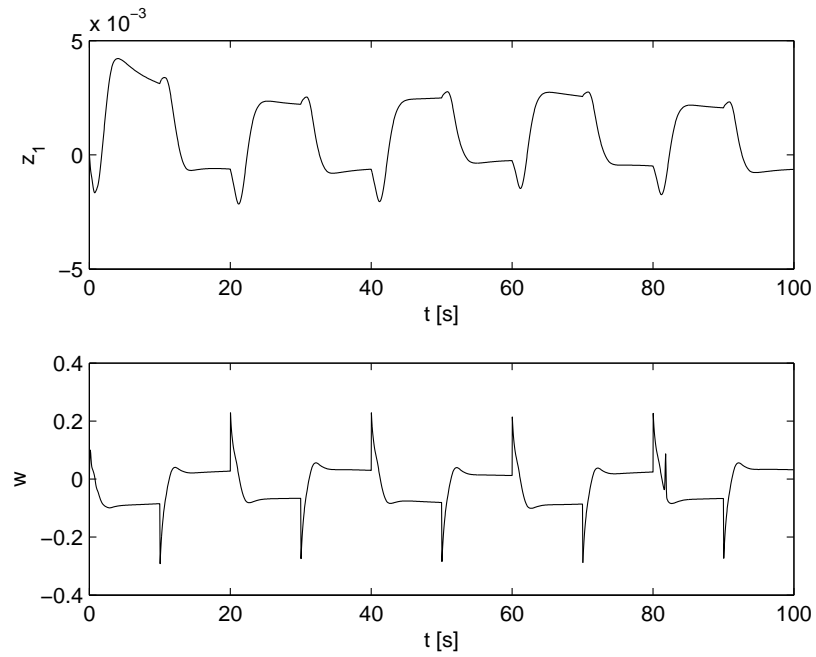


Figure 3.7: Tracking error z_1 (top) and control input w (bottom) for the output feedback system with backlash-like hysteresis

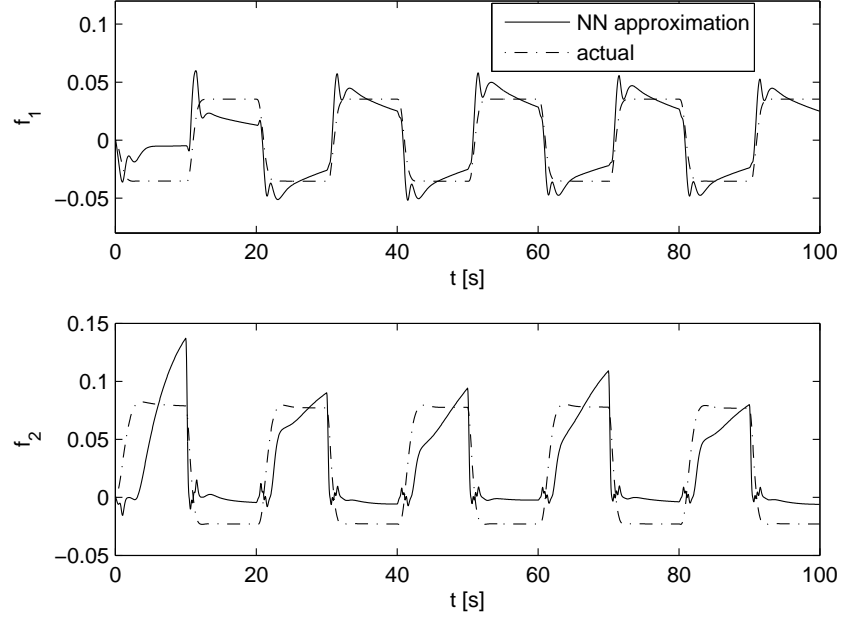


Figure 3.8: Function approximation results: $f_1(y)$ (top) and $f_2(y)$ (bottom) for the output feedback system with backlash-like hysteresis

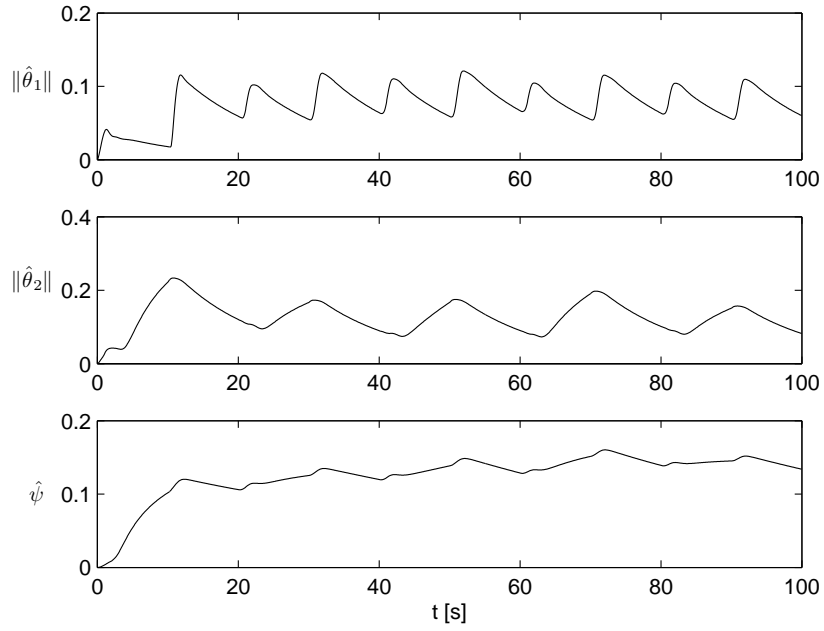


Figure 3.9: Parameter adaptation results for the output feedback system with backlash-like hysteresis: norm of neural weights $\|\hat{\theta}_1\|$ (top); norm of neural weights $\|\hat{\theta}_2\|$ (middle) and bounding parameter $\hat{\psi}$ (bottom)

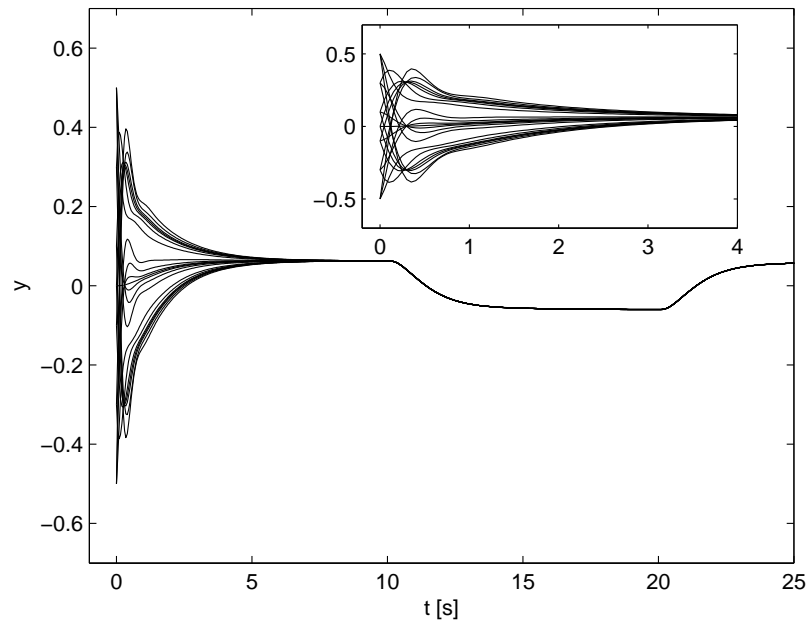


Figure 3.10: Output trajectories for the output feedback system with backlash-like hysteresis with different initial conditions

Chapter 4

Systems with Classic Prandtl-Ishlinskii Hysteresis

4.1 Introduction

Control of a system with hysteresis nonlinearities is challenging, because they are non-differentiable nonlinearities and severely limit system performance by giving rise to undesirable inaccuracy or oscillations, and even lead to closed loop instability [3]. Furthermore, due to the nonsmooth characteristics of hysteresis nonlinearities, traditional control methods are inadequate in dealing with the effects of unknown hysteresis. In [3], adaptive control with an adaptive hysteresis inverse was presented for plants with unknown parameterized hysteresis. Robust control was developed by combining the inverse compensation for a novel dynamic hysteresis model in magnetostriuctive actuators in [120]. In [16], robust adaptive control was investigated for a class of nonlinear system with unknown backlash-like hysteresis, for which, adaptive backstepping control was designed in [17]. Apart from the above hysteresis models, there exist many other hysteresis models in the literature, since hysteresis is a very complex phenomenon. For different kinds of hysteresis models, different compensation methods should be adopted. As such, it is challenging to fuse those hysteresis models with the available control techniques. It appears that the classic Prandtl-Ishlinskii (PI) hysteresis model, which is a subclass of Preisach type model, can be explored in

connection with the existing robust adaptive control methods. In [18] and [19], adaptive variable structure control and adaptive backstepping methods were proposed, respectively, for a class of continuous-time nonlinear dynamic systems preceded by hysteresis nonlinearity with the classic PI hysteresis model representation. However, since the nonlinear functions in most of the above works were assumed to be known, it is therefore of interest to develop methods to deal with unknown nonlinearities, so as to enlarge the class of applicable systems.

Other than hysteresis, time-delay is another problem that is often encountered in physical systems, for example, in the turbojet engines, aircraft systems, microwave oscillators, nuclear reactors, rolling mills, chemical processes, and hydraulic systems, among others [135]. The existence of time-delays in a system frequently becomes a source of instability, and may degrade the control performance. The control of the time-delay systems is challenging since they involve infinite-dimensional functional differential equations, which are more difficult to handle than finite-dimensional ordinary differential equations [136]. To guarantee the stability of time-delay systems, a number of different approaches have been proposed [137]. Lyapunov-Krasovskii functionals [138], combined with the linear matrix inequality (LMI) technique, have been used to establish a framework for the stability and control of time-delay systems [139, 140, 141, 142]. In [143], Lyapunov-Krasovskii functionals were used with backstepping for a class of single-input single-output (SISO) nonlinear time-delay systems with a “triangular structure”, which was later commented that it could not be “constructively obtained” in [144]. The need for knowledge of system nonlinearities was removed with the use of adaptive neural network control in [145], which was extended to a class of multi-input multi-output (MIMO) nonlinear systems in block-triangular form with unknown state delays [146]. Apart from the Lyapunov-Krasovskii method, the Lyapunov-Razumikhin technique has also been investigated for linear time delay systems [147], as well as for nonlinear time delay systems [148, 149].

Although there are some works that deal with hysteresis, or time delay, individually, the combined problem, despite its practical relevance, is largely open in the literature to the best of the author’s knowledge, with the exception of [150], in which turning cutting systems were modeled as plants containing linearly parameterized nonlinearities, backlash hysteresis, and known constant time delay. Motivated by [150], in this

4.2 Problem Formulation and Preliminaries

chapter, several technical contributions are made as follows:

First, the restriction of linearly parameterized nonlinear systems considered in [150], is removed to tackle a larger and more complex class of nonlinear systems with unknown nonlinearities, for which direct approximation based control using neural networks is adopted due to their universal approximation capabilities.

Second, nonlinear systems that are preceded by uncertain hysteresis inputs in the classic PI form, are considered, which is more complex than the backlash type, but can capture the hysteresis phenomenon more accurately. The classic PI hysteresis is fused with adaptive neural control to the reduce the effects of uncertain hysteresis.

Third, the assumption of known constant time delay considered in [150], is relaxed to unknown time-varying delay, for which Lyapunov-Krasovskii functionals are used to compensate.

The organization of this chapter is as follows. The problem formulation and preliminaries are given in Section 4.2. In Section 4.3, adaptive variable structure neural control is developed for a class of SISO time-varying state delay systems with hysteresis by utilizing an integral-type Lyapunov function first, which is extended to MIMO systems later. Results of extensive simulation studies are shown to demonstrate the effectiveness of the approach in Section 4.4, followed by conclusion in Section 4.5.

4.2 Problem Formulation and Preliminaries

Consider the following class of uncertain MIMO nonlinear system Σ_0 consisting of interconnected subsystems in a Brunovsky form with time-varying state delays and uncertain classic PI hysteresis inputs:

$$\Sigma_0 : \begin{cases} \dot{x}_{i,j} &= x_{i,j+1} \\ \dot{x}_{i,n_i} &= f_i(x, \bar{u}_{i-1}) + g_{i,\tau}(x_\tau) + b_i(\bar{x}_i)u_i \\ x_i(t) &= \psi_i(t), \quad t \in [-\tau_{max}, 0] \\ y_i &= x_{i,1} \end{cases} \quad (4.1)$$

where $i = 1, 2, \dots, m$, $j = 1, 2, \dots, n_i - 1$; $x_i = [x_{i,1}, \dots, x_{i,n_i}]^T \in \mathbb{R}^{n_i}$ are the delay-free state variables of the i th subsystem, $\bar{x}_i = [x_1^T, \dots, x_i^T]^T \in \mathbb{R}^{\bar{n}_i}$ with $\bar{n}_i = \sum_{j=1}^i n_j$

4.2 Problem Formulation and Preliminaries

and $x = [x_1^T, x_2^T, \dots, x_m^T]^T \in \mathbb{R}^n$ with $n = \sum_{i=1}^m n_i$; $y_i \in \mathbb{R}$ denotes the i th subsystem output; $f_i(\cdot)$ and $g_{i,\tau}(\cdot)$ are unknown continuous functions; $b_i(\cdot)$ are the unknown differentiable control gains; $\psi_i(t)$ are the smooth and bounded initial functions; $x_\tau = [x_1(t-\tau_1(t))^T, \dots, x_m(t-\tau_m(t))^T]^T$, and $\tau_1(t), \dots, \tau_m(t)$ are unknown time-varying state delays, τ_{max} as will be defined later is a known positive constant; $\bar{u}_i = [u_1, u_2, \dots, u_i]^T$, and $u_i \in \mathbb{R}$ is the input of the the i th subsystem and the output of the i th hysteresis, which is represented as the classic PI hysteresis model with a play operator as follows:

$$u_i(t) = p_{i0}v_i(t) - d_i[v_i](t) \quad (4.2)$$

$$\begin{aligned} p_{i0} &= \int_0^R p_i(r)dr \\ d_i[v_i](t) &= \int_0^R p_i(r)F_{ir}[v_i](t)dr \\ F_{ir}[v_i](0) &= f_{ir}(v_i(0), 0) \\ F_{ir}[v_i](t) &= f_{ir}(v_i(t), F_{ir}[v_i](t_k)), \text{ for } t_k < t \leq t_{k+1} \text{ and } 0 \leq k \leq N-1 \\ f_{ir}(v, w) &= \max(v-r, \min(v+r, w)) \end{aligned} \quad (4.3)$$

where $u_i(t) \in \mathbb{R}$ and $v_i(t) \in \mathbb{R}$ are the output and input of the classic PI hysteresis model respectively; $p_i(r)$ is a given density function, satisfying $p_i(r) \geq 0$ with $\int_0^\infty r p_i(r)dr < \infty$, F_{ir} is known as the play operator. In addition, there are N subintervals, and the function v_i is monotone on each of the subintervals $(t_k, t_{k+1}]$. The density function $p_i(r)$ vanishes for large values of r . As such, it is reasonable to choose a large enough constant R such that the given density function $p_i(R)$ vanishes, despite the fact that $R = \infty$ is commonly chosen as the upper limit of integration in the literature.

Substituting the classic PI hysteresis model (4.2) into the plant (4.1), we obtain the the integrated system Σ_1

$$\Sigma_1 : \begin{cases} \dot{x}_{i,j} &= x_{i,j+1} \\ \dot{x}_{i,n_i} &= f_i(x, \bar{u}_{i-1}) + g_{i,\tau}(x_\tau) + b_i(\bar{x}_i)p_{i0}v_i(t) - b_i(\bar{x}_i)d_i[v_i](t) \\ x_i(t) &= \psi_i(t), \quad t \in [-\tau_{max}, 0] \\ y_i &= x_{i,1} \end{cases} \quad (4.4)$$

4.2 Problem Formulation and Preliminaries

Our control objective is to track the specified desired trajectory y_{id} to a small neighborhood of zero with the output y_i , while ensuring that all the signals in the corresponding closed-loop system is semiglobally uniformly ultimately bounded (SGUUB).

Remark 4.1 *Although it appears possible to rewrite (4.4) into the non-affine form $\dot{x} = f(x, u)$, it still cannot be handled by the method proposed by [42], in which Implicit Function Theorem was adopted to handle the non-affine problem. The reason is that if we want to apply Implicit Function Theorem to a function, one requirement is that the first order derivative of the function is not equal to zero. However, due to the nonsmooth characteristics of hysteresis, the function $f(x, u)$ transformed from (4.4) is non-differentiable and thus does not satisfy the conditions of applying Implicit Function Theorem. Therefore, we need seek for new solutions in this chapter.*

Remark 4.2 *Noticing that $d_i[v_i](t)$ in (4.4) is an integral function of control input signal v_i , which needs to be designed later, we cannot assume $d_i[v_i](t)$ is bounded before we prove the boundedness of control input v_i , even if the output of the classic PI model is bounded for bounded input. Therefore, standard robust adaptive control used for dealing with bounded disturbance cannot be applied here. To solve this problem, we will develop the comprehensive control in the subsequent Section 4.3.*

Assumption 4.1 *There exist two positive constants, b_{i0} and b_{i1} , such that $0 < b_{i0} \leq |b_i(\bar{x}_i)| \leq b_{i1}$, $\forall \bar{x}_i \in \mathbb{R}^{\bar{n}_i}$.*

Remark 4.3 *Assumption 4.1 implies that smooth functions $b_i(\bar{x}_i)$ are either strictly positive or strictly negative, which is reasonable because $b_i(\bar{x}_i)$ being bounded away from zero is the controllable condition of system Σ_1 in (4.4), which is necessary in most control schemes [65, 151]. Without loss of generality, we shall assume that $b_i(\bar{x}_i) > 0$, $\forall \bar{x}_i \in \mathbb{R}^{\bar{n}_i}$. In addition, the constants b_{i0} and b_{i1} need not be known, as they are used in the stability analysis only.*

Assumption 4.2 *The desired trajectory y_{id} and its time derivatives up to the n_i -th order remain bounded, i.e., $\bar{x}_{id} = [y_{id}, \dot{y}_{id}, \ddot{y}_{id}, \dots, y_{id}^{(n_i)}]^T \in \Omega_{id} \subset \mathbb{R}^{n_i+1}$ with known compact set Ω_{id} , $i = 1, \dots, m$.*

4.3 Control Design and Stability Analysis

Assumption 4.3 *The unknown time-varying state delays $\tau_i(t)$ satisfy the following inequalities*

$$0 \leq \tau_i(t) \leq \tau_{\max}, \quad \dot{\tau}_i(t) \leq \bar{\tau}_{\max} < 1, \quad i = 1, \dots, m \quad (4.5)$$

with known constants τ_{\max} and $\bar{\tau}_{\max}$.

Assumption 4.4 *There exist known constants $p_{i0\min}$ and $p_{i\max}$, such that $p_{i0} > p_{i0\min}$, and $p_i(r) \leq p_{i\max}$ for all $r \in [0, R]$, $i = 1, \dots, m$.*

Remark 4.4 *It is reasonable to set an upper bound for the density function $p_i(r)$, based on its properties that $p_i(r) \geq 0$ with $\int_0^R r p_i(r) dr < \infty$.*

Remark 4.5 *According to Lemma 2.5, the unknown continuous functions of delayed states in (4.4), $g_{i,\tau}(x_\tau)$, satisfy the inequality*

$$g_{i,\tau}(x_\tau) \leq \sum_{k=1}^m \varrho_{ik}(x_k(t - \tau_k(t))) \quad (4.6)$$

with $\varrho_{ik}(\cdot)$ being positive continuous functions, $i = 1, \dots, m$. In this chapter, we consider the special case whereby the bounding functions, $\varrho_{ik}(\cdot)$, are known. As for the case of unknown bounding functions, interested readers can refer to [146].

4.3 Control Design and Stability Analysis

In this section, we will carry out adaptive NN control design for system Σ_1 in (4.4) to achieve stable output tracking. In order to illustrate the design methodology clearly, the SISO case (i.e., $m = 1$) is discussed first, which is generalized to the MIMO case (i.e., $m \geq 2$) subsequently. For both cases, the closed-loop system will be proved to be SGUUB by Lyapunov stability analysis.

The following definitions and notations are used throughout the control design and stability analysis. Define x_{id} and e_i as

$$\begin{aligned} x_{id} &= [y_{id}, \dot{y}_{id}, \dots, y_{id}^{(n_i-1)}]^T \\ e_i &= x_i - x_{id} = [e_{i1}, e_{i2}, \dots, e_{in_i}]^T \end{aligned}$$

4.3 Control Design and Stability Analysis

and the filtered tracking error s_i as

$$s_i = \left(\frac{d}{dt} + \lambda_i\right)^{n_i-1} e_{i1} = \sum_{j=1}^{n_i-1} \lambda_{ij} e_{ij} + e_{in_i} \quad (4.7)$$

where λ_{ij} are chosen such that the polynomial $\sum_{j=1}^{n_i-1} \lambda_{ij} e_{ij} + e_{in_i}$ is a Hurwitz polynomial.

4.3.1 Adaptive Variable Structure Neural Control for SISO Case ($m = 1$)

For the SISO case where $m = 1$, system (4.4) can be rewritten in the following form:

$$\Sigma_{11} : \begin{cases} \dot{x}_{1,j} &= x_{1,j+1}, \quad j = 1, 2, \dots, n_1 - 1 \\ \dot{x}_{1,n_1} &= f_1(x_1) + g_{1,\tau}(x_1(t - \tau_1(t))) + b_1(x_1)p_{10}v_1(t) - b_1(x_1)d_1[v_1](t) \\ x_1(t) &= \psi_1(t), \quad t \in [-\tau_{\max}, 0] \\ y_1 &= x_{1,1} \end{cases} \quad (4.8)$$

Substituting (4.8) into (4.7) leads to

$$\dot{s}_1 = f_1(x_1) + g_{1,\tau}(x_1(t - \tau_1(t))) + b_1(x_1)p_{10}v_1 - b_1(x_1)d_1[v_1](t) + \nu_1 \quad (4.9)$$

where $\nu_1 = \sum_{j=1}^{n_1-1} \lambda_{1j} e_{1,j+1} - y_{1d}^{(n_1)}$.

Define the following integral Lyapunov function candidate, which was firstly proposed in [152] to avoid control singularity:

$$V_{s1} = \int_0^{s_1} \frac{\sigma}{b_1(\bar{x}_1^+, \sigma + \beta_1)} d\sigma \quad (4.10)$$

where $\beta_1 = y_{1d}^{(n_1-1)} - \sum_{j=1}^{n_1-1} \lambda_{1j} e_{1j}$, and $\bar{x}_1^+ = [x_{1,1}, \dots, x_{1,n_1-1}]^T$.

Then, V_{s1} can be rewritten as the following form by using the First Mean Value Theorem for Integrals

$$V_{s1} = \frac{\lambda_{s1} s_1^2}{b_1(\bar{x}_1^+, \lambda_{s1} s_1 + \beta_1)}, \quad \lambda_{s1} \in (0, 1)$$

According to Assumption 4.1, $0 < b_{10} \leq b_1(x_1)$, it is clear that V_{s1} is positive definite with respect to s_1 .

4.3 Control Design and Stability Analysis

Differentiating V_{s1} with respect to time t , we obtain

$$\begin{aligned}\dot{V}_{s1} &= \frac{\partial V_{s1}}{\partial s_1} \dot{s}_1 + \frac{\partial V_{s1}}{\partial \bar{x}_1^+} \dot{\bar{x}}_1^+ + \frac{\partial V_{s1}}{\partial \beta_1} \dot{\beta}_1 \\ &= \frac{s_1}{b_1(x_1)} \dot{s}_1 + \int_0^{s_1} \sigma \left[\frac{\partial b_1^{-1}(\bar{x}_1^+, \sigma + \beta_1)}{\partial \bar{x}_1^+} \dot{\bar{x}}_1^+ \right] d\sigma + \dot{\beta}_1 \int_0^{s_1} \sigma \left[\frac{\partial b_1^{-1}(\bar{x}_1^+, \sigma + \beta_1)}{\partial \beta_1} \right] d\sigma\end{aligned}\quad (4.11)$$

Due to $\partial b_1^{-1}(\bar{x}_1^+, \sigma + \beta_1) / \partial \beta_1 = \partial b_1^{-1}(\bar{x}_1^+, \sigma + \beta_1) / \partial \sigma$ and $\dot{\beta}_1 = -\nu_1$, it is shown that

$$\dot{\beta}_1 \int_0^{s_1} \sigma \left[\frac{\partial b_1^{-1}(\bar{x}_1^+, \sigma + \beta_1)}{\partial \beta_1} \right] d\sigma = -\frac{\nu_1 s_1}{b_1(x_1)} + \int_0^{s_1} \frac{\nu_1}{b_1(\bar{x}_1^+, \sigma + \beta_1)} d\sigma \quad (4.12)$$

Substituting (4.9) and (4.12) into (4.11) results in

$$\begin{aligned}\dot{V}_{s1} &= \frac{s_1}{b_1(x_1)} \left[f_1(x_1) + g_{1,\tau}(x_1(t - \tau_1(t))) + b_1(x_1)p_{10}v_1 - b_1(x_1)d_1[v_1](t) + \nu_1 \right] \\ &\quad + \int_0^{s_1} \sigma \left[\sum_{k=1}^{n_1-1} \frac{\partial b_1^{-1}(\bar{x}_1^+, \sigma + \beta_1)}{\partial x_{1k}} x_{1,k+1} \right] d\sigma - \frac{\nu_1 s_1}{b_1(x_1)} \\ &\quad + \int_0^{s_1} \frac{\nu_1}{b_1(\bar{x}_1^+, \sigma + \beta_1)} d\sigma\end{aligned}\quad (4.13)$$

Using (4.6) and Young's inequality, (4.13) becomes

$$\begin{aligned}\dot{V}_{s1} &\leq s_1 Q_1(Z_1) + s_1 \left[p_{10}v_1 - d_1[v_1](t) \right] + \frac{1}{2} \varrho_{11}^2(x_1(t - \tau_1(t))) \\ &\quad + \frac{s_1^2}{2b_1^2(x_1)}\end{aligned}\quad (4.14)$$

where

$$\begin{aligned}Q_1(Z_1) &= \frac{f_1(x_1)}{b_1(x_1)} + \frac{1}{s_1} \int_0^{s_1} \left[\sigma \sum_{k=1}^{n_1-1} \frac{\partial b_1^{-1}(\bar{x}_1^+, \sigma + \beta_1)}{\partial x_{1k}} x_{1,k+1} + \frac{\nu_1}{b_1(\bar{x}_1^+, \sigma + \beta_1)} \right] d\sigma \\ &= \frac{f_1(x_1)}{b_1(x_1)} + \int_0^1 \left[\theta s_1 \sum_{k=1}^{n_1-1} \frac{\partial b_1^{-1}(\bar{x}_1^+, \theta s_1 + \beta_1)}{\partial x_{1k}} x_{1,k+1} + \frac{\nu_1}{b_1(\bar{x}_1^+, \theta s_1 + \beta_1)} \right] d\theta\end{aligned}$$

with $Z_1 = [x_1^T, s_1, \nu_1, \beta_1]^T \in \mathbb{R}^{n_1+3}$.

To overcome the design difficulties from the unknown time-varying delays $\tau_1(t)$ in (4.14), the following Lyapunov-Krasovskii functional can be considered [114]:

$$V_{U1}(t) = \frac{1}{2(1 - \bar{\tau}_{\max})} \int_{t-\tau_1(t)}^t \varrho_{11}^2(x_1(\tau)) d\tau \quad (4.15)$$

4.3 Control Design and Stability Analysis

The time derivative of V_{U_1} can be expressed as follows:

$$\dot{V}_{U_1}(t) = \frac{1}{2(1 - \bar{\tau}_{\max})} \left[\varrho_{11}^2(x_1(t)) - \varrho_{11}^2(x_1(t - \tau_1(t)))(1 - \dot{\tau}_1(t)) \right] \quad (4.16)$$

which can be used to cancel the time-delay term on the right hand side of (4.14), thus circumvent the design difficulty due to the unknown time-varying delay $\tau_1(t)$, without introducing any additional uncertainties to the system. For concise notation, the time variables t and $t - \tau_1(t)$ will be omitted whenever the time-varying delay term is eliminated, in the remainder of the section.

Combining (4.14) and (4.16), we obtain

$$\dot{V}_{s_1} + \dot{V}_{U_1} \leq s_1 h_1(Z_1) + s_1 \left[p_{10} v_1 - d_1[v_1](t) \right] \quad (4.17)$$

where

$$h_1(Z_1) = Q_1(Z_1) + \frac{s_1}{2b_1^2(x_1)} + \frac{1}{2(1 - \bar{\tau}_{\max})s_1} \varrho_{11}^2(x_1) \quad (4.18)$$

Remark 4.6 Note that $h_1(Z_1)$ in (4.18) contains the term $\frac{1}{2(1 - \bar{\tau}_{\max})s_1} \varrho_{11}^2(x_1)$, which is not well-defined at $s_1 = 0$ and may lead to the controller singularity problem, if we utilize $h_1(Z_1)$ to construct the control law. As such, care must be taken to guarantee the boundedness of the control as discussed in [114]. It is noted that the controller singularity takes place at the point $s_1 = 0$, where the control objective is supposed to be achieved. From a practical point of view, once the system reaches its origin, no control action should be taken for less power consumption. As $s_1 = 0$ is hard to detect owing to the existence of measurement noise, it is more practical to relax our control objective of convergence to a “ball” rather than the origin.

Define the following compact sets

$$\Omega_{Z_1} = \left\{ [x_1^T, s_1, \nu_1, \beta_1]^T \mid x_1 \in \Omega_1, x_{1d} \in \Omega_{1d} \right\} \quad (4.19)$$

$$\Omega_{c_{s_1}} = \{s_1 \mid |s_1| < c_{s_1}, x_{1d} \in \Omega_{1d}\} \quad (4.20)$$

$$\Omega_{Z_1}^0 = \Omega_{Z_1} - \Omega_{c_{s_1}} \quad (4.21)$$

where $\Omega_1 \subset \mathbb{R}^{n_1}$ is a sufficiently large compact set satisfying $\Omega_1 \supset \Omega_{10}$ defined later in Theorem 4.1, and c_{s_1} is a positive design constant that can be chosen arbitrarily

4.3 Control Design and Stability Analysis

small and “—” in (4.21) is used to denote the complement set of set $\Omega_{c_{s_1}}$. In addition, it has been shown that $\Omega_{Z_1}^0$ is a compact set in [114].

Let $\hat{W}_1^T S(Z_1)$ be the approximation of the function $h_1(Z_1)$, defined in (4.18), on the compact set $\Omega_{Z_1}^0$. Then, using the radial basis function neural networks (RBFNNs) in Section 2.3.3, we have

$$h_1(Z_1) = \hat{W}_1^T S(Z_1) - \tilde{W}_1^T S(Z_1) + \varepsilon_1(Z_1) \quad (4.22)$$

where the approximation error $\varepsilon_1(Z_1)$ satisfies $|\varepsilon_1(Z_1)| \leq \varepsilon_1^*$ with positive constant ε_1^* , $\forall Z_1 \in \Omega_{Z_1}^0$.

For (4.17), we design a control law as follows

$$v_1 = -q(s_1|c_{s_1}) \frac{\text{sgn}(s_1)}{p_{10\min}} [k_{10}(t)|s_1| + |\hat{W}_1^T S(Z_1)|] + v_{1h} \quad (4.23)$$

$$v_{1h} = -q(s_1|c_{s_1}) \frac{\text{sgn}(s_1)}{p_{10\min}} \int_0^R \hat{p}_1(t, r) |F_{1r}[v_1](t)| dr \quad (4.24)$$

$$k_{10}(t) = q(s_1|c_{s_1})(k_{11} + k_{12}(t) + \frac{1}{2}) \quad (4.25)$$

where $\hat{p}_1(t, r)$ is the estimate of the density function $p_1(r)$, k_{11} is a positive constant, and $k_{12}(t)$ chosen as

$$k_{12}(t) = q(s_1|c_{s_1}) \frac{k_{13}}{2(1 - \bar{\tau}_{\max})s_1^2} \int_{t-\tau_{\max}}^t \varrho_{11}^2(x_1(\tau)) d\tau \quad (4.26)$$

with k_{13} as a positive constant specified by the designer.

The adaptation laws are designed as follows

$$\dot{\hat{W}}_1 = q(s_1|c_{s_1}) \Gamma_1 [S(Z_1)s_1 - \sigma_{w_1} \hat{W}_1] \quad (4.27)$$

$$\frac{\partial}{\partial t} \hat{p}_1(t, r) = \begin{cases} -q(s_1|c_{s_1}) \eta_1 \sigma_{p_1} \hat{p}_1(t, r), & \text{if } \hat{p}_1(t, r) \geq p_{1\max}; \\ q(s_1|c_{s_1}) \eta_1 [|s_1| |F_{1r}[x_{1,n_1}](t)| - \sigma_{p_1} \hat{p}_1(t, r)], & \text{if } 0 \leq \hat{p}_1(t, r) < p_{1\max}. \end{cases} \quad (4.28)$$

with $\Gamma_1 > 0$, σ_{w_1} , σ_{p_1} and η_1 are strictly positive constants.

Remark 4.7 The term v_{1h} in (4.24) is used to cancel the effect caused by the hysteresis term $d_1[v_1](t)$. Unlike traditional robust adaptive controller designs, where

4.3 Control Design and Stability Analysis

$d_1[v_1](t)$ is either assumed to be bounded by a constant or a known function, $d_1[v_1](t)$ here is presented as an integral function of control input signal v_1 , and there are no assumptions on its boundedness. Considering that the density function $p_1(r)$ is not a function of time, it can be treated as a “parameter” of the hysteresis model and adaption law can be developed to obtain an estimate of it. This is crucial for the success of the adaption law design [18].

Remark 4.8 From (4.23) and (4.24), we notice that both sides of (4.23) contain the control signal v_1 , because v_{1h} depends on v_1 as can be seen from (4.24). This is known as the fixed-point problem, where the solvability of v_1 can be proved following the proof of Theorem 1.4 about the existence of the hysteresis inverse operator in [15]. Since it is difficult to obtain the explicit solution for v_1 from (4.23), we introduce several possible implementation methods instead of solving v_1 directly from (4.23). One is the time-scale separation approach, recently proposed in [153]: the control signal $v_1(t)$ is a solution of a “fast” dynamical equation, which means the dynamics of the controller are faster than that of the system plant. Thus, time-scale separation is achieved between the system plant and the controller dynamics using the singular perturbation theory. Second method is adopting the numerical implementation of the inverse hysteresis operator as in [15], where a real-time inverse feed-forward control was designed for piezo-electric actuators. In this chapter, we introduce a small delay to evaluate the input: at time t , we use $v_1(t - \Delta t)$ to compute v_{1h} in (4.24) for suitably small Δt , such that $v_1(t)$ in (4.23) becomes a function of $s_1, \hat{W}_1, \hat{p}_1(t, r), v_1(t - \Delta t)$. The limitation of this method is that its accuracy depends on the choice of Δt . The effects of the variations of Δt will be investigated later in the simulation part in Section 4.4.

Theorem 4.1 Consider the closed-loop system consisting of the plant (4.8), the control laws (4.23) (4.24) and adaptation laws (4.27) (4.28). Under Assumptions 4.1-4.4, given some initial conditions $x_1(0), \hat{W}_1(0)$, belong to Ω_{10} , we can conclude that the overall closed-loop neural control system is SGUUB in the sense that all of the signals in the closed-loop system are bounded, i.e., the states and weights in the closed-loop

4.3 Control Design and Stability Analysis

system will remain in the compact set Ω_1 defined by

$$\Omega_1 = \left\{ s_1, \tilde{W}_1 \mid |s_1| \leq \sqrt{2\mu_1}, \quad \|\tilde{W}_1\| \leq \sqrt{\frac{2\mu_1}{\lambda_{\min}(\Gamma_1^{-1})}} \right\} \quad (4.29)$$

with

$$\begin{aligned} \mu_1 &= \frac{\mu_{11}}{\lambda_{11}} + V_1(0) \\ \mu_{11} &= \frac{\sigma_{p_1} R}{2} p_{1\max}^2 + \frac{\sigma_{w_1}}{2} \|W_1^*\|^2 + \frac{\varepsilon_1^{*2}}{2} \end{aligned} \quad (4.30)$$

$$\lambda_{11} = \min \left\{ \frac{b_{10}k_{11}}{\lambda_{s1}}, k_{13}, \frac{\sigma_{w_1}}{\lambda_{\max}(\Gamma_1^{-1})}, \sigma_{p_1}\eta_1 \right\} \quad (4.31)$$

$$V_1(0) = V_{s1}(0) + V_{U_1}(0) + \frac{1}{2} \tilde{W}_1^T(0) \Gamma_1^{-1} \tilde{W}_1(0) + \frac{1}{2\eta_1} \int_0^R \tilde{p}_1^2(0, r) dr$$

and the tracking error will converge to a neighborhood of zero. In addition, the states and weights in the closed-loop system will eventually converge to the compact set Ω_s defined by

$$\Omega_{1s} = \left\{ s_1, \tilde{W}_1 \mid |s_1| \leq \sqrt{2\mu_1^*}, \quad \|\tilde{W}_1\| \leq \sqrt{\frac{2\mu_1^*}{\lambda_{\min}(\Gamma_1^{-1})}} \right\} \quad (4.32)$$

where $\mu_1^* = \frac{\mu_{11}}{\lambda_{11}}$.

Proof: The method of proof is generally similar to that in our previous works [129, 154], although the details of analysis are different and more complex, due to the presence of time delay and hysteresis in the system. In this proof, we will show that for a compact set Ω_{NN} , on which the NN approximation is valid, there exist some control parameters and a non-empty initial compact set Ω_{10} , such that as long as the initial conditions start in Ω_{10} , the states and weights will remain in the conservative compact set Ω_1 , and finally converge to the compact set Ω_{1s} . Both of them belong to the chosen compact set Ω_{NN} . The proof includes two steps, and one could see the whole picture at the end of the proof of Step 2.

Step 1: Suppose that both the states and weights belong to Ω_{NN} , i.e., $\{x_1, \hat{W}_1\} \in \Omega_{NN}, \forall t \geq 0$, on which NN approximation (4.22) is valid.

4.3 Control Design and Stability Analysis

Consider the following Lyapunov function candidate

$$V_1(t) = V_{s1}(t) + V_{U1}(t) + \frac{1}{2}\tilde{W}_1^T \Gamma_1^{-1} \tilde{W}_1 + \frac{1}{2\eta_1} \int_0^R \tilde{p}_1^2(t, r) dr \quad (4.33)$$

where $\tilde{W}_1 = \hat{W}_1 - W_1$ and $\tilde{p}_1(t, r) = \hat{p}_1(t, r) - p(r)$.

Differentiating $V_1(t)$ with respect to time t leads to

$$\dot{V}_1(t) = \dot{V}_{s1}(t) + \dot{V}_{U1}(t) + \tilde{W}_1^T \Gamma_1^{-1} \dot{\tilde{W}}_1 + \frac{1}{\eta_1} \int_0^R \tilde{p}_1(t, r) \frac{\partial}{\partial t} \hat{p}_1(t, r) dr \quad (4.34)$$

Substituting (4.17) into (4.34) leads to

$$\begin{aligned} \dot{V}_1(t) \leq & s_1 h_1(Z_1) + s_1 [p_{10} v_1 - d_1[v_1](t)] + \tilde{W}_1^T \Gamma_1^{-1} \dot{\tilde{W}}_1 \\ & + \frac{1}{\eta_1} \int_0^R \tilde{p}_1(t, r) \frac{\partial}{\partial t} \hat{p}_1(t, r) dr \end{aligned} \quad (4.35)$$

Considering the adaptive neural control laws and adaptation laws from (4.23)-(4.28), the stability analysis is carried out in the following two regions, respectively.

- **Region 1:** If $|s_1| \geq c_{s1}$, then $q_1(s_1|c_{s1}) = 1$. Noting (4.22) and submitting (4.23) into (4.35), we have

$$\begin{aligned} \dot{V}_1(t) \leq & -s_1 \tilde{W}_1^T S(Z_1) + s_1 \varepsilon_1(Z_1) - k_{10}(t) s_1^2 + s_1 [p_{10} v_{1h} - d_1[v_1](t)] \\ & + \tilde{W}_1^T \Gamma_1^{-1} \dot{\tilde{W}}_1 + \frac{1}{\eta_1} \int_0^R \tilde{p}_1(t, r) \frac{\partial}{\partial t} \hat{p}_1(t, r) dr \end{aligned} \quad (4.36)$$

Using Young's Inequality, we have

$$s_1 \varepsilon_1(Z_1) \leq \frac{s_1^2}{2} + \frac{\varepsilon_1^{*2}}{2} \quad (4.37)$$

Substituting (4.25), (4.27) and (4.37) into (4.36) leads to

$$\begin{aligned} \dot{V}_1(t) \leq & -k_{11} s_1^2 - k_{13} V_{U1} - \sigma_{w1} \tilde{W}_1^T \hat{W}_1 + \frac{\varepsilon_1^{*2}}{2} + s_1 [p_{10} v_{1h} - d_1[v_1](t)] \\ & + \frac{1}{\eta_1} \int_0^R \tilde{p}_1(t, r) \frac{\partial}{\partial t} \hat{p}_1(t, r) dr \end{aligned} \quad (4.38)$$

For the third term in (4.38), by completion of squares, we have

$$-\sigma_{w1} \tilde{W}_1^T \hat{W}_1 \leq -\frac{\sigma_{w1}}{2} \|\tilde{W}_1\|^2 + \frac{\sigma_{w1}}{2} \|W_1^*\|^2 \quad (4.39)$$

4.3 Control Design and Stability Analysis

For the last two terms in (4.38), using (4.3) and (4.24), we have

$$\begin{aligned}
& s_1 \left[p_{10} v_{1h} - d_1[v_1](t) \right] + \frac{1}{\eta_1} \int_0^R \tilde{p}_1(t, r) \frac{\partial}{\partial t} \hat{p}_1(t, r) dr \\
= & s_1 \left[-\frac{\text{sgn}(s_1) p_{10}}{p_{10\min}} \int_0^R \hat{p}_1(t, r) |F_{1r}[v](t)| dr - \int_0^R p_1(r) F_{1r}[v](t) dr \right] \\
& + \frac{1}{\eta_1} \int_0^R \tilde{p}_1(t, r) \frac{\partial}{\partial t} \hat{p}_1(t, r) dr \\
\leq & -|s_1| \int_0^R \hat{p}_1(t, r) |F_{1r}[v](t)| dr + |s_1| \int_0^R p_1(r) |F_{1r}[v](t)| dr \\
& + \frac{1}{\eta_1} \int_0^R \tilde{p}_1(t, r) \frac{\partial}{\partial t} \hat{p}_1(t, r) dr \\
\leq & -|s_1| \int_0^R \tilde{p}_1(t, r) |F_{1r}[v](t)| dr + \frac{1}{\eta_1} \int_0^R \tilde{p}_1(t, r) \frac{\partial}{\partial t} \hat{p}_1(t, r) dr \quad (4.40)
\end{aligned}$$

According to (4.28), the adaptation law for the estimate of density function $\hat{p}_1(t, r)$ is divided to two cases, due to the different regions which $\hat{p}_1(t, r)$ belongs to. Therefore, we also need to consider two cases for the analysis of (4.40):

(a) $r \in R_{1\max} = \{r : \hat{p}_1(t, r) \geq p_{1\max}\} \subset [0, R]$.

According to (4.28), we have

$$\tilde{p}_1(t, r) \geq 0 \quad (4.41)$$

$$\frac{\partial}{\partial t} \hat{p}_1(t, r) = -\eta_1 \sigma_{p_1} \hat{p}_1(t, r) \quad (4.42)$$

Substituting (4.41) and (4.42) into (4.40), we have

$$\begin{aligned}
& -|s_1| \int_{r \in R_{1\max}} \tilde{p}_1(t, r) |F_{1r}[v](t)| dr + \frac{1}{\eta_1} \int_{r \in R_{1\max}} \tilde{p}_1(t, r) \frac{\partial}{\partial t} \hat{p}_1(t, r) dr \\
\leq & -\sigma_{p_1} \int_{r \in R_{1\max}} \tilde{p}_1(t, r) \hat{p}_1(t, r) dr \quad (4.43)
\end{aligned}$$

(b) $r \in R_{1\max}^c$, which is the complement set of $R_{1\max}$ in $[0, R]$, i.e., $0 \leq \hat{p}_1(t, r) < p_{1\max}$.

In this case, from (4.28), we have

$$\frac{\partial}{\partial t} \hat{p}_1(t, r) = \eta_1 [|s_1| |F_{1r}[v](t)| - \sigma_{p_1} \hat{p}_1(t, r)] \quad (4.44)$$

4.3 Control Design and Stability Analysis

Substituting (4.44) into (4.40), we have

$$\begin{aligned} & -|s_1| \int_{r \in R_{1\max}^c} \tilde{p}_1(t, r) |F_{1r}[v](t)| dr + \frac{1}{\eta_1} \int_{r \in R_{1\max}^c} \tilde{p}_1(t, r) \frac{\partial}{\partial t} \hat{p}_1(t, r) dr \\ & \leq -\sigma_{p_1} \int_{r \in R_{1\max}^c} \tilde{p}_1(t, r) \hat{p}_1(t, r) dr \end{aligned} \quad (4.45)$$

Combining (4.40), (4.43) and (4.45), we know that

$$\begin{aligned} & s_1 \left[p_{10} v_{1h} - d_1[v_1](t) \right] + \frac{1}{\eta_1} \int_0^R \tilde{p}_1(t, r) \frac{\partial}{\partial t} \hat{p}_1(t, r) dr \\ & \leq -\sigma_{p_1} \int_0^R \tilde{p}_1(t, r) \hat{p}_1(t, r) dr \end{aligned} \quad (4.46)$$

By completion of squares, we have

$$-\sigma_{p_1} \tilde{p}_1(t, r) \hat{p}_1(t, r) \leq -\frac{\sigma_{p_1}}{2} \tilde{p}_1^2(t, r) + \frac{\sigma_{p_1}}{2} p_1^2(r) \quad (4.47)$$

Integrating both sides of (4.47) over $[0, R]$ results in

$$-\sigma_{p_1} \int_0^R \tilde{p}_1(t, r) \hat{p}_1(t, r) dr \leq -\frac{\sigma_{p_1}}{2} \int_0^R \tilde{p}_1^2(t, r) dr + \frac{\sigma_{p_1}}{2} \int_0^R p_1^2(r) dr \quad (4.48)$$

According to Assumption 4.4, we know that $p_1(r) \leq p_{1\max}$. Therefore,

$$-\sigma_{p_1} \int_0^R \tilde{p}_1(t, r) \hat{p}_1(t, r) dr \leq -\frac{\sigma_{p_1}}{2} \int_0^R \tilde{p}_1^2(t, r) dr + \frac{\sigma_{p_1} R}{2} p_{1\max}^2 \quad (4.49)$$

Substituting (4.39), (4.46) and (4.49) into (4.38), we have

$$\begin{aligned} \dot{V}_1(t) & \leq -k_{11} s_1^2 - k_{13} V_{U1} - \frac{\sigma_{w_1}}{2} \|\tilde{W}_1\|^2 - \frac{\sigma_{p_1}}{2} \int_0^R \tilde{p}_1^2(t, r) dr + \frac{\sigma_{p_1} R}{2} p_{1\max}^2 \\ & \quad + \frac{\sigma_{w_1}}{2} \|W_1^*\|^2 + \frac{\varepsilon_1^{*2}}{2} \\ & \leq -\lambda_{11} V_1(t) + \mu_{11} \end{aligned} \quad (4.50)$$

where

$$\begin{aligned} \lambda_{11} &= \min \left\{ \frac{b_{10} k_{11}}{\lambda_{s1}}, k_{13}, \frac{\sigma_{w_1}}{\lambda_{\max}(\Gamma_1^{-1})}, \sigma_{p_1} \eta_1 \right\} \\ \mu_{11} &= \frac{\sigma_{p_1} R}{2} p_{1\max}^2 + \frac{\sigma_{w_1}}{2} \|W_1^*\|^2 + \frac{\varepsilon_1^{*2}}{2} \end{aligned}$$

Multiplying (4.50) by $e^{\lambda_{11}t}$ and integrating over $[0, t]$, we have

4.3 Control Design and Stability Analysis

$$0 \leq V_1(t) \leq \frac{\mu_{11}}{\lambda_{11}} + [V_1(0) - \frac{\mu_{11}}{\lambda_{11}}]e^{-\lambda_{11}t} \leq \mu_1 \quad (4.51)$$

where $\mu_1 = \frac{\mu_{11}}{\lambda_{11}} + V_1(0)$. Therefore, according to the definition of $V_1(t)$ in (4.33),

$$\|\tilde{W}_1\| \leq \sqrt{2\mu_1/\lambda_{\min}(\Gamma_1^{-1})}, \quad |s_1| \leq \sqrt{2b_{11}V_1(t)} \leq \sqrt{2b_{11}\mu_1}$$

Region 2: If $|s_1| < c_{s_1}$, then $q_1(s_1|c_{s_1}) = 0$. In this case, the control signal $v_1 = 0$, $v_{1h} = 0$, $\dot{W}_1 = 0$, $\frac{\partial}{\partial t}\hat{p}_1(t, r) = 0$, i.e., all the signals are kept bounded.

Define $\pi_1 = [e_{11}, \dots, e_{1, n_1-1}]^T \in \mathbb{R}^{n_1-1}$. From (4.7), we know that (i) there is a state space representation for mapping $s_1 = [\Lambda^T \ 1]e_1$, i.e., $\dot{\pi}_1 = A_{s_1}\pi_1 + b_{s_1}s_1$ with $\Lambda_1 = [\lambda_{11}, \dots, \lambda_{1, n_1-1}]^T$, $b_{s_1} = [0, \dots, 0, 1]^T$, A_{s_1} being a stable matrix; (ii) there are positive constants c_{10} and λ_1 such that $\|e^{A_{s_1}t}\| \leq c_{10}e^{-\lambda_1 t}$, and (iii) the solution of π_1 is

$$\pi_1(t) = e^{A_{s_1}t}\pi_1(0) + \int_0^t e^{A_{s_1}(t-\tau)}b_{s_1}s_1(\tau)d\tau$$

Accordingly, it follows that

$$\begin{aligned} \|\pi_1(t)\| &\leq c_{10}\|\pi_1(0)\|e^{-\lambda_1 t} + c_{10} \int_0^t e^{-\lambda_1(t-\tau)}|s_1(\tau)|d\tau \\ &\leq c_{10}\|\pi_1(0)\| + \frac{c_{10}\sqrt{2b_{11}\mu_1}}{\lambda_1} \end{aligned} \quad (4.52)$$

Noting $s_1 = \Lambda_1^T \pi_1 + e_{1n_1}$ and $e_1 = [\pi_1^T, e_{1n_1}]^T$, we have

$$\|e_1\| \leq \|\pi_1\| + |e_{1n_1}| \leq (1 + \|\Lambda_1\|)\|\pi_1\| + |s_1|$$

Substituting (4.52) into the above inequality leads to

$$\|e_1\| \leq c_{10}(1 + \|\Lambda_1\|)\|\pi_1(0)\| + [1 + \frac{(1 + \|\Lambda_1\|)c_{10}}{\lambda_1}]\sqrt{2b_{11}\mu_1}$$

Therefore, we can conclude that all the closed-loop signals are semi-globally uniformly ultimately bounded for some initial conditions, and the tracking error will converge to a neighborhood of zero.

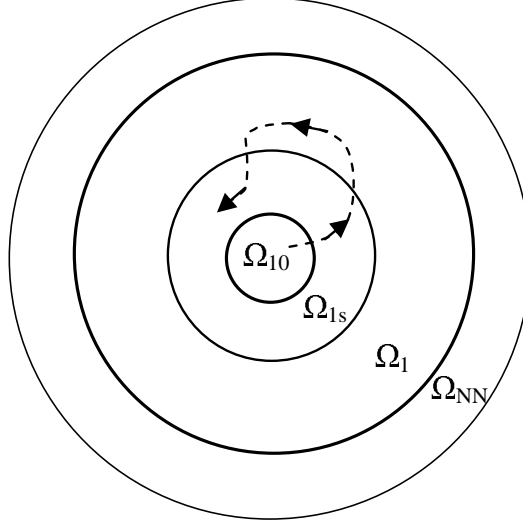


Figure 4.1: Compact sets

Furthermore, from (4.51), we also can have

$$0 \leq V_1(t) \leq \mu_1^*, \quad t \rightarrow \infty \quad (4.53)$$

where $\mu_1^* = \frac{\mu_{11}}{\lambda_{11}}$. Therefore,

$$\|\tilde{W}_1\| \leq \sqrt{2\mu_1^*/\lambda_{\min}(\Gamma_1^{-1})}, \quad |s_1| \leq \sqrt{2b_{11}V_1(t)} \leq \sqrt{2b_{11}\mu_1^*}$$

as $t \rightarrow \infty$.

Step 2: In this step, we prove that there exist some control parameters and a non-empty initial compact set Ω_{10} , such that as long as initial conditions belong in Ω_{10} , the states and the weights under the proposed control, for $t > 0$, will never escape from the conservative compact set Ω_1 , which belongs to the chosen compact set Ω_{NN} , as shown in Figure 4.1.

From the definition of the bounds of the compact sets Ω_1 in (4.29) and Ω_{1s} in (4.32), we can see that for a given Ω_{NN} , there exist some $V_1(0), \mu_{11}, \lambda_{11}$ such that $\Omega_1 \subset \Omega_{NN}$ and $\Omega_{1s} \subset \Omega_{NN}$. From the definitions of μ_{11} and λ_{11} in (4.30)(4.31) as follows

$$\begin{aligned} \mu_{11} &= \frac{\sigma_{p_1} R}{2} p_{1\max}^2 + \frac{\sigma_{w_1}}{2} \|W_1^*\|^2 + \frac{\varepsilon_1^{*2}}{2} \\ \lambda_{11} &= \min \left\{ \frac{b_{10} k_{11}}{\lambda_{s1}}, k_{13}, \frac{\sigma_{w_1}}{\lambda_{\max}(\Gamma_1^{-1})}, \sigma_{p_1} \eta_1 \right\} \end{aligned}$$

4.3 Control Design and Stability Analysis

we can see that the values of μ_{11} and λ_{11} depend on the choice of the control parameters $k_{11}, k_{13}, \lambda_{\max}(\Gamma_1^{-1})$ and η_1 . Therefore, for a given NN compact set Ω_{NN} , there exist some control parameters such that $\Omega_1 \subset \Omega_{NN}$ for a $V(0) = V_{\max} > 0$. Then, we define the initial compact set Ω_{10} as the set of initial conditions $s_1(0), \hat{W}_1(0)$ such that $V(0) < V_{\max}$. Therefore, for all $s_1(0), \hat{W}_1(0)$ that belong to Ω_{10} , we have $\Omega_1 \subset \Omega_{NN}$ for $t > 0$. If Ω_1 and Ω_{1s} are larger than Ω_{NN} , this means that the initial conditions do not belong to a valid initial compact set Ω_{10} . This completes the proof. ■

4.3.2 Adaptive Variable Structure Neural Control for MIMO Case ($m \geq 2$)

In the foregoing discussions, we design control for the SISO case by Lyapunov synthesis design, so as to elucidate the main ideas of our control design. In this section, we extend the previous result to the MIMO case (4.4). System (4.4) is block triangular with respect to inputs u , as seen in the fact that nonlinearities $f_i(x, \bar{u}_{i-1})$ only contain inputs from the preceding subsystems. This structure of interconnection facilitates systematic recursive design.

Substituting (4.4) into (4.7) leads to

$$\begin{aligned} \dot{s}_i &= f_i(x, \bar{u}_{i-1}) + g_{i,\tau}(x_1(t - \tau_1(t)), \dots, x_m(t - \tau_m(t))) + b_i(\bar{x}_i)p_{i0}v_i(t) \\ &\quad - b_i(\bar{x}_i)d_i[v_i](t) + \nu_i \end{aligned} \quad (4.54)$$

where $\nu_i = \sum_{j=1}^{n_i-1} \lambda_{ij}e_{i,j+1} - y_{id}^{(n_i)}$.

Define the following integral Lyapunov function candidate,

$$V_{si} = \int_0^{s_i} \frac{\sigma}{b_i(\bar{x}_i^+, \sigma + \beta_i)} d\sigma \quad (4.55)$$

where $\beta_i = y_{id}^{(n_i-1)} - \sum_{j=1}^{n_i-1} \lambda_{ij}e_{ij}$, and $\bar{x}_i^+ = [x_1^T, \dots, x_{i-1}^T, x_{i,1}, \dots, x_{i,n_i-1}]^T$.

Applying First Mean Value Theorem for Integrals to (4.55), we have

$$V_{si} = \frac{\lambda_{si}s_i^2}{b_i(\bar{x}_i^+, \lambda_{si}s_i + \beta_i)}, \quad \lambda_{si} \in (0, 1)$$

which is positive definite with respect to s_i due to Assumption 4.1, $0 < b_{i0} \leq b_i(\bar{x}_i)$.

4.3 Control Design and Stability Analysis

Differentiating V_{si} with respect to time t , we obtain

$$\begin{aligned}
\dot{V}_{si} &= \frac{\partial V_{si}}{\partial s_i} \dot{s}_i + \frac{\partial V_{si}}{\partial \bar{x}_i^+} \dot{\bar{x}}_i^+ + \frac{\partial V_{si}}{\partial \beta_i} \dot{\beta}_i \\
&= \frac{s_i}{b_i(\bar{x}_i)} \left[f_i(x, \bar{u}_{i-1}) + g_{i,\tau}(x_1(t - \tau_1(t)), \dots, x_m(t - \tau_m(t))) \right. \\
&\quad \left. + b_i(\bar{x}_i) p_{i0} v_i(t) - b_i(\bar{x}_i) d_i[v_i](t) + \nu_i \right] \\
&\quad + \sum_{j=1}^{i-1} g_{i,\tau}(x_1(t - \tau_1(t)), \dots, x_m(t - \tau_m(t))) \int_0^{s_i} \sigma \left[\frac{\partial b_i^{-1}(\bar{x}_i^+, \sigma + \beta_i)}{\partial x_{jn_j}} \right] d\sigma \\
&\quad + \int_0^{s_i} \sigma \left\{ \sum_{j=1}^i \sum_{k=1}^{n_j-1} \frac{\partial b_i^{-1}(\bar{x}_i^+, \sigma + \beta_i)}{\partial x_{jk}} x_{j,k+1} + \sum_{j=1}^{i-1} \frac{\partial b_i^{-1}(\bar{x}_i^+, \sigma + \beta_i)}{\partial x_{jn_j}} \left[f_j(x, \bar{u}_{i-1}) \right. \right. \\
&\quad \left. \left. + b_j(\bar{x}_j) u_j(v_j) \right] \right\} d\sigma - \frac{\nu_i s_i}{b_i(\bar{x}_i)} + \int_0^{s_i} \frac{\nu_i}{b_i(\bar{x}_i^+, \sigma + \beta_i)} d\sigma
\end{aligned} \tag{4.56}$$

Using (4.6), after some manipulations, (4.56) becomes

$$\begin{aligned}
\dot{V}_{si} &\leq s_i Q_i + s_i \left[p_{i0} v_i(t) - d_i[v_i](t) \right] + \frac{|s_i|}{|b_i(\bar{x}_i)|} \sum_{k=1}^m \varrho_{ik}(x_k(t - \tau_k(t))) \\
&\quad + \sum_{j=1}^{i-1} \sum_{k=1}^m \varrho_{jk}(x_k(t - \tau_k(t))) s_i^2 \int_0^1 \theta \left[\frac{\partial b_i^{-1}(\bar{x}_i^+, \theta s_i + \beta_i)}{\partial x_{jn_j}} \right] d\theta
\end{aligned} \tag{4.57}$$

where

$$\begin{aligned}
Q_i(Z_i) &= \frac{f_i(x, \bar{u}_{i-1})}{b_i(\bar{x}_i)} + \int_0^1 \left\{ \theta s_i \left[\sum_{j=1}^i \sum_{k=1}^{n_j-1} \frac{\partial b_i^{-1}(\bar{x}_i^+, \sigma + \beta_i)}{\partial x_{jk}} x_{j,k+1} \right. \right. \\
&\quad \left. \left. + \sum_{j=1}^{i-1} \frac{\partial b_i^{-1}(\bar{x}_i^+, \theta s_i + \beta_i)}{\partial x_{jn_j}} [f_j(x, \bar{u}_{i-1}) + b_j(\bar{x}_j) u_j(v_j)] \right] \right. \\
&\quad \left. + \frac{\nu_i}{b_i(\bar{x}_i^+, \theta s_i + \beta_i)} \right\} d\theta
\end{aligned}$$

with $Z_i = [x^T, s_i, \nu_i, \beta_i, v_1, \dots, v_{i-1}]^T \in \mathbb{R}^{(\sum_{i=1}^m n_i) + i + 2}$.

By utilizing Young's inequality, we obtain that

$$\frac{|s_i|}{|b_i(\bar{x}_i)|} \sum_{k=1}^m \varrho_{ik}(x_k(t - \tau_k(t))) \leq \frac{m s_i^2}{2 b_i^2(\bar{x}_i)} + \frac{1}{2} \sum_{k=1}^m \varrho_{ik}^2(x_k(t - \tau_k(t))) \tag{4.58}$$

And

$$\sum_{j=1}^{i-1} \sum_{k=1}^m \varrho_{jk}(x_k(t - \tau_k(t))) s_i^2 \int_0^1 \theta \left[\frac{\partial b_i^{-1}(\bar{x}_i^+, \theta s_i + \beta_i)}{\partial x_{jn_j}} \right] d\theta$$

4.3 Control Design and Stability Analysis

$$\leq \frac{1}{2} \sum_{j=1}^{i-1} \sum_{k=1}^m \varrho_{jk}^2(x_k(t - \tau_k(t))) + \frac{ms_i^4}{2} \sum_{j=1}^{i-1} \left(\int_0^1 \theta \left[\frac{\partial b_i^{-1}(\bar{x}_i^+, \theta s_i + \beta_i)}{\partial x_{jn_j}} \right] d\theta \right)^2 \quad (4.59)$$

Substituting (4.58) and (4.59) into (4.57), we have

$$\begin{aligned} \dot{V}_{si} \leq & s_i Q_i + s_i [p_{i0} v_i(t) - d_i[v_i](t)] + \frac{ms_i^2}{2b_i^2(\bar{x}_i)} + \frac{1}{2} \sum_{j=1}^i \sum_{k=1}^m \varrho_{jk}^2(x_k(t - \tau_k(t))) \\ & + \frac{ms_i^4}{2} \sum_{j=1}^{i-1} \left(\int_0^1 \theta \left[\frac{\partial b_i^{-1}(\bar{x}_i^+, \theta s_i + \beta_i)}{\partial x_{jn_j}} \right] d\theta \right)^2 \end{aligned} \quad (4.60)$$

To overcome the design difficulties from the unknown time-varying delays $\tau_1(t), \dots, \tau_m(t)$ in (4.60), the following Lyapunov-Krasovskii functional can be considered:

$$V_{U_i}(t) = \frac{1}{2(1 - \bar{\tau}_{\max})} \sum_{j=1}^i \sum_{k=1}^m \int_{t-\tau_k(t)}^t \varrho_{jk}^2(x_k(\tau)) d\tau \quad (4.61)$$

The time derivative of V_{U_i} can be expressed as follows:

$$\begin{aligned} \dot{V}_{U_i}(t) = & \frac{1}{2(1 - \bar{\tau}_{\max})} \left[\sum_{j=1}^i \sum_{k=1}^m \varrho_{jk}^2(x_k(t)) \right. \\ & \left. - \sum_{j=1}^i \sum_{k=1}^m \varrho_{jk}^2(x_k(t - \tau_k(t))) (1 - \dot{\tau}_k(t)) \right] \end{aligned} \quad (4.62)$$

which can be used to cancel the time-delay term on the right hand side of (4.60).

Combining (4.60) and (4.62), we obtain

$$\dot{V}_{si} + \dot{V}_{U_i} \leq s_i h_i(Z_i) + s_i [p_{i0} v_i(t) - d_i[v_i](t)] \quad (4.63)$$

where

$$\begin{aligned} h_i(Z_i) = & Q_i(Z_i) + \frac{ms_i}{2b_i^2(\bar{x}_i)} + \frac{1}{2(1 - \bar{\tau}_{\max})s_i} \sum_{j=1}^i \sum_{k=1}^m \varrho_{jk}^2(x_k(t)) \\ & + \frac{ms_i^3}{2} \sum_{j=1}^{i-1} \left(\int_0^1 \theta \left[\frac{\partial b_i^{-1}(\bar{x}_i^+, \theta s_i + \beta_i)}{\partial x_{jn_j}} \right] d\theta \right)^2 \end{aligned} \quad (4.64)$$

Define the following compact sets

$$\Omega_{Z_1} = \left\{ [x^T, s_1, \nu_1, \beta_1]^T \mid x_j \in \Omega_j, j = 1, \dots, m, x_{1d} \in \Omega_{1d} \right\} \quad (4.65)$$

4.3 Control Design and Stability Analysis

$$\Omega_{Z_i} = \left\{ [x^T, s_i, \nu_i, \beta_i, v_1, \dots, v_{i-1}]^T \mid x_j \in \Omega_j, j = 1, \dots, m, x_{kd} \in \Omega_{kd}, \right. \\ \left. k = 1, \dots, i, \hat{W}_j \in \Omega_j, j = 1, \dots, i-1 \right\} \quad (4.66)$$

$$\Omega_{c_{s_i}} = \{s_i \mid |s_i| < c_{s_i}, x_{id} \in \Omega_{id}\} \quad (4.67)$$

$$\Omega_{Z_i}^0 = \Omega_{Z_i} - \Omega_{c_{s_i}} \quad (4.68)$$

where $\Omega_j \subset R^{n_j}$ is a sufficiently large compact set satisfying $\Omega_j \supset \Omega_{j0}$ defined later in Theorem 4.2, and c_{s_i} is a positive design constant that can be chosen arbitrarily small. The compact set $\Omega_{Z_i}^0$ is the complement set of set $\Omega_{c_{s_i}}$.

Let $\hat{W}_i^T S(Z_i)$ be the approximation of the function $h_i(Z_i)$, defined in (4.64), on the compact set $\Omega_{Z_i}^0$. Then, using RBFNNs, we have

$$h_i(Z_i) = \hat{W}_i^T S(Z_i) - \tilde{W}_i^T S(Z_i) + \varepsilon_i(Z_i) \quad (4.69)$$

where the approximation error $\varepsilon_i(Z_i)$ satisfies $|\varepsilon_i(Z_i)| \leq \varepsilon_i^*$ with positive constant ε_i^* , $\forall Z_i \in \Omega_{Z_i}^0$.

Similar to the procedures of Section 4.3.1, we design the following control law for the system in (4.4):

$$v_i = -q(s_i|c_{s_i}) \frac{\text{sgn}(s_i)}{p_{i0\min}} [k_{i0}(t)|s_i| + |\hat{W}_i^T S(Z_i)|] + v_{ih} \quad (4.70)$$

$$v_{ih}(t) = -q(s_i|c_{s_i}) \frac{\text{sgn}(s_i)}{p_{i0\min}} \int_0^R \hat{p}_i(t, r) |F_{ir}[v_i](t)| dr \quad (4.71)$$

$$k_{i0}(t) = q(s_i|c_{s_i}) [k_{i1} + k_{i2}(t) + \frac{1}{2}] \quad (4.72)$$

where $\hat{p}_i(t, r)$ denotes the estimate of the density function $p_i(r)$; k_{i1} is any positive constant, and $k_{i2}(t)$ is chosen as

$$k_{i2}(t) = q(s_i|c_{s_i}) \frac{k_{i3}}{2(1 - \bar{\tau}_{\max}) s_i^2} \sum_{j=1}^i \sum_{k=1}^m \int_{t-\tau_{\max}}^t \varrho_{jk}^2(x_k(\tau)) d\tau \quad (4.73)$$

with k_{i3} a positive constant specified by the designer.

The adaptation laws are chosen as

$$\dot{\hat{W}}_i = q(s_i|c_{s_i}) \Gamma_i [S(Z_i) s_i - \sigma_{w_i} \hat{W}_i] \quad (4.74)$$

$$\frac{\partial}{\partial t} \hat{p}_i(t, r) = \begin{cases} -q(s_i|c_{s_i}) \eta_i \sigma_{p_i} \hat{p}_i(t, r), & \text{if } \hat{p}_i(t, r) \geq p_{i\max}; \\ q(s_i|c_{s_i}) \eta_i [|s_i| |F_{ir}[x_{i,n_i}](t)| - \sigma_{p_i} \hat{p}_i(t, r)], & \text{if } 0 \leq \hat{p}_i(t, r) < p_{i\max}. \end{cases} \quad (4.75)$$

4.3 Control Design and Stability Analysis

with $\Gamma_i > 0$, σ_{w_i} , σ_{p_i} and η_i are strictly positive constants.

Based on the above design for control and adaptation laws, we are ready to establish the following result for the MIMO case.

Theorem 4.2 *Consider the closed-loop system consisting of the plant (4.4), the control laws (4.70) (4.71) and adaptation laws (4.74) (4.75). Under Assumptions 4.1-4.4, given some initial conditions $x_i(0)$, $\hat{W}_i(0)$, belong in Ω_{i0} , we can conclude that the overall closed-loop neural control system is SGUUB in the sense that all of the signals in the closed-loop system are bounded, i.e., the states and weights in the closed-loop system will remain in the compact set defined by*

$$\Omega_i = \left\{ s_i, \tilde{W}_i \mid |s_i| \leq \sqrt{2\mu_i}, \quad \|\tilde{W}_i\| \leq \sqrt{\frac{2\mu_i}{\lambda_{\min}(\Gamma_i^{-1})}} \right\} \quad (4.76)$$

with

$$\begin{aligned} \mu_i &= \frac{\mu_{i1}}{\lambda_{i1}} + V_i(0) \\ \mu_{i1} &= \frac{\sigma_{p_i} R}{2} p_{i\max}^2 + \frac{\sigma_{w_i}}{2} \|W_i^*\|^2 + \frac{\varepsilon_i^2}{2} \\ \lambda_{i1} &= \min \left\{ \frac{b_{i0} k_{i1}}{\lambda_{si}}, k_{i3}, \frac{\sigma_{w_i}}{\lambda_{\max}(\Gamma_i^{-1})}, \sigma_{p_i} \eta_i \right\} \\ V_i(0) &= V_{si}(0) + V_{Ui}(0) + \frac{1}{2} \tilde{W}_i^T(0) \Gamma_i^{-1} \tilde{W}_i(0) + \frac{1}{2\eta_i} \int_0^R \tilde{p}_i^2(0, r) dr \end{aligned}$$

and the tracking error will converge to a neighborhood of zero. In addition, the states and weights in the closed-loop system will eventually converge to the compact set defined by

$$\Omega_{is} = \left\{ s_i, \tilde{W}_i \mid |s_i| \leq \sqrt{2\mu_i^*}, \quad \|\tilde{W}_i\| \leq \sqrt{\frac{2\mu_i^*}{\lambda_{\min}(\Gamma_i^{-1})}} \right\} \quad (4.77)$$

where

$$\mu_i^* = \frac{\mu_{i1}}{\lambda_{i1}}$$

Proof: The proof is built on that of Theorem 4.1, and for the conciseness, we will only outline the general approach without going into specific details. For the i -th

4.3 Control Design and Stability Analysis

subsystem, we design v_i that takes into account the inputs from the preceding $(i-1)$ subsystems, i.e. \bar{v}_{i-1} . Suppose that both the states and the weights belong to Ω_{NN} , i.e., $\{x_j, \hat{W}_i\} \in \Omega_{NN}, \forall t \geq 0$, on which NN approximation (4.69) is valid.

Consider the following Lyapunov function candidate

$$V_i(t) = V_{si}(t) + V_{U_i}(t) + \frac{1}{2} \tilde{W}_i^T \Gamma_i^{-1} \tilde{W}_i + \frac{1}{2\eta_i} \int_0^R \tilde{p}_i^2(t, r) dr \quad (4.78)$$

where $\tilde{W}_i = \hat{W}_i - W_i$ and $\tilde{p}_i(t, r) = \hat{p}_i(t, r) - p_i(r)$.

Differentiating $V_i(t)$ with respect to time t leads to

$$\dot{V}_i(t) = \dot{V}_{si}(t) + \dot{V}_{U_i}(t) + \tilde{W}_i^T \Gamma_i^{-1} \dot{\tilde{W}}_i + \frac{1}{\eta_i} \int_0^R \tilde{p}_i(t, r) \frac{\partial}{\partial t} \hat{p}_i(t, r) dr \quad (4.79)$$

Substituting (4.63) into (4.79) leads to

$$\begin{aligned} \dot{V}_i(t) \leq & s_i h_i(Z_i) + s_i [p_{i0} v_i - d_i[v_i](t)] + \tilde{W}_i^T \Gamma_i^{-1} \dot{\tilde{W}}_i \\ & + \frac{1}{\eta_i} \int_0^R \tilde{p}_i(t, r) \frac{\partial}{\partial t} \hat{p}_i(t, r) dr \end{aligned} \quad (4.80)$$

Considering the adaptive neural control laws and adaptation laws from (4.70)-(4.75), the stability analysis is carried out in the following two regions, respectively.

- **Region 1:** If $|s_i| \geq c_{s_i}$, then $q_i(s_i|c_{s_i}) = 1$. Noting (4.69) and submitting (4.70) into (4.80), we have

$$\begin{aligned} \dot{V}_i(t) \leq & -s_i \tilde{W}_i^T S(Z_i) + s_i \varepsilon_1(Z_i) - k_{i0}(t) s_i^2 + s_i [p_{i0} v_{ih} - d_i[v_i](t)] \\ & + \tilde{W}_i^T \Gamma_i^{-1} \dot{\tilde{W}}_i + \frac{1}{\eta_i} \int_0^R \tilde{p}_i(t, r) \frac{\partial}{\partial t} \hat{p}_i(t, r) dr \end{aligned} \quad (4.81)$$

Using Young's Inequality, we have

$$s_i \varepsilon_i(Z_i) \leq \frac{s_i^2}{2} + \frac{\varepsilon_i^{*2}}{2} \quad (4.82)$$

Substituting (4.72), (4.74) and (4.82) and into (4.81) leads to

$$\begin{aligned} \dot{V}_i(t) \leq & -k_{i1} s_i^2 - k_{i3} V_{U_i} - \sigma_{w_i} \tilde{W}_i^T \hat{W}_i + \frac{\varepsilon_i^{*2}}{2} + s_i [p_{i0} v_{ih} - d_i[v_i](t)] \\ & + \frac{1}{\eta_i} \int_0^R \tilde{p}_i(t, r) \frac{\partial}{\partial t} \hat{p}_i(t, r) dr \end{aligned} \quad (4.83)$$

4.3 Control Design and Stability Analysis

For the third term in (4.83), by completion of squares, we have

$$-\sigma_{w_i} \tilde{W}_i^T \hat{W}_i \leq -\frac{\sigma_{w_i}}{2} \|\tilde{W}_i\|^2 + \frac{\sigma_{w_i}}{2} \|W_i^*\|^2 \quad (4.84)$$

For the last two terms in (4.83), we can obtain the similar conclusions as (4.46) and (4.49):

$$\begin{aligned} & s_i \left[p_{i0} v_{ih} - d_i[v_i](t) \right] + \frac{1}{\eta_i} \int_0^R \tilde{p}_i(t, r) \frac{\partial}{\partial t} \hat{p}_i(t, r) dr \\ & \leq -\sigma_{p_i} \int_0^R \tilde{p}_i(t, r) \hat{p}_i(t, r) dr \\ & \leq -\frac{\sigma_{p_i}}{2} \int_0^R \tilde{p}_i^2(t, r) dr + \frac{\sigma_{p_i} R}{2} p_{i\max}^2 \end{aligned} \quad (4.85)$$

Substituting (4.84) and (4.85) into (4.83), we have

$$\begin{aligned} \dot{V}_i(t) & \leq -k_{i1} s_1^2 - k_{i3} V_{Ui} - \frac{\sigma_{w_i}}{2} \|\tilde{W}_i\|^2 - \frac{\sigma_{p_i}}{2} \int_0^R \tilde{p}_i^2(t, r) dr + \frac{\sigma_{p_i} R}{2} p_{i\max}^2 \\ & \quad + \frac{\sigma_{w_i}}{2} \|W_i^*\|^2 + \frac{\varepsilon_i^{*2}}{2} \\ & \leq -\lambda_{i1} V_i(t) + \mu_{i1} \end{aligned} \quad (4.86)$$

where

$$\begin{aligned} \lambda_{i1} &= \min \left\{ \frac{b_{i0} k_{i1}}{\lambda_{si}}, k_{i3}, \frac{\sigma_{w_i}}{\lambda_{\max}(\Gamma_i^{-1})}, \sigma_{p_i} \eta_i \right\} \\ \mu_{i1} &= \frac{\sigma_{p_i} R}{2} p_{i\max}^2 + \frac{\sigma_{w_i}}{2} \|W_i^*\|^2 + \frac{\varepsilon_i^{*2}}{2} \end{aligned}$$

Multiplying (4.86) by $e^{\lambda_{i1} t}$ and integrating over $[0, t]$, we have

$$0 \leq V_i(t) \leq \frac{\mu_{i1}}{\lambda_{i1}} + [V_i(0) - \frac{\mu_{i1}}{\lambda_{i1}}] e^{-\lambda_{i1} t} \leq \mu_i \quad (4.87)$$

where $\mu_i = \frac{\mu_{i1}}{\lambda_{i1}} + V_i(0)$. Therefore,

$$\|\tilde{W}_i\| \leq \sqrt{2\mu_i / \lambda_{\min}(\Gamma_i^{-1})}, \quad |s_i| \leq \sqrt{2b_{i1} V_i(t)} \leq \sqrt{2b_{i1} \mu_i} \quad (4.88)$$

Region 2: If $|s_i| < c_{s_i}$, then $q_i(s_i | c_{s_i}) = 0$. In this case, the control signal $v_i = 0$, $v_{ih} = 0$, $\dot{W}_i = 0$, $\frac{\partial}{\partial t} \hat{p}_i(t, r) = 0$, i.e., all the signals are kept bounded.

Similar to the discussion in Theorem 4.1, we can conclude that the overall closed-loop neural control system is SGUUB in the sense that all of the signals in the closed-loop system are bounded, i.e., the states and weights in the closed-loop system will remain in the compact set Ω_i defined in (4.76), and will eventually converge to the compact set defined by (4.77). This completes the proof. ■

4.4 Simulation Results

In this section, results of extensive simulation studies are presented to demonstrate the effectiveness of the proposed adaptive NN approach to deal with uncertain nonlinear systems under the effects of time delay and hysteresis. For clear illustration, we consider first a simplified SISO plant with first-order dynamics, and study the tracking performance of the controller, as well as perform detailed analysis on the effects of control parameter variations. Subsequently, a MIMO plant consisting of two interconnected second-order subsystems is tackled, and the closed loop properties and tracking behavior are investigated.

4.4.1 SISO Case

For the SISO case, we consider the following first-order scalar nonlinear system with hysteresis and state delay:

$$S_1 : \begin{cases} \dot{x} &= \frac{1-e^{-x}}{1+e^{-x}} + 0.1x(t - \tau(t)) + u \\ y &= x \end{cases} \quad (4.89)$$

where y is the plant output; u is the plant input and the output of the classic PI hysteresis model as in (4.2): $u = p_0 v - \int_0^R p(r) F_r[v](t) dr$, with $p(r) = 0.35e^{-0.003(r-1)^2}$ for $r \in [0, 100]$, $p_{\max} = 0.35$, $p_{0\min} = 0.35$; the time-varying delay $\tau(t) = 1 - 0.5 \cos(t)$, $\tau_{\max} = 2$, $\bar{\tau}_{\max} = 0.6$. The objective is to design control v such that the output y can track the desired trajectory $y_d = \sin(2t) + 0.1 \cos(6.7t)$.

We adopt the control law and adaption laws designed in Section 4.3.1 in the following:

$$v = -q(s|c_s) \frac{\text{sgn}(s)}{p_{0\min}} [k_0(t)|s| + |\hat{W}^T S(Z)|] + v_h \quad (4.90)$$

$$v_h = -q(s|c_s) \frac{\text{sgn}(s)}{p_{0\min}} \int_0^R \hat{p}(t, r) |F_r[v](t)| dr \quad (4.91)$$

$$k_0(t) = q(s|c_s) [k_1 + k_2(t) + \frac{1}{2}] \quad (4.92)$$

$$k_2(t) = q(s|c_s) \frac{k_3}{2(1 - \bar{\tau}_{\max})s^2} \int_{t-\tau_{\max}}^t \varrho^2(x(\tau)) d\tau \quad (4.93)$$

$$\dot{\hat{W}} = q(s|c_s) \Gamma_1 [S(Z)s - \sigma_w \hat{W}] \quad (4.94)$$

$$\frac{\partial}{\partial t} \hat{p}(t, r) = \begin{cases} -q(s|c_s) \eta \sigma_p \hat{p}(t, r), & \text{if } \hat{p}(t, r) \geq p_{\max} \\ q(s|c_s) \eta [|s| |F_r[v](t)| - \sigma_p \hat{p}(t, r)], & \text{if } 0 \leq \hat{p}(t, r) < p_{\max} \end{cases} \quad (4.95)$$

where $s = e = y - y_d$, and $\hat{p}(t, r)$ is the estimate of the density function of $p(r)$. The input of the neural networks is $Z = [x, \dot{y}_d] \in \mathbb{R}^2$. Employing ten nodes for each input dimension, we end up with $10^2 = 100$ nodes for the network $\hat{W}^T S(Z)$. The bounding function for the time delay term is chosen as $\varrho(x(\tau)) = 0.1|x(\tau)|$, and the following initial conditions and controller design parameters are adopted in the simulation: $x(0) = 0.5$, $v(0) = 0$, $\hat{p}(0, r) = 0$, $\hat{W}(0) = 0$, $\Gamma = \text{diag}\{1.0\}$, $\sigma = 0.1$, $\eta = 0.2$, $\sigma_p = 0.05$, $k_1 = 0.1$, $k_3 = 0.001$, $\epsilon = 0.05$, $c_s = 0.0001$.

The simulation results for SISO plant S_1 , as described in (4.89), are shown in Figures 4.2 -4.11. From Figure 4.2, we can observe that good tracking performance is achieved. At the same time, the boundedness of the control signals are shown in Figure 4.3. It is noted that there is a large difference between the v and u , indicating the significant hysteresis effect. In particular, we highlight the importance of the term v_h in (4.90), which is used to mitigate the effect caused by the hysteresis term $\int_0^R p(r) F_r[v](t) dr$ in the classic PI hysteresis model $u = p_0 v - \int_0^R p(r) F_r[v](t) dr$, as discussed in Remark 4.7. The comparison of tracking errors in the presence and absence of v_h is shown in Figure 4.4, and it is seen that with v_h , the tracking error resulting from hysteresis is attenuated accordingly. Figures 4.5 and 4.6 show the nonlinear approximation capability of neural networks $\hat{W}^T S(Z)$ and the norm of NN weights respectively. The behavior of the estimate of the density function, $\hat{p}(t, r)$, is also indicated in Figure 4.7.

To investigate the effects of the control parameters on the tracking performance, and to provide recommendations for their selection, we provide the following comparison results for the design constants k_1 and η in Figures 4.8 and 4.9. First of all, as

shown in Figure 4.8, the tracking error can be reduced by increasing the parameter k_1 . Secondly, from (4.95) and Figure 4.9, we know that higher learning rate, i.e. increase of η , results in better tracking performance. While the above results seem to indicate that k_1 and η should be large, caution must be exercised in the choice of these parameters, due to the fact that there are some tradeoffs between the control performance and other issues. In particular, for the case of control gain k_1 , the price to be paid is the high gain control, which also can be seen from (4.90) and (4.92). Problems associated with high gain control include sensitivity to measurement noise, excitation of high frequency unmodelled dynamics, as well as excessive control efforts. A similar tradeoff exists with regard to the parameter η , which represents the learning rate of the density function estimate $\hat{p}(t, r)$, in (4.95). In general, if η is chosen to be too large, then the stability and robustness of the system may be compromised in a similar way as high gain control.

Need to mention that, due to the use of sign function $\text{sgn}(\cdot)$, controllers (4.90) and (4.91) become discontinuous, which may excite unmodelled high-frequency plant dynamics and cause the chattering phenomenon. To avoid the undesired chattering phenomenon, we replace the sign function in the above control laws with the saturation function $\text{sat}(\frac{s}{\epsilon})$, which is defined as:

$$\text{sat}(*) = \begin{cases} 1 & \text{if } * \geq \epsilon \\ \frac{*}{\epsilon} & \text{if } |*| < \epsilon \\ -1 & \text{if } * < -\epsilon \end{cases} \quad (4.96)$$

where ϵ is a very small positive constant. Therefore, the different choices of ϵ also can affect the tracking performance, as shown in Figure 4.10. The smaller ϵ , the closer the saturation function approximate the sign function. As such, though the better tracking performance can be achieved with the smaller ϵ , the chattering phenomenon will become more serious, as a result, which degrades the performance finally.

In addition, as discussed in previous Remark 4.8, we adopt a numerical method by introducing a small delay Δt to implement the control v in (4.90) instead of solving it directly. The choices of the delay Δt affect the performance as shown in Figure 4.11. With the increasing of Δt , the performance becomes worse. In this chapter, we choose $\Delta t = T$, where $T = 0.005$ is the sampling time.

4.4.2 MIMO Case

Consider the following MIMO nonlinear system consisting of two interconnected second-order subsystems with time delay and hysteresis:

$$S_2 : \begin{cases} \dot{x}_{11} &= x_{12} \\ \dot{x}_{12} &= x_{11}x_{12} + u_1 + 0.1x_{11}(t - \tau_1(t)) \\ \dot{x}_{21} &= x_{22} \\ \dot{x}_{22} &= x_{11}x_{21} + u_2 + 0.2x_{21}(t - \tau_2(t)) \\ y_1 &= x_{11} \\ y_2 &= x_{21} \end{cases}$$

where y_i are the plant outputs, $i = 1, 2$; u_i are the plant inputs and the outputs of the classic PI hysteresis model as in (4.2): $u_i = p_0 v_i - \int_0^R p(r) F_r[v_i](t) dr$ with $p(r) = 0.08e^{-0.0024(r-1)^2}$ for $r \in [0, 100]$, $p_{\max} = 0.35$, $p_{0\min} = 0.1$; the time-varying delays $\tau_1(t) = 0.2(1 + \sin(t))$, $\tau_2(t) = 1 - 0.5 \cos(t)$, $\tau_{\max} = 2$, $\bar{\tau}_{\max} = 0.6$. The objective is to design control v_i such that the output y_i can track the desired trajectory $y_{di} = 0.5 \sin(t)$, $i = 1, 2$.

The control law and adaption laws in (4.70)-(4.75) are adopted. The inputs of the neural networks are $Z_1 = [s_1, x, \nu_1, \beta_1] \in \mathbb{R}^7$ and $Z_2 = [s_2, x, \nu_2, \beta_2, v_1] \in \mathbb{R}^8$, where $\nu_i = \lambda_i(\dot{y}_i - \dot{y}_{id}) - \dot{y}_{id}$, $\beta_i = \dot{y}_{id} - \lambda_i(y_i - y_{id})$, $i = 1, 2$. Employing three nodes for each input dimension, we end up with 3^7 nodes for the network $\hat{W}_1^T S(Z_1)$, and 3^8 nodes for the network $\hat{W}_2^T S(Z_2)$. The bounding functions for the time delay term are chosen as $\varrho_1(x_1(\tau)) = 0.1|x_{11}(\tau)|$, $\varrho_2(x_2(\tau)) = 0.2|x_{22}(\tau)|$, and the following initial conditions and controller design parameters are adopted in the simulation: $x_{11}(0) = -0.4$, $x_{12}(0) = x_{21}(0) = x_{22}(0) = 0.5$, $v_1(0) = v_2(0) = 0$, $\hat{p}_1(0, r) = \hat{p}_2(0, r) = 0$, $\hat{W}_1(0) = \hat{W}_2(0) = 0$, $\Gamma_1 = \text{diag}\{1.0\}$, $\Gamma_2 = \text{diag}\{0.025\}$, $\sigma_1 = 0.2$, $\sigma_1 = 2.5$, $\eta_1 = \eta_2 = 0.01$, $\sigma_{p1} = \sigma_{p2} = 0.05$, $k_{11} = k_{21} = 0.1$, $k_{13} = k_{23} = 0.001$, $\lambda_1 = 2.5$, $\lambda_2 = 2.0$, $c_{s_1} = c_{s_2} = 0.0001$.

Simulation results for MIMO plant S_2 , as described in (4.97), are shown in Figs 4.12-4.19. From Figures 4.12, it is seen that good tracking performance is achieved despite large initial tracking errors e_1 and e_2 , and they converge to a small neighborhood of zero in a relatively short time. At the same time, it can be observed, in Figures

4.13, 4.14 and 4.15, that the control signals, norms of NN weights, and states x_{12} , x_{22} remain bounded. Figure 4.16 shows the nonlinear approximation capability of neural networks $\hat{W}_1^T S(Z_1)$ and $\hat{W}_2^T S(Z_2)$. Similar relationships between variations of control parameters and effects on tracking performance, as shown for the SISO case, can be verified for the MIMO case as well in Figures 4.17-4.19.

4.5 Conclusion

Adaptive variable structure neural control has been proposed for a class of uncertain MIMO nonlinear systems with unknown state time-varying delays and classic PI hysteresis nonlinearities. The uncertainties from unknown time-varying delays have been compensated for through the use of appropriate Lyapunov-Krasovskii functionals. The effect of the unknown hysteresis with the classic PI models was also mitigated using the proposed control. The controller has been made to be free from singularity problem by utilizing integral Lyapunov function. Based on the principle of sliding mode control, the developed controller can guarantee that all signals involved are semi-globally uniformly ultimately bounded. Simulation results have verified the effectiveness of the proposed approach.

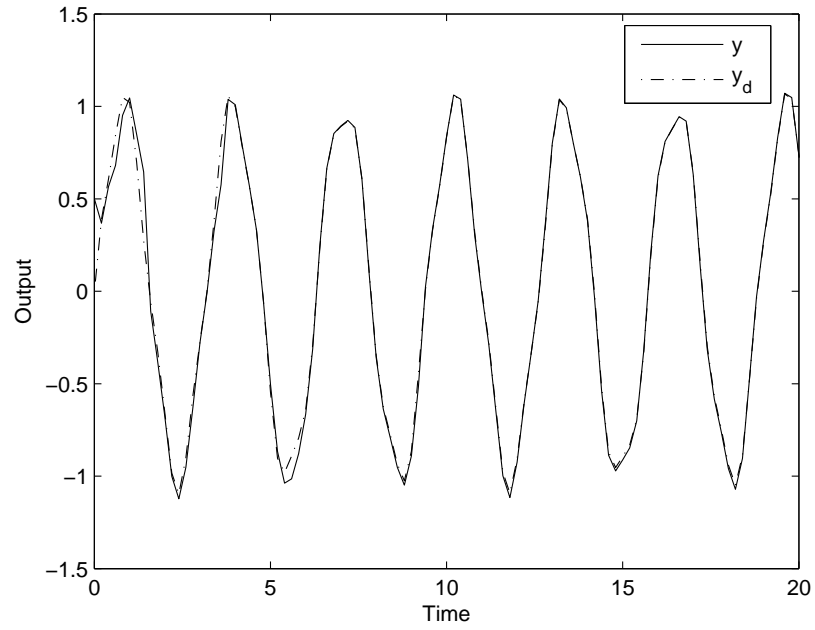


Figure 4.2: Output tracking performance of SISO plant S_1 with classic PI hysteresis

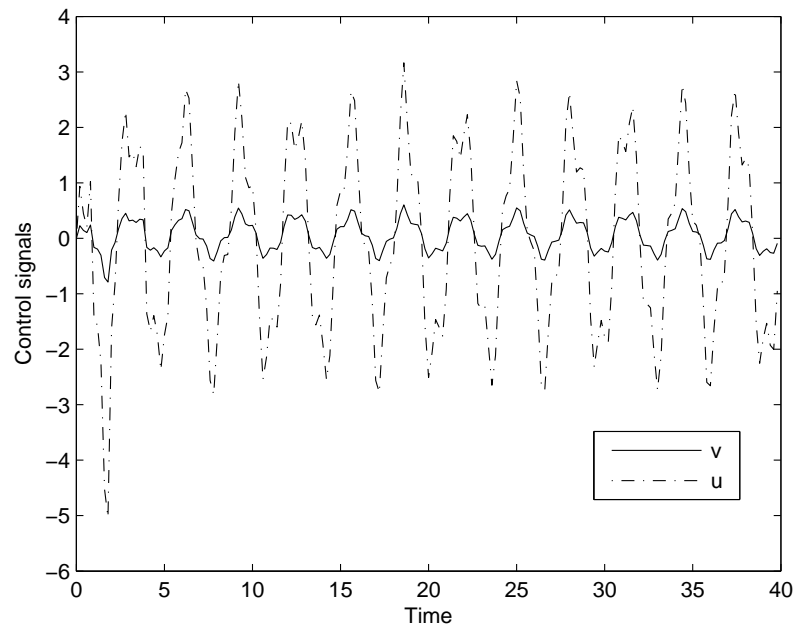


Figure 4.3: Control signals of SISO plant S_1 with classic PI hysteresis

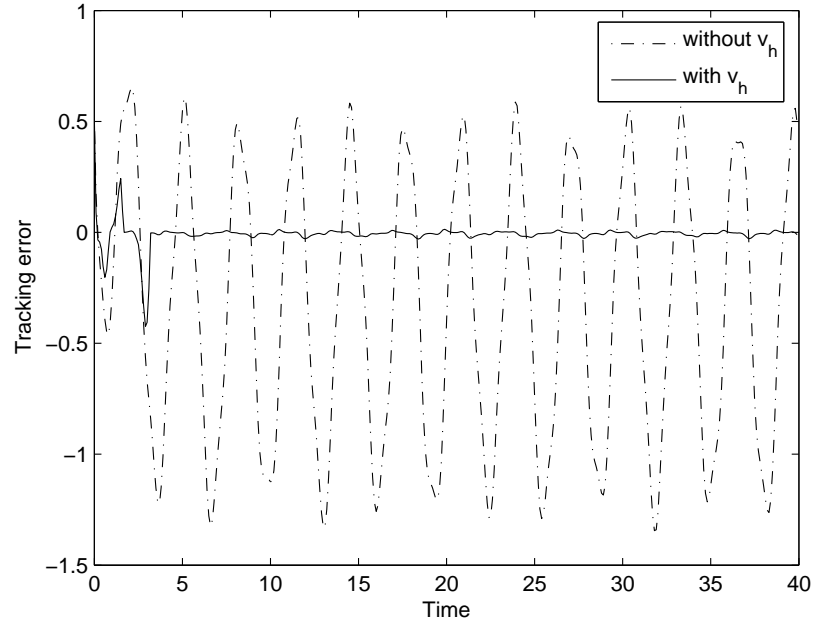


Figure 4.4: Tracking error comparison result of SISO plant S_1 with classic PI hysteresis and w/o v_h

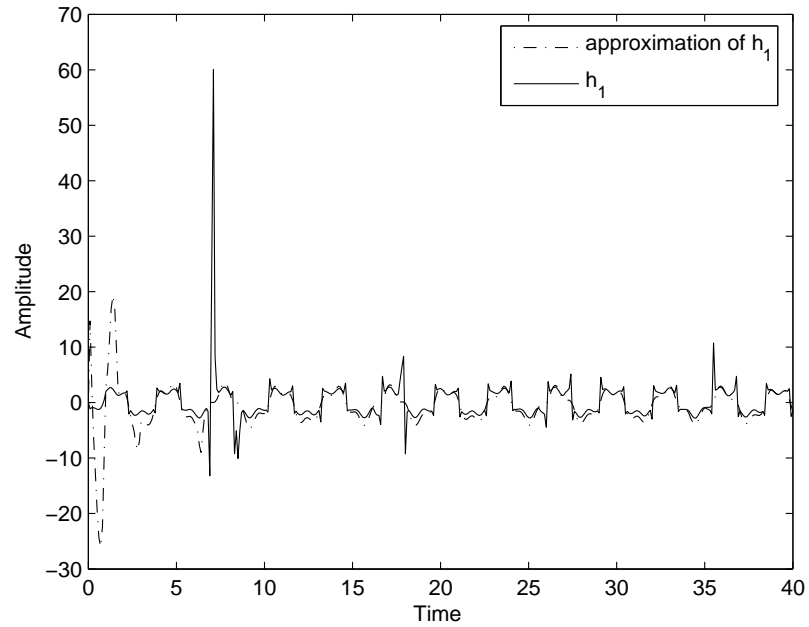


Figure 4.5: Learning behavior of neural networks of SISO plant S_1 with classic PI hysteresis

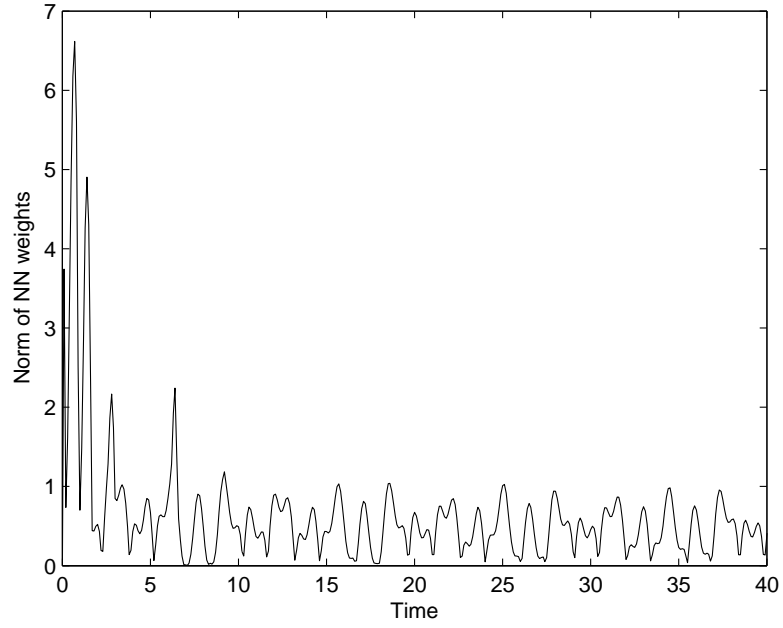


Figure 4.6: Norm of NN weights of SISO plant S_1 with classic PI hysteresis

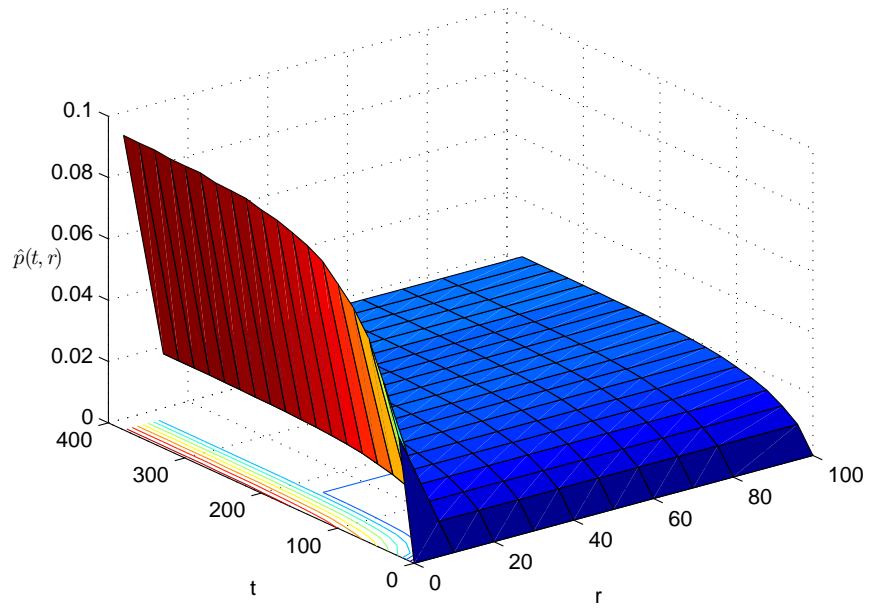


Figure 4.7: The behavior of the estimate values of the density function, $\hat{p}(t, r)$

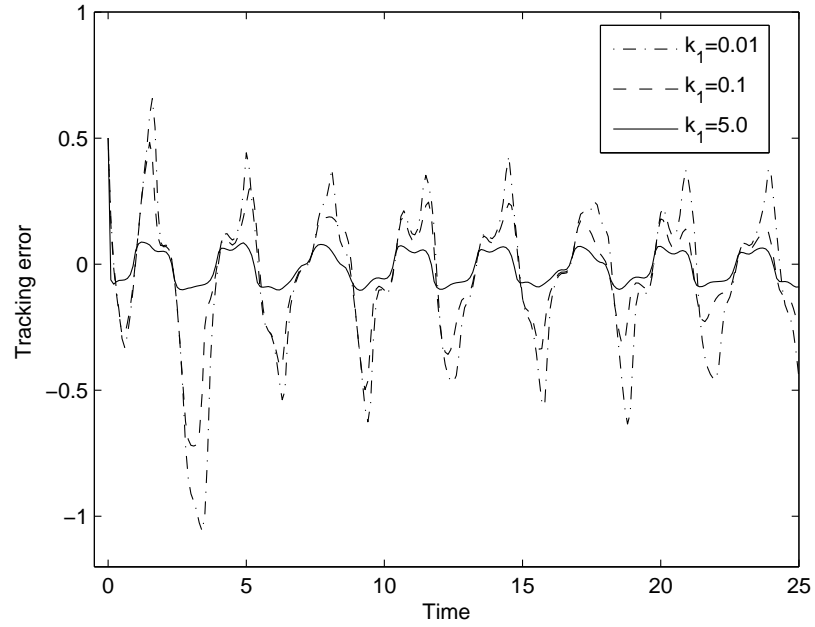


Figure 4.8: Tracking error comparison result of SISO plant S_1 with classic PI hysteresis for different k_1

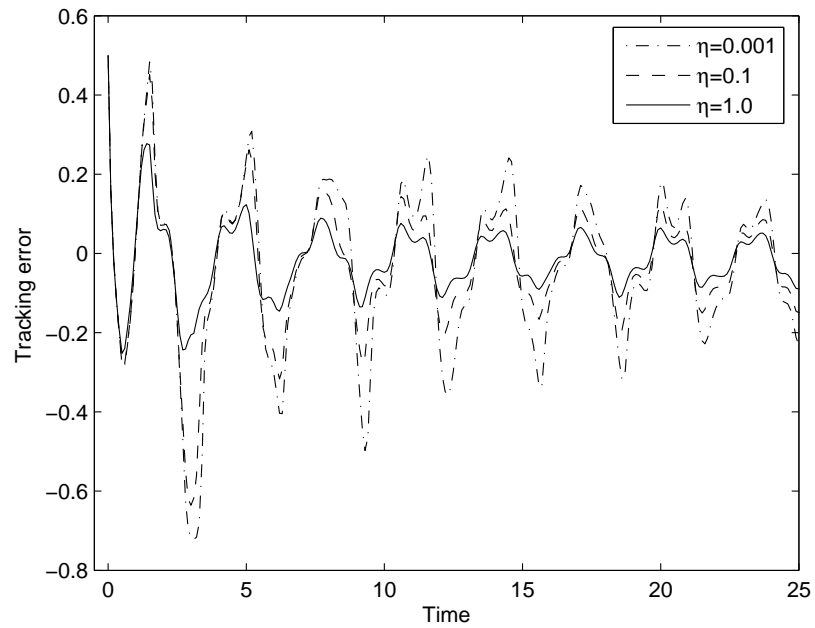


Figure 4.9: Tracking error comparison result of SISO plant S_1 with classic PI hysteresis for different η

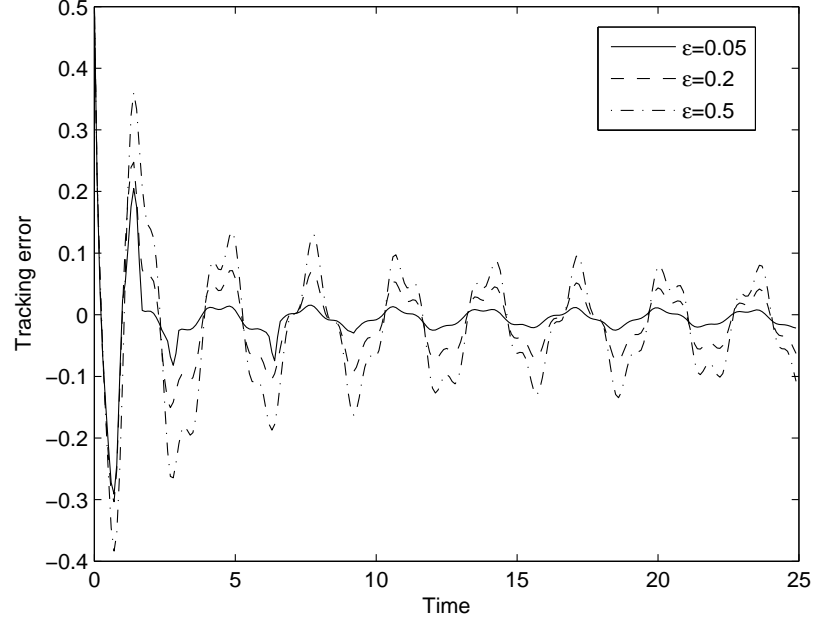


Figure 4.10: Tracking error comparison result of SISO plant S_1 with classic PI hysteresis for different ϵ

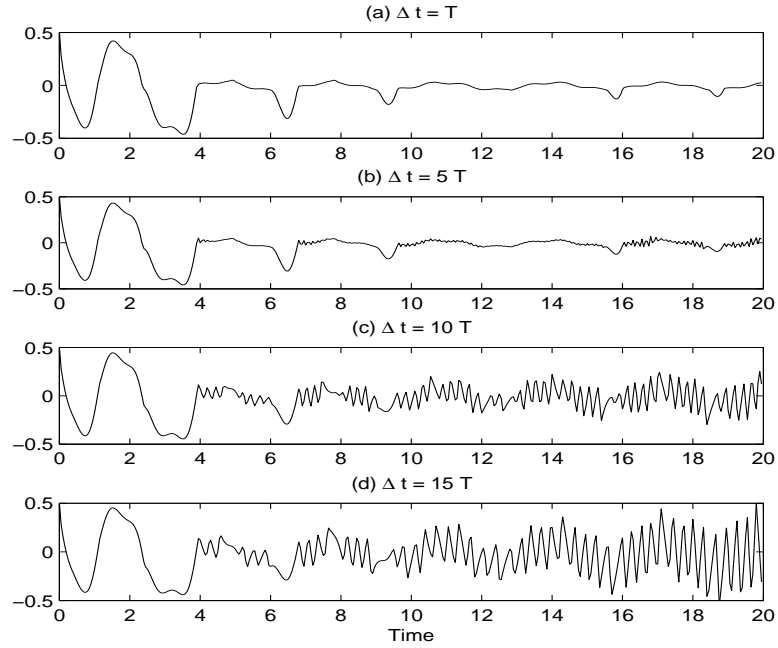


Figure 4.11: Tracking error comparison result of SISO plant S_1 with classic PI hysteresis for different delay Δt as pointed in Remark 4.8 (the sampling time $T = 0.005$)

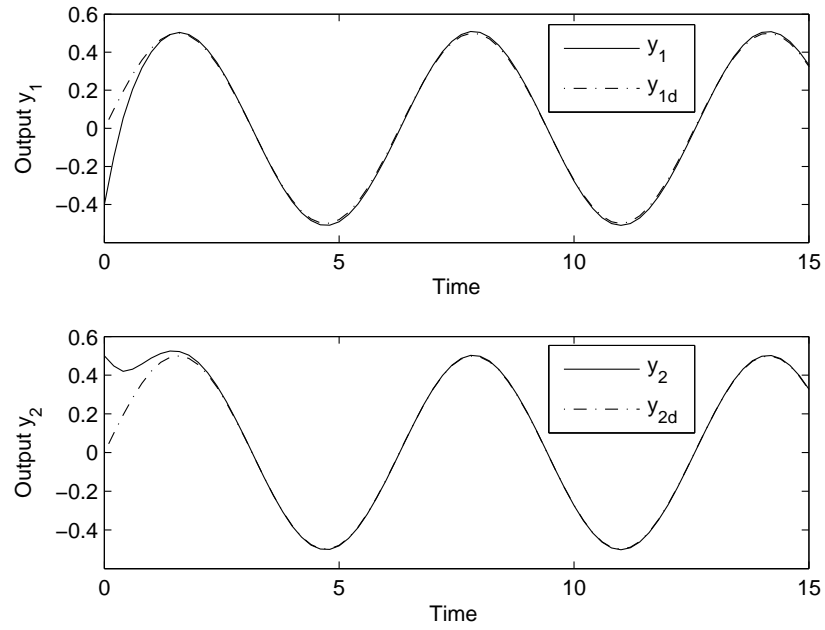


Figure 4.12: Output tracking performance of MIMO plant S_2 with classic PI hysteresis

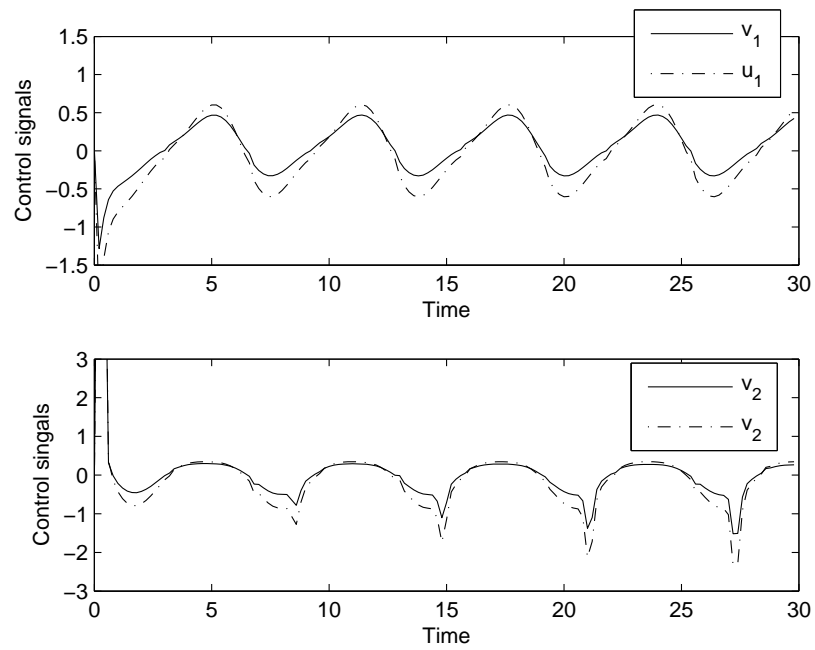


Figure 4.13: Control signals of MIMO plant S_2 with classic PI hysteresis

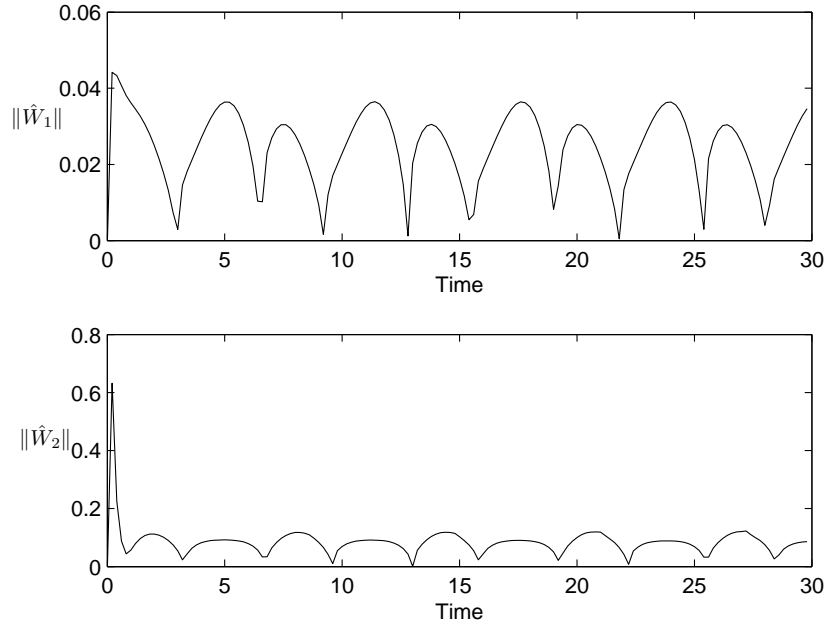


Figure 4.14: Norm of NN weights of MIMO plant S_2 with classic PI hysteresis

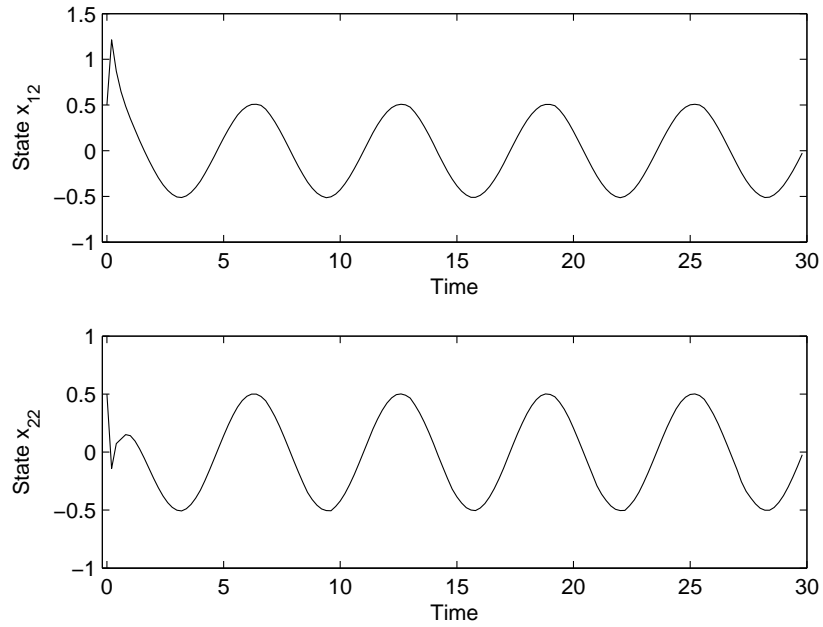


Figure 4.15: Other states of MIMO plant S_2 with classic PI hysteresis

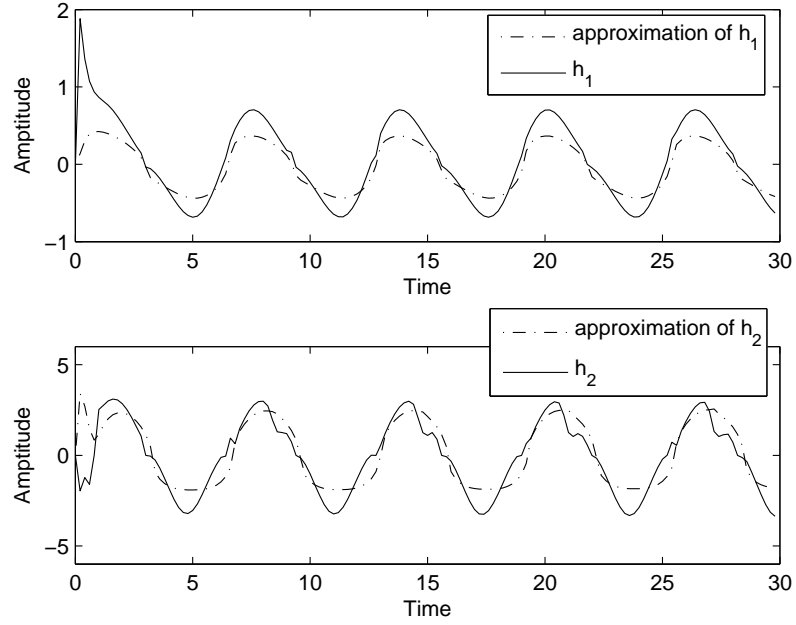


Figure 4.16: Learning behavior of neural networks of MIMO plant S_2 with classic PI hysteresis

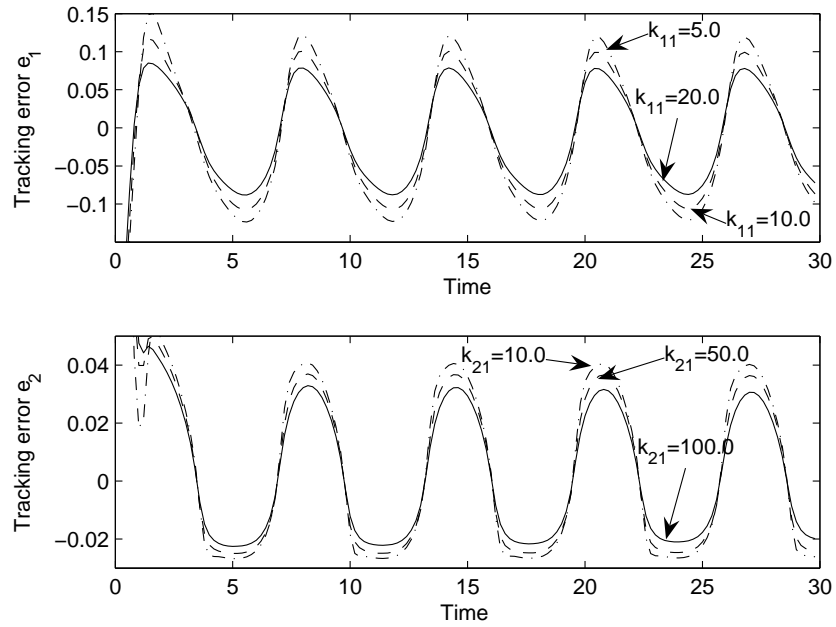


Figure 4.17: Tracking error comparison result of MIMO plant S_2 with classic PI hysteresis for different k_{11} and k_{21}

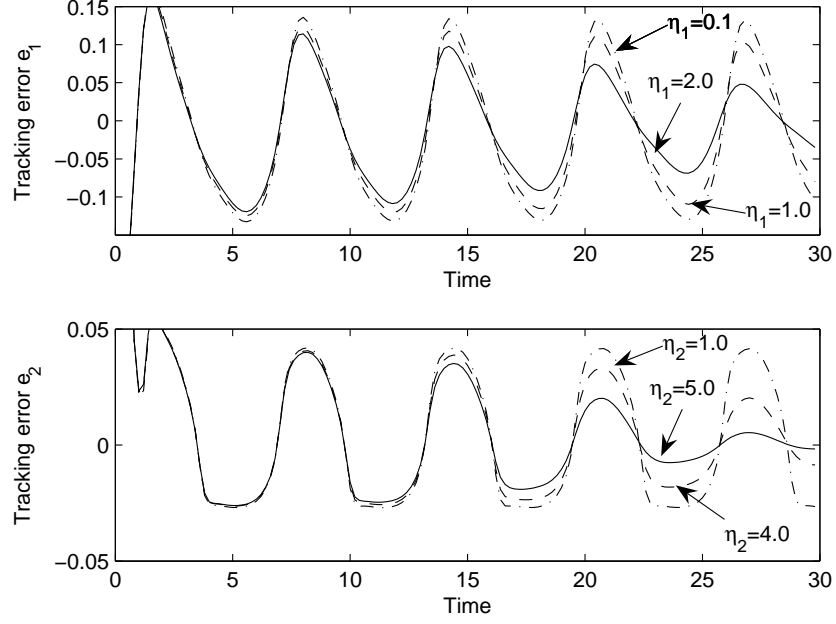


Figure 4.18: Tracking error comparison result of MIMO plant S_2 with classic PI hysteresis for different η_1 and η_2

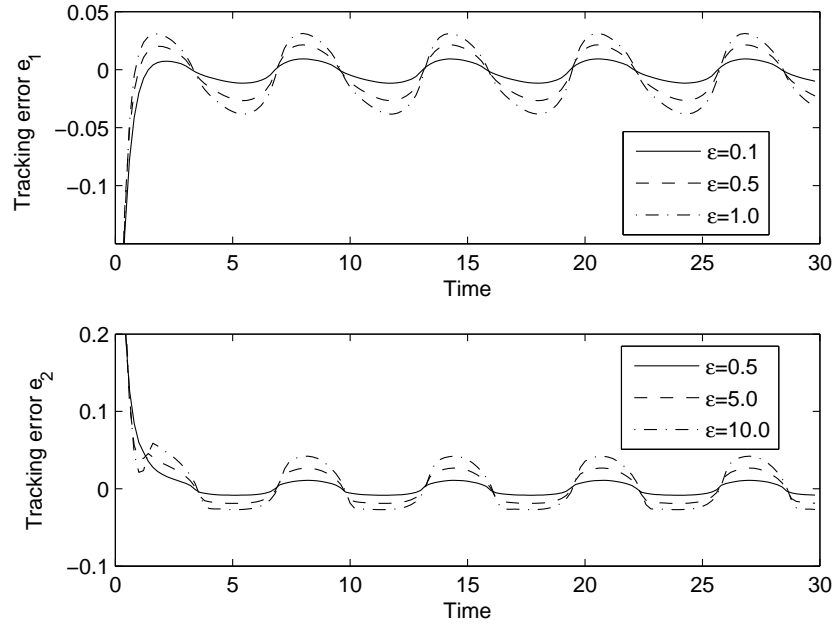


Figure 4.19: Tracking error comparison result of MIMO plant S_2 with classic PI hysteresis for different ϵ

Chapter 5

Systems with Generalized Prandtl-Ishlinskii Hysteresis

5.1 Introduction

Hysteresis nonlinearities are common in smart material-based actuators, such as piezoceramics and shape memory alloys. It is challenging to fuse the available hysteresis models with the existing control methods, due to the nonsmooth characteristics of hysteresis nonlinearities. One of the most common approaches is to construct an inverse operator to cancel the effects of the hysteresis as in [3] and [120]. However, it is a challenging task to construct the inverse operator for the hysteresis, due to the complexity and uncertainty of hysteresis. To circumvent these difficulties, alternative control approaches that do not need an inverse model have also been developed in [16, 17, 18, 19]. In [16] and [17], robust adaptive control and adaptive backstepping control were, respectively, investigated for a class of nonlinear system with unknown backlash-like hysteresis. In [18] and [19], adaptive variable structure control and adaptive backstepping methods, respectively, were proposed for a class of continuous-time nonlinear dynamic systems preceded by a hysteresis nonlinearity with the classic Prandtl-Ishlinskii (PI) model representation.

Compared with the above works, in this chapter, we consider a class of unknown

nonlinear systems in pure-feedback form which are preceded by a generalized PI hysteresis input. Compared with the backlash-like hysteresis and the classic PI hysteresis model, the generalized PI hysteresis model proposed in [106] can capture the hysteresis phenomenon more accurately and accommodate more general classes of hysteresis shapes, by adjusting both the density function and the input function. However, the difficulty here in dealing with the generalized PI hysteresis model lies in that the input function in the generalized PI hysteresis model is unknown and non-affine. Motivated by [99, 101, 155], in this chapter, we adopt the Mean Value Theorem to transform the unknown non-affine input function to a partially affine form, which can be seen as a multiplication of control term with a function of control and handled by extending some available techniques for affine nonlinear system control in the literature.

For pure-feedback systems, the cascade and non-affine properties make it difficult to find the explicit virtual controls and the actual control to stabilize the pure-feedback systems. In [97] and [98], much simpler pure-feedback systems where the last one or two equations were assumed to be affine, were discussed. In [100], an “ISS-modular” approach combined with small gain theorem was presented for adaptive neural control of the completely non-affine pure-feedback system. In this chapter, we also consider a class of unknown nonlinear systems in pure-feedback form. The non-affine problem in the control variable and virtual ones is dealt with by adopting the Mean Value Theorem, motivated by the works [99, 101, 155], without the assumptions that the last one or two equations are affine as in [97] and [98]. The unknown virtual control directions are dealt with by using Nussbaum functions.

The main contributions are highlighted as follows:

- (i) to the best of the author’s knowledge, it is the first time, in the literature, that the tracking control problem of unknown nonlinear systems in pure-feedback form with the generalized PI hysteresis input is investigated;
- (ii) the difficulty in dealing with the generalized PI hysteresis model, i.e., the non-affine problem of the uncertain nonlinear input function in the generalized PI hysteresis model, is solved by adopting the Mean Value Theorem;
- (iii) different from the previous works [18, 19], the σ -modification is included in the

5.2 Problem Formulation and Preliminaries

adaptation law of estimate of density function, $\hat{p}(t, r)$, to establish the different closed-loop stability; and

- (iv) the combination of the Mean Value Theorem and Nussbaum functions are also used to solve the non-affine and unknown virtual control direction problems in the pure-feedback nonlinear systems, without the assumptions that the last one or two equations are affine as in [97, 98].

The organization of this chapter is as follows. The problem formulation and preliminaries are given in Section 5.2. In Section 5.3, adaptive neural control is developed for a class of unknown nonlinear systems in pure-feedback form with the uncertain generalized PI hysteresis input. The closed-loop system stability is analyzed as well. Results of extensive simulation studies are shown to demonstrate the effectiveness of the approach in Section 5.4, followed by the conclusion in Section 5.5.

5.2 Problem Formulation and Preliminaries

Consider the following class of unknown nonlinear system in pure-feedback form whose input is preceded by the uncertain generalized PI hysteresis:

$$\begin{aligned}\dot{x}_j &= f_j(\bar{x}_j, x_{j+1}), \quad 1 \leq j \leq n-1 \\ \dot{x}_n &= f_n(\bar{x}_n, u) + d(t) \\ y &= x_1\end{aligned}\tag{5.1}$$

where $\bar{x}_j = [x_1, \dots, x_j]^T \in \mathbb{R}^j$ is the vector of states of the first j differential equations, and $\bar{x}_n = [x_1, \dots, x_n]^T \in \mathbb{R}^n$; $f_j(\cdot)$ and $f_n(\cdot)$ are unknown smooth functions; $d(t)$ is a bounded disturbance; $y \in \mathbb{R}$ is the output of the system; and $u \in \mathbb{R}$ is the input of the system and the output of the hysteresis nonlinearity, which is represented by the generalized PI model in [106] as follows

$$\begin{aligned}u(t) &= h(v)(t) - \int_0^D p(r) F_r[v](t) dr \\ F_r[v](0) &= h_r(v(0), 0) \\ F_r[v](t) &= h_r(v(t), F_r[v](t_i)), \text{ for } t_i < t \leq t_{i+1}, \quad 0 \leq i \leq N-1 \\ h_r(v, w) &= \max(v - r, \min(v + r, w))\end{aligned}\tag{5.2}$$

5.2 Problem Formulation and Preliminaries

where v is the input to the hysteresis model; $0 = t_0 < t_1 < \dots < t_N = t_E$ is a partition of $[0, t_E]$ such that the function v is monotone on each of the subintervals $(t_i, t_{i+1}]$; $p(r)$ is a given density function, satisfying $p(r) \geq 0$ with $\int_0^\infty rp(r)dr < \infty$; D is a constant so that density function $p(r)$ vanishes for large values of D ; $F_r[v](t)$ is known as the play operator; and $h(v)$ is the hysteresis input function that satisfies the following assumptions [106]:

Assumption 5.1 *The function $h : \mathbb{R} \rightarrow \mathbb{R}$ is odd, non-decreasing, locally Lipschitz continuous, and satisfies $\lim_{v \rightarrow \infty} h(v) \rightarrow \infty$ and $\frac{dh(v)}{dv} > 0$ for almost every $v \in \mathbb{R}$.*

Assumption 5.2 *The growth of the hysteresis function $h(v)$ is smooth, and there exist positive constants h_0 and h_1 such that $0 < h_0 \leq \frac{dh(v)}{dv} \leq h_1$.*

The objective is to design an adaptive neural controller $v(t)$ for system (5.1)–(5.2) such that all signals in the closed-loop system are bounded, while the output y follows the specified desired trajectory y_d to a small neighborhood of zero.

Remark 5.1 *Compared with the classic PI hysteresis model, the difficulty in dealing with the generalized PI hysteresis model lies in that the input function $h(v)$ is unknown, which needs some new treatments. In this chapter, motivated by the works [99, 101, 155], the Mean Value Theorem is adopted to transform the unknown non-affine input function to a partially affine form, which can be seen as a multiplication of a control term with a function of control. As such, the available techniques for affine nonlinear system control in the literature can be extended to solve this problem.*

Remark 5.2 *Although it appears possible to rewrite (5.1) and (5.2) into the non-affine form $\dot{x} = f(x, v)$, it still cannot be directly handled by the method proposed by [99], in which the Mean Value Theorem and Implicit Function Theorem were adopted to handle the non-affine problem. The reason is that if we want to apply the Mean Value Theorem and Implicit Function Theorem to a function, one requirement is that the first order derivative of the function is not equal to zero. However, due to the nonsmooth characteristics of hysteresis, the function $f(x, v)$ transformed from (5.1)*

5.2 Problem Formulation and Preliminaries

and (5.2) is non-differentiable and thus does not satisfy the conditions of applying the Mean Value Theorem and Implicit Function Theorem. Therefore, only the Mean Value Theorem is applied to the smooth functions in (5.1), namely, $f_j(\cdot)$, $f_n(\cdot)$ and the hysteresis input function $h(v)$. For the nonsmooth function $F_r[v](t)$ in (5.2), a new treatment needs to be developed later.

Remark 5.3 *There are many physical processes whose dynamics can be described by nonlinear differential equations of form (5.1) and (5.2). Examples include some chemical reaction processes such as the continuously stirred tank reactor (CSTR) system given in [41, 156]. Within the tank reactor, two chemicals are mixed and react to produce compound A at a concentration C_a . The control objective is to manipulate the coolant flow rate q_c to control the concentration C_a at a desired value. The system is a pure-feedback system, which is non-affine in the control input q_c . According to [157] and [158], the control valve that controls the coolant flow rate, q_c , exhibits considerable hysteresis. Since the generalized PI hysteresis model can capture the hysteresis phenomenon more accurately and accommodate more general classes of hysteresis shapes by adjusting both the density function and the input function, the generalized PI hysteresis model can be adopted to represent the hysteresis nonlinearity between the coolant flow rate, q_c , and the aperture of the control valve, v . Therefore, we can regard the CSTR system as a physical example of pure feedback systems with input hysteresis of form (5.1) and (5.2).*

Assumption 5.3 *The desired trajectory y_d , and their time derivatives up to the n th order $y_d^{(n)}$, are continuous and bounded.*

Based on Assumption 5.3, we define the trajectory vector $\bar{x}_{d(j+1)} = [y_d \ \dot{y}_d \ \dots \ y_d^{(j)}]^T$, $j = 1, \dots, n-1$, which is a vector from the y_d to its j -th time derivative, $y_d^{(j)}$, which will be used in the subsequent control design.

Assumption 5.4 *There exists an unknown constant d^* such that $|d(t)| \leq d^*$.*

Assumption 5.5 *There exist a known constant p_{\max} , such that $p(r) \leq p_{\max}$ for all $r \in [0, D]$.*

5.2 Problem Formulation and Preliminaries

Remark 5.4 *It is reasonable to set an upper bound for the density function $p(r)$, based on its properties that $p(r) \geq 0$ with $\int_0^\infty rp(r)dr < \infty$.*

According to the Mean Value Theorem [113], we can express $f_j(\cdot, \cdot)$ in (5.1) as follows:

$$\begin{aligned} f_j(\bar{x}_j, x_{j+1}) &= f_j(\bar{x}_j, x_{j+1}^0) + \frac{\partial f_j(\bar{x}_j, x_{j+1})}{\partial x_{j+1}} \Big|_{x_{j+1}=x_{j+1}^{\theta_j}} \times (x_{j+1} - x_{j+1}^0), 1 \leq j \leq n-1 \\ f_n(\bar{x}_n, u) &= f_n(\bar{x}_n, u^0) + \frac{\partial f_n(\bar{x}_n, u)}{\partial u} \Big|_{u=u^{\theta_n}} \times (u - u^0) \end{aligned} \quad (5.3)$$

where $x_{j+1}^{\theta_j} = \theta_j x_{j+1} + (1 - \theta_j)x_{j+1}^0$, with $0 < \theta_j < 1$, $1 \leq j \leq n-1$, and $x_n^{\theta_n} = \theta_n u + (1 - \theta_n)u^0$, with $0 < \theta_n < 1$.

By choosing $x_{j+1}^0 = 0$ and $x_n^0 = 0$, (5.3) can be written as

$$\begin{aligned} f_j(\bar{x}_j, x_{j+1}) &= f_j(\bar{x}_j, 0) + \frac{\partial f_j(\bar{x}_j, x_{j+1})}{\partial x_{j+1}} \Big|_{x_{j+1}=x_{j+1}^{\theta_j}} x_{j+1}, 1 \leq j \leq n-1 \\ f_n(\bar{x}_n, u) &= f_n(\bar{x}_n, 0) + \frac{\partial f_n(\bar{x}_n, u)}{\partial u} \Big|_{u=u^{\theta_n}} u \end{aligned} \quad (5.4)$$

For convenience of analysis, we define $g_j(\bar{x}_j, x_{j+1}^{\theta_j}) = \frac{\partial f_j(\bar{x}_j, x_{j+1})}{\partial x_{j+1}} \Big|_{x_{j+1}=x_{j+1}^{\theta_j}}$ and $g_n(\bar{x}_n, u^{\theta_n}) = \frac{\partial f_n(\bar{x}_n, u)}{\partial u} \Big|_{u=u^{\theta_n}}$, which are also unknown nonlinear functions.

Substituting (5.4) into (5.1), we have

$$\begin{aligned} \dot{x}_j &= f_j(\bar{x}_j, 0) + g_j(\bar{x}_j, x_{j+1}^{\theta_j})x_{j+1}, \quad 1 \leq j \leq n-1 \\ \dot{x}_n &= f_n(\bar{x}_n, 0) + g_n(\bar{x}_n, u^{\theta_n})u + d(t) \\ y &= x_1 \end{aligned} \quad (5.5)$$

In addition, according to the Mean Value Theorem [113], there also exists a constant θ_0 ($0 < \theta_0 < 1$) such that the unknown input function $h(v)$ in (5.2) satisfies the following property

$$h(v) = h(v^*) + \frac{\partial h(\cdot)}{\partial v} \Big|_{v=v^{\theta_0}} (v - v^*)$$

where $v^{\theta_0} = \theta_0 v + (1 - \theta_0)v^*$.

According to Assumptions 5.1 and 5.2, and the Implicit Function Theorem [64], we can find v^* such that $h(v^*) = 0$. Defining

$$g_0(v^{\theta_0}) = \frac{\partial h(\cdot)}{\partial v} \Big|_{v=v^{\theta_0}}$$

5.3 Control Design and Stability Analysis

we have

$$h(v) = g_0(v^{\theta_0})(v - v^*)$$

Therefore, we can rewrite (5.2) as

$$u(t) = g_0(v^{\theta_0})v - g_0(v^{\theta_0})v^* - \int_0^D p(r)F_r[v](t)dr \quad (5.6)$$

Substituting (5.6) into (5.5) leads to our unified system:

$$\begin{aligned} \dot{x}_j &= f_j(\bar{x}_j, 0) + g_j(\bar{x}_j, x_{j+1}^{\theta_j})x_{j+1}, \quad 1 \leq j \leq n-1 \\ \dot{x}_n &= f_n(\bar{x}_n, 0) + g_n(\bar{x}_n, u^{\theta_n})[g_0(v^{\theta_0})v - g_0(v^{\theta_0})v^* - \int_0^D p(r)F_r[v](t)dr] + d(t) \\ y &= x_1 \end{aligned} \quad (5.7)$$

Assumption 5.6 *There exist constants \underline{g}_j and \bar{g}_j such that $0 < \underline{g}_j \leq |g_j(\cdot)| \leq \bar{g}_j < \infty$, for $j = 1, \dots, n$.*

Remark 5.5 *Assumption 5.6 implies that smooth functions $g_j(\cdot)$ for $j = 1, \dots, n$ are strictly either positive or negative, which is reasonable because $g_j(\cdot)$ being away from zero is the controllable condition of system (5.7), which is made in most control schemes [65, 151]. Without loss of generality, we shall assume that $g_n(\bar{x}_n, u^{\theta_n}) > 0$, while no knowledge is required of the signs of $g_j(\cdot)$, $j = 1, 2, \dots, n-1$.*

5.3 Control Design and Stability Analysis

In this section, we will investigate adaptive neural control for the system (5.7) using the backstepping method [65] combined with neural networks approximation. The backstepping design procedure contains n steps and involves the following change of coordinates: $z_1 = x_1 - y_d$, $z_i = x_i - \alpha_{i-1}$, $i = 2, \dots, n$, where α_i is a virtual control which shall be developed for the corresponding i -subsystem based on an appropriate Lyapunov function V_i . The control law $v(t)$ is designed in the last step to stabilize the

5.3 Control Design and Stability Analysis

entire closed-loop system, and deal with the hysteresis term. The closed-loop system can be proved to be SGUUB by Lyapunov stability analysis.

Step 1: Since $z_1 = x_1 - y_d$ and $z_2 = x_2 - \alpha_1$, the derivative of z_1 is

$$\begin{aligned}\dot{z}_1 &= f_1(\bar{x}_1, 0) + g_1(\bar{x}_1, x_2^{\theta_1})x_2 - \dot{y}_d \\ &= f_1(x_1, 0) + g_1(\bar{x}_1, x_2^{\theta_1})(z_2 + \alpha_1) - \dot{y}_d \\ &= g_1(\bar{x}_1, x_2^{\theta_1})(z_2 + \alpha_1) + Q_1(Z_1)\end{aligned}\tag{5.8}$$

where $Q_1(Z_1) = f_1(\bar{x}_1, 0) - \dot{y}_d$ with $Z_1 = [\bar{x}_1, \dot{y}_d] \in \Omega_{Z_1} \subset \mathbb{R}^2$.

To compensate for the unknown function $Q_1(Z_1)$, we can use the radial basis function neural networks (RBFNNs) in Section 2.3.3, $\hat{W}_1^T S(Z_1)$, with $\hat{W}_1 \in \mathbb{R}^{l \times 1}$, $S(Z_1) \in \mathbb{R}^{l \times 1}$, and the NN node number $l > 1$, to approximate the function $Q_1(Z_1)$ on the compact set Ω_{Z_1} as follows

$$Q_1(Z_1) = \hat{W}_1^T S(Z_1) - \tilde{W}_1^T S(Z_1) + \varepsilon_1(Z_1)\tag{5.9}$$

where the approximation error $\varepsilon_1(Z_1)$ satisfies $|\varepsilon_1(Z_1)| \leq \varepsilon_1^*$ with positive constant ε_1^* .

Substituting (5.9) into (5.8), we obtain

$$\dot{z}_1 = g_1(\bar{x}_1, x_2^{\theta_1})(z_2 + \alpha_1) + \hat{W}_1^T S(Z_1) - \tilde{W}_1^T S(Z_1) + \varepsilon_1(Z_1)\tag{5.10}$$

Choose the following virtual control law and adaption laws:

$$\begin{aligned}\alpha_1 &= N(\zeta_1)[k_1 z_1 + \hat{W}_1^T S(Z_1)] \\ \dot{\zeta}_1 &= k_1 z_1^2 + z_1 \hat{W}_1^T S(Z_1) \\ \dot{\hat{W}}_1 &= \Gamma_1[z_1 S(Z_1) - \sigma_1 \hat{W}_1]\end{aligned}\tag{5.11}$$

where $\Gamma_1 = \Gamma_1^T \in \mathbb{R}^{l \times l} > 0$, $k_1 > 0$ and $\sigma_1 > 0$ are design parameters.

Consider the following Lyapunov function candidate

$$V_1 = \frac{1}{2}z_1^2 + \frac{1}{2}\tilde{W}_1^T \Gamma_1^{-1} \tilde{W}_1\tag{5.12}$$

5.3 Control Design and Stability Analysis

The time derivative of (5.12) along with (5.10) and (5.11) is

$$\begin{aligned}\dot{V}_1 &= z_1 \dot{z}_1 + \tilde{W}_1^T \Gamma_1^{-1} \dot{\tilde{W}}_1 \\ &\leq -k_1 z_1^2 + [g_1(\bar{x}_1, x_2^{\theta_1}) N_1(\zeta_1) + 1] \dot{\zeta}_1 + g_1(\bar{x}_1, x_2^{\theta_1}) z_1 z_2 - \sigma_1 \tilde{W}_1^T \hat{W}_1 + |z_1| \varepsilon_1^*\end{aligned}\quad (5.13)$$

By using Young's inequality, we obtain the following inequalities:

$$\begin{aligned}-\sigma_1 \tilde{W}_1^T \hat{W}_1 &\leq -\frac{\sigma_1 \|\tilde{W}_1\|^2}{2} + \frac{\sigma_1 \|W_1^*\|^2}{2} \\ |z_1| \varepsilon_1^* &\leq \frac{z_1^2}{4c_{11}} + c_{11} \varepsilon_1^{*2} \\ g_1(\bar{x}_1, x_2^{\theta_1}) z_1 z_2 &\leq \frac{z_1^2}{4c_{12}} + c_{12} g_1^2(\bar{x}_1, x_2^{\theta_1}) z_2^2\end{aligned}\quad (5.14)$$

Substituting (5.14) into (5.13) results in

$$\begin{aligned}\dot{V}_1 &\leq -(k_1 - \frac{1}{4c_{11}} - \frac{1}{4c_{12}}) z_1^2 + [g_1(\bar{x}_1, x_2^{\theta_1}) N_1(\zeta_1) + 1] \dot{\zeta}_1 - \frac{\sigma_1 \|\tilde{W}_1\|^2}{2} \\ &\quad + c_{12} g_1^2(\bar{x}_1, x_2^{\theta_1}) z_2^2 + \frac{\sigma_1 \|W_1^*\|^2}{2} + c_{11} \varepsilon_1^{*2} \\ &\leq -\gamma_1 V_1 + [g_1(\bar{x}_1, x_2^{\theta_1}) N_1(\zeta_1) + 1] \dot{\zeta}_1 + \rho_1 + c_{12} g_1^2(\bar{x}_1, x_2^{\theta_1}) z_2^2\end{aligned}\quad (5.15)$$

where γ_1 and ρ_1 are positive constants, which are defined as

$$\gamma_1 = \min \left\{ 2(k_1 - \frac{1}{4c_{11}} - \frac{1}{4c_{12}}), \frac{\sigma_1}{\lambda_{\max}(\Gamma_1^{-1})} \right\}, \quad \rho_1 = \frac{\sigma_1 \|W_1^*\|^2}{2} + c_{11} \varepsilon_1^{*2}$$

Multiplying both sides of (5.15) by $e^{\gamma_1 t}$ yields

$$\frac{d}{dt}(V_1 e^{\gamma_1 t}) \leq \rho_1 e^{\gamma_1 t} + [g_1(\bar{x}_1, x_2^{\theta_1}) N_1(\zeta_1) + 1] \dot{\zeta}_1 e^{\gamma_1 t} + c_{12} g_1^2(\bar{x}_1, x_2^{\theta_1}) z_2^2 e^{\gamma_1 t} \quad (5.16)$$

Integrating (5.16) over $[0, t]$, we have

$$\begin{aligned}V_1 &\leq \frac{\rho_1}{\gamma_1} + [V_1(0) - \frac{\rho_1}{\gamma_1}] e^{-\gamma_1 t} + e^{-\gamma_1 t} \int_0^t [g_1(\bar{x}_1, x_2^{\theta_1}) N_1(\zeta_1) + 1] \dot{\zeta}_1 e^{\gamma_1 \tau} d\tau \\ &\quad + e^{-\gamma_1 t} \int_0^t c_{12} g_1^2(\bar{x}_1, x_2^{\theta_1}) z_2^2 e^{\gamma_1 \tau} d\tau\end{aligned}\quad (5.17)$$

$$\begin{aligned}&\leq \frac{\rho_1}{\gamma_1} + V_1(0) + e^{-\gamma_1 t} \int_0^t [g_1(\bar{x}_1, x_2^{\theta_1}) N_1(\zeta_1) + 1] \dot{\zeta}_1 e^{\gamma_1 \tau} d\tau \\ &\quad + e^{-\gamma_1 t} \int_0^t c_{12} g_1^2(\bar{x}_1, x_2^{\theta_1}) z_2^2 e^{\gamma_1 \tau} d\tau\end{aligned}\quad (5.18)$$

5.3 Control Design and Stability Analysis

Noting Assumption 5.6, the last term of (5.18) $e^{-\gamma_1 t} \int_0^t c_{12} g_1^2(\bar{x}_1, x_2^{\theta_1}) z_2^2 e^{\gamma_1 \tau} d\tau$ has the following property

$$\begin{aligned} e^{-\gamma_1 t} \int_0^t c_{12} g_1^2(\bar{x}_1, x_2^{\theta_1}) z_2^2 e^{\gamma_1 \tau} d\tau &\leq e^{-\gamma_1 t} \int_0^t c_{12} \bar{g}_1^2 z_2^2 e^{\gamma_1 \tau} d\tau \\ &\leq \bar{g}_1^2 \sup_{\tau \in [0, t]} [z_2^2(\tau)] e^{-\gamma_1 t} \int_0^t c_{12} e^{\gamma_1 \tau} d\tau \\ &\leq \frac{c_{12}}{\gamma_1} \bar{g}_1^2 \sup_{\tau \in [0, t]} [z_2^2(\tau)] \end{aligned} \quad (5.19)$$

where \bar{g}_1 is the upper bound for $|g_1(\cdot)|$ as defined in Assumption 5.6.

Therefore, if z_2 can be kept bounded over a finite time interval $[0, t_f)$, then we can obtain the boundedness of the term $e^{-\gamma_1 t} \int_0^t c_{12} g_1^2(\bar{x}_1, x_2^{\theta_1}) z_2^2 e^{\gamma_1 \tau} d\tau$. Furthermore, (5.18) can be written as

$$V_1 \leq c_1 + e^{-\gamma_1 t} \int_0^t [g_1(\bar{x}_1, x_2^{\theta_1}) N_1(\zeta_1) + 1] \dot{\zeta}_1 e^{\gamma_1 \tau} d\tau \quad (5.20)$$

where $c_1 = \frac{\rho_1}{\gamma_1} + V_1(0) + \frac{c_{12}}{\gamma_1} \bar{g}_1^2 \sup_{\tau \in [0, t_f]} [z_2^2(\tau)]$. According to Lemma 2.4, we can conclude that V_1 , ζ_1 , \hat{W}_1 , $\int_0^t [g_1(\bar{x}_1, x_2^{\theta_1}) N_1(\zeta_1) + 1] \dot{\zeta}_1 e^{\gamma_1 \tau} d\tau$ are all bounded on $[0, t_f)$. According to Proposition 2 [159], $t_f = \infty$ and we know that z_1 and \hat{W}_1 are SGUUB. The boundedness of z_2 will be dealt with in the following steps.

Step j ($2 \leq j < n$): Similar to the procedure of Step 1, we define $z_j = x_j - \alpha_{j-1}$. Its derivative is

$$\begin{aligned} \dot{z}_j &= \dot{x}_j - \dot{\alpha}_{j-1} \\ &= f_j(\bar{x}_j, 0) + g_j(\bar{x}_j, x_{j+1}^{\theta_j}) x_{j+1} - \dot{\alpha}_{j-1} \end{aligned} \quad (5.21)$$

Since α_{j-1} is a function of $\bar{x}_{j-1}, \bar{x}_{dj}, \zeta_{j-1}, \hat{W}_1, \dots, \hat{W}_{j-1}$, its derivative, $\dot{\alpha}_{j-1}$, can be expressed as

$$\begin{aligned} \dot{\alpha}_{j-1} &= \sum_{k=1}^{j-1} \frac{\partial \alpha_{j-1}}{\partial x_k} \dot{x}_k + \phi_{j-1} \\ &= \sum_{k=1}^{j-1} \frac{\partial \alpha_{j-1}}{\partial x_k} f_k(\bar{x}_k, x_{k+1}) + \phi_{j-1} \end{aligned} \quad (5.22)$$

where

$$\phi_{j-1} = \frac{\partial \alpha_{j-1}}{\partial \zeta_{j-1}} \dot{\zeta}_{j-1} + \frac{\partial \alpha_{j-1}}{\partial \bar{x}_{dj}} \dot{\bar{x}}_{dj} + \sum_{k=1}^{j-1} \frac{\partial \alpha_{j-1}}{\partial \hat{W}_k} \dot{\hat{W}}_k \quad (5.23)$$

5.3 Control Design and Stability Analysis

which is computable. As such, $\dot{\alpha}_{j-1}$ can be seen as a function of $\bar{x}_j, \frac{\partial \alpha_{j-1}}{\partial x_1}, \dots, \frac{\partial \alpha_{j-1}}{\partial x_{j-1}}, \phi_{j-1}$. Further, we can rewrite (5.21) as

$$\dot{z}_j = g_j(\bar{x}_j, x_{j+1}^{\theta_j})(z_{j+1} + \alpha_j) + Q_j(Z_j) \quad (5.24)$$

where $Z_j = [\bar{x}_j, \frac{\partial \alpha_{j-1}}{\partial x_1}, \dots, \frac{\partial \alpha_{j-1}}{\partial x_{j-1}}, \phi_{j-1}] \in \Omega_{Z_j} \subset \mathbb{R}^{2j}$, and $Q_j(Z_j) = f_j(\bar{x}_j, 0) - \dot{\alpha}_{j-1}$ is an unknown function that can be approximated by the RBFNNs, $\hat{W}_j^T S(Z_j)$, on the compact set Ω_{Z_j} as

$$Q_j(Z_j) = \hat{W}_j^T S(Z_j) - \tilde{W}_j^T S(Z_j) + \varepsilon_j(Z_j) \quad (5.25)$$

where the approximation error $\varepsilon_j(Z_j)$ satisfies $|\varepsilon_j(Z_j)| \leq \varepsilon_j^*$ with positive constant ε_j^* . Substituting (5.25) into (5.21), we obtain

$$\dot{z}_j = g_j(\bar{x}_j, x_{j+1}^{\theta_j})(z_{j+1} + \alpha_j) + \hat{W}_j^T S(Z_j) - \tilde{W}_j^T S(Z_j) + \varepsilon_j(Z_j) \quad (5.26)$$

The following virtual control laws and adaption laws are considered:

$$\begin{aligned} \alpha_j &= N(\zeta_j)[k_j z_j + \hat{W}_j^T S(Z_j)] \\ \dot{\zeta}_j &= k_j z_j^2 + z_j \hat{W}_j^T S(Z_j) \\ \dot{\hat{W}}_j &= \Gamma_j [z_j S(Z_j) - \sigma_j \hat{W}_j] \end{aligned} \quad (5.27)$$

where $\Gamma_j = \Gamma_j^T > 0$, k_j and σ_j are positive constants.

Define the following Lyapunov function candidate

$$V_j = \frac{1}{2} z_j^2 + \frac{1}{2} \tilde{W}_j^T \Gamma_j^{-1} \tilde{W}_j \quad (5.28)$$

Similar to the procedures outlined in Step 1, with the help of Young's Inequality, the derivative of V_j in (5.28) along (5.26) and (5.27) can be obtained as

$$\begin{aligned} \dot{V}_j &\leq -(k_j - \frac{1}{4c_{j1}} - \frac{1}{4c_{j2}}) z_j^2 + [g_1(\bar{x}_j, x_{j+1}^{\theta_j}) N_j(\zeta_j) + 1] \dot{\zeta}_j - \frac{\sigma_j \|\tilde{W}_j\|^2}{2} \\ &\quad + c_{j2} g_j^2(\bar{x}_j, x_{j+1}^{\theta_j}) z_{j+1}^2 + \frac{\sigma_j \|W_j^*\|^2}{2} + c_{j1} \varepsilon_j^{*2} \\ &\leq -\gamma_j V_j + [g_j(\bar{x}_j, x_{j+1}^{\theta_j}) N_j(\zeta_j) + 1] \dot{\zeta}_j + \rho_j + c_{j2} g_j^2(\bar{x}_j, x_{j+1}^{\theta_j}) z_{j+1}^2 \end{aligned} \quad (5.29)$$

where γ_j and ρ_j are positive constants defined as

$$\gamma_j = \min \left\{ 2(k_j - \frac{1}{4c_{j1}} - \frac{1}{4c_{j2}}), \frac{\sigma_j}{\lambda_{\max}(\Gamma_j^{-1})} \right\}, \quad \rho_j = \frac{\sigma_j \|W_j^*\|^2}{2} + c_{j1} \varepsilon_j^{*2} \quad (5.30)$$

5.3 Control Design and Stability Analysis

Multiplying both sides of (5.29) by $e^{\gamma_j t}$ and integrating over $[0, t]$, we have

$$\begin{aligned} V_j &\leq \frac{\rho_j}{\gamma_j} + [V_j(0) - \frac{\rho_j}{\gamma_j}]e^{-\gamma_j t} + e^{-\gamma_j t} \int_0^t [g_j(\bar{x}_j, x_{j+1}^{\theta_j})N_j(\zeta_j) + 1]\dot{\zeta}_j e^{\gamma_j \tau} d\tau \\ &\quad + e^{-\gamma_j t} \int_0^t c_{j2} g_j^2(\bar{x}_j, x_{j+1}^{\theta_j}) z_{j+1}^2 e^{\gamma_j \tau} d\tau \end{aligned} \quad (5.31)$$

$$\begin{aligned} &\leq \frac{\rho_j}{\gamma_j} + V_j(0) + e^{-\gamma_j t} \int_0^t [g_j(\bar{x}_j, x_{j+1}^{\theta_j})N_j(\zeta_j) + 1]\dot{\zeta}_j e^{\gamma_j \tau} d\tau \\ &\quad + e^{-\gamma_j t} \int_0^t c_{j2} g_j^2(\bar{x}_j, x_{j+1}^{\theta_j}) z_{j+1}^2 e^{\gamma_j \tau} d\tau \end{aligned} \quad (5.32)$$

Similarly, as discussed in Step 1, if z_{j+1} can be kept bounded over a finite time interval $[0, t_f)$, we can readily guarantee the boundedness of the extra term

$e^{-\gamma_j t} \int_0^t c_{j2} g_j^2(\bar{x}_j, x_{j+1}^{\theta_j}) z_{j+1}^2 e^{\gamma_j \tau} d\tau$ in (5.32) as follows

$$e^{-\gamma_j t} \int_0^t c_{j2} g_j^2(\bar{x}_j, x_{j+1}^{\theta_j}) z_{j+1}^2 e^{\gamma_j \tau} d\tau \leq \frac{c_{j2}}{\gamma_j} \bar{g}_j^2 \sup_{\tau \in [0, t]} [z_{j+1}^2(\tau)] \quad (5.33)$$

Therefore, (5.32) can be written as

$$V_j \leq c_j + e^{-\gamma_j t} \int_0^t [g_j(\bar{x}_j, x_{j+1}^{\theta_j})N_j(\zeta_j) + 1]\dot{\zeta}_j e^{\gamma_j \tau} d\tau \quad (5.34)$$

where $c_j = \frac{\rho_j}{\gamma_j} + V_j(0) + \frac{c_{j2}}{\gamma_j} \bar{g}_j^2 \sup_{\tau \in [0, t_f]} [z_{j+1}^2(\tau)]$. Then, applying Lemma 2.4, the boundedness of V_j , ζ_j , \dot{W}_j , $\int_0^t [g_j(\bar{x}_j, x_{j+1}^{\theta_j})N_j(\zeta_j) + 1]\dot{\zeta}_j e^{\gamma_j \tau} d\tau$ can be readily obtained. The boundedness of z_{j+1} will be dealt with in the Step $(j+1)$.

Step n: This is the final step, in which we will design the control input $v(t)$. Since $z_n = x_n - \alpha_{n-1}$, its derivative is given by

$$\begin{aligned} \dot{z}_n &= f_n(\bar{x}_n, 0) + g_n(\bar{x}_n, u^{\theta_n})[g_0(v^{\theta_0})v - g_0(v^{\theta_0})v^* - \int_0^D p(r)F_r[v](t)dr] + d(t) - \dot{\alpha}_{n-1} \\ &= g_n(\bar{x}_n, u^{\theta_n})[g_0(v^{\theta_0})v - g_0(v^{\theta_0})v^* - \int_0^D p(r)F_r[v](t)dr] + Q_n(Z_n) + d(t) \\ &= g_n(\bar{x}_n, u^{\theta_n})[g_0(v^{\theta_0})v - g_0(v^{\theta_0})v^* - \int_0^D p(r)F_r[v](t)dr] + \hat{W}_n^T S(Z_n) \\ &\quad - \tilde{W}_n^T S(Z_n) + \varepsilon_n(Z_n) + d(t) \end{aligned} \quad (5.35)$$

where $\hat{W}_n^T S(Z_n)$ is used to approximate the unknown function $Q_n(Z_n) = f_n(x, 0) - \dot{\alpha}_{n-1}$ on the compact set $\Omega_{Z_n} \subset \mathbb{R}^n$ with $Z_n = [\bar{x}_n, \frac{\partial \alpha_{n-1}}{\partial x_1}, \dots, \frac{\partial \alpha_{n-1}}{\partial x_{n-1}}, \phi_{n-1}] \in \Omega_{Z_n} \subset \mathbb{R}^{2n}$, and the approximation error $\varepsilon_n(Z_n)$ satisfies $|\varepsilon_n(Z_n)| \leq \varepsilon_n^*$ with positive constant ε_n^* .

5.3 Control Design and Stability Analysis

Choose the following Lyapunov function candidate

$$V_n = \frac{1}{2}z_n^2 + \frac{1}{2}\tilde{W}_n^T \Gamma_n^{-1} \tilde{W}_n + \frac{1}{2\gamma_d}\tilde{d}^2 + \frac{\bar{g}_n}{2\gamma_p} \int_0^D \tilde{p}^2(t, r) dr \quad (5.36)$$

where $\tilde{d} = \hat{d} - d^*$, $\tilde{p}(t, r) = \hat{p}(t, r) - p_{\max}$, \hat{d} and $\hat{p}(t, r)$ are the estimates of the disturbance bound d^* and the density function of $p(r)$ respectively, $\Gamma_n = \Gamma_n^T > 0$, and γ_d, γ_p are positive constants.

The derivative of V_n defined in (5.36) along (5.35) is

$$\begin{aligned} \dot{V}_n &= z_n g_n(\bar{x}_n, u^{\theta_n}) [g_0(v^{\theta_0})v - \int_0^D p(r) F_r[v](t) dr] - z_n g_n(\bar{x}_n, u^{\theta_n}) g_0(v^{\theta_0}) v^* \\ &\quad + z_n \hat{W}_n^T S(Z_n) - z_n \tilde{W}_n^T S(Z_n) + z_n \varepsilon_n(Z_n) + z_n d(t) + \tilde{W}_n^T \Gamma_n^{-1} \dot{W}_n + \frac{1}{\gamma_d} \tilde{d} \dot{\tilde{d}} \\ &\quad + \frac{\bar{g}_n}{\gamma_p} \int_0^D \tilde{p}(t, r) \frac{\partial}{\partial t} \tilde{p}(t, r) dr \end{aligned} \quad (5.37)$$

From Assumptions 5.2 and 5.6, we know that $|g_n(x, u^{\theta_n}) g_0 v^*| \leq C$, where C is a positive constant. And due to $|\varepsilon_n(Z_n)| \leq \varepsilon_n^*$, and Assumption 5.4, (5.37) can be written as

$$\begin{aligned} \dot{V}_n &\leq z_n g_n(\bar{x}_n, u^{\theta_n}) [g_0(v^{\theta_0})v - \int_0^D p(r) F_r[v](t) dr] + z_n \hat{W}_n^T S(Z_n) - z_n \tilde{W}_n^T S(Z_n) \\ &\quad + |z_n|(C + \varepsilon_n^*) + |z_n|d^* + \tilde{W}_n^T \Gamma_n^{-1} \dot{W}_n + \frac{1}{\gamma_d} \tilde{d} \dot{\tilde{d}} + \frac{\bar{g}_n}{\gamma_p} \int_0^D \tilde{p}(t, r) \frac{\partial}{\partial t} \tilde{p}(t, r) dr \end{aligned} \quad (5.38)$$

The following control laws and adaption laws are proposed:

$$v = N(\zeta_n) \left[k_n z_n + \hat{W}_n^T S(Z_n) + \hat{d} \tanh\left(\frac{z_n}{\omega}\right) \right] + v_h \quad (5.39)$$

$$v_h = -\text{sign}(z_n) \int_0^D \frac{\hat{p}(t, r)}{h_0} |F_r[v](t)| dr \quad (5.40)$$

$$\dot{\zeta}_n = k_n z_n^2 + z_n \hat{W}_n^T S(Z_n) + z_n \hat{d} \tanh\left(\frac{z_n}{\omega}\right) \quad (5.41)$$

$$\dot{\hat{W}}_n = \Gamma_n [z_n S(Z_n) - \sigma_n \hat{W}_n] \quad (5.42)$$

$$\dot{\hat{d}} = \gamma_d [z_n \tanh\left(\frac{z_n}{\omega}\right) - \sigma_d \hat{d}] \quad (5.43)$$

$$\frac{\partial}{\partial t} \hat{p}(t, r) = \begin{cases} -\gamma_p \sigma_p \hat{p}(t, r), & \text{if } \hat{p}(t, r) \geq p_{\max} \\ \gamma_p [|z_n| |F_r[v](t)| - \sigma_p \hat{p}(t, r)], & \text{if } 0 \leq \hat{p}(t, r) < p_{\max} \end{cases} \quad (5.44)$$

where σ_p and ω are positive constants.

5.3 Control Design and Stability Analysis

Remark 5.6 The term v_h in (5.39) is used to cancel the effect caused by the non-differentiable hysteresis term $\int_0^D p(r)F_r[v](t)dr$. Due to the integral form of $\int_0^D p(r)F_r[v](t)dr$, we cannot make assumptions on its boundedness, and thus cannot design the traditional robust adaptive control. However, considering that the density function $p(r)$ is not a function of time, it can be treated as a “parameter” of the hysteresis model, and an adaptation law can be developed to obtain an estimate of it.

Substituting (5.39)-(5.43) into (5.38), and using Young’s Inequality and the following property of the hyperbolic tangent function $\tanh(\cdot)$ [76, 160]:

$$0 \leq |z_n| - z_n \tanh\left(\frac{z_n}{\omega}\right) \leq 0.2785\omega,$$

we obtain that

$$\begin{aligned} \dot{V}_n \leq & -(k_n - \frac{1}{4c_{n1}})z_n^2 + [g_n(x, u^{\theta_n})g_0(v^{\theta_0})N_n(\zeta_n) + 1]\dot{\zeta}_n - \frac{\sigma_n\|\tilde{W}_n\|^2}{2} - \frac{\sigma_d\tilde{d}^2}{2} \\ & + \frac{\sigma_n\|W_j^*\|^2}{2} + \frac{\sigma_d d^{*2}}{2} + 0.2785\omega d^* + c_{n1}(\varepsilon_n^* + C)^2 \\ & + g_n(x, u^{\theta_n}) \left[-g_0(v^{\theta_0})|z_n| \int_0^D \frac{\hat{p}(t, r)}{h_0} |F_r[v](t)|dr - z_n \int_0^D p(r)F_r[v](t)dr \right] \\ & + \frac{\bar{g}_n}{\gamma_p} \int_0^D \tilde{p}(t, r) \frac{\partial}{\partial t} \tilde{p}(t, r) dr \end{aligned} \quad (5.45)$$

where c_{n1} is a positive constant.

Notice that the last two terms of (5.45) can be written as

$$\begin{aligned} & g_n(x, u^{\theta_n}) \left[-g_0(v^{\theta_0})|z_n| \int_0^D \frac{\hat{p}(t, r)}{h_0} |F_r[v](t)|dr - z_n \int_0^D p(r)F_r[v](t)dr \right] \\ & + \frac{\bar{g}_n}{\gamma_p} \int_0^D \tilde{p}(t, r) \frac{\partial}{\partial t} \tilde{p}(t, r) dr \\ \leq & g_n(x, u^{\theta_n}) \left[-|z_n| \int_0^D \hat{p}(t, r) |F_r[v](t)|dr + |z_n| \int_0^D p_{\max} |F_r[v](t)|dr \right] \\ & + \frac{\bar{g}_n}{\gamma_p} \int_0^D \tilde{p}(t, r) \frac{\partial}{\partial t} \tilde{p}(t, r) dr \\ \leq & -g_n(x, u^{\theta_n})|z_n| \int_0^D \tilde{p}(t, r) |F_r[v](t)|dr + \frac{\bar{g}_n}{\gamma_p} \int_0^D \tilde{p}(t, r) \frac{\partial}{\partial t} \tilde{p}(t, r) dr \end{aligned} \quad (5.46)$$

5.3 Control Design and Stability Analysis

According to (5.44), the adaptation law for the estimate of density function $\hat{p}(t, r)$ comprises two cases, due to the different regions which $\hat{p}(t, r)$ belong to. Therefore, we also need to consider two cases for the analysis of (5.46):

Case(a): When $r \in D_{\max} = \{r : \hat{p}(t, r) \geq p_{\max}\} \subset [0, D]$, according to (5.44), we have

$$\tilde{p}(t, r) \geq 0 \quad (5.47)$$

$$\frac{\partial}{\partial t} \hat{p}(t, r) = -\gamma_p \sigma_p \hat{p}(t, r) \quad (5.48)$$

Substituting (5.47) and (5.48) into (5.46), we have

$$\begin{aligned} & -g_n(x, u^{\theta_n})|z_n| \int_{r \in D_{\max}} \tilde{p}(t, r) |F_r[v](t)| dr + \frac{\bar{g}_n}{\gamma_p} \int_{r \in D_{\max}} \tilde{p}(t, r) \frac{\partial}{\partial t} \tilde{p}(t, r) dr \\ & \leq -\sigma_p \bar{g}_n \int_{r \in D_{\max}} \tilde{p}(t, r) \hat{p}(t, r) dr \end{aligned} \quad (5.49)$$

Case (b): When $r \in D_{\max}^c$, which is the complement set of D_{\max} in $[0, D]$, i.e., $0 \leq \hat{p}(t, r) < p_{\max}$.

In this case, from (5.44), we have

$$\tilde{p}(t, r) < 0 \quad (5.50)$$

$$\frac{\partial}{\partial t} \hat{p}(t, r) = \gamma_p [|z_n| |F_r[v](t)| - \sigma_p \hat{p}(t, r)] \quad (5.51)$$

Substituting (5.50) and (5.51) into (5.46), we have

$$\begin{aligned} & -g_n(x, u^{\theta_n})|z_n| \int_{r \in D_{\max}^c} \tilde{p}(t, r) |F_r[v](t)| dr + \frac{\bar{g}_n}{\gamma_p} \int_{r \in D_{\max}^c} \tilde{p}(t, r) \frac{\partial}{\partial t} \tilde{p}(t, r) dr \\ & \leq -g_n(x, u^{\theta_n})|z_n| \int_{r \in D_{\max}^c} \tilde{p}(t, r) |F_r[v](t)| dr + \bar{g}_n |z_n| \int_{r \in D_{\max}^c} \tilde{p}(t, r) |F_r[v](t)| dr \\ & \quad -\sigma_p \bar{g}_n \int_{r \in D_{\max}^c} \tilde{p}(t, r) \hat{p}(t, r) dr \\ & \leq -\sigma_p \bar{g}_n \int_{r \in D_{\max}^c} \tilde{p}(t, r) \hat{p}(t, r) dr \end{aligned} \quad (5.52)$$

Combining Case (a) with Case (b), (5.46) can be written as

$$g_n(x, u^{\theta_n}) [-g_0(v^{\theta_0})|z_n| \int_0^D \frac{\hat{p}(t, r)}{h_0} |F_r[v](t)| dr - z_n \int_0^D p(r) F_r[v](t) dr]$$

5.3 Control Design and Stability Analysis

$$\begin{aligned}
& + \frac{\bar{g}_n}{\gamma_p} \int_0^D \tilde{p}(t, r) \frac{\partial}{\partial t} \tilde{p}(t, r) dr \\
\leq & -g_n(x, u^{\theta_n}) |z_n| \int_{r \in D_{\max}} \tilde{p}(t, r) |F_r[v](t)| dr + \frac{\bar{g}_n}{\gamma_p} \int_{r \in D_{\max}} \tilde{p}(t, r) \frac{\partial}{\partial t} \tilde{p}(t, r) dr \\
& -g_n(x, u^{\theta_n}) |z_n| \int_{r \in D_{\max}^c} \tilde{p}(t, r) |F_r[v](t)| dr + \frac{\bar{g}_n}{\gamma_p} \int_{r \in D_{\max}^c} \tilde{p}(t, r) \frac{\partial}{\partial t} \tilde{p}(t, r) dr \\
= & -\sigma_p \bar{g}_n \int_{r \in D_{\max}} \tilde{p}(t, r) \hat{p}(t, r) dr - \sigma_p \bar{g}_n \int_{r \in D_{\max}^c} \tilde{p}(t, r) \hat{p}(t, r) dr \\
= & -\sigma_p \bar{g}_n \int_0^D \tilde{p}(t, r) \hat{p}(t, r) dr \tag{5.53}
\end{aligned}$$

By Young's Inequality, we have

$$-\sigma_p \bar{g}_n \tilde{p}(t, r) \hat{p}(t, r) \leq -\frac{\sigma_p \bar{g}_n}{2} \tilde{p}^2(t, r) + \frac{\sigma_p \bar{g}_n}{2} p_{\max}^2 \tag{5.54}$$

Integrating both sides of (5.54) over $[0, D]$ results in

$$-\sigma_{p1} \bar{g}_n \int_0^D \tilde{p}(t, r) \hat{p}(t, r) dr \leq -\frac{\sigma_p \bar{g}_n}{2} \int_0^D \tilde{p}^2(t, r) dr + \frac{\sigma_p \bar{g}_n D}{2} p_{\max}^2 \tag{5.55}$$

Therefore, according to (5.55), we can rewrite (5.53) further as

$$\begin{aligned}
& g_n(x, u^{\theta_n}) [-g_0(v^{\theta_0}) |z_n| \int_0^D \frac{\hat{p}(t, r)}{h_0} |F_r[v](t)| dr - z_n \int_0^D p(r) F_r[v](t) dr] \\
& + \frac{\bar{g}_n}{\gamma_p} \int_0^D \tilde{p}(t, r) \frac{\partial}{\partial t} \tilde{p}(t, r) dr \\
\leq & -\frac{\sigma_p \bar{g}_n}{2} \int_0^D \tilde{p}^2(t, r) dr + \frac{\sigma_p \bar{g}_n D}{2} p_{\max}^2 \tag{5.56}
\end{aligned}$$

Substituting (5.56) into (5.45), we have

$$\begin{aligned}
\dot{V}_n & \leq -(k_n - \frac{1}{4c_{n1}}) z_n^2 + [g_n(x, u^{\theta_n}) g_0(v^{\theta_0}) N_n(\zeta_n) + 1] \dot{\zeta}_n - \frac{\sigma_n \|\tilde{W}_n\|^2}{2} - \frac{\sigma_d \tilde{d}^2}{2} \\
& - \frac{\sigma_p \bar{g}_n}{2} \int_0^D \tilde{p}^2(t, r) dr + \frac{\sigma_n \|W_j^*\|^2}{2} + \frac{\sigma_d d^{*2}}{2} + 0.2785 \omega d^* + c_{n1} (\varepsilon_n^* + C)^2 \\
& + \frac{\sigma_p \bar{g}_n D}{2} p_{\max}^2 \\
& \leq -\gamma_n V_n + [g_n(x, u^{\theta_n}) g_0(v^{\theta_0}) N_n(\zeta_n) + 1] \dot{\zeta}_n + \rho_n \tag{5.57}
\end{aligned}$$

where γ_n and ρ_n are positive constants defined as

$$\begin{aligned}
\gamma_n & = \min \left\{ 2(k_n - \frac{1}{4c_{n1}}), \frac{\sigma_n}{\lambda_{\max}(\Gamma_n^{-1})}, \sigma_d \gamma_d, \sigma_p \gamma_p \right\} \\
\rho_n & = \frac{\sigma_n \|W_n^*\|^2}{2} + \frac{\sigma_d d^{*2}}{2} + 0.2785 \omega d^* + c_{n1} (\varepsilon_n^* + C)^2 + \frac{\sigma_p \bar{g}_n D}{2} p_{\max}^2 \tag{5.58}
\end{aligned}$$

5.3 Control Design and Stability Analysis

Multiplying both sides of (5.57) and integrating over $[0, t]$, we have

$$V_n \leq \frac{\rho_n}{\gamma_n} + [V_n(0) - \frac{\rho_n}{\gamma_n}]e^{-\gamma_n t} + e^{-\gamma_n t} \int_0^t [g_n(x, u^{\theta_n})g_0(v^{\theta_0})N_n(\zeta_n) + 1]\dot{\zeta}_n e^{\gamma_n \tau} d\tau \quad (5.59)$$

$$\begin{aligned} &\leq \frac{\rho_n}{\gamma_n} + V_n(0) + e^{-\gamma_n t} \int_0^t [g_n(x, u^{\theta_n})g_0(v^{\theta_0})N_n(\zeta_n) + 1]\dot{\zeta}_n e^{\gamma_n \tau} d\tau \\ &\leq c_n + e^{-\gamma_n t} \int_0^t [g_n(x, u^{\theta_n})g_0(v^{\theta_0})N_n(\zeta_n) + 1]\dot{\zeta}_n e^{\gamma_n \tau} d\tau \end{aligned} \quad (5.60)$$

where $c_n = \frac{\rho_n}{\gamma_n} + V_n(0)$. According to Assumptions 5.1, 5.2, and 5.6, we can regard $g_n(x, u)g_0(v)$ in (5.60) as $g(\cdot)$, which is a time-varying parameter and takes values in the known closed intervals $I = [h_0 \underline{g}_n, h_1 \bar{g}_n]$, with $0 \notin I$. Using Lemma 2.4, we can conclude that $V_n(t), \zeta_n(t)$ and hence $\bar{z}_n(t), \hat{W}_n, \hat{\bar{d}}_n$ are SGUUB. From the boundedness of $z_n(t)$, the boundedness of the extra term $e^{-\gamma_{n-1}t} \int_0^t c_{(n-1)} 2g_{n-1}^2(\bar{x}_{n-1}, x_{n-1}^{\theta_{n-1}}) z_n^2 e^{\gamma_{n-1}\tau} d\tau$ at Step $(n-1)$ is readily obtained. Applying Lemma 2.4 for $(n-1)$ times backward, it can be seen from the above iterative design procedure that $V_j, z_j, \hat{W}_j, \hat{\bar{d}}_j$, and hence, x_j , are SGUUB on $[0, t_f]$.

Remark 5.7 *In order to use Lemma 2.4 to establish closed-loop stability, we need to express \dot{V}_n in the form of $\dot{V}_n = -\gamma_n V_n + [g_n(x, u^{\theta_n})g_0(v^{\theta_0})N_n(\zeta_n) + 1]\dot{\zeta}_n + \rho_n$ as in (5.57). Thus, we need to adopt the σ -modification form in the adaptation law of $\hat{p}(t, r)$ as in (5.44). This is different from the previous works [18, 19], where no σ -modification was included since only the property $\dot{V} \leq 0$ was to be obtained.*

The following theorem shows the stability and control performance of the closed-loop adaptive system.

Theorem 5.1 *Consider the closed-loop system consisting of the plant (5.1), preceded by unknown hysteresis nonlinearities (5.2), and the control laws and adaptation laws (5.39). Under Assumptions 5.3-5.5, and given any initial conditions $z_i(0), \hat{W}_i(0), \hat{\bar{d}}(0)$ ($i = 1, 2, \dots, n$) belonging to Ω_0 , the overall closed-loop neural control system is SGUUB, in the sense that all of the signals are bounded. Specifically, the states and weights in the closed-loop system will remain in the compact set Ω defined*

5.3 Control Design and Stability Analysis

by

$$\Omega = \left\{ z_j, \tilde{W}_j, \tilde{d} \mid |z_j| \leq \sqrt{2\mu_j}, \quad \|\tilde{W}_j\| \leq \sqrt{\frac{2\mu_j}{\lambda_{\min}(\Gamma_j^{-1})}}, \right. \\ \left. |\tilde{d}| \leq \sqrt{2\gamma_d\mu_n}, \quad j = 1, 2, \dots, n \right\} \quad (5.61)$$

and eventually converge to the compact set Ω_s defined by

$$\Omega_s = \left\{ z_j, \tilde{W}_j, \tilde{d} \mid |z_j| \leq \sqrt{2\mu_j^*}, \quad \|\tilde{W}_j\| \leq \sqrt{\frac{2\mu_j^*}{\lambda_{\min}(\Gamma_j^{-1})}}, \right. \\ \left. |\tilde{d}| \leq \sqrt{2\gamma_d\mu_n^*}, \quad j = 1, 2, \dots, n \right\} \quad (5.62)$$

where

$$\begin{aligned} \mu_j &= c_j + c_{j0}, \quad j = 1, 2, \dots, n, \\ c_n &= \frac{\rho_n}{\gamma_n} + V_n(0), \\ V_n(0) &= \frac{1}{2}z_n^2(0) + \frac{1}{2}\tilde{W}_n^T(0)\Gamma_n^{-1}\tilde{W}_n(0) + \frac{1}{2\gamma_d}\tilde{d}_n^2(0) + \frac{\bar{g}_n}{2\gamma_p} \int_0^D \tilde{p}^2(0, r)dr, \\ c_j &= \frac{\rho_j}{\gamma_j} + V_j(0) + \frac{2c_{j2}}{\gamma_j}\bar{g}_j^2(c_{j+1} + c_{j+1,0}), \\ V_j(0) &= \frac{1}{2}z_j^2(0) + \frac{1}{2}\tilde{W}_j^T(0)\Gamma_j^{-1}\tilde{W}_j(0), \quad j = 1, 2, \dots, n-1, \\ \mu_j^* &= c'_j + c_{j0}, \quad j = 1, 2, \dots, n, \\ c'_n &= \frac{\rho_n}{\gamma_n}, \\ c'_j &= \frac{\rho_j}{\gamma_j} + \frac{2c_{j2}}{\gamma_j}\bar{g}_j^2(c_{j+1} + c_{j+1,0}), \quad j = 1, 2, \dots, n-1, \end{aligned}$$

and c_{j0} being the upper bound of $e^{-\gamma_j t} \int_0^t [g_j(\bar{x}_j, x_{j+1}^{\theta_j})N_j(\zeta_j) + 1]\dot{\zeta}_j e^{\gamma_j \tau} d\tau$, $j = 1, 2, \dots, n$.

Proof: For any given initial compact set Ω_0 , i.e., $\{z_i(0), \hat{W}_i(0), \hat{d}(0)\} \in \Omega_0$ ($i = 1, 2, \dots, n$), we can always construct a corresponding compact set Ω_{NN} comprising $\Omega_{Z_1}, \dots, \Omega_{Z_n}$, which is larger than Ω_0 and can be as large as we want, on which the NN approximation is valid. Based on the previous iterative derivation procedures from Step 1 to Step n of backstepping, from (5.20), (5.34) and (5.60), and according to Lemma 2.4, we can conclude that $V_j, z_j, \hat{W}_j, \hat{\tilde{d}}$, and hence, x_j , are SGUUB, $i = 1, 2, \dots, n$, i.e., all the signals in the closed-loop system are bounded.

5.3 Control Design and Stability Analysis

Noting the definition of V_n in (5.36), and letting c_{n0} be the upper bound of the term $e^{-\gamma_n t} \int_0^t [g_n(x, u^{\theta_n}) g_0 N_n(\zeta_n) + 1] \dot{\zeta}_n e^{\gamma_n \tau} d\tau$, $c_n = \frac{\rho_n}{\gamma_n} + V_n(0)$, $\mu_n = c_n + c_{n0}$ in (5.60), we have

$$|z_n| \leq \sqrt{2\mu_n}, \quad \|\tilde{W}_n\| \leq \sqrt{\frac{2\mu_n}{\lambda_{\min}(\Gamma_n^{-1})}}, \quad |\tilde{d}| \leq \sqrt{2\gamma_d \mu_n}.$$

Similarly, in the rest of steps from $(n-1)$ to 1 , letting c_{j0} be the upper bound of $e^{-\gamma_j t} \int_0^t [g_j(\bar{x}_j, x_{j+1}^{\theta_j}) N_j(\zeta_j) + 1] \dot{\zeta}_j e^{\gamma_j \tau} d\tau$, $c_j = \frac{\rho_j}{\gamma_j} + V_j(0) + \frac{2c_{j2}}{\gamma_j} \bar{g}_j^2(c_{j+1} + c_{j+1,0})$ and $\mu_j = c_j + c_{j0}$ in (5.34), we can obtain

$$|z_j| \leq \sqrt{2\mu_j}, \quad \|\tilde{W}_j\| \leq \sqrt{\frac{2\mu_j}{\lambda_{\min}(\Gamma_j^{-1})}}, \quad j = 1, \dots, n-1.$$

Furthermore, we can rewrite (5.59) as

$$V_n \leq \mu_n^* + [V_n(0) - \frac{\rho_n}{\gamma_n}] e^{-\gamma_n t}$$

where $\mu_n^* = c'_n + c_{n0}$, $c'_n = \frac{\rho_n}{\gamma_n}$, and c_{n0} be the upper bound of the term $e^{-\gamma_n t} \int_0^t [g_n(x, u^{\theta_n}) g_0 N_n(\zeta_n) + 1] \dot{\zeta}_n e^{\gamma_n \tau} d\tau$. As $t \rightarrow \infty$, we have

$$V_n \leq \mu_n^*$$

Therefore, based on the definition of V_n in (5.36), we can conclude that when $t \rightarrow \infty$, the following inequalities are true:

$$|z_n| \leq \sqrt{2\mu_n^*}, \quad \|\tilde{W}_n\| \leq \sqrt{\frac{2\mu_n^*}{\lambda_{\min}(\Gamma_n^{-1})}}, \quad |\tilde{d}| \leq \sqrt{2\gamma_d \mu_n^*}$$

A similar conclusion can be made about z_j , \hat{W}_j as follows

$$|z_j| \leq \sqrt{2\mu_j^*}, \quad \|\tilde{W}_j\| \leq \sqrt{\frac{2\mu_j^*}{\lambda_{\min}(\Gamma_j^{-1})}}, \quad j = 1, \dots, n-1$$

with $\mu_j^* = c'_j + c_{j0}$ and $c'_j = \frac{\rho_j}{\gamma_j} + \frac{2c_{j2}}{\gamma_j} \bar{g}_j^2(c_{j+1} + c_{j+1,0})$ as $t \rightarrow \infty$.

In addition, from the definition of the bounds of the compact sets Ω in (5.61) and Ω_s in (5.62), and the definitions of ρ_j , γ_j in (5.30) and ρ_n , γ_n (5.58), we can see that the size of the compact sets Ω and Ω_s depends on the choice of the control parameters σ_j , $\lambda_{\max}(\Gamma_j^{-1})$, σ_d , σ_p , ω , \bar{g}_n , γ_p , c_{j1} , c_{j2} , k_j . In particular, by decreasing

$\sigma_j, c_{j1}, c_{j2}, \lambda_{\max}(\Gamma_j^{-1}), \sigma_n, \sigma_d, \sigma_p, \omega, c_{n1}, \lambda_{\max}(\Gamma_n^{-1})$, and increasing $k_j, k_n, \gamma_d, \gamma_p$, we can reduce $\mu_j, \mu_j^*, \mu_n, \mu_n^*$, and thus, the size of the compact sets Ω and Ω_s will decrease. Therefore, as long as the initial conditions start in Ω_0 , there exist some control parameters such that the states and weights will remain in the conservative compact set Ω , and finally converge to the compact set Ω_s . Both of them belong to the chosen compact set Ω_{NN} . This completes the proof. ■

5.4 Simulation Results

In this section, simulation studies are presented to demonstrate the effectiveness of the proposed adaptive NN approach to deal with uncertain nonlinear systems in pure-feedback form preceded by the generalized PI hysteresis. Consider the following second-order nonlinear system with the generalized PI hysteresis:

$$\begin{aligned} \dot{x}_1 &= x_2 + 0.05 \sin(x_2) \\ \dot{x}_2 &= \frac{1 - e^{-x_2}}{1 + e^{-x_2}} + u + 0.1 \sin(u) + 0.1 \sin(6t) \\ y &= x_1 \end{aligned} \tag{5.63}$$

where u represents the output of the hysteresis described by the generalized PI model $u(t) = h(v)(t) - \int_0^D p(r) F_r[v](t) dr$ with the density function $p(r) = 0.08e^{-0.0024(r-1)^2}$, $r \in [0, 100]$, and $h(v)(t) = 0.4(|v| \arctan(v) + v)$. We can check that the plant (5.63) satisfies Assumptions 5.4 to 5.5. Our objective is to make the output of system (5.63), y , to track the desired trajectory, $y_d = 0.8 \sin(0.5t) + 0.1 \cos(t)$.

We adopt the control law and adaption laws designed in Section 5.3 in the following:

$$\begin{aligned} \alpha_1 &= N(\zeta_1)[k_1 z_1 + \hat{W}_1^T S(Z_1)] \\ v &= N(\zeta_2) \left[k_2 z_2 + \hat{W}_2^T S(Z_2) + \hat{d} \tanh\left(\frac{z_2}{\omega}\right) \right] + v_h \\ v_h &= -\text{sign}(z_2) \int_0^D \frac{\hat{p}(t, r)}{h_0} |F_r[v](t)| dr \\ \dot{\zeta}_1 &= k_1 z_1^2 + z_1 \hat{W}_1^T S(Z_1) \\ \dot{\zeta}_2 &= k_2 z_2^2 + z_2 \hat{W}_2^T S(Z_2) + z_2 \hat{d} \tanh\left(\frac{z_2}{\omega}\right) \end{aligned}$$

$$\begin{aligned}
\dot{\hat{W}}_1 &= \Gamma_1[z_1 S(Z_1) - \sigma_1 \hat{W}_1] \\
\dot{\hat{W}}_2 &= \Gamma_2[z_2 S(Z_2) - \sigma_2 \hat{W}_2] \\
\dot{\hat{d}} &= \gamma_d[z_2 \tanh(\frac{z_2}{\omega}) - \sigma_d \hat{d}] \\
\frac{\partial}{\partial t} \hat{p}(t, r) &= \begin{cases} -\gamma_p \sigma_p \hat{p}(t, r), & \text{if } \hat{p}(t, r) \geq p_{\max} \\ \gamma_p [|z_2| |F_r[v](t)| - \sigma_p \hat{p}(t, r)], & \text{if } 0 \leq \hat{p}(t, r) < p_{\max} \end{cases} \quad (5.64)
\end{aligned}$$

where $z_1 = x_1 - y_d$, $z_2 = x_2 - \alpha_1$. The Nussbaum function is chosen as $N(\zeta) = \exp(\zeta^2) \cos((\pi/2)\zeta)$. The inputs of the neural networks are $Z_1 = [x_1, y_d] \in \mathbb{R}^2$ and $Z_2 = [x_1, x_2, \frac{\partial \alpha_1}{\partial x_1}, \phi_1] \in \mathbb{R}^4$, where $\phi_1 = \frac{\partial \alpha_1}{\partial \zeta_1} \dot{\zeta}_1 + \frac{\partial \alpha_1}{\partial y_d} \dot{y}_d + \frac{\partial \alpha_1}{\partial \hat{W}_1} \dot{\hat{W}}_1$. The following initial conditions and controller design parameters are adopted in the simulation: $x_1(0) = 0.2$, $x_2(0) = \zeta_1(0) = \zeta_2(0) = \hat{d}(0) = 0.0$, $\hat{W}_1(0) = \hat{W}_2(0) = 0.0$, $k_1 = k_2 = 1.0$, $\Gamma_1 = 0.01I_{25}$, $\sigma_1 = 0.0$, $\Gamma_2 = 0.2I_{256}$, $\sigma_2 = 0.002$, $\sigma_p = 0.2$, $\gamma_p = 0.06$, $p_{\max} = 0.1$, $\omega = 0.1$, $h_0 = 0.35$.

In practice, the selection of the centers and widths of RBF has a great influence on the performance of the designed controller. According to [111], Gaussian RBF NNs arranged on a regular lattice on \mathbb{R}^n can uniformly approximate sufficiently smooth functions on closed, bounded subsets. Accordingly, in the following simulation studies, the centers and widths are chosen on a regular lattice in the respective compact sets. Specifically, we employ 5 nodes for each input dimension of $\hat{W}_1^T S(Z_1)$ and 4 nodes for each input dimension of $\hat{W}_2^T S(Z_2)$, and, thus, we end up with 25 nodes (i.e., $l_1 = 25$) with centers $\mu_l = 1.0$ ($l = 1, 2, \dots, l_1$) evenly spaced in $[-4.0, +4.0] \times [-4.0, +4.0]$ and widths $\eta_l = 1.0$ ($l = 1, 2, \dots, l_1$) for neural network $\hat{W}_1^T S(Z_1)$; and 256 nodes (i.e., $l_2 = 256$) with centers μ_l ($l = 1, 2, \dots, l_2$) evenly spaced in $[-4.0, +4.0] \times [-4.0, +4.0] \times [-4.0, +4.0] \times [-4.0, +4.0]$ and widths $\eta_l = 1.0$ ($l = 1, 2, \dots, l_1$) for neural network $\hat{W}_2^T S(Z_2)$.

Due to the use of sign function $\text{sgn}(\cdot)$, the control signal v_h (5.40) becomes discontinuous, which may excite unmodelled high-frequency plant dynamics and cause the

chattering phenomenon. To avoid the undesired chattering phenomenon, we will replace the sign function in v_h with the following saturation function in the simulation:

$$\text{sat}(*) = \begin{cases} 1 & \text{if } * \geq \epsilon \\ \frac{*}{\epsilon} & \text{if } |*| < \epsilon \\ -1 & \text{if } * < -\epsilon \end{cases}$$

where ϵ is a small positive constant and chosen as 0.05 in this section.

The simulation results are shown in Figures 5.1-5.6. From Figure 5.1, we observe that good tracking performance is achieved and the tracking error converges to a small neighborhood of zero in less than one period of oscillation. At the same time, other signals, including the state x_2 , control signal v , hysteresis output u , NN weights norms $\|W_1\|$, $\|W_2\|$, Nussbaum function signals $\zeta_1, \zeta_2, N(\zeta_1), N(\zeta_2)$, and the disturbance parameter estimate \hat{d} are kept bounded, as seen in Figures 5.2-5.6. It is noted that there is a large difference between the signals v and u in Figure 5.3, which indicates the significant hysteresis effect. In particular, in all figures, there are two obvious spikes at around 4 and 8 seconds, which result from the Nussbaum functions $N(\zeta_1), N(\zeta_2)$.

5.5 Conclusion

Adaptive neural control has been proposed for a class of unknown nonlinear systems in pure-feedback form preceded by the uncertain generalized PI hysteresis. We adopted the Mean Value Theorem to solve the non-affine problem both in system unknown nonlinear functions and unknown input function in the generalized PI hysteresis model, and used Nussbaum function to deal with the problem of the unknown virtual control directions. The closed-loop control system has been theoretically shown to be SGUUB using Lyapunov synthesis method. Simulation results have verified the effectiveness of the proposed approach.

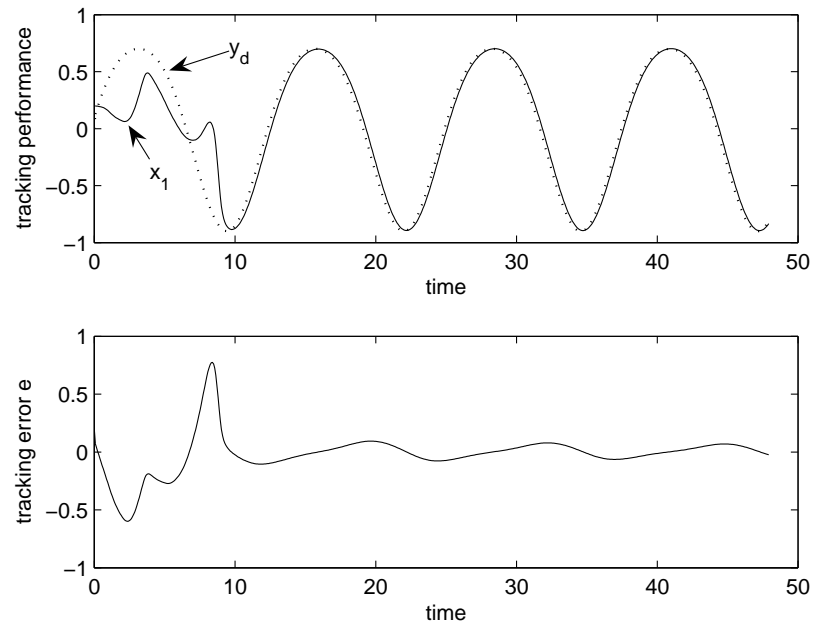


Figure 5.1: Tracking performance for the pure-feedback system with generalized PI hysteresis

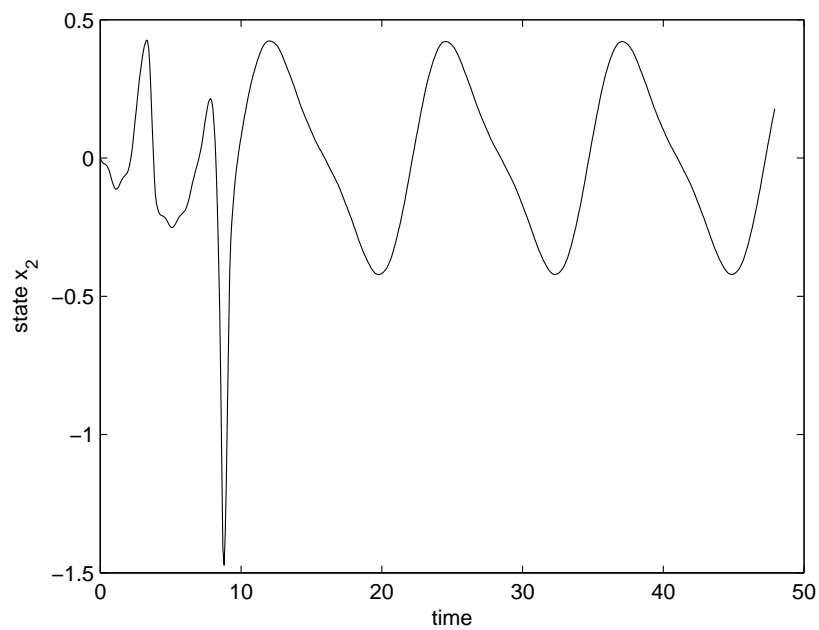


Figure 5.2: State x_2 for the pure-feedback system with generalized PI hysteresis

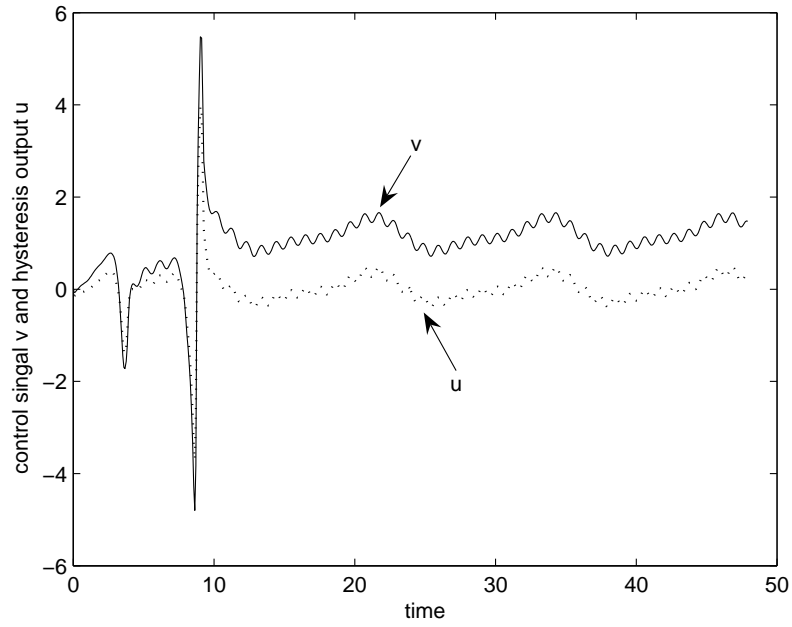


Figure 5.3: Control signals for the pure-feedback system with generalized PI hysteresis

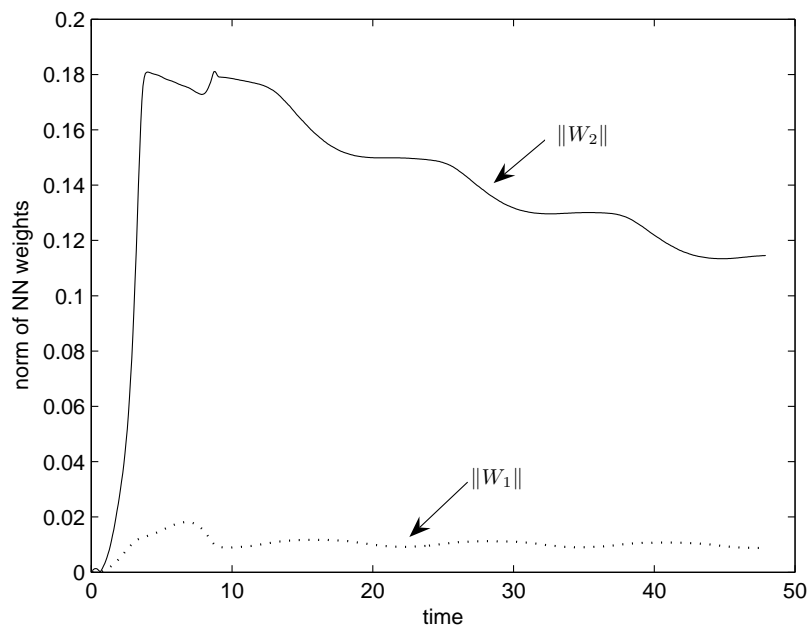


Figure 5.4: Norm of NN weights for the pure-feedback system with generalized PI hysteresis

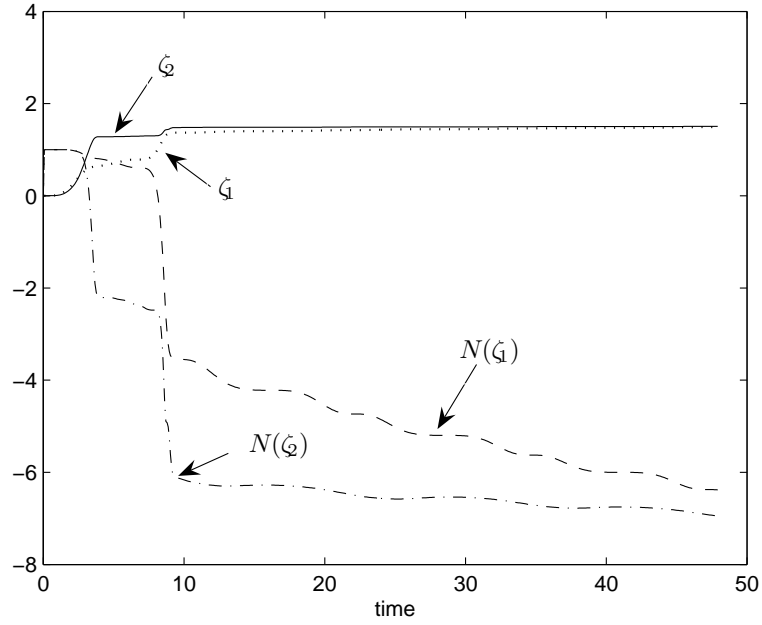


Figure 5.5: Nussbaum function signals for the pure-feedback system with generalized PI hysteresis

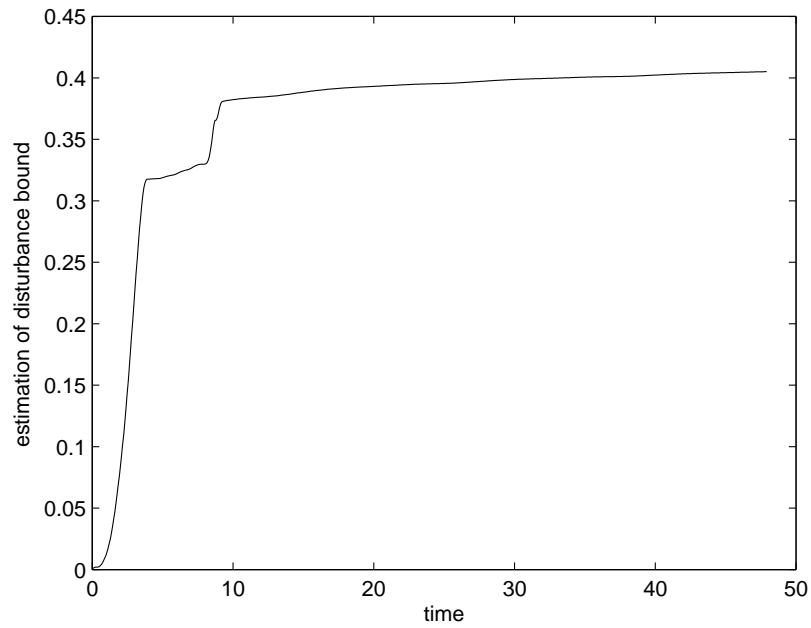


Figure 5.6: Estimation of disturbance bound, \hat{d} , for the pure-feedback system with generalized PI hysteresis

Chapter 6

Conclusions and Further Research

6.1 Conclusions

This thesis focused on exploring new avenues to fuse different hysteresis models with the available control techniques to achieve both stabilization and strict tracking precision requirements for the concerned uncertain nonlinear systems without constructing a hysteresis inverse. The results presented in this thesis can be considered as a stepping stone to be used toward the development of a general control framework for the systems with hysteretic behavior. The key results are as follows:

- **Strict-Feedback Systems with Backlash-Like Hysteresis.**

For a class of strict-feedback nonlinear systems preceded by unknown backlash-like hysteresis, adaptive dynamic surface control (DSC) was developed without constructing a hysteresis inverse by exploring the characteristics of backlash-like hysteresis, which can be described by two parallel lines connected via horizontal line segments. Through transforming the backlash-like hysteresis model into a linear-in-control term plus a bounded “disturbance-like” term, standard robust adaptive control used for dealing with bounded disturbances was applied. The explosion of complexity in traditional backstepping design was avoided by utilizing DSC. Function uncertainties were compensated for using neural networks (NNs) due to their universal approximation capabilities. Through Lyapunov

synthesis, the closed-loop control system has been proved to be semi-globally uniformly ultimately bounded (SGUUB), and the tracking error converged to a small neighborhood of zero. Simulation results have been provided to illustrate the performance of the proposed approach.

- **Output Feedback Systems with Backlash-Like Hysteresis.**

Adaptive neural observer backstepping has been proposed for state estimation and function on-line approximation using only output measurements to achieve the output tracking for a class of output feedback nonlinear systems subject to function uncertainties and backlash-like hysteresis. The Barrier Lyapunov Function (BLF) has been incorporated into Lyapunov synthesis to address two open and challenging problems in the neuro-control area. By ensuring the boundedness of the BLF, we can actively (i) determine the compact set *a priori*, on which NN approximation is valid; and (ii) ensure the argument of the unknown function remain within the specified set. The SGUUB stability of the closed-loop system has been provided and the effectiveness of the proposed approach has been illustrated using a numerical example. The present approach would provide both theoretical criteria and practical insights for the design and implementation of NN based control. It can be considered as a supplement or an improvement to the state of art in neuro-control field.

- **MIMO Systems with Classic Prandtl-Ishlinskii Hysteresis**

Adaptive variable structure neural control is proposed for a class of uncertain multi-input multi-output (MIMO) nonlinear systems under the effects of classic Prandtl-Ishlinskii (PI) hysteresis and time-varying state delays. Although there are some works that deal with hysteresis, or time delay, individually, the combined problem, despite its practical relevance, is largely open in the literature to the best of the author's knowledge. The unknown time-varying delay uncertainties are compensated for using appropriate Lyapunov-Krasovskii functionals in the design. Unlike backlash-like hysteresis, standard robust adaptive control used for dealing with bounded disturbances cannot be applied here, since no assumptions can be made on the boundedness of the hysteresis term of the classic PI model. By investigating the properties of PI classic hysteresis, the effect of

6.2 Recommendations for Further Research

the uncertain PI classic hysteresis was also mitigated using the proposed control. The controller has been made to be free from singularity problem by utilizing integral Lyapunov function. Based on the principle of sliding-mode control, the developed controller can guarantee that all signals involved are SGUUB. Simulation results have verified the effectiveness of the proposed approach.

- **Pure-Feedback Systems with Generalized Prandtl-Ishlinskii Hysteresis**

Adaptive neural control has been investigated for a class of unknown nonlinear systems in pure-feedback form with the generalized Prandtl-Ishlinskii (PI) hysteresis input. Compared with the backlash-like hysteresis model and the classic PI hysteresis model, the generalized PI hysteresis model can capture the hysteresis phenomenon more accurately and accommodate more general classes of hysteresis shapes by adjusting not only the density function but also the input function. The difficulty of the control of such class of systems lies in the non-affine problem in both system unknown nonlinear functions and unknown input function in the generalized PI hysteresis model. To overcome this difficulty, we adopted the meanvalue theorem to solve the nonaffine problem in both system unknown nonlinear functions and unknown input function in the generalized PI hysteresis model, and used Nussbaum function to deal with the problem of the unknown virtual control directions. The closed-loop control system has been theoretically shown to be SGUUB using the Lyapunov synthesis method. Simulation results have verified the effectiveness of the proposed approach.

6.2 Recommendations for Further Research

This section presents several possible directions that are recommended for extending the results developed in this thesis:

- **Variability in Hysteresis Modeling.**

In this thesis, we focused on a specific hysteresis model for a class of concerned

6.2 Recommendations for Further Research

nonlinear system. In practice, the hysteretic behavior of the actuators has variability due to some factors, such as fluctuation of the temperature. Therefore, more investigations are needed to include this variability in hysteresis modeling and to fuse these hysteresis models with the available control techniques to mitigate the effects of hysteresis while satisfying the basic requirements for the concerned system.

- **Practical Applications.**

As mentioned, hysteresis nonlinearities are common in many industrial processes, especially in position control of smart material-based actuators. Both computer simulations and experimental work need to be carried out extensively to verify the effectiveness and expose the limitations of the proposed controllers in this thesis, especially in the face of real time response, tolerances, measurement noise and modeling compatibility with practical systems, etc.

- **Generalization of the solution of NN open problems.**

Though the solution of NN open problems was presented for uncertain output feedback systems in Chapter 3.2, the proposed method could be generalized to many more classes of systems with state-dependent uncertain nonlinearities, which makes the problem becomes much more challenging. One way is to follow a similar approach as that in our recently published result [161], where Barrier Lyapunov Functions are adopted to handle full state constraints for strict feedback systems. The analysis will be much more involved, requiring the checking of feasibility conditions on the initial states and control parameters. The case of uncertain strict feedback systems is still an ongoing topic of research for us.

Bibliography

- [1] H. T. Banks and R. C. Smith, “Hysteresis modeling in smart material systems,” *Journal of Applied Mechanics and Engineering*, vol. 5, no. 1, pp. 31–45, 2000.
- [2] C. A. Dickinson, D. C. Hughes, and J. T. Wen, “Hysteresis in shape memory alloy actuators: the control issues,” *Proceedings of SPIE*, vol. 2715, pp. 494–506, 1996.
- [3] G. Tao and P. V. Kokotovic, “Adaptive control of plants with unknown hysteresees,” *IEEE Transactions on Automatic Control*, vol. 40, no. 2, pp. 200–212, 1995.
- [4] G. Tao and F. L. Lewis, *Adaptive Control of Nonsmooth Dynamic Systems*. Springer, 2001.
- [5] X. Tan and J. S. Baras, “Recursive identification of hysteresis in smart materials,” in *Proceedings of the 2004 American Control Conference*, pp. 3857–3862, 2004.
- [6] J. W. Macki, P. Nistri, and P. Zecca, “Mathematical models for hysteresis,” *SIAM Review*, vol. 35, no. 1, pp. 94–123, 1993.
- [7] S. O. Reza Moheimani and G. C. Goodwin, “Guest editorial introduction to the special issue on dynamics and control of smart structures,” *IEEE Transactions on Control Systems Technology*, vol. 9, no. 1, pp. 3–4, 2001.
- [8] Q. Wang, *Robust Adaptive Controls of Nonlinear Systems with Actuator Hysteresis Represented by Prandtl-Ishlinskii Models*. PhD thesis, Concordia University, Canada, 2006.

-
- [9] P. Ge and M. Jouaneh, "Tracking control of a piezoceramic actuator," *IEEE Transactions on Control Systems Technology*, vol. 4, no. 3, pp. 209–216, 1996.
 - [10] W. S. Galinaitis, *Two methods for modeling scalar hysteresis and their use in controlling actuators with hysteresis*. PhD thesis, Virginia Polytechnic Institute and State University, Blacksburg, VA, 1999.
 - [11] S. Mittal and C.-H. Meng, "Hysteresis compensation in electromagnetic actuators through Preisach model inverse," *IEEE/ASME Transactions on Mechatronics*, vol. 5, no. 4, pp. 394–409, 2000.
 - [12] D. Croft, G. Shed, and S. Devasia, "Creep, hysteresis, and vibration compensation for piezoactuators: Atomic force microscopy application," *Journal of Dynamic Systems, Measurement, and Control*, vol. 123, no. 1, pp. 35–43, 2001.
 - [13] Y. Bernard, E. Mendes, and F. Bouillault, "Dynamic hysteresis modeling based on Preisach model," *IEEE Transactions on Magnetics*, vol. 38, no. 2, pp. 885–888, 2002.
 - [14] G. Webb, A. Kurdila, and D. Lagoudas, "Adaptive hysteresis model for model reference control with actuator hysteresis," *Journal of Guidance, Control, and Dynamics*, vol. 23, no. 3, pp. 459–465, 2000.
 - [15] P. Krejci and K. Kuhnen, "Inverse control of systems with hysteresis and creep," *IEE Proceedings-Control Theory and Applications*, vol. 148, no. 3, pp. 185–192, 2001.
 - [16] C. Y. Su, Y. Stepanenko, J. Svoboda, and T. P. Leung, "Robust adaptive control of a class of nonlinear systems with unknown backlash-like hysteresis," *IEEE Transactions on Automatic Control*, vol. 45, no. 12, pp. 2427–2432, 2000.
 - [17] J. Zhou, C. Wen, and Y. Zhang, "Adaptive backstepping control design of a class of uncertain nonlinear systems with unknown backlash-like hysteresis," *IEEE Transactions on Automatic Control*, vol. 49, no. 10, pp. 1751–1757, 2004.
 - [18] C. Y. Su, Q. Wang, X. Chen, and S. Rakheja, "Adaptive variable structure control of a class of nonlinear systems with unknown Prandtl-Ishlinskii hysteresis," *IEEE Transactions on Automatic Control*, vol. 50, no. 12, pp. 2069–2074, 2005.

- [19] Q. Wang and C. Y. Su, “Robust adaptive control of a class of nonlinear systems including actuator hysteresis with Prandtl-Ishlinskii presentations,” *Automatica*, vol. 42, no. 5, pp. 859–867, 2006.
- [20] W. S. McCulloch and W. Pitts, “A logical calculus of the ideas immanent in nervous activity,” *Bulletin of Mathematical Biophysics*, vol. 5, no. 4, pp. 115–133, 1943.
- [21] G. Cybenko, “Approximation by superpositions of a sigmoidal function,” *Mathematics of Control, Signals and Systems*, vol. 2, no. 4, pp. 303–314, 1989.
- [22] T. Khanna, *Foundations of Neural Networks*. Reading, Mass.: Addison-Wesley, 1990.
- [23] K. I. Funahashi, “On the approximate realization of continuous mappings by neural networks,” *Neural Networks*, vol. 2, no. 3, pp. 183–192, 1989.
- [24] K. Hornik, M. Stinchcombe, and H. White, “Multilayer feedforward networks are universal approximators,” *Neural Networks*, vol. 2, no. 5, pp. 359–366, 1989.
- [25] V. Cherkassky, D. Gehring, and F. Mulier, “Comparison of adaptive methods for function estimation from samples,” *IEEE Transactions on Neural Networks*, vol. 7, no. 4, pp. 969–984, 1996.
- [26] N. Sadegh, “A perception network for functional identification and control of nonlinear systems,” *IEEE Transactions on Neural Networks*, vol. 4, no. 6, pp. 982–988, 1993.
- [27] A. R. Barron, “Universal approximation bounds for superpositions for a sigmoidal function,” *IEEE Transactions on Information Theory*, vol. 39, no. 3, pp. 930–945, 1993.
- [28] A. S. Poznyak, E. N. Sanchez, and W. Yu, *Differential Neural Networks for Robust Nonlinear Control : Identification, State Estimation and Trajectory Tracking*. Singapore; River Edge, N.J.: World Scientific, 2001.
- [29] B. Widrow and F. W. Smith, “Pattern-recognizing control systems,” in *Computer and Information Sciences: Collected Papers on Learning, Adaptation and*

- Control in Information Systems* (J. Tou and R. Wilcox, eds.), COINS symposium proceedings, pp. 288–317, Washington DC: Spartan Books, 1964.
- [30] J. S. Albus, “A new approach to manipulator control: the cerebellar model articulation controller (CMAC),” *Journal of Dynamic Systems, Measurement, and Control*, vol. 97, pp. 220–227, 1975.
 - [31] D. E. Rumelhart, G. E. Hinton, and R. J. Williams, “Learning internal representations by error-propagation,” in *Parallel Distributed Processing* (D. E. Rumelhart and R. J. McClelland, eds.), vol. 1, ch. 8, pp. 318–362, Cambridge, Mass.: MIT Press, 1986.
 - [32] K. S. Narendra and K. Parthasarathy, “Identification and control of dynamic systems using neural networks,” *IEEE Transactions on Neural Networks*, vol. 1, no. 1, pp. 4–27, 1990.
 - [33] K. S. Narendra and S. Mukhopadhyay, “Adaptive control of nonlinear multivariable systems using neural networks,” *Neural Networks*, vol. 7, no. 5, pp. 737–752, 1994.
 - [34] D. Psaltis, A. Sideris, and A. A. Yamamura, “A multilayered neural network controller,” *IEEE Control Systems Magazine*, vol. 8, no. 2, pp. 17–21, 1988.
 - [35] L. Jin, P. N. Nikiforuk, and M. M. Gupta, “Direct adaptive output tracking control using multilayered neural networks,” *IEE Proceedings - Control Theory and Applications*, vol. 140, no. 6, pp. 393–398, 1993.
 - [36] M. M. Polycarpou and P. A. Ioannou, “Learning and convergence analysis of neural-type structured networks,” *IEEE Transactions on Neural Networks*, vol. 3, no. 1, pp. 39–50, 1992.
 - [37] F. C. Chen and H. K. Khalil, “Adaptive control of a class of nonlinear discrete-time systems using neural networks,” *IEEE Transactions on Automatic Control*, vol. 40, no. 5, pp. 791–801, 1995.
 - [38] A. U. Levin and K. S. Narendra, “Control of nonlinear dynamical systems using neural networks - Part II: observability, identification, and control,” *IEEE Transactions on Neural Networks*, vol. 7, no. 1, pp. 30–42, 1996.

- [39] C. J. Goh, “Model reference control of non-linear systems via implicit function emulation,” *International Journal of Control*, vol. 60, no. 1, pp. 91–115, 1994.
- [40] T. Zhang, S. S. Ge, and C. C. Hang, “Neural-based direct adaptive control for a class of general nonlinear systems,” *International Journal of Systems Science*, vol. 28, no. 10, pp. 1011–1020, 1997.
- [41] S. S. Ge, C. C. Hang, and T. Zhang, “Nonlinear adaptive control using neural networks and its application to CSTR systems,” *Journal of Process Control*, vol. 9, no. 4, pp. 313–323, 1999.
- [42] S. S. Ge, C. C. Hang, and T. Zhang, “Adaptive neural network control of nonlinear systems by state and output feedback,” *IEEE Transactions on Systems Man and Cybernetics-Part B: Cybernetics*, vol. 29, no. 6, pp. 818–828, 1999.
- [43] C. Wang and S. S. Ge, “Adaptive backstepping control of uncertain Lorenz system,” *International Journal of Bifurcation and Chaos*, vol. 11, no. 4, pp. 1115–1119, 2001.
- [44] P. E. Moraal and J. W. Grizzle, “Observer design for nonlinear systems with discrete-time measurements,” *IEEE Transactions on Automatic Control*, vol. 40, no. 3, pp. 395–404, 1995.
- [45] A. M. Dabroom and H. K. Khalil, “Output feedback sampled-data control of nonlinear systems using high-gain observers,” *IEEE Transactions on Automatic Control*, vol. 46, no. 11, pp. 1712–1725, 2001.
- [46] F. L. Lewis, S. Jagannathan, and A. Yesilidrek, *Neural Network Control of Robot Manipulators and Nonlinear Systems*. London: Taylor and Francis, 1999.
- [47] S. S. Ge, T. H. Lee, and C. J. Harris, *Adaptive Neural Network Control of Robotic Manipulators*. River Edge, NJ: World Scientific, 1998.
- [48] A. T. Vemuri and M. M. Polycarpou, “Neural-network-based robust fault diagnosis in robotic systems,” *IEEE Transactions on neural networks*, vol. 8, no. 6, pp. 1410–1420, 1997.

- [49] A. T. Vemuri, M. M. Polycarpou, and S. A. Diakourtis, "Neural network based fault detection in robotic manipulators," *IEEE Transactions on Robotics and Automation*, vol. 14, no. 2, pp. 342–348, 1998.
- [50] K. J. Hunt, D. Sbarbaro, R. Żbikowski, and P. J. Gawthrop, "Neural networks for control systems - A survey," *Automatica*, vol. 28, no. 6, pp. 1083–1112, 1992.
- [51] K. Najim, *Process Modeling and Control in Chemical Engineering*. New York: Marcel Dekker, 1989.
- [52] G. K. Kel'mans, A. S. Poznyak, and A. V. Chernitser, "Local optimization algorithms in asymptotic control of nonlinear dynamic plants," *Automation and Remote Control*, vol. 38, no. 11, pp. 1639–1652, 1977.
- [53] A. M. Shaw and F. J. Doyle, "Multivariable nonlinear control applications for a high purity distillation column using a recurrent dynamic neuron model," *Journal of Process Control*, vol. 7, no. 4, pp. 255–268, 1997.
- [54] R. Ordonez, J. Zumberge, J. T. Spooner, and K. M. Passino, "Adaptive fuzzy control: Experiments and comparative analyses," *IEEE Transactions on Fuzzy Systems*, vol. 5, no. 2, pp. 167–188, 1997.
- [55] J. T. Spooner, M. Maggiore, R. Ordonez, and K. M. Passino, *Stable Adaptive Control and Estimation for Nonlinear Systems - Neural and Fuzzy Approximator Techniques*. New York: Wiley, 2002.
- [56] M. Brown and C. J. Harris, *Neurofuzzy Adaptive Modelling and Control*. New York: Prentice-Hall, 1994.
- [57] G. C. Goodwin and K. S. Sin, *Adaptive Filtering Prediction and Control*. Englewood Cliffs, N. J.: Prentice-Hall, 1984.
- [58] B. B. Petersen and K. S. Narendra, "Bounded error adaptive control," *IEEE Transactions on Automatic Control*, vol. 27, no. 6, pp. 1161–1168, 1982.
- [59] C. Samson, "Stability analysis of adaptively controlled systems subject to bounded disturbances," *Automatica*, vol. 19, no. 1, pp. 81–86, 1983.

- [60] K. S. Narendra and A. M. Annaswamy, “A new adaptive law for robust adaptation without persistent excitation,” *IEEE Transactions on Automatic Control*, vol. 32, no. 2, pp. 134–145, 1987.
- [61] P. A. Ioannou and J. Sun, *Robust Adaptive Control*. Upper Saddle River, NJ: PTR Prentice-Hall, 1996.
- [62] K. Nam and A. Araposthathis, “A model reference adaptive control scheme for pure-feedback nonlinear systems,” *IEEE Transactions on Automatic Control*, vol. 33, no. 9, pp. 803–811, 1988.
- [63] S. Sastry and A. Isidori, “Adaptive control of linearizable systems,” *IEEE Transactions on Automatic Control*, vol. 34, no. 11, pp. 1123–1131, 1989.
- [64] H. K. Khalil, *Nonlinear Systems*. Upper Saddle River, NJ: Prentice Hall, 1996.
- [65] M. Krstić, I. Kanellakopoulos, and P. V. Kokotović, *Nonlinear and Adaptive Control Design*. New York: Wiley, 1995.
- [66] S. S. Ge, C. C. Hang, T. H. Lee, and T. Zhang, *Stable Adaptive Neural Network Control*. Boston: Kluwer Academic, 2002.
- [67] K. S. Narendra and A. M. Annaswamy, *Stable Adaptive Systems*. Englewood Cliffs, NJ: Prentice Hall, 1989.
- [68] K. S. Narendra and S. Mukhopadhyay, “Adaptive control using neural networks and approximate models,” *IEEE Transactions on Neural Networks*, vol. 8, no. 3, pp. 475–485, 1997.
- [69] T. Parisini and R. Zoppoli, “Neural networks for feedback feedforward nonlinear control systems,” *IEEE Transactions on Neural Networks*, vol. 5, no. 3, pp. 436–449, 1994.
- [70] J. T. Spooner and K. M. Passino, “Stable adaptive control using fuzzy systems and neural networks,” *IEEE Transactions on Fuzzy Systems*, vol. 4, no. 3, pp. 339–359, 1996.

- [71] J. T. Spooner and K. M. Passino, “Adaptive control of a class of decentralized nonlinear systems,” *IEEE Transactions on Automatic Control*, vol. 41, no. 2, pp. 280–284, 1996.
- [72] T. Parisini and R. Zoppoli, “Neural networks for nonlinear state estimation,” *International Journal of Robust and Nonlinear Control*, vol. 4, no. 2, pp. 231–248, 1994.
- [73] T. Parisini and R. Zoppoli, “Neural approximations for multistage optimal control of nonlinear stochastic systems,” *IEEE Transactions on Automatic Control*, vol. 41, no. 6, pp. 889–895, 1996.
- [74] J. H. Braslavsky, R. H. Middleton, and J. S. Freudenberg, “Cheap control performance of a class of nonright-invertible nonlinear systems,” *IEEE Transactions on Automatic Control*, vol. 47, no. 8, pp. 1314–1319, 2002.
- [75] H. K. Khalil, “Adaptive output feedback control of nonlinear systems represented by input-output models,” *IEEE Transactions on Automatic Control*, vol. 41, no. 2, pp. 177–188, 1996.
- [76] M. M. Polycarpou and P. A. Ioannou, “A robust adaptive nonlinear control design,” *Automatica*, vol. 32, no. 3, pp. 423–427, 1996.
- [77] F. L. Lewis, A. Yesildirek, and K. Liu, “Multilayer neural-net robot controller with guaranteed tracking performance,” *IEEE Transactions on Neural Networks*, vol. 7, no. 2, pp. 388–399, 1996.
- [78] M. M. Polycarpou, “Stable adaptive neural control scheme for nonlinear systems,” *IEEE Transactions on Automatic Control*, vol. 41, no. 3, pp. 447–451, 1996.
- [79] A. Yesildirek and F. L. Lewis, “Feedback linearization using neural networks,” *Automatica*, vol. 31, no. 11, pp. 1659–1664, 1995.
- [80] T. Zhang, S. S. Ge, and C. C. Hang, “Design and performance analysis of a direct adaptive controller for nonlinear systems,” *Automatica*, vol. 35, no. 11, pp. 1809–1817, 1999.

- [81] I. Kanellakopoulos, P. V. Kokotović, and A. S. Morse, “Systematic design of adaptive controllers for feedback linearizable systems,” *IEEE Transactions on Automatic Control*, vol. 36, no. 11, pp. 1241–1253, 1991.
- [82] O. Adetona, E. Garcia, and L. H. Keel, “Stable adaptive control of unknown nonlinear dynamic systems using neural networks,” in *Proceedings of the 1999 American Control Conference*, pp. 1072 –1076, 1999.
- [83] I. Kanellakopoulos, P. V. Kokotović, and R. Marino, “An extended direct scheme for robust adaptive nonlinear control,” *Automatica*, vol. 27, no. 2, pp. 247–255, 1991.
- [84] G. Campion and G. Bastin, “Indirect adaptive state feedback control of linearly parametrized non-linear systems,” *International Journal of Adaptive Control and Signal Processing*, vol. 4, no. 5, pp. 345–358, 1990.
- [85] I. Kanellakopoulos, *Adaptive Control of Nonlinear Systems*. PhD thesis, University of Illinois, Urbana, 1991.
- [86] J. S. Freudenberg and R. H. Middleton, “Properties of single input, two output feedback systems,” *International Journal of Control*, vol. 72, no. 16, pp. 1446–1465, 1999.
- [87] G. Chen, J. Chen, and R. Middleton, “Optimal tracking performance for SIMO systems,” *IEEE Transactions on Automatic Control*, vol. 47, no. 10, pp. 1770–1775, 2002.
- [88] S. S. Ge, C. C. Hang, and T. Zhang, “Stable adaptive control for nonlinear multivariable systems with a triangular control structure,” *IEEE Transactions on Automatic Control*, vol. 45, no. 6, pp. 1221–1225, 2000.
- [89] D. N. Godbole and S. S. Sastry, “Approximate decoupling and asymptotic tracking for MIMO systems,” in *Proceedings of the 32nd IEEE Conference on Decision and Control*, pp. 2754–2759, 1993.
- [90] A. Isidori, *Nonlinear Control Systems*. Berlin; New York: Springer, 3rd ed., 1995.

- [91] H. Nijmeijer and J. M. Schumacher, “The regular local noninteracting control problem for nonlinear control systems,” *SIMA Journal on Control and Optimization*, vol. 24, no. 6, pp. 1232–1245, 1986.
- [92] H. Nijmeijer and A. J. van der Schaft, *Nonlinear Dynamical Control Systems*. New York: Springer, 1990.
- [93] H. Nijmeijer and W. Respondek, “Decoupling via dynamic compensation for nonlinear control systems,” in *Proceedings of the 25th IEEE Conference on Decision and Control*, pp. 192–197, 1986.
- [94] W. Lin and C. J. Qian, “Semi-global robust stabilization of nonlinear systems by partial state and output feedback,” in *Proceedings of the 37th IEEE Conference on Decision and Control*, pp. 3105–3110, 1998.
- [95] A. Trebi-Ollennu and B. A. White, “Robust output tracking for MIMO nonlinear systems: An adaptive fuzzy systems approach,” *IEE Proceedings - Control Theory and Applications*, vol. 144, no. 6, pp. 537–544, 1997.
- [96] N. Hovakimyan, F. Nardi, and A. J. Calise, “A novel error observer-based adaptive output feedback approach for control of uncertain systems,” *IEEE Transactions on Automatic Control*, vol. 47, no. 8, pp. 1310–1314, 2002.
- [97] S. S. Ge and C. Wang, “Adaptive NN control of uncertain nonlinear pure-feedback systems,” *Automatica*, vol. 38, no. 4, pp. 671–682, 2002.
- [98] D. Wang and J. Huang, “Adaptive neural network control for a class of uncertain nonlinear systems in pure-feedback form,” *Automatica*, vol. 38, no. 8, pp. 1365–1372, 2002.
- [99] S. S. Ge and J. Zhang, “Neural-network control of nonaffine nonlinear system with zero dynamics by state and output feedback,” *IEEE Transactions on Neural Networks*, vol. 14, no. 4, pp. 900–918, 2003.
- [100] C. Wang, D. J. Hill, S. S. Ge, and G. Chen, “An ISS-modular approach for adaptive neural control of pure-feedback systems,” *Automatica*, vol. 42, no. 5, pp. 723–731, 2006.

- [101] H. Du, H. Shao, and P. Yao, “Adaptive neural network control for a class of low-triangular-structured nonlinear systems,” *IEEE Transactions on Neural Networks*, vol. 17, no. 2, pp. 509–514, 2006.
- [102] J. Y. Choi and J. A. Farrel, “Adaptive observer backstepping control using neural networks,” *IEEE Transactions on Neural Networks*, vol. 12, no. 5, pp. 1103–1112, 2001.
- [103] M. Krasnosel’skii and A. Pokrovskii, *Systems with Hysteresis*. Berlin; New York: Springer-Verlag, 1989.
- [104] M. Brokate and J. Sprekels, *Hysteresis and Phase Transitions*. New York: Springer, 1996.
- [105] A. Visintin, *Differential Models of Hysteresis*. Berlin; New York: Springer, 1994.
- [106] O. Klein and P. Krejci, “Outwards pointing hysteresis operators and asymptotic behaviour of evolution equations,” *Nonlinear Analysis: Real World Applications*, vol. 4, no. 5, pp. 755–785, 2003.
- [107] J. R. Rice, *The Approximation of Functions*. Reading, Mass.: Addison-Wesley, 1964.
- [108] A. Barron., “Approximation and estimation bounds for superposition for a sigmoidal function,” in *Proc. 4th Ann. Workshop on Computational Learning Theory*, (San Mateo), pp. 243–249, Morgan Kanffman, 1991.
- [109] S. Haykin, *Neural Networks: A Comprehensive Foundations*. Pearson Education, 2nd ed., 1998.
- [110] C. A. Micchelli, “Interpolation of scattered data: distance matrices and conditionally positive definite functions,” *Constructive Approximation*, vol. 2, no. 1, pp. 11–22, 1986.
- [111] R. M. Sanner and J. E. Slotine, “Gaussian networks for direct adaptive control,” *IEEE Transactions on Neural Networks*, vol. 3, no. 6, pp. 837–863, 1992.

- [112] J. A. Farrell and M. M. Polycarpou, *Adaptive Approximation Based Control*. Hoboken, NJ: Wiley, 2006.
- [113] T. M. Apostol, *Mathematical Analysis*. Reading, MA: Addison-Wesley, 2nd ed., 1974.
- [114] S. S. Ge, F. Hong, and T. H. Lee, “Adaptive neural control of nonlinear time-delay systems with unknown virtual control coefficients,” *IEEE Transactions on Systems Man and Cybernetics-Part B: Cybernetics*, vol. 34, no. 1, pp. 499–516, 2004.
- [115] W. Lin and C. Qian, “Adaptive control of nonlinearly parameterized systems: the smooth feedback case,” *IEEE Transactions on Automatic Control*, vol. 47, no. 8, pp. 1249–1266, 2002.
- [116] K. P. Tee, S. S. Ge, and E. H. Tay, “Barrier Lyapunov Functions for the control of output-constrained nonlinear systems,” *Automatica*, vol. 45, no. 4, pp. 918–927, 2009.
- [117] K. B. Ngo, R. Mahony, and Z. P. Jiang, “Integrator backstepping using barrier functions for systems with multiple state constraints,” in *Proceedings of the 44th IEEE Conference on Decision and Control and 2005 European Control Conference*, pp. 8306–8312, 2005.
- [118] B. Ren, S. S. Ge, K. P. Tee, and T. H. Lee, “Adaptive neural control for output feedback nonlinear systems using a Barrier Lyapunov Function,” *submitted to IEEE Transactions on Neural Networks*, 2009.
- [119] E. D. Sontag, *Mathematical Control Theory: Deterministic Finite Dimensional Systems*. New York: Springer, 2nd ed., 1998.
- [120] X. Tan and J. S. Baras, “Modeling and control of hysteresis in magnetostrictive actuators,” *Automatica*, vol. 40, no. 9, pp. 1469–1480, 2004.
- [121] D. Swaroop, J. K. Hedrick, P. P. Yip, and J. C. Gerdes, “Dynamic surface control for a class of nonlinear systems,” *IEEE Transactions on Automatic Control*, vol. 45, no. 10, pp. 1893–1899, 2000.

- [122] D. Wang and J. Huang, "Neural network-based adaptive dynamic surface control for a class of uncertain nonlinear systems in strict-feedback form," *IEEE Transactions on Neural Networks*, vol. 16, no. 1, pp. 195–202, 2005.
- [123] J. A. Farrel, "Stability and approximator convergence in nonparametric nonlinear adaptive control," *IEEE Transactions on Neural Networks*, vol. 9, no. 5, pp. 1008–1020, 1998.
- [124] M. M. Polycarpou and M. J. Mears, "Stable adaptive tracking of uncertain systems using nonlinearly parametrized on-line approximators," *International Journal of Control*, vol. 70, no. 3, pp. 363–384, 1998.
- [125] Y. H. Kim and F. L. Lewis, "Neural network output feedback control of robot manipulators," *IEEE Transactions on Robotics and Automation*, vol. 15, no. 2, pp. 301–309, 1999.
- [126] S. Seshagiri and H. K. Khalil, "Output feedback control of nonlinear systems using RBF neural networks," *IEEE Transactions on Neural Networks*, vol. 11, no. 1, pp. 69–79, 2000.
- [127] J. Stoev, J. Y. Choi, and J. Farrell, "Adaptive control for output feedback nonlinear systems in the presence of modeling errors," *Automatica*, vol. 38, no. 10, pp. 1761–1767, 2002.
- [128] N. Hovakimyan, F. Nardi, A. Calise, and N. Kim, "Adaptive output feedback control of uncertain nonlinear systems using single-hidden-layer neural networks," *IEEE Transactions on Neural Networks*, vol. 13, no. 6, pp. 1420–1431, 2002.
- [129] S. S. Ge and C. Wang, "Adaptive neural control of uncertain MIMO nonlinear systems," *IEEE Transactions on Neural Networks*, vol. 15, no. 3, pp. 674–692, 2004.
- [130] S. S. Ge, C. C. Hang, and T. Zhang, "A direct method for robust adaptive nonlinear control with guaranteed transient performance," *Systems & Control Letters*, vol. 37, no. 5, pp. 275–284, 1999.

- [131] Y. Zhao and J. A. Farrell, “Locally weighted online approximation-based control for nonaffine systems,” *IEEE Transactions on Neural Networks*, vol. 18, no. 6, pp. 1709–1724, 2007.
- [132] K. P. Tee, S. S. Ge, and E. H. Tay, “Adaptive control of electrostatic microactuators with bidirectional drive,” *IEEE Transactions on Control Systems Technology*, vol. 17, no. 2, pp. 340 – 352, 2009.
- [133] Z. Ding, “Adaptive stabilisation of extended nonlinear output feedback systems,” *IEE Proceedings - Control Theory and Applications*, vol. 148, no. 3, pp. 268–272, 2001.
- [134] X. Ye, “Adaptive nonlinear output-feedback control with unknown high-frequency gain sign,” *IEEE Transactions on Automatic Control*, vol. 46, no. 1, pp. 112–115, 2001.
- [135] P. L. Liu and T. J. Su, “Robust stability of interval time-delay systems with delay-dependence,” *Systems & Control Letters*, vol. 33, no. 4, pp. 231–239, 1998.
- [136] L. Dugard and E. Veriest, *Stability and Control of Time-delay Systems*. Berlin; New York: Springer-Verlag, 1997.
- [137] J.-P. Richard, “Time-delay systems: an overview of some recent advances and open problems,” *Automatica*, vol. 39, no. 10, pp. 1667–1694, 2003.
- [138] J. Hale, *Theory of Functional Differential Equations*. New York: Springer-Verlag, 2nd ed., 1977.
- [139] V. B. Kolmanovskii and J. P. Richard, “Stability of some linear systems with delays,” *IEEE Transactions on Automatic Control*, vol. 44, no. 5, pp. 984–989, 1999.
- [140] S.-I. Niculescu, *Delay Effects on Stability: A Robust Control Approach*. New York: Springer, 2001.
- [141] K. Gu, V. L. Kharitonov, and J. Chen, *Stability of Time-delay Systems*. Boston: Birkhäuser, 2003.

- [142] V. L. Kharitonov and D. Melchor-Aguilar, “Lyapunov-Krasovskii functionals for additional dynamics,” *International Journal of Robust Nonlinear Control*, vol. 13, no. 9, pp. 793–804, 2003.
- [143] S. K. Nguang, “Robust stabilization of a class of time-delay nonlinear systems,” *IEEE Transactions on Automatic Control*, vol. 45, no. 4, pp. 756–762, 2000.
- [144] S. Zhou, G. Feng, and S. K. Nguang, “Comments on ‘robust stabilization of a class of time-delay nonlinear systems’,” *IEEE Transactions on Automatic Control*, vol. 47, no. 9, pp. 1586–1586, 2002.
- [145] S. S. Ge, F. Hong, and T. H. Lee, “Adaptive neural network control of nonlinear systems with unknown time delays,” *IEEE Transactions on Automatic Control*, vol. 48, no. 11, pp. 2004–2010, 2003.
- [146] S. S. Ge and K. P. Tee, “Approximation-based control of nonlinear MIMO time-delay systems,” *Automatica*, vol. 43, no. 1, pp. 31–43, 2007.
- [147] Y. Sun, J. Hsieh, and H. Yang, “On the stability of uncertain systems with multiple time-varying delays,” *IEEE Transactions on Automatic Control*, vol. 42, no. 1, pp. 101–105, 1997.
- [148] B. Xu and Y. Liu, “An improved Razumikhin-type theorem and its applications,” *IEEE Transactions on Automatic Control*, vol. 39, no. 4, pp. 839–841, 1994.
- [149] M. Jankovic, “Control Lyapunov-Razumikhin functions and robust stabilization of time delay systems,” *IEEE Transactions on Automatic Control*, vol. 46, no. 7, pp. 1048–1060, 2001.
- [150] J. Pan, C.-Y. Su, and Y. Stepanenko, “Modeling and robust adaptive control of metal cutting mechanical systems,” in *Proceedings of the 2001 American Control Conference*, pp. 1268–1273, 2001.
- [151] R. Sepulchre, M. Janković, and P. V. Kokotović, *Constructive Nonlinear Control*. London; New York: Springer, 1997.

- [152] S. S. Ge, C. C. Hang, and T. Zhang, “A direct adaptive controller for dynamic systems with a class of nonlinear parameterizations,” *Automatica*, vol. 35, no. 4, pp. 741–747, 1999.
- [153] N. Hovakimyan, E. Lavretsky, and A. Sasane, “Dynamic inversion for nonaffine-in-control systems via time-scale separation. Part I,” *Journal of Dynamical and Control Systems*, vol. 13, no. 4, pp. 451–465, 2007.
- [154] T. P. Zhang and S. S. Ge, “Adaptive neural control of MIMO nonlinear state time-varying delay systems with unknown dead-zones and gain signs,” *Automatica*, vol. 43, no. 6, pp. 1021–1033, 2007.
- [155] M. S. de Queiroz, J. Hu, D. M. Dawson, T. Burg, and S. R. Donepudi, “Adaptive position/force control of robot manipulators without velocity measurements: Theory and experimentation,” *IEEE Transactions on Systems Man and Cybernetics-Part B: Cybernetics*, vol. 27, no. 5, pp. 796–809, 1997.
- [156] G. Lightbody and G. W. Irwin, “Direct neural model reference adaptive control,” *IEE Proceedings-Control Theory and Applications*, vol. 142, no. 1, pp. 31–43, 1995.
- [157] L. O. Santos, P. A. Afonso, J. A. A. M. Castro, N. M. C. Oliveira, and L. T. Biegler, “On-line implementation of nonlinear MPC: an experimental case study,” *Control Engineering Practice*, vol. 9, no. 8, pp. 847–857, 2001.
- [158] W. F. Ramirez and B. A. Turner, “The dynamic modeling, stability, and control of a continuous stirred tank chemical reactor,” *AIChE Journal*, vol. 15, no. 6, pp. 853–860, 1969.
- [159] E. P. Ryan, “A universal adaptive stabilizer for a class of nonlinear systems,” *Systems & Control Letters*, vol. 16, no. 3, pp. 209–218, 1991.
- [160] B. Yao and M. Tomizuka, “Adaptive robust control of SISO nonlinear systems in a semi-strict feedback form,” *Automatica*, vol. 33, no. 5, pp. 893–900, 1997.
- [161] K. P. Tee and S. S. Ge, “Control of nonlinear systems with full state constraint using a barrier lyapunov function,” in *Proceedings of the Joint 48th*

IEEE Conference on Decision and Control and 28th Chinese Control Conference, pp. 8618–8623, 2009.

Author's Publications

The contents of this thesis are based on the following papers that have been published or accepted by peer-reviewed journals and conferences.

Journal Papers:

1. B. Ren, S. S. Ge, T. H. Lee and C.-Y. Su, "Adaptive Neural Control for a Class of Nonlinear Systems with Uncertain Hysteresis Inputs and Time-Varying State Delays", *IEEE Transactions on Neural Networks*, vol. 20, no. 7, pp. 1148-1164, 2009.
2. B. Ren, S. S. Ge, C.-Y. Su and T. H. Lee, "Adaptive Neural Control for a Class of Uncertain Nonlinear Systems in Pure-Feedback Form with Hysteresis Input", *IEEE Transactions on Systems, Man, and Cybernetics - Part B: Cybernetics*, vol. 39, no. 2, pp. 431-443, 2009.
3. P. P. San, B. Ren, S. S. Ge and T. H. Lee, "Adaptive Neural Network Control of Hard Disk Drives with Hysteresis Friction Nonlinearity", *IEEE Transactions on Control Systems Technology*, accepted.
4. B. Ren, S. S. Ge, K. P. Tee and T. H. Lee, "Adaptive Neural Control for Output Feedback Nonlinear Systems Using a Barrier Lyapunov Function", *IEEE Transactions on Neural Networks*, accepted.

Conference Papers:

1. B. Ren, P. P. San, S. S. Ge and T. H. Lee, "Adaptive Dynamic Surface Control for a Class of Strict-Feedback Nonlinear Systems with Unknown Backlash-Like Hysteresis", Proceedings of the 2009 American Control Conference, pp. 4482-4487, St. Louis, MO, USA June 10-12, 2009.

2. B. Ren, S. S. Ge, T. H. Lee, and C.-Y. Su, "Adaptive Neural Control for Uncertain Nonlinear Systems in Pure-feedback Form with Hysteresis Input", Proceedings of the 47th IEEE Conference on Decision and Control, pp. 86-91, Cancun, Mexico, December 9-11, 2008.
3. S. S. Ge, B. Ren, T. H. Lee, C.-Y. Su, "Adaptive Neural Control of SISO Non-Affine Nonlinear Time-Delay Systems with Unknown Hysteresis Input", Proceedings of the 2008 American Control Conference, pp.4203-4208, Seattle, Washington, USA, June 11-13, 2008.
4. B. Ren, P. P. San, S. S. Ge and T. H. Lee, "Robust Adaptive NN Control of Hard Disk Drives with Hysteresis Friction Nonlinearity", Proceedings of the 17th IFAC World Congress, pp.2538-2543, Seoul, Korea, July 6-11, 2008.
5. T. H. Lee, B. Ren and S. S. Ge, "Adaptive Neural Control of SISO Time-Delay Nonlinear Systems with Unknown Hysteresis Input", Proceedings of the 17th IFAC World Congress, pp.248-253, Seoul, Korea, July 6-11, 2008.